Evolutionary Strategies Against Antimicrobial Resistance

Farhan Rahman Chowdhury

A Thesis
In the Department of
Biology

Presented in Partial Fulfillment of the Requirements

for the Degree of

Doctor of Philosophy (Biology) at

Concordia University

Montréal, Québec, Canada

June 2025

CONCORDIA UNIVERSITY

School o	f Graduate Studies	
This is to	certify that the thesis prepared	
By:	Farhan Rahman Chowdhury	
	Entitled: Evolutionary Strategies Again	nst Antimicrobial Resistance
and subn	nitted in partial fulfillment of the require	ments for the degree of
Doctor o	of Philosophy Biology	
-	s with the regulations of the University arty and quality.	nd meets the accepted standards with respect to
Signed b	y the final examining committee:	
	Dr. Andreas Bergdahl	Chair
	Dr. Bastien Castagner	External Examiner
	Dr. Paul Joyce	External to Program
	Dr. Isabelle Benoit-Gelber	Examiner
	Dr. Steve C. C. Shih	Examiner
	Dr. Brandon Findlay	Thesis Supervisor
Approve	ed by	
	Dr. Robert Weladji, Graduate Prog	gram Director
August 1	5, 2025	
	Dr. Pascale Sicotte, Dean of Facul	ty of Arts and Science

Abstract

Evolutionary Strategies Against Antimicrobial Resistance

Farhan Rahman Chowdhury, PhD Concordia University, 2025

Antibiotic resistance threatens to undo many of the advancements of modern medicine. A slow antibiotic development pipeline makes it impossible to outpace bacterial evolution, making alternative strategies essential to combat resistance. In this study, I use large scale experimental evolutions powered by the soft agar gradient evolution (SAGE) platform to investigate the evolutionary trade-offs associated with antibiotic resistance, and how they can be leveraged to combat the emergence of resistance.

The study begins with the finding that a chloramphenicol (CHL) resistant *Escherichia coli* (*E. coli*) mutant exhibits a markedly reduced rate of resistance evolution against other antibiotics. I show that this slow adaptation is linked to the fitness costs associated with resistance, which bacteria often readily overcome through compensatory evolution. Further screening identifies fitness costs which cannot be easily compensated for, highlighting an opportunity to exploit these trade-offs to slow down the emergence of resistance. However, the translatory potential of the findings from SAGE to the clinic remained unclear.

To test the utility and clinical relevance of SAGE, I first expand its applicability to a broader range of antibiotics by supplementing the evolution medium with xanthan gum. Xanthan gum is a water-binding polysaccharide that significantly reduces synaeresis of the agar-based medium, enhancing evolution in SAGE. To demonstrate its capacity to uncover resistance mechanisms I use this modified platform to characterize the evolution of resistance to the lipopeptide tridecaptin A₁—an

antibiotic previously thought to be impervious to resistance. I then assess the clinical applicability of the evolutionary trade-offs observed in SAGE-derived mutants by comparing outcomes from SAGE to those obtained using other widely used laboratory evolution platforms, as well as clinical bacterial datasets. These analyses reveal that SAGE more accurately reproduces clinically relevant patterns of fitness trade-offs than the alternative platforms tested. One such trade-off, collateral sensitivity (CS), has recently been proposed to be useful in mitigating resistance in sequential antibiotic therapies, where antibiotics are applied one after the other. But large-scale evolutionary studies to determine its role and effectiveness in sequential regimens were missing.

I use over 450 evolution experiments to test the role of CS in resistance mitigation in four proposed drug pairs. I find that resistance to both drugs evolves readily, and that collateral sensitivity does not hinder the evolution of multidrug resistance or promote resensitization. However, if resistance to drug B reduces susceptibility to A in an A-B drug sequence, a phenomenon I term backward CS, resistance to A can be reduced. As an example, I demonstrate that β -lactam resistant *E. coli* cells frequently lower their resistance to β -lactams upon aminoglycoside resistance acquisition due to conflicting modifications to the proton motive force and efflux pumps. This suggests that the levels of resistance evolved can be kept in check by leveraging backwards CS to resensitize cells as antibiotic resistance evolves. However, the levels of resensitization achieved were two-fold on average, often not sufficient to reduce resistance below clinical breakpoints.

Finally, I introduce sequential antibiotic regimens composed of three drugs or "tripartite loops" to contain resistance within a closed drug cycle. Through 424 discrete adaptive laboratory evolution experiments I show that as bacteria sequentially evolve resistance to the drugs in a loop, they

continually trade their past resistance for fitness gains, reverting back to sensitivity via four-to-eight-fold reductions in resistance on average. Through fitness and genomic analyses, I find that tripartite loops guide bacterial strains towards evolutionary paths that mitigate fitness costs and reverse resistance to component drugs in the loops, driving levels of resensitization not achievable through previously suggested pairwise regimens. I then apply this strategy to reproducibly resensitize or eradicate four multidrug-resistant clinical isolates over the course of 216 evolutionary experiments. Resensitization occurred even when bacteria adapted through plasmid-bound mutations instead of chromosomal changes, showing the robustness of this strategy.

In conclusion, this work demonstrates that the evolutionary trade-offs accompanying antibiotic resistance can be strategically exploited to limit or reverse resistance evolution. I highlight the importance of studying the evolutionary aspect of antibiotic resistance to inform rational treatment strategies and restore efficacy of existing antibiotics. As the pace of novel antibiotic discovery continues to lag behind resistance evolution, such evolution-based approaches may be essential for extending the lifespan of our current antimicrobial arsenal.

Acknowledgements

When I chat with students who are thinking about grad school and joining a lab, I tell them that it's not enough to just be interested in the work that the lab is doing. I recommend talking to current students and alumni about their time in the lab. It's a great way to get a feel for what it's like to work there, both in terms of the environment and the people. I didn't do any of that before joining the Findlay lab. I liked what the lab was working on, I got accepted in the lab after a meeting with Dr. Brandon Findlay, and I was off to join the lab on the other side of the planet. Knowing what I know now about the lab and the people in it, I would, a hundred percent, do it again.

Since day 1, Dr. Findlay has given me the freedom to work the way I wanted, when I wanted, within the rough confines of my projects. I never felt rushed or pushed towards a direction I did not want to take, and I always felt like my opinions were valued. The weekly one-on-one meetings (I think I had a weekly meeting almost every working week) did not feel like an exam (even though the first few were a little intimidating because I knew potato at the time about the field of science I have written this thesis on), and his responses to my failed experiments were never discouraging, always constructive. The amount I've learned from him—everything from basic evolutionary biology and microbiology to designing experiments, writing papers and scholarship applications, and giving presentations—is honestly kind of insane. It's easy to get buried in your own experiments and data and lose sight of the goal, but he's always helped me reorient. He's also given me invaluable career advice, kept track of my timelines, and reminded me to think about what comes next (because I definitely did not). For these, and for everything else I missed writing here, I cannot thank him enough. If I do not get a custom Findlay lab printed souvenir before I leave the lab, I will withdraw all the thank-yous though.

I am grateful to my committee members, Isabelle Benoit Gelber and Steve C. C. Shih for their feedback and guidance during my PhD. They were consistently encouraging in every meeting and offered perspectives different from my own, which helped shape the direction of my research and ultimately allowed me to bring it to a timely and meaningful conclusion.

I am not known for my social skills. I was confident-ish that I could handle myself in the lab when I first joined, but fitting in a new lab with new people was my biggest fear. But I got lucky again. Very lucky. Day 1 (or 2 or some single digit), I remember meeting Lydia Rili (MSc, Findlay lab) who was so incredibly warm and welcoming. I remember being invited to have tea with her and another wonderful soul, Nathalie Reid (PhD, Joyce lab) that day. I never felt not-out-of-place so quickly in a new place before. I'm lucky to be able to call them my friends.

Soon after, I had my first real interaction with Laura Domínguez (PhD candidate, Findlay lab), who showed me how to make a SAGE plate (if you're going to read the thesis after, you'll learn too much about these plates; if you're not, you probably don't care). I'd meet Prerna Singh (PhD candidate, Findlay lab) a few months later when she joined the lab. Some people say you don't really make real friends in the workplace. Laura and Prerna are some of my best friends I've ever had. They made coming to the lab something I could still look forward to when things (experiments and plans and all that) were going south. I'd always have their support on pretty much anything I did, and it was always reassuring (?) to hear "mine's not working either" when I cried about my work. All the coffee breaks, lunch breaks, trips to Hive, random breaks for gossip and venting sessions combined made the lab (we didn't eat/drink inside the lab) feel FUN! I will miss being in the same lab with these two goofs, terribly. I hope we can forever remain PhrienDs.

Every member of the Findlay lab that I've ever interacted with are amazing people. I'm going to miss Marcus Simoes' (MSc candidate, Findlay lab) incredible cooking (and potlucks) and our chats about gaming, and Elena Ali's (MSc candidate, Findlay lab) energy and her Whatsapp stickers. I'd like to thank all the wonderful interns and undergraduate research students that worked in the Findlay lab, especially Joana Schnubel (research intern in the Findlay lab at the time, from University of Mannheim) for bringing her contagious energy into the lab, and Rayan Djavedani Hadji (MSc research intern in the Findlay lab at the time, from University of Strasbourg) for constantly keeping the mood light with his sense of humor. It's wild how quickly Rayan and I became friends.

Veronica Banari (Mitacs Globalink Intern in the Findlay lab when we met), and Vlada Lesnic (CHEM 450 student in the Findlay lab when we met) deserve a separate paragraph. They're both incredibly talented and hardworking young scientists, and their work on one of my projects (which is part of this thesis) played a huge role in its success.

I always tell my wife, Sumaiya, that if she weren't here, I'd have finished my PhD ~a year sooner. BUT, I would not remain sane. She has been my biggest personal cheerleader throughout this journey. She has always been by my side, supportive, loving and understanding when work required long hours (which has been most days) and working on weekends and holidays (which has been most weekends and holidays). I believe that most people would NOT put up with this. She helped me disconnect from lab tragedies and recharge ready for the next day. She stops me from drowning in work: she is my anchor, my safe space, and the person who reminds me that

there's more to life than experiments and deadlines. These paragraphs are in no particular order of importance. If they were, this one wouldn't be here.

There is no way I would have made it this far without my mother, Irine, and my sister, Suzana. Strictly speaking in terms of education, I do not think I could've learned to do basic addition and subtraction or the mathematical tables without my mom and her infinite patience. She was my first teacher, and she inspires me to be the person I want to be. My sister's discipline and grit are something I can only dream of having, but I do dream of it. We've been through some incredibly difficult times together, but they've always supported me and believed in every step I took. They guided me toward paths, still aligned with my dreams, that I never would have found on my own. I am a gigantic negative Nancy, and I almost always assume the worst to happen. For example, I never thought I could actually start a PhD here, let alone finish it. If not for their encouragement and support and the frequent "STFU, stop crying", I probably wouldn't have even tried.

There're so many people who worked tirelessly behind the scenes to keep our work in the lab running smoothly. I thank Mila Anohina for tirelessly womanning the central stores, and Kevin Kay from the shipping docks for processing all shipping smoothly. I'm grateful to the security personnel who let me in after hours and holidays, the technical staff that kept our equipment running, and the janitorial staff who kept our spaces clean. The PhD thesis cover page allows only a singular name, but if it didn't, there would be a 'see more' button.

Contribution of Authors

Chapter 2:

- Farhan Rahman Chowdhury: Experimental design, experimentation, preparation of figures, writing the manuscript.
- Brandon Findlay: Conceptualization, experimental design, editing the manuscript.

Chapter 3:

- Farhan Rahman Chowdhury: Experiments, preparation of figures and writing related to evolution, synaeresis testing, motility and diffusion assays,
- Laura Domínguez Mercado: Experiments, preparation of figures and writing related to genomics and allelic exchange.
- Katya Kharitonov: Oct-TriA₁ synthesis.
- Brandon Findlay: Conceptualization, experimental design, editing the manuscript.

Chapter 4:

- Farhan Rahman Chowdhury: Conceptualization, experimental design, 40% of all evolution experiments and susceptibility testing; all genomics and phenotypic analysis of mutants, experiments with the *marR*-containing plasmid and clinical data analysis; preparation of figures, writing the manuscript.
- Veronica Banari: 40% of all evolution experiments and susceptibility testing.
- Vlada Lesnic: 20% of all evolution experiments and susceptibility testing.
- Brandon Findlay: Conceptualization, experimental design, editing the manuscript.

Chapter 5:

- Farhan Rahman Chowdhury: Experimental design, experimentation, preparation of figures, writing the manuscript.
- Brandon Findlay: Conceptualization, experimental design, editing the manuscript.

Chapter 6:

- Farhan Rahman Chowdhury: Experimental design, experimentation, preparation of figures, writing the manuscript.
- Brandon Findlay: Conceptualization, experimental design, editing the manuscript.

Table of Contents

Abstract	iii
Acknowledgements	vi
Contribution of Authors	X
Table of Contents	xi
List of Figures	xiv
List of Tables	
List of Abbreviations	
Chapter 1. Introduction	
1.1. Laboratory tools to study antibiotic resistance evolution	
1.2. Leveraging fitness penalties of resistance to combat resistance evolution	
1.3. Sequential antibiotic therapies and collateral sensitivity	
1.3.1. Mechanisms of collateral sensitivity	
1.3.2. Collateral sensitivity and cyclic antibiotic therapies	
1.3.3. The pitfalls of collateral sensitivity	
1.3.4. An improved SAGE leads to the elucidation of the mechanism of resistance aga	
the "evolution proof" antibiotic octyl-TriA ₁	
1.3.5. Large scale laboratory evolutions predicts clinical outcomes and leads to the	2 1
discovery of a novel mechanism of collateral sensitivity	25
1.3.6. The role of collateral sensitivity in antibiotic resensitization	
1.4. Collateral sensitivity-independent sequential regimens that produce large and	,
repeatable resensitizations	29
Chapter 2. Fitness costs of antibiotic resistance impede the evolution of resistance to	
other antibiotics	
2.1. Introduction2.2. Results	
2.2.1. Evolution of high-level resistance to chloramphenicol via SAGE	
2.2.2. Chloramphenicol resistant cells are fitness impaired2.2.3. Fitness costs delay the evolution of resistance and alter evolutionary trajector	
2.2.4. Evolution against streptomycin	
2.2.5. Improving fitness of chloramphenicol-resistant cells restores resistance poten	
to nitrofurantoin but not streptomycin	
2.2.6. Impaired resistance evolution is not linked to chloramphenicol resistance	
2.3. Discussion	
2.4. Materials and methods	
2.4.1. Bacterial strain and growth conditions	
2.4.2. SAGE evolutions	
2.4.3. Growth measurements	
2.4.4. Fitness improvements via flat-concentration SAGE plates	
2.4.5. MIC assays	
2.4.6. Whole genome sequencing	

Chapter	· 3.	De novo evolution of antibiotic resistance to Oct-TriA ₁	59
3.1.	Intro	oduction	59
3.2.		ılts	
3.2.	.1.	Standard SAGE medium fails to generate resistance to polymyxin B	61
3.2.	2.	Xanthan gum supplementation reduces synaeresis in agar hydrogels	
3.2.		Supplementation with xanthan gum enhanced the evolution of polymyxin B	
	stance		
3.2.4.		volution of resistance to Oct-TriA ₁	66
3.2.4.		Genetic analysis of Oct-TriA ₁ -resistant mutants	
_	.6.	Allelic exchange in genes involved in phospholipid transport and outer members.	
		confirmed their involvement in resistance to Oct-TriA ₁	
3.3.	•	cussion	
3.3. 3.4.		erials and Methods	
3.4. 3.4.		Bacterial Strain and Growth Conditions	
_			
3.4.		Oct-TriA ₁ synthesis	
3.4.		SAGE evolutions	
3.4.		MIC Assays	
3.4.		Synaeresis tests	
3.4.		Bacterial Motility tests	
3.4.		Generation of the XAM-adapted WT strain	
3.4.		Fitness measurements	
3.4.		WGS and variant calling	
3.4.		Gene ontology enrichment analysis	
3.4.	.11.	Allelic exchange mutant generation.	
3.4.	.12.	Keio collection strains Kan cassette curing	80
3.4.	.13.	Strains	80
Chapter		Large scale laboratory evolution uncovers clinically relevant collateral	0.2
antibioti		sitivity	
4.1.	Intro	oduction	82
4.2.	Resu	ılts	83
	1.	SAGE produces lower collateral sensitivities and higher cross resistances	
con	nparec	to other ALE platforms	83
4.2.		Tigecycline resistance evolves via similar pathways across ALE platforms	
4.2.	.3.	Polymyxin collateral sensitivity is linked to Lon protease deactivation	
4.2.	4.	MarR deactivation neutralizes Lon deactivation-driven polymyxin collateral	
sens	sitivit	y	92
4.2.	•	Strong intra-class cross-resistance, but not collateral sensitivity, is prevalent in	
clin	ical E	. coli	
4.2.		CS relationships rarely appear in clinical strains and their prevalence is best	,
		by SAGE	98
4.3.		sussion	
4.4.		erials and Methods	
4.4.		Bacterial strain and growth conditions	
4.4.		Susceptibility assays	
		ALE experiments	103

4.4.4.	Whole genome sequencing and analysis	10 4
4.4.5.	Exopolysaccharide assay	
4.4.6.	MarR complementation	105
4.4.7.	Clinical strains and data analysis	106
4.4.8.	Data and materials availability:	
Chapter 5.	Sequential antibiotic exposure restores antibiotic susceptibility	107
5.1. Int	oduction	107
5.2. Re	sults	110
5.2.1.	A SAGE-based evolution platform to test pairwise drug sequences	110
5.2.2.	Forward CS does not promote extinctions, resistance drops or resensitization	is in
clonal p	opulations	114
5.2.3.	Backward CS can drive resistance drops	118
5.2.4.	POL resensitization is multifactorial	121
5.3. Dis	cussion	122
5.4. Ma	terials and Methods	125
5.4.1.	Bacterial strain and growth conditions	125
5.4.2.	SAGE Evolutions	125
5.4.3.	MIC assays	126
5.4.4.	Flat plates	126
5.4.5.	Whole genome sequencing and analysis	127
5.4.6.	Hexanes tolerance assay	127
5.4.7.	Antibiotic free soft agar plates	128
Chapter 6.	Tripartite loops reverse antibiotic resistance	129
-	Tripartite loops reverse antibiotic resistance	
6.1. Int		129
6.1. Int	oduction	129 132
6.1. Inta	roductionsults	129 132 132
6.1. Into 6.2. Res 6.2.1.	Tripartite drug loops that resensitize bacteria to antibiotics PIP resistance is important for resensitization	129 132 132
6.1. Intr 6.2. Re 6.2.1. 6.2.2.	roductionsults Tripartite drug loops that resensitize bacteria to antibiotics	129 132 132
6.1. Int. 6.2. Res 6.2.1. 6.2.2. 6.2.3. 6.2.4.	Tripartite drug loops that resensitize bacteria to antibiotics	129 132 132 135
6.1. Int. 6.2. Res 6.2.1. 6.2.2. 6.2.3. 6.2.4.	Tripartite drug loops that resensitize bacteria to antibiotics	129 132 135 137
6.1. Int. 6.2. Res 6.2.1. 6.2.2. 6.2.3. 6.2.4. mechan	Tripartite drug loops that resensitize bacteria to antibiotics	129 132 135 137 141
6.1. Introduced for the following forms of th	Tripartite drug loops that resensitize bacteria to antibiotics	129 132 135 137 141 147 ttions
6.1. Introduced for the following forms of th	Tripartite drug loops that resensitize bacteria to antibiotics	129 132 135 137 141 147 150
6.1. Introduced for the following forms of th	Tripartite drug loops that resensitize bacteria to antibiotics	129 132 135 137 141 147 150 150
6.1. Introduced for the following forms of th	Tripartite drug loops that resensitize bacteria to antibiotics	129 132 135 137 141 147 150 153
6.1. Introduced for the following forms of th	Tripartite drug loops that resensitize bacteria to antibiotics	129 132 135 137 141 147 150 153 153
6.1. Introduced for the following forms of th	Tripartite drug loops that resensitize bacteria to antibiotics PIP resistance is important for resensitization Resensitizations are independent of CS and principally mitigate fitness loss. Whole genome sequencing sheds light on resistance and resensitization sms NIT-PIP-GEN loop reduces clinically acquired NIT resistance Bypassing chromosomal adaptations against PIP does not abolish resensitization terials and Methods Bacterial strain and growth conditions SAGE evolutions Susceptibility testing	129 132 135 137 141 147 150 153 153 154
6.1. Introduced for the following forms of th	Tripartite drug loops that resensitize bacteria to antibiotics	129 132 135 137 141 147 153 153 154 154
6.1. Introduced for the following forms of th	Tripartite drug loops that resensitize bacteria to antibiotics PIP resistance is important for resensitization Resensitizations are independent of CS and principally mitigate fitness loss. Whole genome sequencing sheds light on resistance and resensitization sms. NIT-PIP-GEN loop reduces clinically acquired NIT resistance Bypassing chromosomal adaptations against PIP does not abolish resensitization streials and Methods. Bacterial strain and growth conditions SAGE evolutions Susceptibility testing Flat plates Fitness measurements	129 132 135 137 141 147 150 153 153 154 154
6.1. Introduction of the control of	Tripartite drug loops that resensitize bacteria to antibiotics PIP resistance is important for resensitization Resensitizations are independent of CS and principally mitigate fitness loss. Whole genome sequencing sheds light on resistance and resensitization sms NIT-PIP-GEN loop reduces clinically acquired NIT resistance Bypassing chromosomal adaptations against PIP does not abolish resensitization susceptibility testing SAGE evolutions Susceptibility testing Flat plates Fitness measurements Whole genome sequencing	129 132 135 137 141 147 153 153 154 155 155
6.2. Research 6.2.1. 6.2.2. 6.2.3. 6.2.4. mechan 6.2.5. 6.2.6. 6.3. Dis 6.4. Ma 6.4.1. 6.4.2. 6.4.3. 6.4.4. 6.4.5. 6.4.6.	Tripartite drug loops that resensitize bacteria to antibiotics PIP resistance is important for resensitization Resensitizations are independent of CS and principally mitigate fitness loss. Whole genome sequencing sheds light on resistance and resensitization sms. NIT-PIP-GEN loop reduces clinically acquired NIT resistance Bypassing chromosomal adaptations against PIP does not abolish resensitization streials and Methods. Bacterial strain and growth conditions SAGE evolutions Susceptibility testing Flat plates Fitness measurements	129 132 135 137 141 147 153 153 154 155 155

7.1.	Key Findings	
7.2.	Limitations	
7.3.	Future Work	
7.4.	Conclusion	165
Referen	nces	168
Append	lices	196
Supp	lementary Materials for Chapter 2	196
	lementary Materials for Chapter 3	
Supp	lementary Materials for Chapter 4	219
	lementary Materials for Chapter 5	
Supp	lementary Materials for Chapter 6	224
List of	Figures	
Figure 1	1.1 The SAGE platform	11
Figure 1	1.2 Fitness costs can be leveraged to restore antibiotic susceptibility in a population	13
Figure 1	1.3 Reciprocal CS	19
Figure 1	.4 Antibiotic resensitization in clonal bacterial populations	22
Figure 1	1.5 Forward and Backward collateral sensitivity.	28
Figure 1	1.6 Trading resistance for fitness	30
Figure 2	2.1 Evolution of chloramphenicol resistance incurs fitness costs	35
Figure 2	2.2 Tracking movement of bacterial populations in SAGE revealed resistance evolution	n
impairn	nents	39
Figure 2	2.3 STR resistance is delayed in the fitness-impaired OM background	44
Figure 2	2.4 Passaging cells through "flat" SAGE lanes improves fitness of the OM	48
	3.1 Synaeresis limits SAGE.	
Figure 3	3.2 Evolution of antibiotic resistance.	65
_	3.3 Mutations identified in the evolved strains.	
_	4.1 Evolution of antibiotic resistance using three different ALEs.	
	4.2 Genomic and phenotypic analysis reveals mechanism of POL CS in TIG resistant	
	4.3 Uropathogenic <i>E. coli</i> antimicrobial susceptibilities reveal a rare CS relationship	
_	ed by laboratory evolution.	97
-	5.1 The concept of forward and backward collateral sensitivity	
	5.2 A SAGE-based evolution platform to study sequential antibiotic application	
_	5.3 Extinctions, MIC reductions and resensitizations in drug pairs	
_	5.4 GEN resistance disrupts efflux-mediated PIP resistance.	
	5.5 Resensitization of POL resistant strains.	
_	5.1 Tripartite loops improve antibiotic resensitization	
_	5.2 PIP aids resensitization in tripartite loops	
	6.3 Resensitization does not correlate with CS but mitigates fitness loss	

Figure 6.4 Tracking genomic changes through the GEN-PIP-NIT loop	14
Figure 6.5 The NIT-PIP-GEN loop reduces clinically acquired NIT resistance	1 8
List of Tables	
Table 2.1 The OM exhibited a multidrug resistant phenotype	36
Table 3.1 Details of Oct-TriA1 mutants sampled from SAGE	57
Table 4.1 Changes in POL MIC after introduction of the pUC57-marR plasmid in strains with	
different MarR mutations9	_
Table 5.1 WT MICs	11
Table 5.2 Mutations in the PIP and PIP-GEN adapted strains that affect efflux and the electron	
transport chain respectively	13

List of Abbreviations

Abbreviation Definition

ALE Adaptive Laboratory Evolution

AMR Antimicrobial Resistance
ANOVA Analysis of Variance

AU Arbitrary Units

AUC Area Under the Curve

CFZ Cefazolin

CHL Chloramphenicol
CIP Ciprofloxacin

COL Colistin

CR Cross Resistance
CS Collateral Sensitivity

DOX Doxycycline GEN Gentamicin

GP Gradient Plating ALE system

IPTG isopropyl β-D-1-thiogalactopyranoside

LPS Lipopolysaccharide

LQ Serial Transfer-based ALE system

MDR Multidrug-resistant

MHA Mueller Hinton Agar, Cation Adjusted
MHB Mueller Hinton Broth, Cation Adjusted
MIC Minimum Inhibitory Concentration

NIT Nitrofurantoin
OMC Omadacycline
PIP Piperacillin

PMF Proton Motive Force

POL Polymyxin B

SAGE Soft Agar Gradient Evolution ALE system

STR Streptomycin
TET Tetracycline
TIG Tigecycline

Chapter 1. Introduction

Since their introduction in 1945, antibiotics have revolutionized medicine, turning once-fatal infections into manageable conditions. They are essential in treating a wide range of illnesses—from common infections like strep throat to severe diseases such as meningitis [1]. Modern medical procedures, including cancer therapies, organ transplants, and open-heart surgeries would be nearly impossible without effective antibiotics [2,3]. For vulnerable groups such as individuals with weakened immune systems, these drugs are critical for preventing and managing life-threatening bacterial infections [4,5]. Their use in the clinic contributed to a dramatic 20–30 year increase in life expectancy across the developed world according to data from 2016 [2,6]. But today, poor antibiotic stewardship, inadequate drug regulations and widespread misuse in livestock have created one of the greatest challenges in modern healthcare: antimicrobial resistance (AMR) [7–10]. In 2021 alone, AMR was directly responsible for over 1.1 million deaths and contributed to an estimated 4.7 million more. Projections suggest that by 2050, annual AMR-related deaths could exceed 8 million [11,12].

Beta-lactams are some of the most widely used antibiotics, with them sharing a common β-lactam ring in their structure [13]. They work by binding penicillin-binding proteins in bacteria and disrupting the synthesis of peptidoglycan, a key component in bacterial cell wall. This class can be further divided into subclasses: penicillins, cephalosporins, carbapenems, and monobactams [13]. Penicillin is the first true antibiotic discovered in 1928 by Alexander Fleming, produced by the mold *Penicillium notatum* [13]. Cephalosporins were discovered through research on a *Cephalosporium* fungus in 1948 [14]. They are structurally similar to penicillin and hence have a similar mechanism of action but contain a seven-membered dihydrothiazine ring instead of the

five-membered thiazolidine ring found in penicillin [15]. Most clinically used cephalosporins are semisynthetic, with modifications made to broaden its spectrum of activity against bacterial pathogens and to evade resistance mechanisms [15]. The first carbapenem, thienamycin, was discovered in 1976 from the bacterium *Streptomyces cattleya* [16]. More stable synthetic variants like imipenem and meropenem were then developed that were viable for clinical use [16]. They contain a β-lactam ring which, unlike in penicillin, is fused to a five-membered ring, and the sulfur atom at position 1 in penicillin is replaced with a carbon atom [16]. Again, these modifications allow these molecules to bypass resistance mechanisms in bacteria that evolved against penicillins [16]. Monobactams were discovered in the 1980s, characterized by a monocyclic beta-lactam ring, unlike the bicyclic structure found in penicillins and cephalosporins [17]. They were first isolated from bacteria like *Chromobacterium*, *Gluconobacter*, *Acetobacter*, *Pseudomonas*, *Agrobacterium*, and Flexibacter, and chemical modifications led to the first potent monobactam called aztreonam, active against Gram-negative bacteria [18]. Aztreonam is known to be stable against a variety of β-lactamases, enzymes that can degrade β-lactams to confer resistance in bacteria [18].

Aminoglycosides, another class of broad-spectrum antibiotics characterized by a core structure of amino sugars linked to a dibasic aminocyclitol, were first discovered in 1944 with the isolation of streptomycin from *Streptomyces griseus* [19]. Further research led to the discovery of other aminoglycosides like neomycin, kanamycin, gentamicin, and tobramycin, either from *Streptomyces* or *Micromonospora* species or through chemical modifications [19]. They inhibit protein synthesis by binding to the 30S ribosomal subunit and are active against various Grampositive and Gram-negative organisms [19].

Tetracyclines, derivatives of the polycyclic naphthacene-carboxamides were discovered as natural products from Streptomyces in 1948 [20]. They inhibit protein synthesis by binding to the 30S ribosomal subunit and exhibit activity against both Gram-positive and Gram-negative bacteria [20]. Tetracyclines are commonly used to treat various bacterial infections including acne, chlamydia, and respiratory tract infections [20].

The development of *quinolone* antibiotics began with the discovery of an antibacterial compound from the antimalarial drug chloroquine, which led to the creation of the first quinolone, nalidixic acid in 1962 [21]. While nalidixic acid was only effective for urinary tract infections (UTIs) and led to rapid resistance, it served as a foundational model for future developments [21]. By modifying its structure, researchers introduced a fluorine at position 6 and a piperazine ring at position 7, leading to a major breakthrough with norfloxacin [21]. This compound was the first *fluoroquinolone* and exhibited a broader spectrum of activity improved absorption, but it was still not ideal for systemic use [21]. Further research rapidly produced compounds like ciprofloxacin and levofloxacin which were well-absorbed and effective against a wider range of systemic infections [21].

The first *macrolide*, erythromycin, was discovered in 1950 from a *Streptomyces* strain [22]. Further research led to the development of semi-synthetic macrolides like azithromycin and clarithromycin, with improved properties like better absorption and fewer side effects compared to erythromycin [22]. Macrolides are protein synthesis inhibitors, targeting the 50S ribosomal subunit of bacteria [22]. They exhibit a broad spectrum of activity, effective against many Grampositive bacteria and some Gram-negative bacteria [22].

Lipopeptides like the polymyxins were first discovered in 1947, isolated as a secondary metabolite from a flask of fermenting *Paenibacillus polymyxa* var. colistinus [23]. Another lipopeptide, daptomycin, was discovered in 1983 making it one of the newer antibiotics to enter clinical use [23]. Their precise mechanism of action is still debated. Polymyxins, such as colistin, primarily target lipopolysaccharide in the outer membrane of gram-negative bacteria, displacing stabilizing cations and causing destabilization [23]. This allows the antibiotic to traverse the outer membrane and disrupt the cytoplasmic membrane [23]. In contrast, daptomycin targets phosphatidylglycerol in the membranes of Gram-positive bacteria [23]. With the help of calcium ions, daptomycin inserts into the membrane, disrupting its integrity, which leads to a loss of essential ions and ATP [23]. While membrane disruption is a key factor, daptomycin's action may also involve inhibiting cell wall synthesis by interfering with enzymes and precursors located in the membrane [23].

Glycopeptides inhibit the synthesis of the bacterial cell wall in a different way than β-lactams. The first glycopeptide, vancomycin, was isolated in 1953 from the soil bacterium soil bacterium Amycolatopsis orientalis [24]. They primarily inhibit bacterial cell wall synthesis by binding to the peptidoglycan precursor, lipid II, preventing its incorporation into the cell wall [24]. This binding, which involves hydrogen bonding to the d-alanyl-d-alanine terminus of lipid II, sterically hinders the activity of enzymes involved in cell wall construction [24]. Glycopeptides are generally active against Gram-positive bacteria, and vancomycin, the most well-known of this class is clinically used to treat serious Gram-positive infections [24].

About 75% of all antibiotics in use today and discussed above are natural products or are based on natural products derived from bacteria or fungi [26]. These organisms produce antibiotics to carve

out a niche of their own and defend it against invaders and predators [27,28]. Producers of these compounds are often intrinsically resistant to their effects, but in time, other microorganisms evolved the ability to resist these antimicrobials and compete with the producers. As such, the evolution of antibiotic resistance is ancient and a natural consequence of the interactions between microorganisms and their environment [29]. However, it was not until the introduction of antibiotics in the clinic in the 1940s that antibiotic resistance mechanisms became widespread in bacterial pathogens [25]. Today, resistance has been seen to all antibiotics developed [25].

Bacteria can evolve resistance against antibiotics via a number of different mechanisms [30]. They can produce enzymes like β -lactamases and aminoglycoside-modifying enzymes that break down or modify the antibiotic of interest, rendering them ineffective [31,32]. They can reduce the net uptake of antibiotics by disrupting the permeability of their cell or outer membranes e.g., by altering their porin channels [33], and/or use efflux pumps, transmembrane proteins that use energy to transport toxins like antibiotics out of the cell [34]. They can also directly modify the cellular components or proteins that antibiotics target, preventing effective binding interactions [35]. All this can be accomplished through either mutation of chromosomal DNA or acquisition of mobile genetic elements like plasmids, changing bacterial phenotypes far more rapidly than new drugs can be developed [36].

Discovery of new antibiotics has slowed down since the golden age of antibiotics in the 1950s to 1970s, due to scientific challenges in identifying unique bacterial targets, lengthy and expensive development processes, regulatory complexities, and diminishing financial returns for pharmaceutical companies [37]. A mere 12 antimicrobials have been approved since 2017, and

only three novel classes of antibiotics were introduced in the last three decades (oxazolidinones, cyclic lipopeptides, and the triazaacenaphthylene gepotidacin) [38–40]. Worse, of the roughly 50 new antibiotics currently in clinical trials, only three are active against Gram-negative bacteria [40,41]. These bacteria are inherently more resistant to antibiotics, and WHO's critical priority list of pathogens that require new antibiotics is composed entirely of Gram-negative pathogens [42,43].

To keep up with AMR, innovative strategies to combat resistance are required. Bacterial evolution is at the center of the AMR crisis, but attempts at understanding and modulating bacterial evolution to manage AMR has been underexplored [44]. My research in the Findlay lab seeks to address this gap by applying an eco-evolutionary perspective to AMR. The key motivation for my work is the concept that evolutionary gains often come at a cost, or trade-off [61]. These trade-offs are well-documented in fields like cancer biology [62], but they remain poorly understood in the context of antibiotic resistance management. In this thesis, I describe my work on studying the evolution of resistance and its associated trade-offs and leveraging these trade-offs to design sustainable antibiotic therapies that are resilient against AMR.

1.1. Laboratory tools to study antibiotic resistance evolution

Studying evolution in natural environments presents considerable challenges, due to the inherent complexity of the environment and a multitude of interacting variables that are difficult to isolate and control [45]. Laboratory evolution, also known as adaptive laboratory evolution (ALE), offers a powerful and tractable approach to overcome these limitations. Advances in ALE, especially involving microorganisms like bacteria, have massively improved our understanding of the

principles of evolution because the short microbial generation times offer access to long evolutionary timescales [46]. By establishing controlled experimental conditions, researchers can directly observe and manipulate evolution of bacterial populations, shedding light onto the fundamental mechanisms driving adaptation.

Probably the most well-known microbial evolution experiment is the long-term evolution experiment (LTEE) [46]. The LTEE has been tracking the evolution of 12 replicate populations of *E. coli* since 1987, and has provided invaluable insights into the dynamics of adaptation by natural selection [45]. The LTEE has shown that bacterial populations can continue to adapt and gain fitness in the same environment even after >60,000 generations, contrary to earlier assumptions that fitness plateaus after just a few thousand generations. [45]. Another key finding from this experiment has been the evolution of the ability to utilize citrate as a carbon source in *E. coli*, an organism that was known to be unable to utilize citrate in the presence of oxygen [45,46].

The LTEE experiment utilizes *batch culturing*, where a bacterial population is grown in a fixed volume of nutrient medium until resources are depleted or at a fixed time point, after which the experiment is restarted with a fresh batch of medium and a subset of the evolved population (the transfer population) [47]. As bacteria grow in the medium, mutants with alleles that are better adapted to growth and survival may arise. If an allele confers a significant selective advantage, they can "sweep" and replace the existing allele in the population to get "fixed" before the next transfer. If not, the transfer of the bacterial population imposes a selection bottleneck, the size of which is determined by the size (volume) of the transfer. This bottleneck introduces genetic drift,

where random alleles are selected to start the next batch of culture and the process of selection restarts [46,47].

Batch culturing has been adapted to rapid serial transfer-based methods of ALE, where two-fold antibiotic dilution gradients in growth medium are set up to study the evolution of antibiotic resistance. Bacteria are transferred after they reach a fixed population size (often measured as OD₆₀₀ of the growth medium) or at a fixed time point into increasingly higher concentrations of antibiotics [48]. Robotics have allowed automation of at least parts of serial transfer-based ALEs, increasing throughput and minimizing user intervention [49]. This method has also been adapted to solid media based methods, where bacteria are streaked on a petri dish and allowed to grow overnight, after which a single randomly selected colony is restreaked onto another dish containing a higher concentration of an antibiotic [45]. A variation of this method, the gradient plating-based method, involves streaking bacterial populations onto agar plates that contain a gradient of antibiotic concentration ranging from low to high from one end of the plate to another. Bacteria are streaked or spread throughout entire plates, and the bacteria growing closest to the side of the plate with the highest concentration of the antibiotic is restreaked over the same plate [50,51]. This method circumvents the need to perform different dilutions of antibiotics in agar since a single dilution can be used to prepare all the gradient plates. Many studies have used these platforms to probe bacterial evolution against different stressors, including antibiotics, because of their simplicity and low cost [52–56].

Another ALE platform, called the morbidostat, uses *continuous culturing* instead of batch culturing and enables real-time monitoring of microbial adaptation to antibiotics [57]. Unlike

tracks microbial growth rates and dynamically modulates drug levels to maintain a steady inhibition assessed via optical density measurements. The platform is fully automated and can be controlled using computer programs with minimal user intervention, and hence may be ideal for long-term evolution studies [57]. However, continuous culture methods are more complex and costly to set up and maintain than batch cultures, and they carry a higher risk of contamination [58–60]. Additionally, the number of replicate evolution experiments that can be carried out in morbidostats is limited, reducing throughput [45,57].

Microfluidic devices have now been designed to study bacterial evolution. These devices provide precise control over the supply of media and supplements to cell cultures, and are useful to study evolution at the single-cell level [61]. Since cells can attach to surfaces with some population turnover, microfluidic platforms are an excellent choice for studying biofilms [62]. However, they have limitations in terms of throughput and scalability, and the setup and operation can be technically complex [63].

In 2016, the *microbial evolution and growth arena* (MEGA) plate [64] gained widespread media attention for its striking demonstration of real-time bacterial evolution and the development of antibiotic resistance [65–68]. MEGA plates are rectangular plates layered with agar containing a gradient of antibiotic concentrations, overlaid by soft agar to permit bacterial movement. Bacteria introduced at one end migrate outward, with only resistant mutants able to colonize areas with higher drug levels. Bacteria can be harvested from the end of the plates to collect resistant mutants for analysis, or from different areas of the plate to reconstruct the mutational paths adopted by the

bacteria to evolve resistance [64]. The MEGA plate captures a key aspect of bacterial evolution in nature and clinical settings: the ability of bacteria to migrate between areas with different selective pressures. When selection is spatially structured, evolutionary dynamics change such that a successful mutant simply needs to be the first to reach and persist in a new, unoccupied area instead of outcompeting neighboring cells for resources, accelerating resistance evolution [64]. MEGA also requires minimal user involvement after setup and inoculation [64], but the large size (~50 x 20 inches) of the plates makes handling and scale up impractical.

The ALE platform used in all evolution experiments described in this thesis is the *soft agar* gradient evolution (SAGE) platform [69]. SAGE operates on the same foundational principles as the MEGA plate but utilizes standard rectangular lab dishes (Figure 1.1), preserving the key advantages of MEGA while massively enhancing scalability and ease of use [69]. Its capacity to generate resistance to all major classes of antibiotics against Gram-negative bacteria has been previously reported [69]. The smooth, continuous antibiotic gradient in SAGE instead of the two-fold increments of the serial transfer based methods popularly used [70,71] allows sequential acquisition of small-effect mutations towards high-level resistance, a phenomenon commonly seen in clinical settings [72,73]. In chapters three and four, I detail my contributions on optimizing the SAGE platform further and provide experimental and clinical evidence supporting its use for antibiotic resistance evolution studies.

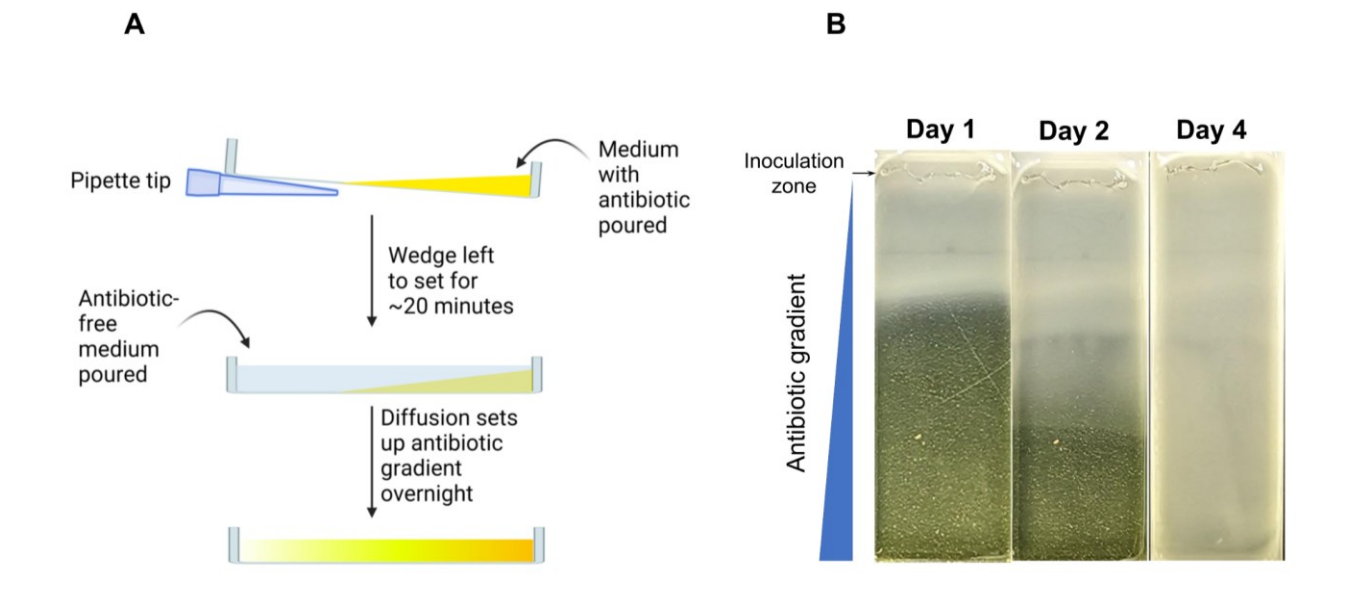


Figure 1.1 The SAGE platform.

(A) To prepare SAGE plates, soft-agar is poured into 4-well plates raised on one side using P1000 pipette tips. After gelling, the supports are removed and a second agar layer is poured to an even depth. Plates are rested at room temperature overnight to allow diffusion between the two layers. Detailed methodology on preparing a SAGE plate can be found in chapter 3. (B) Evolution of antibiotic resistance in SAGE wells. As bacteria grow and deplete resources around their inoculation zone, they move down the plate to access nutrients and space. But as they move down, they face an increasing antibiotic challenge, and resistant mutants are selected for. As mutants arise, they leave their sensitive counterparts behind to move towards the end of the plate.

1.2. Leveraging fitness penalties of resistance to combat resistance evolution

The evolution of antibiotic resistance in bacteria often carries a biological cost. [74–76]. This cost can come in different forms, including slower growth rates, reduced motility, and increased sensitivity to stressors [75,77–79]. For example, when exposed to a class of antibiotics called aminoglycosides, bacteria frequently acquire mutations in key components of the electron transport chain, leading to reduced cellular respiration. Since aminoglycoside uptake across the inner membrane depends on a threshold membrane potential generated by the electron transport

chain [80], lowering this activity can make cells resistant to aminoglycosides [81]. However, this adaptation imposes a significant trade-off, as diminished respiration compromises bacterial growth rates [82].

Multiple studies have now shown that fitness costs imposed on resistant mutants can allow their wild type counterparts to outcompete and replace them when the antibiotic pressure is removed, *resensitizing* the population to the initial antibiotic applied (Figure 1.2) [83–85]. This, in theory, can allow an antibiotic to be reused during therapy. However, during therapy ceasing antibiotic application is not practical, necessitating a switch to a different antibiotic. Switching antibiotics can sometimes still give the wild type bacteria enough time to expand and replace the resistant population before antibiotic concentrations hit inhibitory levels in the target site [86]. Application of one antibiotic after another, often called a *sequential antibiotic therapy*, has been proposed to limit resistance evolution and resensitize bacteria to antibiotics [52,87]. Sequential therapies may be crucial for long-term antibiotic treatments [88–91] where the chances of resistance evolution are high [92,93].

Sequential therapy is less explored than other modalities like combination therapy, where more than one antibiotic is applied at a time (the standard of care for diseases like tuberculosis) [94]. Although combination therapy has been suggested to counteract resistance [95], it has been repeatedly shown to accelerate resistance evolution [87,96–98]. A few clinical studies have shown sequential therapy to be comparable or superior over combination therapy against *H. pylori* infections [99–102]. However, sequential therapy still remains underutilized [94], partly because it is not well understood and is thus unpredictable. For instance, we do not fully understand what

happens to the population that is resistant to the previous antibiotic (pink bacteria in Figure 1.2) when a new antibiotic is applied. While one study proposed a possible dynamic for antibiotic resensitization in a mixed experimental population (Figure 1.2) [52], we do not know what happens if an antibiotic therapy completely eradicates the susceptible population and leaves behind only the resistant subpopulation. Prolonged antibiotic therapies during the treatment of cystic fibrosis, chronic liver disease and respiratory infections, and recurring urinary tract infections can clear wild type or low-level resistant populations completely, eliminating competition for resistant cells [103–106]. Can sequential therapy still be useful in mitigating resistance in these conditions?

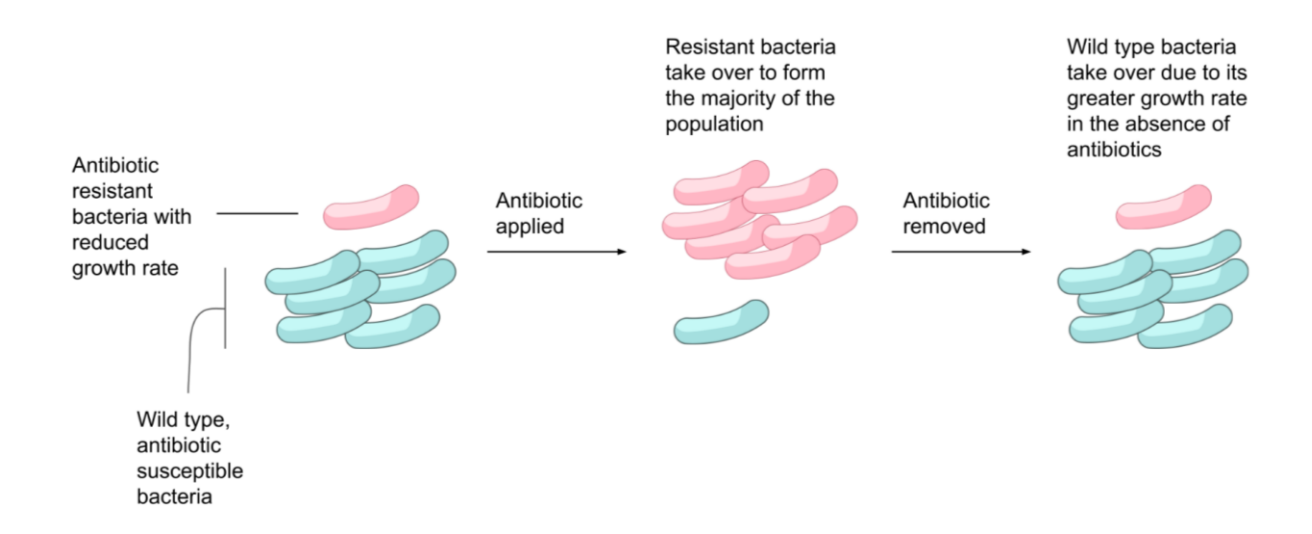


Figure 1.2 Fitness costs can be leveraged to restore antibiotic susceptibility in a population.

When bacteria are exposed to an antibiotic, rare mutants that can resist the antibiotic expand to form the majority of the population despite their reduced growth rates, since the wild type bacteria are killed by the antibiotic. But if the antibiotic pressure is removed, any remaining wild type bacteria can outcompete the resistant mutants due to their improved ability to grow, consume nutrients and occupy space.

The usefulness of sequential therapy to counter resistance evolution hinges on the presence of fitness costs of resistance. These costs frequently appear in laboratory evolution experiments [83–85,107], but apparent 'cost-free' mutants commonly appear in the clinic [108–111]. The presence of these cost-free mutations can be explained almost entirely by compensatory evolution, which occurs when the fitness costs carried by resistance mutations are mitigated or compensated for by other mutations occurring elsewhere in the genome [110–113]. For example, bacteria lose or reduce the number of outer membrane porins to become resistant to a number of drugs, concurrently limiting their ability to take in nutrients. The resulting impairment in growth can be rapidly compensated for through mutations that upregulate phosphate acquisition—an essential process for growth and survival [114]. To date, studies that explored sequential evolution could not fully account for compensatory evolution [52,83,115–117]. Given the tremendous potential of compensatory evolution to shape the fitness landscape of resistance evolution, attempts should be made to directly account for it during evolution studies to avoid inflating the benefits of sequential therapies.

In chapter 2, I set out to tackle these problems by investigating the effects of antibiotic resistance in clonal populations of *Escherichia coli* (*E. coli*) on fitness and evolution. In this thesis, a bacterial strain is defined as resistant to an antibiotic when the minimum inhibitory concentration (MIC) of an antibiotic, the concentration required to inhibit bacterial growth completely, is above the clinical resistance breakpoint for that antibiotic set by the European Committee on Antimicrobial Susceptibility Testing (EUCAST) [63] or by the Clinical & Laboratory Standards Institute (CLSI) [64] when EUCAST breakpoints are unavailable. Unlike arbitrary resistance cut-offs, clinical

breakpoints take into account achievable tissue concentrations when a patient or animal is given a standard antibiotic dose [118].

First, I describe a novel parameter, the rate of movement of bacterial fronts in SAGE plates [43] as an easily trackable measure of the rate of resistance evolution. Using this, I show that resistance to chloramphenicol, a protein synthesis inhibitor antibiotic, imposes severe fitness costs in the form of reduced growth and motility, and impairs their ability to further evolve resistance to secondary antibiotics like streptomycin, an aminoglycoside, and nitrofurantoin, a nitrofuran. I find that this impairment is not dependent on the identity of the antibiotic evolved to or the evolving bacterial strain, but on the presence of a fitness cost of resistance. In line with this, I show that low-cost resistant mutants are not impaired in their evolution rates. This suggests that sequential application of carefully chosen antibiotics can slow down subsequent resistance evolution.

Next, I incorporate experimental compensatory evolution to test the stability of these impairments. Compensatory evolution experiments are often tedious to perform, requiring month-long serial passages [112,113,119]. Leveraging the limited intermixing of populations in soft agar, I develop a soft agar-based platform called "flat plates" which allowed compensatory evolution within a week. Using these plates, I show that chloramphenicol-resistant mutants can rapidly improve their fitness, jumping back to levels comparable to wild type bacteria. Mitigation of fitness costs leads to restoration of wildtype-level adaptation rates against nitrofurantoin, but interestingly, fails to improve adaptation rates against streptomycin, suggesting that this impairment is difficult to overcome. Together, this study provides a framework for the identification of antibiotics whose

resistance mechanisms impose impairments stable against compensatory evolution to design sequential antibiotic therapies that are less prone to resistance.

1.3. Sequential antibiotic therapies and collateral sensitivity

The fitness costs of resistance may slow down the evolution of resistance in sequential therapies, but they don't stop multidrug resistance from emerging. In fact, in chapter 2, I report several fitness-impaired, chloramphenicol-resistant *E. coli* that go on to evolve multidrug resistance. This may not be surprising since, given enough time, bacteria can probably overcome most antibacterial challenges [120]. This implies that in a long enough antibiotic therapy, the component drugs of a sequential regimen may all fail due to resistance evolution [121]. In the next phase of research I determined if antibiotic resensitization could be reliably achieved in clonal bacterial populations during sequential therapy, forestalling or preventing the evolution of multidrug resistance.

This work was driven by prior research on collateral sensitivity (CS) a form of evolutionary tradeoff where evolution of resistance to one antibiotic comes at the cost of increased sensitivity (sometimes termed as hypersensitivity, and this term will be used interchangeably with CS in this thesis) to another antibiotic [122]. CS can occur via a number of different mechanisms: certain mutations evolved to resist one antibiotic can improve the net uptake of another, increase the chemical activation of a prodrug, change the cellular functions and regulatory pathways to increase toxicity, or modify the target structure to improve binding of another antibiotic [123].

1.3.1. Mechanisms of collateral sensitivity

Before the proposed benefits of CS in sequential therapy are discussed, a brief understanding of the mechanisms of CS described so far may be helpful. Experimental data on CS mechanisms are still rare [123]. The most well-known example of CS is perhaps the increased net uptake of β -lactams in aminoglycoside resistant bacteria. *E. coli* reduce their electron transport chain activity and the proton motive force (PMF) it generates to become resistant to aminoglycosides [124], but this reduction also weakens efflux pumps like AcrAB-TolC, which are driven by the energy of the PMF [124]. Since bacteria rely on these proteins to pump out β -lactams and other antibiotics, decreasing efflux increases their sensitivity to these antibiotics [124].

Nitrofurantoin CS in mecillinam-resistant bacteria provides an example of CS due to increased chemical activation. *E. coli* exposed to the β-lactam mecillinam can gather mutations in the stringent response regulator *spoT*, which in turn can increase expression of the nitroreductase enzyme NfsB [125]. NfsB is one of the two enzymes responsible for converting the prodrug, nitrofurantoin, into its active antibacterial form, and increased abundance of NfsB increases nitrofurantoin sensitivity [125].

Some resistance mechanisms can increase the toxicity of antibiotics. The absence of the Lon protease in tigecycline resistant bacteria can spare efflux regular proteins from degradation, increasing expression of genes that mediate resistance like *acrAB* [126]. However, deactivation of Lon has widespread effects, one of which is the failure to degrade other toxic proteins. Nitrofurantoin exposure causes DNA damage which induces the production of the cell replication regulator SulA [125]. SulA stops growth to allow DNA repair, and needs to be degraded by the

Lon protease to allow growth to resume [125]. SulA accumulation halts cell division, contributing to increased nitrofurantoin toxicity [125].

Enzymes like β -lactamases can adapt to improve binding of a β -lactam at the cost of another. The β -lactamase CTX-M-15 can evolve to better resist mecillinam but can lose effectiveness against other β -lactams like cefotaxime due to altered antibiotic binding [127].

1.3.2. Collateral sensitivity and cyclic antibiotic therapies

The idea of sequential antibiotic therapies that leverage CS was first introduced in 2013 by Imamovic *et al* [52]. In this study, the authors first identified a number of *pairwise reciprocal* CS interactions. The reciprocity of CS is an important idea in this field of research. Suppose that evolution of resistance to antibiotic A in bacteria renders cells hypersensitive to B (

Figure 1.3, left panel), and evolution of resistance to antibiotic B also induces CS to A (

Figure 1.3, right panel). The drug pair A-B would then be said to exhibit reciprocal CS. It may be intuitive to assume that the changes in resistance levels occur in the same bacterial population, i.e., it might appear that resistance to antibiotic A in a bacterial population X makes it hypersensitive to B, and subsequent evolution of resistance to B in the same population renders it sensitive to A. This is sequential evolution of resistance in a bacterial population, and is not how reciprocal CS is defined. A drug pair A-B is considered to exhibit reciprocal CS if a bacterial population X resistant to A exhibits CS to B, and another bacterial population Y (isogenic to X) exhibits hypersensitivity to antibiotic A as resistance to antibiotic B evolves.

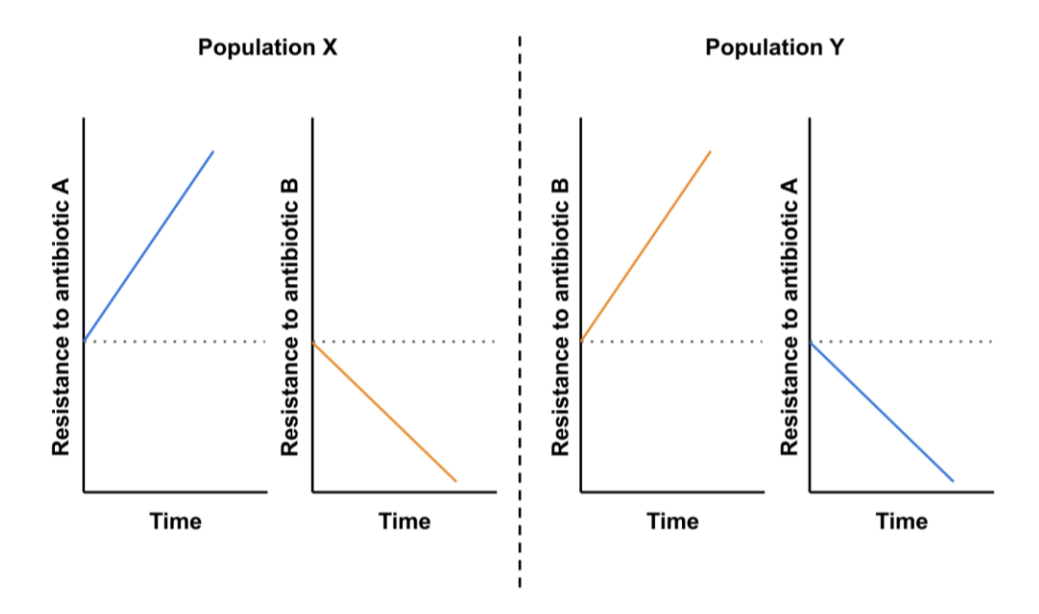


Figure 1.3 Reciprocal CS.

As resistance to antibiotic A increases in population X, cells become more sensitive to antibiotic B at the same time. Resistance to B in another isogenic population Y induces collateral sensitivity to A, making A-B a reciprocal drug pair. The horizontal dotted lines in the graphs represent wild type resistance levels.

Imamovic *et al* [52] identified a number of reciprocal CS interactions. From there, they focused on the pair gentamicin and cefuroxime for their experimental evolution experiments. First, they raised gentamicin resistant *E. coli* via experimental evolution. Then they created an experimental bacterial population composed of 1:1 gentamicin resistant:wild type cells and exposed this population to cefuroxime. Since the gentamicin resistant cells were hypersensitive to cefuroxime, these cells were preferentially killed over the wild type, resensitizing the population to gentamicin. The remaining WT cells were then exposed to cefuroxime. Once these cells evolved resistance to cefuroxime, they were mixed 1:1 with naive WT cells and exposed to gentamicin. Since the cefuroxime resistant cells were hypersensitive to gentamicin, this time they were preferentially killed over the naive cells, resensitizing the population to cefuroxime. Essentially, due to CS, the

antibiotic-resistant populations died out, i.e., went extinct before the wild type, susceptible cells and treatment could be limited to a pairwise, A-B *cycle* in an experimental setting. An A-B pairwise cyclic therapy is, in principle, a type of sequential antibiotic therapy where drugs A and B are cycled one after the other. In this thesis, the term 'loop' is used multiple times interchangeably with 'cycle' to refer to drug sequences where resensitization to an antibiotic in a sequence is targeted or achieved.

This design solves an important problem with 'conventional' sequential therapy, where fitness cost-free resistance can jeopardize the success of sequential therapy due to the ability of resistant populations to compete in growth with the susceptible population. CS, in theory, adds another axis that can be used to select against resistant bacteria, independent of growth rates. Suppose in Figure 1.2, the pink population evolved growth rates comparable to that of the WT and the antibiotic pressure is removed. While the susceptible, wildtype population cannot outcompete the resistant one, if an antibiotic is applied to which the pink population is hypersensitive, the number of pink bacteria will now drop faster than the wildtype, allowing the teal bacteria to take over and reach the same end point in Figure 1.2.

But what happens if the susceptible population is completely eradicated? The CS based cyclic approach still depends on the ability of a susceptible population to clear out the resistant one. A study from Barbosa *et al* [128] examined the effects of CS in drug cycling within clonal populations of *Pseudomonas aeruginosa* (*P. aeruginosa*). They started experiments with eight gentamicin resistant clonal populations that all exhibited CS towards carbenicillin. Then, they exposed them to carbenicillin and found that the majority of populations showed reduced

gentamicin resistance (i.e. they were resensitized to gentamicin) as carbenicillin resistance evolved. The gentamicin resistance was partially conferred by mutations in the sensor histidine kinase PmrB, which modifies the bacterial membrane to reduce its interaction with cationic antibiotics like gentamicin. Carbenicillin-resistant cells gathered mutations in an efflux regulator gene *nalC*, which is known to increase gentamicin susceptibility via unclear mechanisms [129]. They concluded that the effects of the *nalC* mutations counteracted that of *pmrB* to increase gentamicin susceptibility in the carbenicillin resistant cells. But how did CS help achieve this?

The authors suggested that when treatment was switched from gentamicin to carbenicillin, the gentamicin resistant cells found themselves against an antibiotic to which they were hypersensitive. To allow evolution of resistance to carbenicillin, these cells may have reversed their hypersensitivity to carbenicillin, and since the hypersensitivity to carbenicillin is genetically tied to gentamicin resistance (by definition of CS), reversing this hypersensitivity also reversed gentamicin resistance (Figure 1.4).

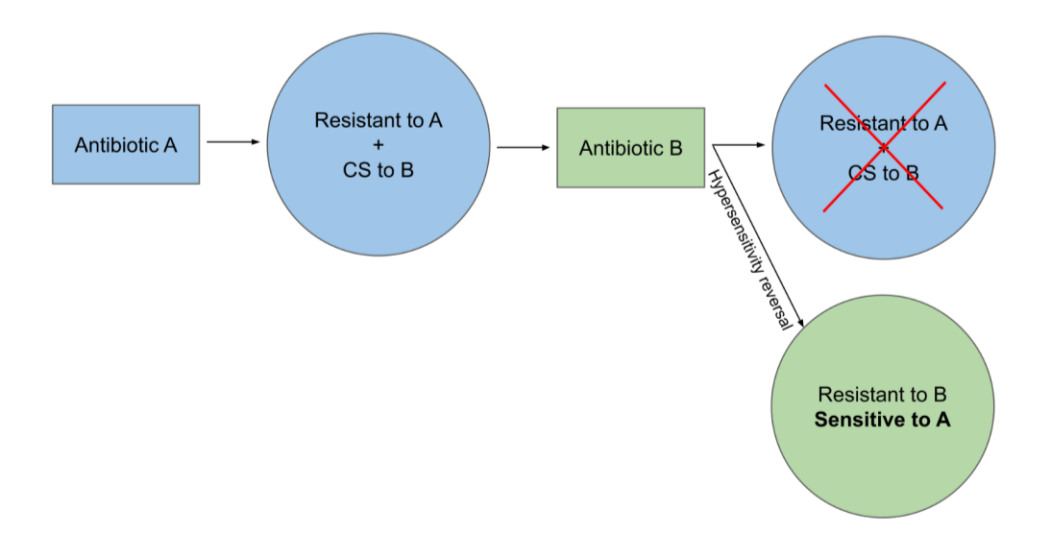


Figure 1.4 Antibiotic resensitization in clonal bacterial populations.

As treatment is switched from antibiotic A to antibiotic B of an A-B reciprocal pair, bacterial populations are inclined to reverse hypersensitivity to B and their associated resistance to A to allow evolution of resistance to B.

1.3.3. The pitfalls of collateral sensitivity

The combined results from the two studies discussed above sparked interest in CS and reciprocal CS relationships, leading to the publication of a large number of studies on novel CS interactions in different bacterial species [129–136]. However, studies that replicate or advance the idea of CS in antibiotic resensitization in cyclic therapies are missing, and some studies have shown that the evolution of CS may not be repeatable since it is contingent on evolution itself being repeatable [54,133,137]. After all, multiple evolutionary pathways to resistance are available to bacteria, many of which may not confer CS [138]. But CS, as with any other evolutionary trade-off, must be evolutionarily repeatable to be useful in combating resistance [139]. Most studies that discovered CS relationships did not investigate the repeatability (sometimes termed *robustness* or *stability*) of the interactions. The frequency of CS evolution cannot be reliably inferred from

existing studies either because evolutionary replicate numbers ranging from one to eight used in most of these studies are insufficient to capture the stochasticity of evolution [54].

The study that proposed the benefits of CS in resensitizing clonal bacterial populations to antibiotics [128] did not repeat their resensitization experiments with 'neutral' clones. They showed that eight replicate populations resistant to drug A and hypersensitive to drug B can be resensitized to A when resistance to B evolves. But we do not know if resensitization would occur if those eight populations did not start with hypersensitivity to B. In fact, reports have now shown that antibiotic switching can affect resistance evolution independently of CS [107,140,141]. Overall, it remains unclear if and to what degree CS disrupts evolution and promotes antibiotic resensitization during antibiotic cycling.

In this thesis, two questions will be addressed: i) how repeatable are reported CS interactions, and ii) how important is CS for antibiotic resensitization in clonal bacterial populations? To pursue answers to these questions, I would require large evolutionary replicate numbers to capture repeatable CS evolution, and to do that, I would need a laboratory evolution platform that could rapidly generate large numbers of resistant mutants. SAGE has already been proven to be fast and high throughput [69]. However, during testing, I found that SAGE struggled with some antibiotics like the β-lactam piperacillin and especially the antimicrobial peptide polymyxin B, which is known to be difficult to evolve resistance against in the laboratory [69,121,142]. Not willing to run into evolution platform-related bottlenecks, I first embarked on a project to improve the SAGE platform.

1.3.4. An improved SAGE leads to the elucidation of the mechanism of resistance against the "evolution proof" antibiotic octyl-TriA₁

In chapter 3, I describe my work on improving SAGE, building a laboratory evolution platform that goes on to become crucial for my research. SAGE evolutions depend on the ability of bacteria to migrate through antibiotic gradients established in soft agar (0.25% agar) [69]. However, synaeresis, the tendency of agar hydrogels to spontaneously shrink over time via continuous expulsion of solvent [143], increases the effective agar concentration and restricts bacterial motility [144]. First, I showed that synaeresis hindered the evolution of resistance to antibiotics like polymyxin B in this platform [145]. To improve the water-retention capacity of the SAGE medium, I screened a number of water-binding polysaccharide additives, finding that the addition of xanthan gum markedly reduces synaeresis in agar. This reduction in synaeresis allowed SAGE gels to retain enough water to support bacteria motility over month-long incubations at 37 °C. Additionally, incorporation of xanthan gum lowered the requirement of agar for gelling of the media. Since the rate of bacterial motility is a function of agar strength [144], and the rate of resistance evolution in SAGE is a function of bacterial motility [145], xanthan gum addition significantly sped up SAGE evolutions. With this modification, I showed that polymyxin B is now an easily evolvable target in SAGE.

To stress test this media, I challenged it with an "evolution proof" antibiotic—octyl-tridecaptin A₁ (Oct-TriA₁)—a compound previously shown to resist the development of bacterial resistance over a 30-day evolution experiment [146]. "Evolution-proof" antibiotics have attracted a lot of attention recently since developing antibiotics immune to resistance evolution could be groundbreaking in the fight against AMR [147]. Using the improved SAGE platform, I demonstrated that resistance

to Oct-TriA₁ can, in fact, emerge within just nine days, overturning previous assumptions about its evolutionary resilience. In collaboration with Laura Domínguez Mercado, a PhD candidate, and Katya Kharitonov, an NSERC USRA intern in the Findlay lab at the time of this work, we described for the first time the mechanism underlying the *de novo* evolution of resistance to this compound. Identifying resistance mechanisms prior to clinical deployment is essential to inform surveillance strategies and extend drug lifespan [148]. As history has repeatedly shown, evolution finds ways to bypass antimicrobial action and the true challenge lies in whether we can predict the routes it may take. Our approach can help uncover these adaptive paths, even for antibiotics previously considered impervious to resistance.

1.3.5. Large scale laboratory evolutions predicts clinical outcomes and leads to the discovery of a novel mechanism of collateral sensitivity

There are a number of different platforms that are available to perform laboratory evolutions like the serial transfer based methods, gradient plating based methods, microfluidic chips, and SAGE [55]. A laboratory is generally free to choose any one platform for their investigations. Unlike many quantitative tools, however, experimental evolution platforms have not been standardized [149,150]. Readings from a mercury-based body temperature thermometer should be the same as that from an IR thermometer, within margins of error. Do all experimental evolution platforms also produce comparable outcomes, or does the choice of the platform affect experimental results? Additionally, how clinically relevant are the predictions made from laboratory evolutions? To improve the generalisability and clinical relevance of my research, I wanted these questions answered before investigating the effects of CS in sequential regimens.

In chapter 4, I describe my work in comparing evolution of antibiotic resistance and its collateral effects via common evolution platforms [151], done in collaboration with Veronica Banari, a Mitacs Globalink Research Intern from FAU Erlangen-Nürnberg in Germany, and Vlada Lesnic, a CHEM 450 research student from Concordia. We generated over 130 resistant mutants and made 540 resistance and CS measurements to show that serial transfer and gradient plating-based platforms agree well on the frequencies of CS, cross-resistance (CR) and resistance levels. However, SAGE produced substantially lower frequencies of CS and higher incidence of CR when compared to the other two platforms. To test the relevance of these CS/CR predictions from the different ALE platforms, we analyzed antimicrobial susceptibility data from over 750 clinical uropathogenic multidrug resistant (MDR) E. coli strains. We found that CS is almost entirely absent, but neutrality or CR is prevalent in clinical data. However, we observed a significant association between increasing omadacycline (a third generation tetracycline) resistance and reduced colistin (polymyxin E) resistance. Interestingly, out of the four drug pairs screened, SAGE showed significant CS in only one of them: a tigecycline (a third generation tetracycline) and polymyxin B pair. Using genomics and phenotypic analysis, we described a novel CS mechanism by showing that cells resistant to tigecycline deactivate the Lon protease and overproduce negatively charged exopolysaccharides, which in turn attracts the polycationic polymyxin B and renders cells hypersensitive to the drug. Together, this work provides important insights into the evolution of collateral phenotypes from different laboratory evolution platforms, and a framework for identifying robust CS with clinical implications.

1.3.6. The role of collateral sensitivity in antibiotic resensitization

With the suitability of the SAGE medium for studying evolution and its collateral effects established, I began probing the role of CS in sequential antibiotic therapies and antibiotic resensitization. In chapter 5, I describe results from over 450 evolution experiments, testing the resilience of four proposed CS-based drug pairs of potential use in sequential therapy. I found that the repeatability of previously reported pairwise CS interactions can vary widely, ranging from a 100% to ~6% chance of evolving CS (from 16 independent evolutionary replicates). Ciprofloxacin and gentamicin were previously reported to have CS interactions [152], but exhibit only a ~6% chance of evolving CS in my experiments. This shows that large scale evolution experiments are required to capture repeatable CS interactions. Next, I investigate pairwise interactions with prevalent CS to investigate the role of CS in antibiotic resensitization during sequential therapy. I find that even drug pairs with ubiquitous CS fail to significantly reduce resistance or promote bacterial extinction, at least when CS is looked at in the way it has been so far.

When we discussed reciprocal CS interactions in section 1.3.2, I explained that a CS interaction in an A-B sequential therapy is reciprocal when resistance to A leads to CS to B, and resistance to B leads to CS to A (Figure 2). Hence, a reciprocal interaction is composed of CS in two *directions* [136], but the two interactions have not been separately described. In this chapter, I introduce two new terms, *forward* CS and *backward* CS (

Figure 1.5) to describe these interactions. To date, only forward CS has been proposed in sequential therapy. When I probed drug pairs that produced significant resensitizations in my dataset, I found instead that backward CS is strongly associated with reductions in resistance. For example, a gentamicin - piperacillin sequence showed strong forward CS interactions, but sequential

evolution against gentamicin - piperacillin showed no significant resensitizations to gentamicin. A piperacillin - gentamicin sequence showed prevalent backward CS, and sequential evolution against the two drugs produced significant reduction in resistance towards piperacillin. I elucidated the mechanism of action of backward CS in this pair, showing that it perturbs the electron transport chain to inhibit aminoglycoside entry and consequently impair β -lactam efflux, resulting in increased β -lactam susceptibility.

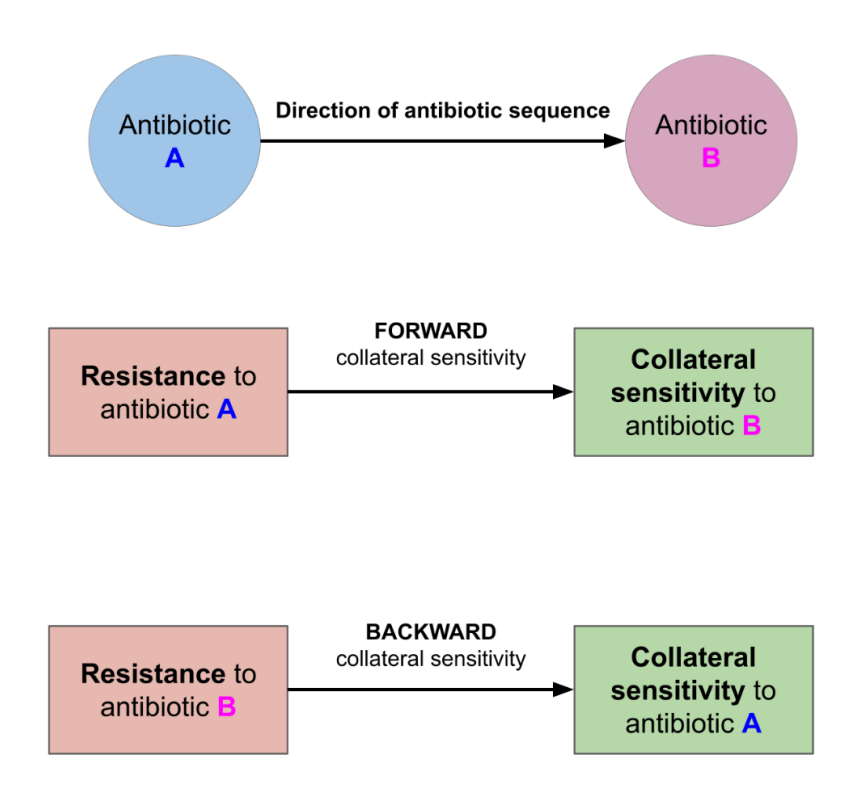


Figure 1.5 Forward and Backward collateral sensitivity.

In an A-B drug pair, where the sequence of antibiotic application is A to B, CS to B upon resistance to A is forward CS, while CS to A upon resistance to B is backward CS. The direction of CS is relative to the direction of the antibiotic sequence.

During my screen, I also discovered a drug pair composed of polymyxin B and tigecycline, where resistance to tigecycline reduces polymyxin B by 64-folds. This is in stark contrast to the two to

four-fold hypersensitivity commonly seen in experimental evolution [123,153]. I show that this level of resensitization occurs via a combination of backward CS and compensatory evolution. Overall, in this chapter, I provide answers to the two questions I began with: the repeatability of CS interactions can vary widely and must be determined via large scale evolutions, and CS may help achieve antibiotic resensitizations only when applied in the right direction. These findings will be important for designing treatment regimens that are less likely to lead to resistance evolution.

1.4. Collateral sensitivity-independent sequential regimens that produce large and repeatable resensitizations

In chapter 5, I showed that forward CS fails to reverse resistance or reduce adaptation rates during sequential regimens, and backward CS may be more useful in antibiotic resensitization. However, backward CS and the associated reduction in resistance was limited to two-folds on average, which may not be sufficient to reduce resistance below clinical breakpoints. Outside the remarkable resensitization magnitudes of the polymyxin B - tigecycline antibiotic pair, there was a lack of complete antibiotic resensitization in the tested drug pairs.

To develop sequential antibiotic regimens that could reliably resensitize bacteria to antibiotics below clinical breakpoints I began with a simple hypothesis: evolving resistance to multiple drugs in a sequence can incur 'stacking' fitness costs in bacteria, and at one point, they would have little left to give. If faced by a new antibiotic challenge, they would then be left with a choice: reverse resistance to a drug and win back the fitness costs paid for that resistance to face this new challenge, or die (

Figure 1.6). In chapter 5, where I tested drug sequences composed of two drugs, fitness costs may not have been large enough for bacteria to trade for resistance. To test this, in chapter 6, I investigate extended sequential regimens composed of three drugs, which I call 'tripartite' sequences.

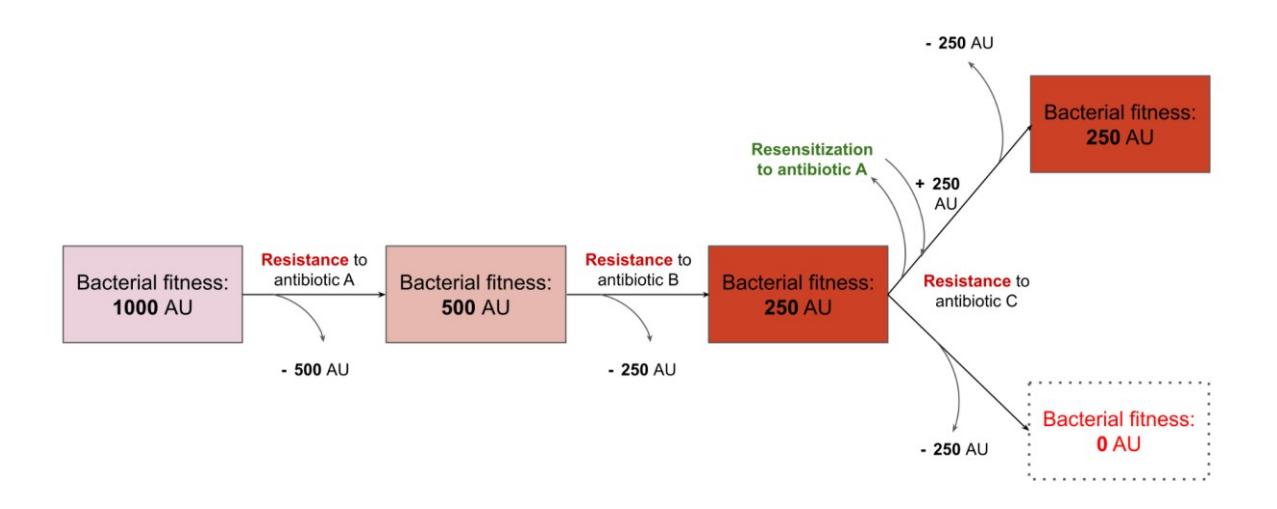


Figure 1.6 Trading resistance for fitness.

After resistance evolves to antibiotics A and B, resistance to C might require a fitness penalty the bacteria may not be able to pay. This can either lead to their death when challenged with C, or resensitization to antibiotic A (or B) to regain fitness to pay for the new challenge, C. AU = arbitrary units. 0 AU represents death/extinction.

First, I extend the gentamicin - piperacillin pair into a tripartite sequence composed of gentamicin - piperacillin - nitrofurantoin. Through 424 discrete adaptive laboratory evolution experiments I find that as bacteria sequentially evolve resistance to the drugs in this tripartite sequence, they reliably trade their past resistance for fitness gains, reverting back to sensitivity to gentamicin. I show that this loop is invertible, with a nitrofurantoin - piperacillin - gentamicin sequence reliably restoring sensitivity to nitrofurantoin. By tracking fitness and genomic changes from each step of evolution, I find that loops guide bacterial strains toward evolutionary paths that mitigate fitness

costs and reverse resistance to component drugs, driving levels of resensitization not achievable through pairwise regimens. I then show that this strategy is robust and not limited to laboratory strains by reproducibly resensitizing or eradicating four multidrug-resistant clinical bacterial isolates using an identical approach. Resensitizations occur even when evolution was complicated via plasmid-bound mutations over chromosomal changes, suggesting that tripartite regimens can be a potent new approach to counter antibiotic resistance.

Collectively, my research offers new insights into laboratory evolution and its clinical relevance, and the role of evolutionary trade-offs in slowing down evolution and resensitizing bacteria to antibiotics. Large-scale laboratory evolutions can be a powerful strategy to discover robust evolutionary trade-offs, and sequential regimens of the right order and length can improve the clinical longevity of antibiotics.

Chapter 2. Fitness costs of antibiotic resistance impede the evolution of

resistance to other antibiotics

Published record: Chowdhury FR and Findlay BL; ACS Infectious Diseases 2023, 9, 10, 1834–

1845.

Available at: doi.org/10.1021/acsinfecdis.3c00156

2.1. Introduction

The rapid rise of antibiotic resistance severely burdens healthcare systems worldwide, increasing

hospital stays and causing increased mortality. A recent study has estimated that infections caused

by antibiotic-resistant pathogens directly led to 1.2 million premature deaths in 2019 alone[11]. If

the current increase in the incidence of these infections continues, the WHO estimates that resistant

pathogens could kill 10 million people and cause more than \$1 trillion in losses annually by the

year 2050[154,155].

The current antibiotic resistance crisis is driven by a combination of the incredible speed at which

bacteria can evolve resistance and a myriad of other factors related to antibiotic stewardship,

including inadequate drug regulations and the widespread use of antibiotics in livestock[10,156].

Critically, the development of new antibiotics has not kept pace with the spread of resistance

mechanisms: only eight new antibiotics have been approved since 2017, most of which are

derivatives of existing antibiotics[42]. To maintain the effectiveness of our current therapies we

urgently need to develop new strategies to combat antibiotic resistant pathogens, and the evolution

of resistance itself.

Evolutionary strategies to combat resistance evolution have gained attention in recent years[116].

The evolution of resistance often incurs a fitness cost to the bacteria, from increased sensitivity to

abiotic stressors, to reduced growth rates and motility [157–159]. Reduced growth and movement

32

rates impede the ability of bacterial populations to acquire nutrients and move away from toxic compounds[157], while reduced fitness can hinder individual mutants' ability to compete with fitter cells that exhibit lower resistance levels[158,159]. However, prolonged antibiotic therapies during the treatment of cystic fibrosis, chronic liver disease, and respiratory infections, and recurring urinary tract infections can clear wildtype or low-level resistant populations completely, eliminating competition for resistant cells[103–106]. This necessitates switching therapy to a different antibiotic to continue effective treatment. Recent studies have highlighted strategies to optimize the design of sequential antibiotic therapy for improved infection clearance and limited resistance evolution[52,84,160]. Most of these studies leverage collateral sensitivity, a phenomenon where resistance to one drug induces hypersensitivity to another, to guide optimal antibiotic switches. However, collateral sensitivity is rare, and its application is limited by contradictory results on evolutionary repeatability and its generalisability across different genetic backgrounds[84,161,162].

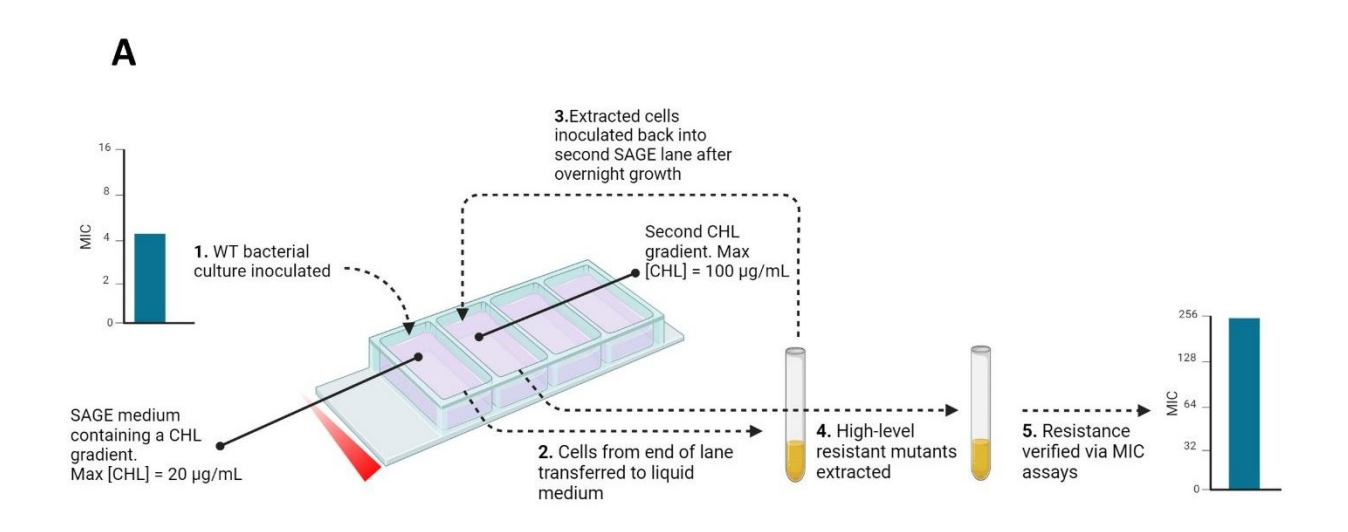
Hypersensitive bacterial populations are often growth-impaired, and Brepoels et al. recently showed that resistance evolution is impaired in hypersensitive bacterial populations independently of collateral sensitivity in certain drug sequences[140,163]. Here we show that evolution of resistance to chloramphenicol (CHL) in *Escherichia coli* K-12 substrain MG1655 cripples its growth rate and movement through soft agar, which impedes its ability to evolve resistance to secondary antibiotics in antibiotic gradients independently of collateral sensitivity. We leveraged the high-throughput mutant generation capacity of the Soft Agar Gradient Evolution (SAGE) system to evolve 16 independent isogenic populations (referred to here as replicates) of wildtype (WT) and CHL-resistant *E. coli* (OM) separately to two different antibiotics, nitrofurantoin (NIT) and streptomycin (STR) in parallel[69]. By tracking distance moved in SAGE plates and observing

growth patterns, we found that resistance was delayed by a day in the majority of OM replicates. We then verified the role of fitness in the adaptation slowdown by evolving CHL-resistant mutants with improved growth and swim rates. These fitter mutants could restore WT-like adaptation rates to nitrofurantoin, but the slowdown in STR-adaptation persisted. Genome sequencing revealed divergent evolutionary trajectories across the differing genetic backgrounds, with fitness costs constraining the available paths to resistance. We suggest that these results are not tied to the primary antibiotic or the genetic background, but to the fitness costs of resistance to the primary antibiotic. Consistent with this view, resistance is also impaired in a cefazolin-resistant mutant of *Escherichia coli* BW25113. Our findings show that resistance mechanisms that incur heavy fitness penalties can serve as an indicator of subsequent evolution impairments which can shape primary antibiotic choices, and the SAGE system can be used to track *in vitro* evolutionary kinetics at high-throughput.

2.2. Results

2.2.1. Evolution of high-level resistance to chloramphenicol via SAGE

We reported the evolution of resistance in *E. coli* MG1655 to a number of antibiotics representing different classes, including chloramphenicol, via the SAGE system before[69]. WT cells were passed through a SAGE plate containing a maximum [CHL] = $20 \mu g/mL$ (WT MIC: $4 \mu g/mL$) (Figure 2.1A). Cells extracted from the end of the plate were grown overnight and inoculated in a second SAGE plate containing a maximum [CHL] = $100 \mu g/mL$. Cells evolved from these plates exhibited CHL MIC of $256 \mu g/mL$.



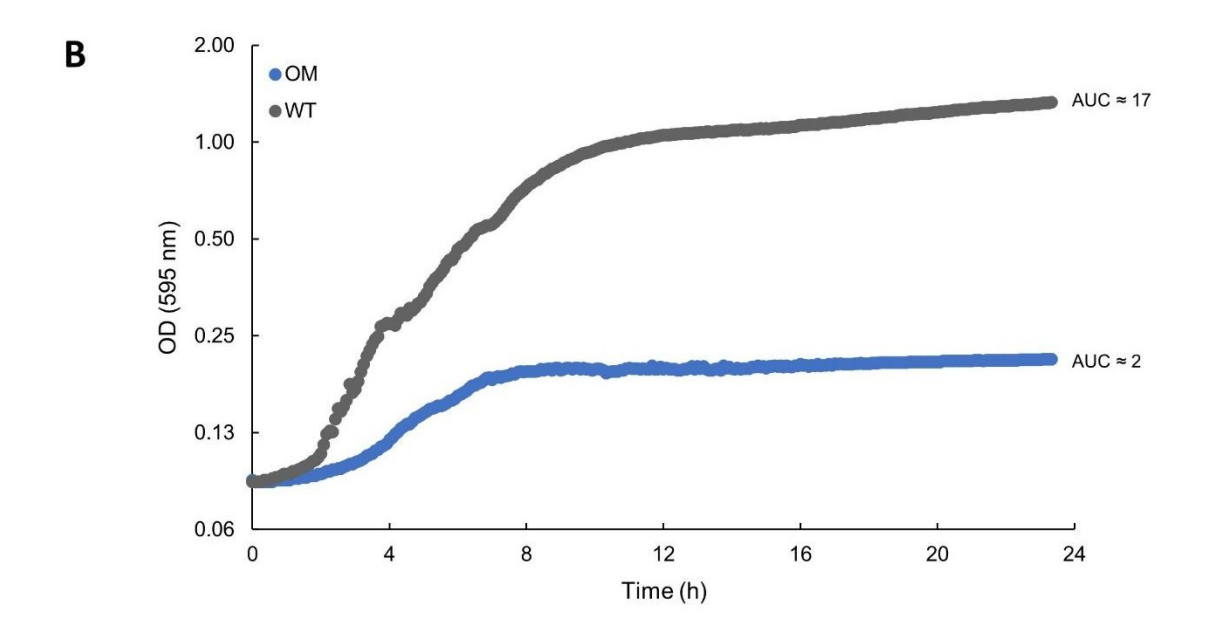


Figure 2.1 Evolution of chloramphenicol resistance incurs fitness costs.

(A) Evolution of chloramphenicol resistance via the SAGE system. WT bacterial culture is inoculated in a CHL gradient (maximum $[CHL] = 20 \mu g/mL$) set up in soft-agar medium. Bacteria moving down a lane to access nutrients and space generate mutants that are able to resist the increasing concentrations of the antibiotic. When cells reach the

end of a lane, they are extracted and cultured overnight and used to inoculate a new CHL gradient (maximum [CHL] = $100 \,\mu\text{g/mL}$). Cells from the end of this secondary lane are extracted and their resistance levels determined. Although depicted in the same plate, a new plate is used for each SAGE evolution cycle. (B) Growth curves of the WT and OM. Area under the curves (AUCs) show the OM to be heavily fitness impaired.

The WT *E. coli* MG1655 used in this study had 75 previously-reported nonsynonymous mutations (Supplementary data) possibly acquired during the 'speed-selection' process, which involves selecting for cells that move the quickest through SAGE medium[69]. The original chloramphenicol-resistant mutant (OM) acquired 54 nonsynonymous mutations distinct from the speed-selected *E. coli* MG1655 progenitor (Supplementary data), including mutations in multiple efflux related genes like *acrB* (a component of the AcrAB-TolC efflux pump), *acrR* (the repressor of *acrAB*), *marR* (the multiple antibiotic resistance repressor, truncated in OM), *mprA/emrA* (repressor of the *marRAB operon*) and *rob* (transcriptional regulator of the *marA/soxS/rob* regulon involved in antibiotic resistance). All of these have been previously implicated in chloramphenicol resistance[164–167]. Upregulation of efflux systems is a common response to antibiotic stress in Gram-negative bacteria[168,169], and efflux pumps are known to confer resistance to a wide range antibiotics classes[170]. As expected, we found the OM to be resistant to many first-line agents susceptible to efflux (Table 2.1).

Table 2.1 The OM exhibited a multidrug resistant phenotype.

Antibiotic	Class	MIC of WT	MIC of OM
		(μg/mL)	(μg/mL)
Amoxicillin	β-lactam	4	16
Ceftazidime	Cephalosporin	≤0.5	4

Cefazolin	Cephalosporin	1	16
Chloramphenicol	Phenicol	16	256
Ciprofloxacin	Fluoroquinolone	0.0156	4
Tetracycline	Tetracycline	1	64
Tigecycline	Tetracycline	≤0.25	2
Trimethoprim	Folic acid synthesis inhibitor	1	16

2.2.2. Chloramphenicol resistant cells are fitness impaired

We observed a slowdown in the movement of OM populations through antibiotic-free soft agar when compared to WT. While WT populations were able to traverse half the plate (40mm) in ~6 h, OM populations required ~24 h to move the same distance (Movie S1). Movement through soft agar is dependent on bacterial growth: the faster cells grow, the quicker they populate and deplete resources from their surroundings, prompting movement to gain access to new space and nutrients via chemotaxis. While the WT quickly formed a high-density band of cells at the leading edge of growth, we observed a significant delay in the formation of this band by the OM (Movie S1). Comparing the speed of these bands showed the OM to be ~2 times slower than the WT.

To link this reduction in movement through soft agar to fitness, we used the area under the curve (AUC) measurements to quantify bacterial growth[140,141]. AUC incorporates three fitness parameters: the lag phase duration, the exponential growth rate, and the yield (maximum cell density). The AUC of the WT population was ~8 times higher than that of the OM, showing large growth deficits (Figure 2.1B).

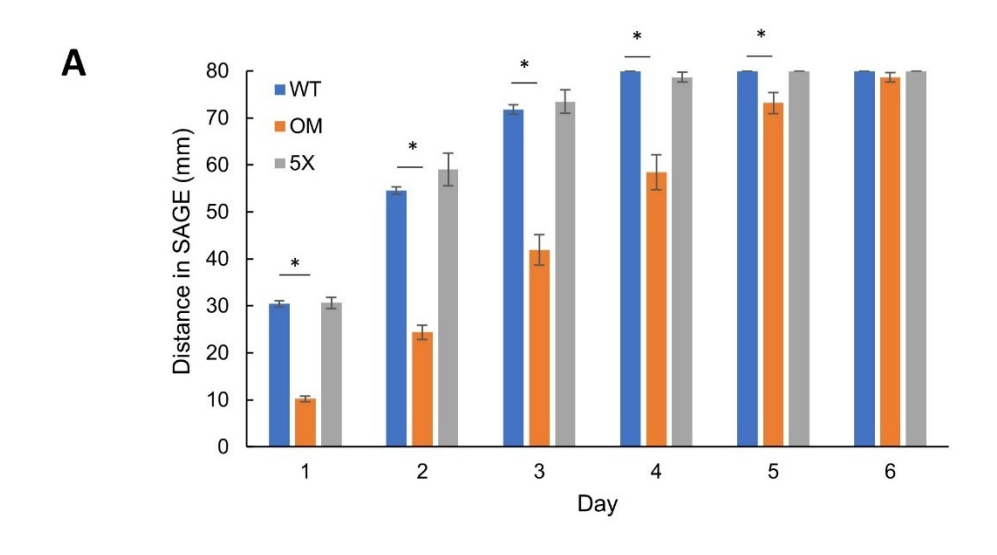
To confirm that accumulation of growth deficits is not a general outcome of SAGE experiments, we also analyzed growth curves for a NIT and a STR-resistant *E. coli* evolved in SAGE. AUCs of both mutants were similar to that of the WT (Figure S2.1). Correspondingly, resistance to STR did not significantly impede growth or movement in SAGE (Movie S1).

Efflux pumps are powered directly by the proton motive force, and are energetically costly[171,172]. In addition to changes in efflux pumps, sequencing of the OM also revealed a truncation in the flagellar basal-body rod protein FlgG, which is essential for cell motility[173]. Cutting down on energetically expensive motility mechanisms may have allowed the mutant to direct more resources towards efflux and growth. A number of other mutations in genes related to metabolism, biosynthesis, the electron transport chain, and membrane transport were also identified in the OM, including a synonymous mutation in the chemotaxis protein CheW (Supplementary data). Together, these data suggest a basis for the fitness and motility defects of the OM.

2.2.3. Fitness costs delay the evolution of resistance and alter evolutionary trajectories

WT populations in NIT SAGE plates (maximum [NIT] = $80 \,\mu\text{g/mL}$; WT MIC: $8 \,\mu\text{g/mL}$) evolved resistance to NIT in a predictable pattern (Figure S2.2A). All 16 replicates evolved in parallel stopped at ~30 mm after 24 h, suggesting that the concentration of antibiotic was growth inhibiting at this point (Figure 2.2A, B). By day 2, all replicates broke through this and a subsequent barrier, fanning out in cones. By the end of day 4, all replicates reached the end of their lanes. Cells extracted from this point had an MIC against NIT of 64 $\mu\text{g/mL}$ (quantified from a randomly selected replicate, R3). Genome sequencing suggests that resistance to NIT evolved via mutations in the nitroreductase genes nfsA and nfsB, and mprA, repressor of the marRAB operon

(Supplementary data). These genes have been commonly associated with nitrofurantoin resistance[125,174]. The purpose of the 29 other mutations in this strain is unclear. Many are involved in metabolism, and may help compensate for the fitness cost of the resistance-conferring mutations. They may also be due to genetic drift, as a number of them were in intergenic regions.



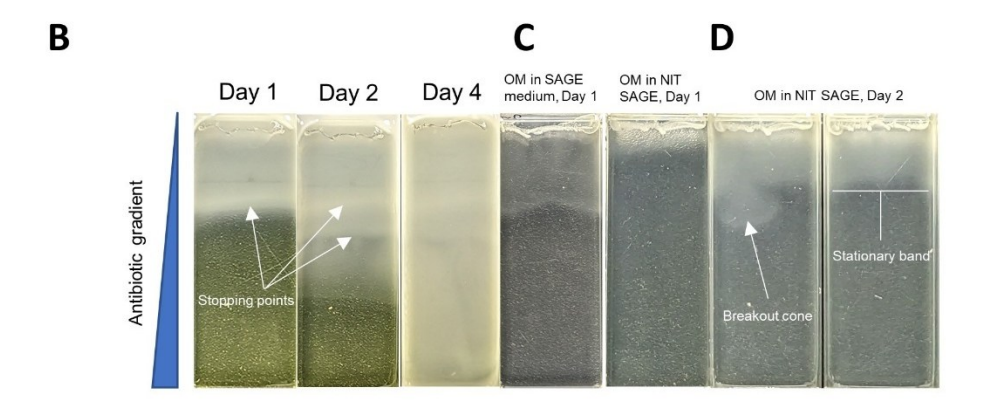


Figure 2.2 Tracking movement of bacterial populations in SAGE revealed resistance evolution impairments. (A) WT populations in NIT SAGE plates (maximum [NIT] = $80 \mu g/mL$ for the WT, $10 \mu g/mL$ for OM and 5X to accommodate hypersensitivity) evolve resistance faster than the OM. Alleviation of fitness deficits in the 5X population allows restoration of WT-like SAGE kinetics. (B) Stopping points of bacterial fronts indicate inhibitory

antibiotic concentrations along the NIT gradient. Cells breaking free from these points indicate emergence of resistance mutation(s) that allow movement into higher antibiotic concentrations. All WT replicates reached the end of their lanes by the end of day 4. (C) Reduced growth and motility of the OM slows their movement speeds in SAGE, but cannot explain the initial delay in distance moved in NIT SAGE plates. Left panel shows a representative lane where the OM moved ~30 mm down a SAGE lane containing no antibiotic after 24 h. The right panel shows the OM confined to ~10 mm after 24 h in a NIT SAGE lane (maximum [NIT] = $10 \mu g/mL$). (D) Observing growth patterns in SAGE allows prediction of resistance emergence. On day 2 in NIT SAGE plates, only 5/16 replicates broke out from the initial stationary bands (left panel), indicating resistance emergence. The rest of the replicates remained as stationary bands (right panel), suggesting delayed resistance evolution. MIC measurements of cells from a breakout cone and stationary band confirmed these predictions (see text). **p<0.01, ****p<0.0001, two-sample t-test assuming unequal variances. Error bars represent the SEM. N = 16 for all SAGE evolutions.

After a pilot run of OM in NIT SAGE (n=4) showed that the bacteria remained confined to within 10 mm of the inoculation site after 24 h (data not shown), we tested for collateral sensitivity of the OM towards NIT. We found the MIC of NIT against OM to be 8-fold lower (1 μg/mL) compared to WT. To our knowledge, collateral sensitivity to nitrofurantoin in chloramphenicol resistant cells has not been reported before. We then repeated evolutions with the OM (n=16), adjusting the NIT gradient to accommodate this increased sensitivity (maximum [NIT] = 10 μg/mL), as has been previously done to eliminate effects of collateral sensitivity on resistance evolution[140]. In contrast to the WT, movement of OM replicates through NIT SAGE plates showed large variation (Figure S2.2B). Cells were again confined to within ~10 mm of the inoculation site after 24 h (figure 2.2A, C), suggesting that the increased sensitivity to NIT was not the cause behind this impaired movement. The stationary phase cell density of the OM was ~5-fold lower than the WT (Figure 2.1B). Since population size can affect evolution by altering mutation supply rates[175], we also inoculated NIT SAGE plates separately with a 5-fold concentrated inoculum of the OM (n = 4). We observed no significant difference in distance moved, except on day 3, where the mean

distance moved by the unstandardized OM (overnight culture) was higher than by the standardized inoculum (p = 0.047) (Table S2.1). Hence, we decided to conduct subsequent experiments with overnight cultures. We also noticed that although fitness deficits in OM impeded the strain's ability to move through soft agar, the movement in NIT SAGE plates at 24 h was $\sim \frac{1}{3}$ the growth in antibiotic-free soft agar. This is significantly slower than expected from changes in movement speed alone (Figure 2.2C).

The increased susceptibility of the OM populations may instead be due to their reduced growth rates. A recent study described how fast-growing cells avoid the intracellular accumulation of antibiotics like macrolides[176]. Although growth rates have not been directly linked to NIT susceptibility before, it has been shown that cells that stay locked in a non-dividing state in *lon* mutants resistant to tetracyclines are known to exhibit increased sensitivity towards nitrofurantoin[123]. By counting the number of OM replicates that showed visible growth beyond the first stopping point (Figure 2.2D), we found that resistance emerged in only 5/16 replicates by the end of day 2. The link between position in the SAGE plate and resistance levels was verified by probing cells drawn from a randomly selected replicate from each position. The MIC of cells (R16) from stationary bands with no signs of 'breakouts' was 1 μg/mL, significantly less than that of cells extracted from breakout cones (R14, 8 μg/mL). By the end of day 6, all replicates generated mutants resistant to nitrofurantoin (MIC (R14): 8 μg/mL), with cells spreading throughout the lanes (Figure 2.2A). Of note, the MIC increase, although 8-folds higher than the base MIC of the OM (from 1 μg/mL to 8 μg/mL), was equal to the base MIC of the WT.

Sequencing of the NIT-evolved OM (R14) did not reveal mutations in any of the genes commonly associated with NIT resistance (*nfsA*, *nfsB*, *ribE*, *oqxA*, *oqxB*, *mprA*, *oxyR*, *marA*, *rob*, *soxS*, *sdsN137*)[125,174] (Supplementary data). It showed 9 non-synonymous mutations compared to

the OM, most of which were in genes related to metabolism. Interestingly, it also contained a second mutation in lolA. The OM strain natively harbored a mutation in the periplasmic chaperone protein LolA, which is essential for lipoprotein trafficking through the periplasm to the outer membrane and membrane integrity[177]. The outer membrane presents a barrier to a number of antibiotics including nitrofurantoin[177,178], and it is hence possible that the mutation in LolA increases cellular access to nitrofurantoin, producing the observed collateral sensitivity. LolA mutants are also known to be severely growth-challenged [179]. The second mutation in the NITevolved OM could then compensate for the increased membrane permeability and growth defect, alleviating the collateral sensitivity towards NIT and allowing these mutants to traverse the SAGE plates without acquiring NIT-resistance mutations. This trajectory has the dual advantage of improving fitness and bypassing collateral sensitivity towards the antibiotic they were put up against. A similar phenomenon was observed in a previous study[163], where during a treatment switch from gentamicin to carbenicillin, a drug-pair that shows reciprocal collateral sensitivity, resensitization to gentamicin may have been favored over multidrug resistance due to trajectories that mitigate both fitness costs and collateral sensitivity. Although we cannot discount the possibility of downregulation of the classical genes involved in NIT-resistance, no mutations were found in any known transcriptional regulators.

2.2.4. Evolution against streptomycin

To test if the delay in resistance evolution is limited to nitrofurantoin, we compared resistance evolution to an unrelated antibiotic, the aminoglycoside streptomycin (STR). In WT populations subjected to STR SAGE (maximum [STR] = $160 \,\mu\text{g/mL}$; WT MIC: $16 \,\mu\text{g/mL}$) resistance evolved via a clear, repeatable trajectory wherein cells stopped at ~40 mm (Figure 2.3A, Figure S2.2C) after 24 h, with mutants breaking free from this stopping point within 48 h. The STR MIC of cells

at the first stopping point showed a 2-fold increase (MICs (R14, R15): 32 μ g/mL) while by the end of day 2, MICs rose to >1024 μ g/mL, indicating the emergence of ribosomal mutations (MICs from R9 - R16)[180]. The 2-fold increase in STR resistance that appeared on day 1 reverted to WT levels after cells were subcultured in antibiotic free medium. This may either indicate selection for a heteroresistant population or the emergence of unstable resistance mutations upon which ribosomal mutations arise[181,182].

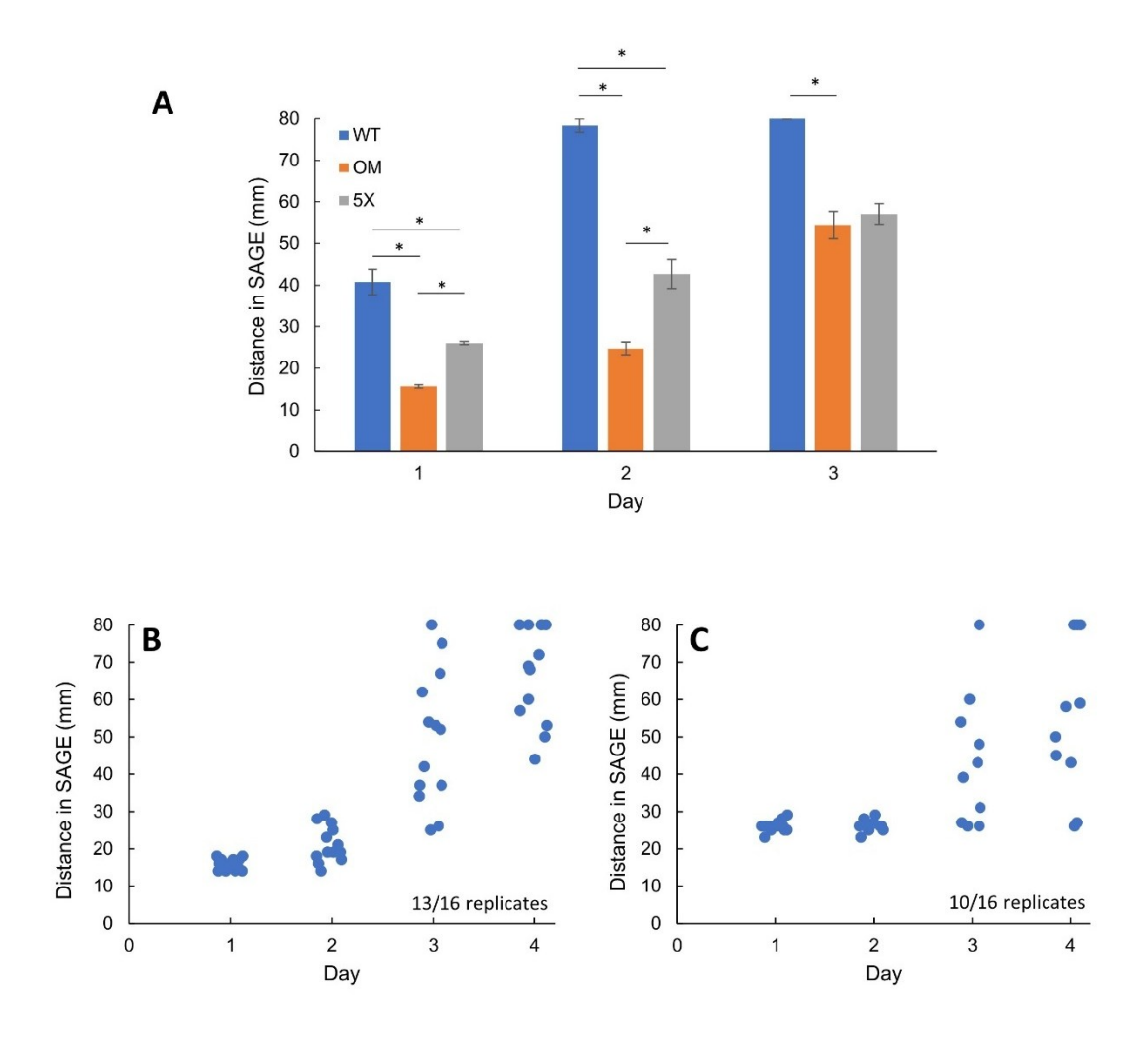


Figure 2.3 STR resistance is delayed in the fitness-impaired OM background.

(A) WT replicates reached the end of STR SAGE plates (max $[STR] = 160 \mu g/mL$) by the end of day 2, whereas significant delays were observed for both the OM and the 5X populations. (B) 13/16 of the OM replicates remained at \leq 29 mm in STR SAGE lanes at the end of day 2, indicating delayed resistance evolution. (C) The delay in STR resistance could not be alleviated via fitness improvements, as 10/16 replicates remained completely stationary at the end of day 2 after hitting their inhibitory concentration step on day 1. Resistance level predictions were confirmed by MIC measurements from cells sampled from random replicates (see text). **p<0.01, ***p<0.001, ****p<0.0001, two-sample t-test assuming unequal variances. Error bars represent the SEM. N = 16 for all SAGE evolutions.

We evolved the OM in SAGE plates using the same parameters used for the WT, since the MIC of STR against both the OM and WT populations were equal. The OM again travelled ~half the distance covered by the WT in 24 h in STR SAGE plates (Figure 2.3A).

Increased susceptibility to antibiotics that bind irreversibly to ribosomes like STR in growth-impaired bacterial populations has been reported before[183]. This repeated slow movement in antibiotic gradients may also indicate the importance of bacterial fitness in their intrinsic ability to resist antibiotics. The majority of the replicates (13/16) stopped at \leq 29 mm after 48 h (Figure 2.3B). Out of the two replicates sampled to quantify STR MIC against cells from this point (R3, R8), R8 showed an MIC of 128 µg/mL (with R3 an MIC of 32 µg/mL). This suggested that resistance to STR in the OM populations may evolve via alternate trajectories, and encouraged us to expand the sample size. Since we did not sample more than two replicates from day 2, and attempting to extract mutants that arose on day 2 at a later time point could include higher-order mutants that could compromise the MIC results, we instead extracted end-point mutants from a total of eight replicates (R1, R5, R7, R8, R9, R12, R13, R16) and compared them with the 8 WT end-point mutants. While all WT mutants showed an MIC \geq 1024 µg/mL, 2 out of the 8 OM replicates (R9, R12) showed an MIC of 512 µg/mL, further suggesting the adoption of alternate

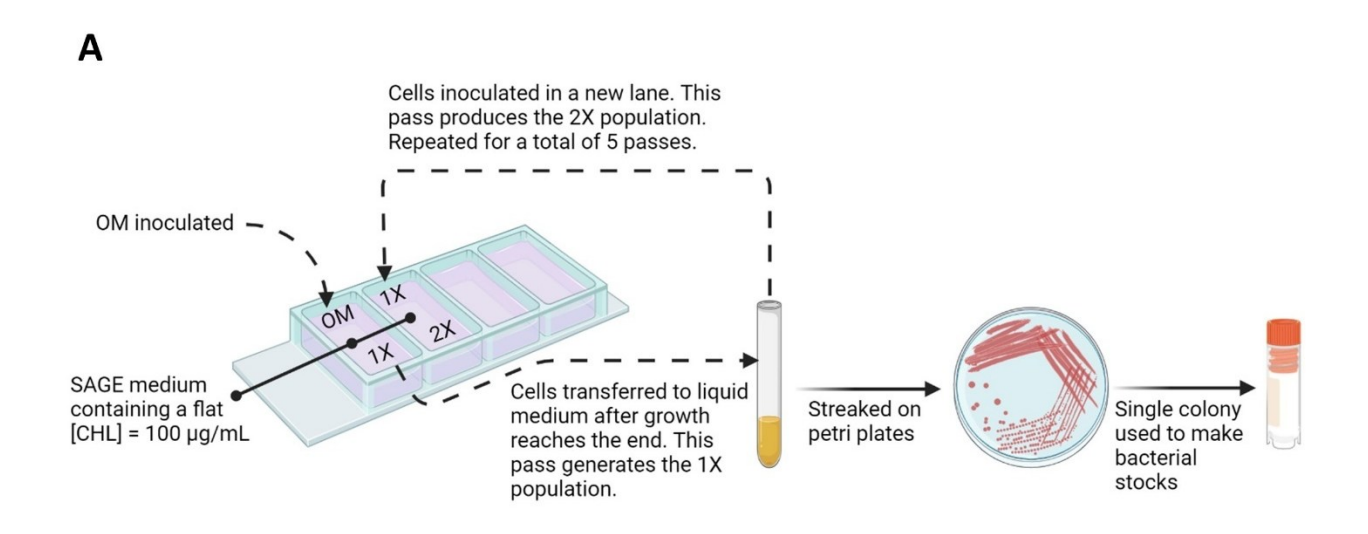
evolutionary paths to resistance by the OM. Sequencing an STR-evolved WT replicate (R5) showed an expected K43R mutation in rpsL, the gene that codes for the S12 protein of the 30S subunit of the ribosome, the target for streptomycin[184]. The replicate also evolved 15 additional mutations on genes broadly involved in metabolism, membrane transport, and integrity (Supplementary data). Mutations in letB (D40G) and rutG (synonymous, A46A), which are involved in membrane integrity, may also contribute to mild STR resistance since membrane stability and voltage dysregulation are implicated in the bactericidal effects of STR[178,185,186]. Although synonymous (A48A), mutations in the outer membrane lipoprotein YaiW have been associated with mild STR resistance before by reducing membrane permeability[187]. We also sequenced 3 replicates of the STR-evolved OM (R7, MIC: >1024 µg/mL; R9, R12, MIC: 512 µg/mL) to identify possible differences in their genome that could explain the differences in MIC. All the 3 STR-evolved OM replicates contained an rpsL mutation (K88R, K88R, and K43R respectively), along with mutations in yafA, bcsB, and pflD in the same position in all 3 replicates (I127V, A390A, P658S respectively). Mutations in these 3 genes were not found in the WT, or in any other strain sequenced in this study. YqfA is involved in the maintenance of optimal membrane energetics and may hence play a role in STR resistance[185]. BcsB, part of the operon bcsQ, codes for a protein with a predicted function in cellulose biosynthesis, but E. coli MG1655 contains a stop codon after the first 5 amino acids of the operon [188,189]. Its repeated appearance in all 3 replicates of the STR-adapted OM may indicate an involvement in either STR resistance or in the mitigation of fitness costs, but literature contains no evidence of these. PflD is a putative pyruvate formate-lyase, and may be an easily accessible compensatory mutation to mitigate fitness deficits via enhancing anaerobic sugar metabolism[190,191]. All 3 replicates also contained a mutation in tRNA-gln (identical C→T mutation in glnX in R7 and R12, and a C→T mutation in glnV in R9)

which has been reported in STR resistant *E. coli* before, and may confer a fitness benefit[187]. Additionally, R9 harbored another ribosomal mutation in the 30S ribosomal subunit protein S7 encoded by *rpsG*. S7 is a translational repressor regulating the synthesis of other gene products including S12 (*rpsL*), and has not been directly linked to STR resistance in *E. coli*. Multiple mutational screens of *rpsG* in other species like *M. smegmatis* and *B. burgdorferi* found no evidence of involvement in STR resistance[192,193]. The rest of the non-overlapping mutations among these 3 replicates and the STR-evolved WT are mostly in genes involved in metabolism. Taken together, these results suggest that mutational paths to resistance to streptomycin in fitness-impaired *E. coli* diverges from that taken by WT, and although all the OM-replicates evolved an *rpsL* mutation, MIC measurements suggest that interactions between the non-overlapping mutations may be reducing the resistance level below what is expected of *rpsL* mutants[194].

2.2.5. Improving fitness of chloramphenicol-resistant cells restores resistance potential to nitrofurantoin but not streptomycin

To test if alleviating the fitness deficits of the resistant cells improves NIT resistance evolution during SAGE, we serially passaged the OM a total of 5 times through "flat" SAGE medium containing a constant 100 μg/mL (MIC: 256 μg/mL) of chloramphenicol (Figure 2.4A). Cells that reached the end of the lanes were extracted after each pass (denoted 1X - 5X). Growing in a constant, permissible concentration of antibiotic, nutrient scarcity and overcrowding becomes the primary driver of evolution, driving selection for fitter cells that can quickly move out to access nutrients and reach the end of the lanes first[115]. *In vitro*, this increase in fitness generally arises from compensatory mutations that mitigate fitness costs[141]. Growth curves of 1X - 5X showed significant improvements in fitness with AUCs ~5-times above the OM, but without much difference within the series (Figure 2.4B) (Figure S2.1). The movement speed of 5X through soft

agar was also significantly improved, with the strain requiring only 8 h to traverse half the plate compared to 24 h by the OM (Movie 1). However, 1X - 5X all maintained their CS towards NIT. Genome sequencing of 5X revealed 17 mutations in genes mostly involved in metabolism (Supplementary data). Importantly, it removed the loss-of-function mutation (introduction of a stop codon) in the flagellar protein FlgG that the OM previously acquired (TAG \rightarrow TGG). This strain also harboured an additional mutation in rpoD, which codes for an RNA polymerase sigma factor essential for exponential growth, and may be compensating for an rpoD mutation in the OM. A mutation was also identified in the methyl-accepting chemotaxis protein Tsr. These mutations may help explain the improved fitness of the 5X.



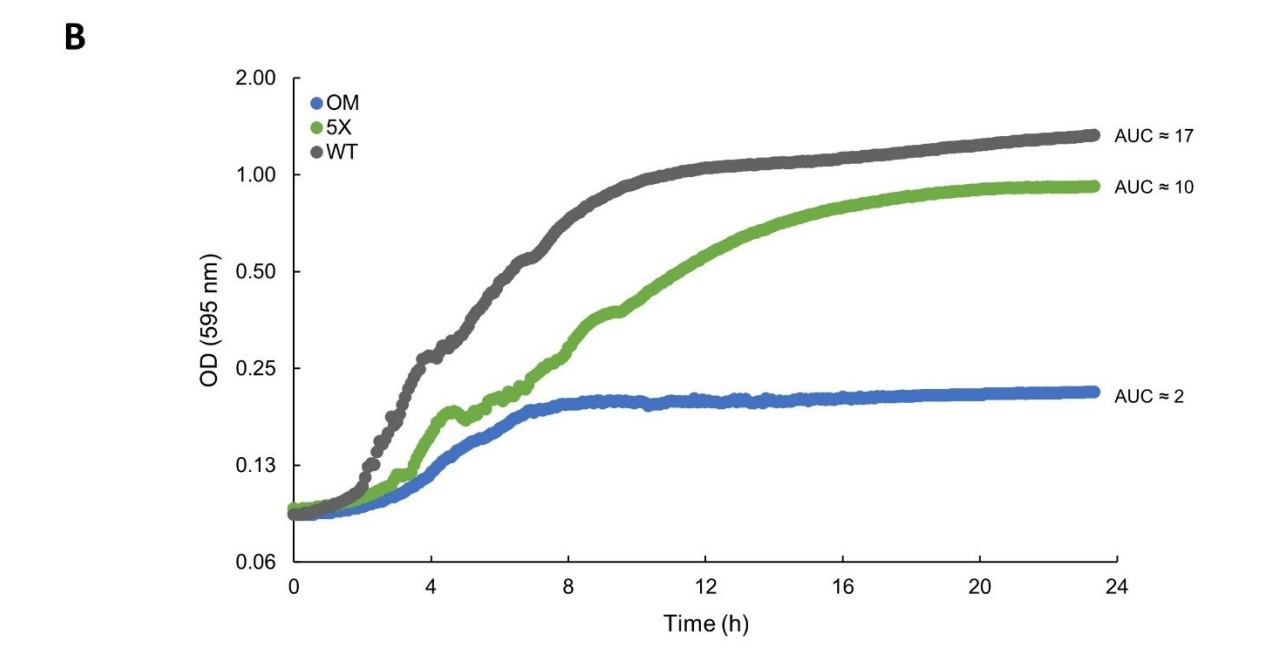


Figure 2.4 Passaging cells through "flat" SAGE lanes improves fitness of the OM.

(A) OM cells are inoculated in SAGE lanes containing a constant [CHL] = $100 \mu g/mL$. Fitter cells move out to the end of the lanes first, which are then extracted and cultured. These cells are denoted 1X. The 1X is inoculated back in a new, identical flat lane to generate 2X. This cycle was repeated until the generation of 5X. Cells were passed on

petri plates and bacterial stocks were prepared after each cycle. (B) The 5X shows significant improvement in fitness as shown by the AUC.

We then repeated the NIT SAGE evolutions with 5X (n = 16). The evolutionary kinetics of the 5Xclosely mirrored that of the WT (Figure 2.2A), implicating the fitness cost of chloramphenicol resistance to be the principal cause behind the slower adaptation to nitrofurantoin. The NIT MIC of cells extracted from one of these plates was 32 µg/mL (R8). Sequencing these cells revealed mutations in *nfsA* and *nfsB*, albeit in positions distinct from that in the WT (Supplementary data). Unexpectedly, the NIT-evolved 5X also showed a large 6279 bp deletion which includes the entire marRAB operon, and the genes encoding YdeA (L-arabinose exporter of the major facilitator superfamily of transporters)[195], MarC (DNA-binding transcriptional dual regulator SoxR)[196], EamA (exporter of metabolites of the cysteine pathway)[197], YdeE (Drug:H+ Antiporter-1 within the major facilitator superfamily of transporters)[198], MgtS (involved in intracellular Mg2+ accumulation)[199], mgtT (involved in intracellular Mg2+ accumulation)[200], MgrR (negative regulator of SoxS)[201], and DgcZ (a diguarylate cyclase that regulates motility and biofilm formation)[202]. Mutations in nitroreductase enzymes have been previously linked to growth defects[203], and it is possible that nitroreductase mutations are incompatible with overexpression of efflux pumps, i.e., the combination may impose debilitating fitness defects. The absence of nitroreductase mutations in the NIT-evolved OM also supports this idea. Removal of the marRAB operon and the other efflux pumps would then allow curbing the energy costs of the efflux systems, allowing access to nitroreductase mutations. To test this hypothesis, we compared the CHL MIC and growth curves of the NIT-evolved OM and 5X. CHL MIC of the NIT-evolved 5X showed a reduction below the OM-level, while the NIT-evolved OM maintained the same resistance level. This reduction in MIC was less than 2-fold, however, as the NIT-evolved 5X exhibited faint

growth in the well containing 128 μ g/mL of CHL, as opposed to saturated growth at the same drug concentration with the NIT-evolved OM. The NIT-evolved 5X also showed a moderate increase in AUC (\approx 12) when compared to the NIT-evolved OM (\approx 9.5) (Figure S2.3). Much like the NIT-evolved WT, the other mutations in the NIT-evolved 5X were mostly in genes involved in metabolism and membrane transport, but in genes distinct from that in the WT. We found no overlapping mutations between the NIT-evolved OM and the NIT-evolved 5X.

In STR SAGE plates, the improved fitness of 5X allowed them to move ~1.5 times the distance moved by the OM in 24 h. However, 10/16 replicates remained completely stationary at this point for an additional 24 h before generating mutants (Figure 2.3C). The STR MIC against cells past this point was >1024 µg/mL (MICs quantified from R2, R3, R9, R13). By day 3, there was no significant difference between the mean distance moved by the OM and 5X (Figure 2.3A). Sequencing of a STR-evolved 5X strain (R3) showed a K88R mutation in rpsL, along with 16 other non-synonymous mutations (Supplementary data). Outside the rpsL mutations, comparing the STR-evolved 5X with the STR-evolved OMs and the STR-evolved WT showed no overlapping mutations except for the ones in genes that code for YfaL (a putative adhesin)[204] and RecD (a exodeoxyribonuclease V subunit)[205], which were shared between 5X R3 and OM R9 (in distinct positions), and in the curcumin reductase CurA between the 5X and the WT (in distinct positions, with the mutation in the WT being synonymous). Overall, while fitness-enhancement improved the movement speeds of bacterial cells in STR gradients, it could not restore WT adaptation rates to STR. Comparison of sequencing data of the STR-evolved WT, OM and 5X end-point mutants revealed mutations in different sets of genes (except for the resistance conferring rpsL mutations), mostly coding for proteins essential in metabolism. Because the 5X still lagged behind the WT in terms of fitness (Figure 2.4B), this could either suggest a certain fitness threshold below which STR resistance is delayed, or that the evolutionary paths to resistance available to a fitnessimpaired background leads to slower adaptation.

2.2.6. Impaired resistance evolution is not linked to chloramphenical resistance

To determine if the reduction in secondary adaptation rates are dependent on the primary antibiotic (ie. chloramphenicol), we generated a cefazolin (CFZ) resistant mutant of *E. coli* K-12 substrain BW25113 (CFZR) (MIC > 512 μ g/mL). This strain exhibited lower fitness compared to the wildtype *E. coli* BW25113 (WTB), though it was not as fitness impaired as OM (Figure S2.4A), able to traverse an entire antibiotic-free plate in 24 h (data not shown). When subject to a NIT challenge (maximum [NIT] = 80 μ g/mL; WTB MIC: 8 μ g/mL; n = 8), CFZR evolved significantly slower than WTB (Figure S2.4B). Similar to the OM in NIT SAGE plates (Figure 2.2D), CFZR did not show signs of breakouts in any replicate lanes on day 2, while all WTB replicates broke free from their first stopping points. This suggests that the reduced rate of adaptation to NIT is independent of the CHL-resistance phenotype and/or the genetic background. This also shows that the magnitude of fitness deficit need not be as great as the difference between the OM and the WT for adaptation to be significantly impaired.

In contrast, a STR-resistant *E. coli* with no detectable fitness deficit (Figure S2.1, Movie S2.1) showed no delay in NIT resistance evolution (data not shown). We routinely recovered NIT-resistant cells from SAGE plates containing max [NIT] of 80 μg/mL by passing them on standard selective agar plates containing 32 μg/mL of NIT (4X MIC). While we were able to recover all replicates of the WTB on selective agar plates, we were only able to obtain 3 out of 8 replicates of the CFZR, suggesting that the majority of the CFZR replicates, despite evolving under the same regime as WTB, developed lower levels of resistance.

2.3. Discussion

Sequential antibiotic therapies that involve changing the antibiotic applied after a duration of treatment have been proposed as a strategy to reduce resistance evolution and improve bacterial clearance [84]. Our study shows that fitness defects due to evolution of resistance to an initial antibiotic can impede the ability of bacteria to adapt to subsequent antibiotics. While growth and fitness measurements can indicate fitness deficits that may lead to reduced adaptation rates, the utility of these effects is contingent on the repeatability of evolution and the frequency with which escape mutants emerge[161]. Large numbers of parallel in vitro evolution experiments are required to account for the stochasticity of evolution. We previously reported the ability of the SAGE system to generate resistance to antibiotics from every major class effective against Gram-negative bacteria [69]. Here, we leverage its ability to run parallel evolutions in the laboratory to show that fitness deficits associated with resistance to CHL repeatedly impedes evolution to secondary antibiotics (Figure 2.2, 2.3). Because the OM showed a multidrug resistance phenotype, possibly due to hyperactive efflux, we investigated adaptation to streptomycin and nitrofurantoin; two drugs that are not efficient efflux targets[170]. Both drugs also exhibit predictable and highly repeatable evolution kinetics in SAGE.

We found that the rate of distance moved by bacteria in SAGE plates is a robust indicator of the adaptation rates to antibiotics since it integrates the rate at which resistance conferring mutations appear with bacterial growth rates and motility. By running 16 replicates in parallel and tracking mutants by their distance moved in SAGE and their growth patterns (Figure 2.2, 2.3), we found that escape mutants that bypassed this delay arose at low frequencies (5/16 for OM evolving to NIT, and 3/16 for OM evolving to STR). MIC values from cells extracted from different positions of SAGE plates aligned well with the expected phenotype.

The delayed adaptation to antibiotics could not be alleviated by equalizing the number of cells added to the SAGE plates (Table S2.1). This may suggest that the increase in mutation supply rate that comes with a larger population[175] may not be enough to compensate for the slow cell turnover rate[206] and the adoption of suboptimal evolutionary trajectories due to epistatic interactions[194] that both reduce antibiotic susceptibility and improve fitness.

Probing cells from different points of growth from SAGE plates can provide insights into evolutionary trajectories. By measuring the MIC of antibiotics against cells from stationary bands collected 24 h into the STR evolution studies, we identified unstable resistant mutants upon which higher-order, stable mutants arose. This is a phenomenon which, to our knowledge, has not been reported for streptomycin before. We also found that 2 out of the 8 STR-evolved OM replicates showed higher susceptibility to STR (MIC: 512 µg/mL) than STR-evolved WT replicates (MIC > 1024 µg/mL for all 8 replicates tested). While the MIC values for these replicates are clearly above the clinical breakpoint of STR, it is interesting to note that compensatory mutations that arise to mitigate fitness defects can negatively affect the resistance levels conferred by resistance conferring mutations.

Generation of fitter mutants through compensatory mutations generally requires continuous subculturing, often for several months[112,113]. A total of five serial passages through soft agar over approximately two weeks generated chloramphenicol-resistant mutants (5X) markedly fitter than the OM (Figure 2.4), with AUC comparable to the WT (Figure 2.4B). When comparing OM and 5X populations adapting to NIT in SAGE plates with identical NIT gradients (maximum [NIT] = $10 \,\mu\text{g/mL}$), resistance in the OM replicates was significantly delayed while the 5X levelled their rates to the WT (Figure 2.2A). 5X also evolved a higher MIC than the OM, which surpassed the maximum concentration of NIT encountered in the plates by about three-fold (OM, R14: 8

μg/mL; 5X, R8: 32 μg/mL). This "overshoot" in resistance has been reported before, and has important consequences since bacteria encountering sub-lethal concentrations of antibiotics can evolve resistance beyond clinical breakpoints[140]. Sequencing revealed that the OM did not acquire mutations in any genes implicated in NIT resistance, while the 5X evolved resistance via mutations in the nitroreductase enzymes classically known to confer NIT resistance. Together, this shows that resistance mechanisms that incur large fitness costs may delay the evolution of resistance and favour, at least when subjected to lower concentrations of antibiotics, the adoption of evolutionary paths that mitigate existing fitness costs over resistance evolution. Contrary to what was observed for NIT, the fitter 5X populations could not restore their STR adaptation potential to WT levels, with resistance being delayed by a day in the majority of the replicates (10/16 replicates) (Figure 2.3C). Sequencing revealed rpsL mutation in the 5X replicate, with the rest of the mutational profile mostly distinct from that of the STR-adapted WT and OM (Supplementary data). The underlying reason behind this slowdown in evolution to STR could not be determined, but the inability to alleviate this slowdown even after multiple passes through SAGE medium suggests that this may be a stable phenotype. Identification of fitness deficits that are stable at the face of fitness-compensation is a major step towards translation of evolutionary trade-offs into effective therapy[207].

The design of sequential antibiotic therapy is not trivial. The primary antibiotic must be selected such that the evolutionary pathways impose deficits that impede subsequent adaptation. A STR-mutant barely exhibits any fitness defects (Figure S2.1), and would not be expected to deviate in evolutionary kinetics from that of the WT (we tested the ability of STR-mutants to generate resistance to NIT in 4 replicates, and did not observe any significant difference from the WT; data not shown). Streptomycin is also antagonized by the bacteriostatic CHL when applied in

combination[208]. Sequential application of antagonistic drugs, in the correct direction, may be a practical option over combination approaches to slow resistance evolution.

In sequential antibiotic regimens where an antibiotic is applied for a short period of time, the antibiotic may not be able to completely eradicate a population that remains at WT resistance levels[209]. Upon cessation of therapy, the WT population may then possess a selective advantage over the antibiotic resistant populations that are often growth impaired. A recent publication also showed how fast-growing bacterial populations can counteract antibiotic susceptibility to dominate bacterial communities independent of specific antibiotic mechanisms[210]. Since not all antibiotic resistance mechanisms incur fitness costs[211], resistance mechanisms that do are important to identify.

The mutations conferring resistance to CHL in the bacterial strain used in this study are primarily linked to upregulation of non-specific efflux pumps, not to alterations in how CHL binds to its target. Since resistance to a wide range of antibiotics is often conferred via mutations in efflux pumps, we expect the rate of resistance evolution to decrease when bacteria evolve resistance to antibiotics via upregulation of these systems, and potentially via other adaptations with significant fitness penalties. This effect may also be independent of the genetic background. To support this notion, we showed that the OM is resistant to a variety of antibiotics (Table 2.1), and a cephalosporin-resistant mutant of *E. coli* K-12 subtrain BW25113 that also exhibited significant fitness defects also exhibited slower adaptation to NIT (Figure S2.4). Furthermore, the fitness-impaired CFZR frequently evolved lower resistance levels than the wildtype strain (5/8 replicates).

Overall, our findings suggest that the fitness costs associated with antibiotic resistance may be exploited to slow down resistance evolution, and the SAGE system can be utilized to identify

evolutionarily stable impairments at high-throughput. We hope that studies like this can guide optimal drug switches to develop sequential antibiotic therapies that are less prone to resistance evolution.

2.4. Materials and methods

2.4.1. Bacterial strain and growth conditions

E. coli K-12 substrain MG1655 (WT) and all subsequent resistant mutants were grown in Mueller Hinton (MH) media at 37 °C. Growth media was supplemented with appropriate antibiotics when growing mutants or extracting mutants from SAGE plates.

2.4.2. SAGE evolutions

SAGE plates were prepared as described previously[69]. Briefly, 6 mL of MH media + 0.25% agar (MHA) supplemented with appropriate antibiotic was poured into each lane of 4-well dishes (Thermo Fisher Scientific, Cat. no. 167063) propped up on one side using p1000 pipette tips. Antibiotic concentrations suitable for evolution were determined via prior MIC testing. The resulting wedge-shaped media were left to set for ~20 minutes before removing the pipette tips and pouring 8 mL of antibiotic free MHA. The plates were left at room temperature overnight to allow diffusion to set up the antibiotic gradient. 50 μL of overnight bacterial culture was inoculated in a line 1-2 mm below the agar surface in each lane, overlaid with ~2.5 mL of mineral oil to reduce drying by evaporation, and incubated at 37 °C. Plates were checked every 24 h to measure maximum distance moved by the bacterial fronts. Resistant mutants were extracted by cutting out ~5x5 mm sections from the end of the plates and dispersing in MH broth (MHB). For the

generation of the OM, these mutants were inoculated back into a second CHL-gradient (Figure 2.1A).

2.4.3. Growth measurements

Absorbance readings at 595 nm of 1/200 dilutions of overnight cultures were recorded using a plate reader (Tecan SunriseTM). To reduce fogging of the plates which interferes with absorbance readings, plate lids were made hydrophilic by pouring in 3 ml of 0.05% Triton X-100 in 20% ethanol and swirling to ensure coverage. After 30 s, excess solution was discarded and lids were air dried[212]. Growth curves were fitted to a logistic equation and AUCs were calculated using the R package *growthcurver*[213] (73).

2.4.4. Fitness improvements via flat-concentration SAGE plates

~13 mL of MHA was poured in a lane of 4-well dishes containing 100 µg/mL of chloramphenicol. Once set, 50 µL of overnight bacterial culture was inoculated as described before. After growth reached the end of lanes (16-20 h of incubation for 1X - 5X, ~48 h for OM), cells were extracted by cutting out ~5x5 mm sections from the end of plates and dispersing in 5 mL MHB supplemented with 100 µg/mL of chloramphenicol. Extracted cells were incubated and used as the inoculum for the next flat lane, up to a total of 5 passages to generate the 5X strain (Figure 2.4A).

2.4.5. MIC assays

MICs were determined as recommended by CLSI[214]. Briefly, 10 point dilutions of antibiotics were made in MHB and inoculated with a 1/200 dilution of 0.5 McFarland standardized inoculum. Plates were incubated overnight and MICs were recorded as the minimum concentration of antibiotic that resulted in no visible growth.

2.4.6. Whole genome sequencing

Sequencing and variant calling were performed by Sequenter (USA). Sequencing was performed on an Illumina NextSeq 2000, and demultiplexing, quality control and adapter trimming was performed with bcl-convert (v3.9.3). Variant calling was carried out using Breseq under default settings[215]. NCBI reference sequence NC_000913.3 for *E. coli* K-12 substrain MG1655 was used for variant calling. Sequencing data have been deposited in the NCBI BioProject database with accession number PRJNA986536. Sequencing quality information is reported in supplementary data.

Chapter 3. De novo evolution of antibiotic resistance to Oct-TriA₁

Published record: Chowdhury FR, Mercado LD, Kharitonov K and Findlay BL; Microbiological

Research 2025;293:128056.

Available at: doi.org/10.1016/j.micres.2025.128056.

3.1. Introduction

Antimicrobial resistance (AMR) is a major global health concern that threatens access to basic

medical interventions. It is estimated that AMR was directly responsible for 1.27 million global

deaths and contributed to 4.95 million deaths in 2019 [216], and it is currently projected that, if

left unchecked, AMR will be responsible for 10 million deaths annually by 2050 [217].

Unfortunately, resistance to many potential new antibiotics can be found in bacterial pathogens

before the drugs' commercial release, due in part to cross-resistance between similar drug

molecules [218]. Studies that describe new antibiotics now often include adaptive laboratory

evolution (ALE) experiments to determine rates of resistance or to elucidate the mechanism of

action, with some antibiotics showing little to no resistance evolution [219-224]. These latter

antibiotics have attracted significant interest as promising candidates for next-generation antibiotic

therapy, and may represent desirable "evolution-proof" or "resistance-proof" agents [225,226].

However, the evolutionary resilience of many of these compounds has only been assessed through

a limited array of ALE experiments, and has generally not been independently verified.

Tridecaptin A₁ is one antibiotic against which laboratory evolution experiments have failed to

describe de novo resistance. Originally isolated from Paenibacillus spp. [227,228], the tridecaptins

are a group of non-ribosomal lipopeptides that act by selectively binding to the cell wall synthesis

precursor lipid II of Gram-negative bacteria and dissipating the proton motive force [220]. Their

59

linear structure is readily accessible to solid phase peptide synthesis, allowing facile construction of tridecaptin analogues [229,230]. Best studied of these is octyl-tridecaptin A₁ (Oct-TriA₁), in which the chiral lipid tail is replaced with a low-cost octyl equivalent with no significant change in antimicrobial activity [231]. Tridecaptins are selective for Gram-negative bacteria, and their potent activity against the majority of the WHO's priority pathogens list [232] makes them exciting antibiotic candidates. They have also been reported to be evolutionarily resilient, with Cochrane *et al.* finding no appreciable resistance to Oct-TriA₁ following a 30-day laboratory evolution experiment [220].

Gram negative bacteria are notoriously difficult to treat, and some recent efforts have focused on targeting the very outer membrane that makes them more resilient. Some examples of such antibiotics include compounds that inhibit LPS biosynthesis or transport, like cerastecin [233], zosurabalpin [234] and analogs [235], L27-11 [236], murepavadin [237], IMB-881[238]. Likewise, antibiotics like darobactin [239] target OM proteins [240]. This strategy seems to confer certain selectivity, enabling development of narrow-spectrum antibiotics which may reduce the likelihood of developing resistance [233,234,236,237]. These antibiotics are especially interesting as their resistance could also lead to loss of virulence, by directly targeting LPS and OM stability [239].

We previously reported the ability of the soft agar gradient evolution (SAGE) system to rapidly generate resistance against antibiotics, including ones difficult to evolve in other platforms [241]. SAGE uses antibiotic gradients and bacteria's natural propensity to swim through soft agar to select for antibiotic-resistant mutants. Unfortunately, the efficacy of SAGE is limited by

synaeresis, the tendency of agar hydrogels to spontaneously shrink over time via continuous expulsion of solvent [242]. In SAGE this hinders bacterial motility [243] and limits experiments to ten days or less. We report here a new SAGE medium that is resistant to synaeresis. Supplemented with xanthan gum, a polysaccharide with excellent water binding capacity [244], this medium has a reduced agar content and is suitable for month-long evolution experiments. We start by showing that resistance to the lipopeptide polymyxin B (PolB), an antibiotic that has proven difficult to evolve resistance to in SAGE [241] and in other platforms [245], can now be quickly achieved via SAGE. We subsequently use this medium to successfully generate resistance against Oct-TriA₁ in Escherichia coli through a 27-day, maintenance free, SAGE experiment. Whole genome sequencing of evolved strains reveals mutations in phospholipid transport, outer membrane (OM) assembly and liopolysaccharide (LPS) biosynthesis. Notably, mutations in the lptD gene appeared consistently across resistant strains, implying its importance in resistance to Oct-TriA₁. We then conduct further investigations into the role of *lptD*, *mlaA* and *ompC* mutations through allelic replacement studies, demonstrating their effect on Oct-TriA₁ and other antibiotics minimum inhibitory concentrations (MICs), as well as their fitness costs.

3.2. Results

3.2.1. Standard SAGE medium fails to generate resistance to polymyxin B

To begin testing the ability of SAGE to generate resistance to lipopeptides, we attempted to evolve resistance to PolB in *Escherichia coli* K-12 substr. BW25113. However, we repeatedly failed to evolve resistance greater than 4-fold the initial value of $0.25 \,\mu\text{g/mL}$. At low PolB concentrations ([PolB]_{max}= $1.25 \,\mu\text{g/mL}$, $5x \,\text{MIC}$), cells quickly covered the plate and on isolation gave MICs that were 2x-4x that of the wildtype strain. However, the susceptibility of these mutants quickly

reverted to wildtype (WT) levels upon subculturing in antibiotic-free media (data not shown), a feature consistent with the heteroresistance often observed with polymyxins like PolB and colistin [246–248]. Growth in plates with a higher [PolB]_{max} (10 µg/mL, 40x MIC) failed to reach the end of the plates (Figure 3.1A, 3.1B). This behaviour is consistent with other ALE platforms, and PolB is known to be difficult to evolve resistance to via ALE [245].

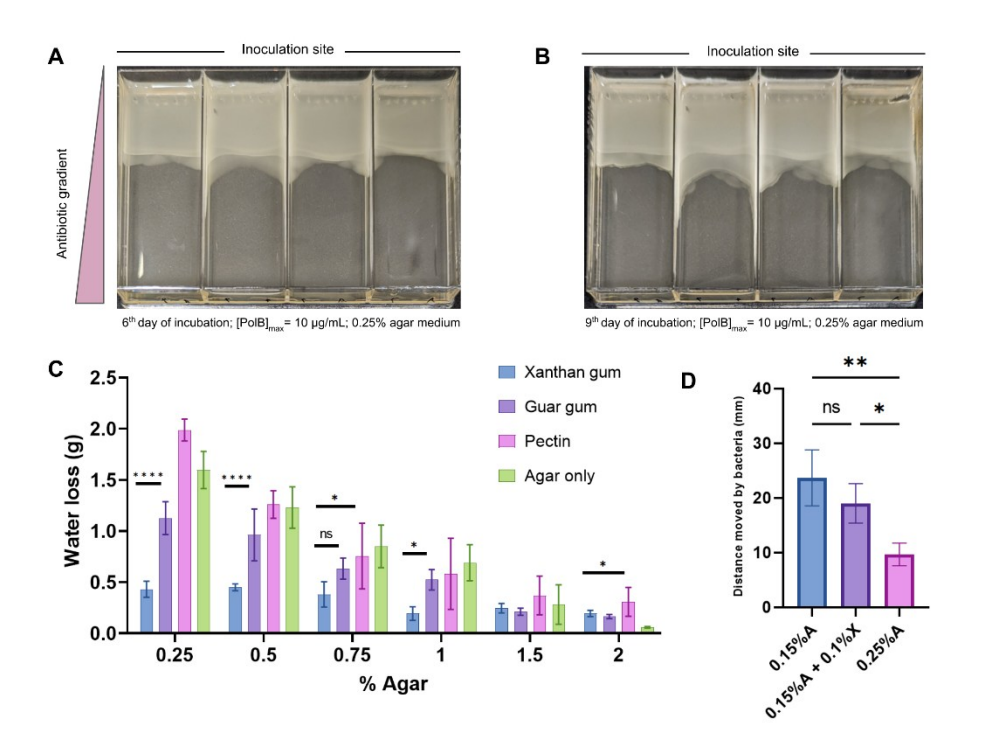


Figure 3.1 Synaeresis limits SAGE.

(A) Cells in 0.25% agar-based PolB SAGE plates ([PolB]_{max}= 10 μ g/mL) remain stationary ~30 mm from the inoculation site. (B) Further incubation results in only small movements of the bacterial front. (C) Xanthan gum outperforms all other additives tested for synaeresis-resistance across a range of agar strengths (n= 5). (D) Distance moved by bacteria in 0.15% agar medium (0.15%A), 0.15% agar + 0.1% xanthan gum medium (0.15%A + 0.1%X), and 0.25% agar medium (0.25%A). Bacteria traverse significantly higher distances in the 0.15%A + 0.1%X medium compared to the 0.25%A (n= 3). *p < 0.05, **p < 0.01, ****p < 0.001, ****p < 0.0001, one-way ANOVA with Fisher's LSD test. Error bars represent SD.

SAGE evolutions rely on the ability of bacteria to move through the antibiotic gradients set up in soft-agar (0.25% agar) [241]. During incubation, synaeresis increases the effective agar concentration, reducing bacterial motility. We noticed that the bacterial front in PolB SAGE plates incubated for more than a week scarcely moved (Figure 3.1A, 3.1B), and hypothesized that synaeresis may be hindering the emergence of chromosomal mutations that confer stable PolB resistance. In line with this, a previous study reported that resistance to PolB in *E. coli* did not evolve for ~6 days (in a liquid evolution platform), after which a rapid increase in resistance was seen [249]. The authors proposed a two-step trajectory of resistance where heteroresistant bacterial populations leverage non-genetic mechanisms to withstand PolB stress at low concentrations, accessing stable chromosomal mutations only when the antibiotic concentrations increased [249]. We thus set out to develop a SAGE medium more suitable for prolonged experiments.

3.2.2. Xanthan gum supplementation reduces synaeresis in agar hydrogels

Polysaccharides like pectin, guar gum, and xanthan gum are able to form hydrogen bonds with water molecules, and are widely used as thickening agents in the food industry [244,250]. We hypothesized that the addition of these water-binding agents to agar gels may help slow down the synaeresis-driven remodeling of the agar matrix by resisting expulsion of water. We first confirmed that *E. coli* cannot utilize these polysaccharides as a carbon source (Supplementary Figure 3.1), then evaluated their effect on the synaeretic properties of agar gels. Each agent was separately added at 0.25% to agar strengths ranging from 0.25% to 2% (all percentages are in w/v), and the extent of synaeresis was evaluated via a modification of the method described by Banerjee *et al.* [251]. Gels supplemented with xanthan gum achieved the highest reduction in water loss at all agar strengths tested (Figure 3.1C). While not a gelling agent itself, xanthan gum could replace

a proportion of the agar while maintaining gel cohesion and limiting synaeresis (Supplementary Figure 3.2), though the medium became viscous at higher xanthan gum strengths.

Next, we tested the effect of addition of xanthan gum on bacterial motility in the SAGE medium. Addition of 0.1% xanthan gum to 0.15% agar had no statistically-significant effect on bacterial motility when compared to 0.15% agar alone, and both offered significant improvements in motility compared to the 0.25% agar medium. (Figure 3.1D, Supplementary Figure 3.3).

3.2.3. Supplementation with xanthan gum enhanced the evolution of polymyxin B resistance

Moving forward, we opted to use a mixture of 0.2% xanthan gum and 0.15% agar (referred to from here on as XAM), a ratio which provided a balance of low viscosity in liquid state and high stability in the gel state, in place of the conventional 0.25% agar base used in SAGE. We found no difference between diffusion rates of malachite green in 0.25% agar and XAM (Supplementary Figure 3.3B), indicating that diffusion rates of antibiotics in XAM should be similar to that in the conventional medium.

To test the performance of the medium in SAGE, we set up a PolB SAGE plate with XAM ([PolB]_{max} in SAGE = $10 \mu g/mL$, 40x MIC). We were able to generate stable PolB resistant mutants within 4 days in 2/4 SAGE lanes (MIC: $16 \mu g/mL$, Figure 3.2A). We suspect that the increase in bacterial movement speed in xanthan gum-supplemented media (Figure 3.1D) reduced the time required for evolution in XAM-SAGE plates by allowing bacteria to reach PolB concentration that selects for stable genomic mutations earlier. By the time cells reached this

concentration in the conventional medium, the medium may have already been too dry to allow movement.

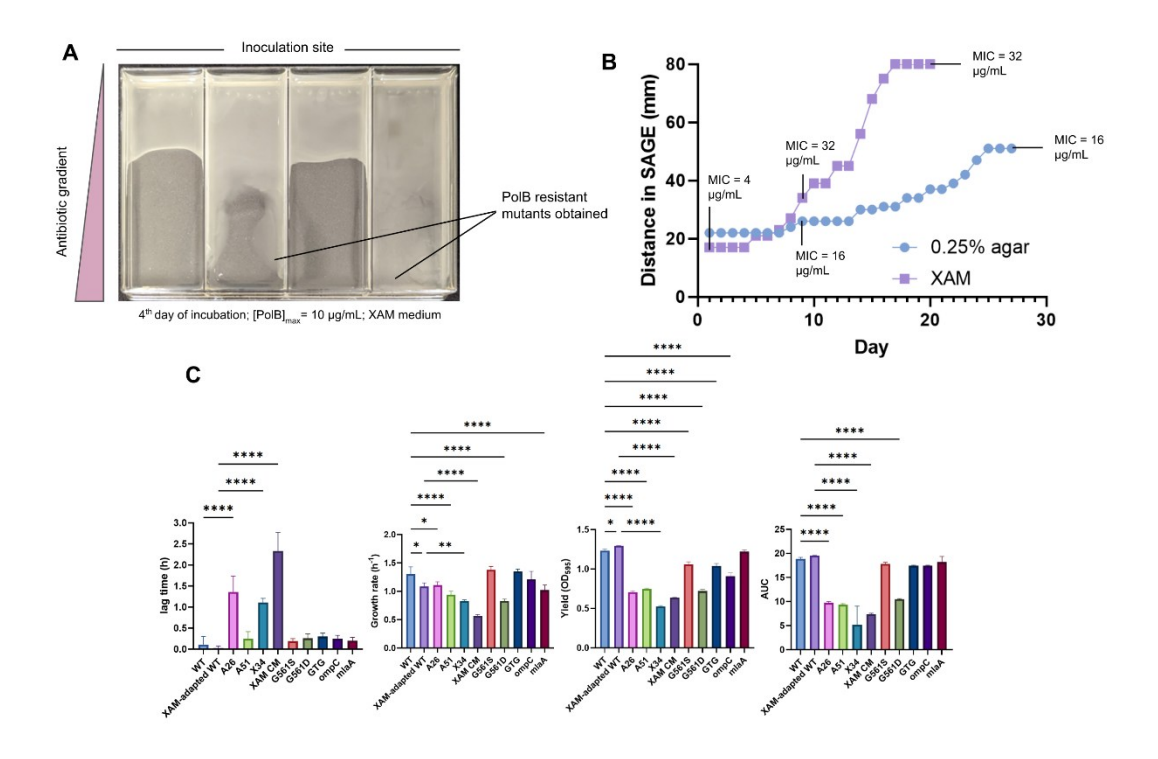


Figure 3.2 Evolution of antibiotic resistance.

(A) Resistance to PolB emerged in 2 out of the 4 replicates in SAGE with XAM ([PolB]_{max}= 10 μg/mL). (B) Distance moved by bacteria swimming through agar or xanthan gum/agar SAGE plates loaded with Oct-TriA₁ at a max concentration of 40 μg/mL. Bacteria moved farther and faster in XAM. MIC of samples from several time points are labelled, with bacteria in XAM achieving a higher MIC (full list of MICs in Table 3.1). (C) Oct-TriA₁ mutants are fitness impaired (n= 3). *p<0.05, **p<0.01, ***p<0.001, p<0.0001, one-way ANOVA with Bonferroni correction. For statistical comparisons, WT values were compared with XAM-adapted WT, A26, A51, G561S, G561D, GTG, ompC and mlaA, and XAM-adapted WT values were compared with XAM34 and XAM CM. Among these comparisons, only statistically significant differences are indicated by asterisks. Error bars represent SD. Results obtained from 3-9 replicates.

3.2.4. Evolution of resistance to Oct-TriA₁

We next sought to evolve resistance to Oct-TriA₁ in XAM. We set up two SAGE lanes in parallel ([Oct-TriA₁]_{max} = $40 \mu g/mL$, 10 x MIC), one with the conventional 0.25% agar medium, and the other with XAM. We followed the evolution of resistance by measuring the maximum distance moved by the bacterial fronts every 24 h (Figure 3.2B). Bacteria moved slowly through the 0.25% agar medium, traversing only about 60% of the lane (~50 mm) by the end of 25th day and remaining stationary for 3 additional days before the experiment was stopped (Figure 3.2B). The small distances moved and thinning agar gel made sampling from this medium beyond 7 days challenging. In contrast, bacteria in the XAM lane moved large distances after breaking free from the initial inhibitory Oct-TriA₁ concentration (Day 7), covering the entire lane by the end of day 17 (Figure 3.2B). The XAM gel also appeared to have retained significantly more water than the agar-based gel at the end of the experiment (data not shown). Samples were collected whenever significant bacterial movement was detected since cells that continued moving towards higher concentration of the antibiotic may have acquired adaptive mutations against Oct-TriA₁. We sampled 20 µL of gel out of the plates every sampling. While sampling may reduce the population size of a mutant on the plate, it is unlikely to alter the evolutionary trajectory. We previously showed that varying population sizes in SAGE plates containing nitrofurantoin did not change the adaptation rate [252]. We tested the MIC of samples A26, A30, A37, A51, XAM34, XAM45, XAM56 and XAM CM ('A' and 'XAM' in the sample IDs denote samplings from 0.25% agar lane and XAM respectively, and the numbers denote the distance in millimeters from the inoculation zone to where cells were sampled; CM = cells extracted from the end of lane, \sim 75 mm) (Table 3.1). The MIC of A26 and XAM34, both from the 9th day of incubation, showed that resistance emerged early, and appeared to remain constant throughout the rest of the experiment (Table 3.1). This could partly be due to partial flattening of the Oct-TriA₁ gradient via diffusion, presenting an antibiotic challenge that allowed bacteria to evolve resistance to a level which remained sufficient for the rest of the plate. Also, since standard MIC assays are based on 2-fold dilution steps, small increases in MIC that might have occurred after the initial increase may not have been resolved via our MIC assays. Overall, mutants from the 0.25% agar-based medium exhibited up to 4x increase in MIC, compared to an 8x increase in XAM (Table 3.1).

Table 3.1 Details of Oct-TriA1 mutants sampled from SAGE.

Media in SAGE lane	Sampling day	Oct-TriA ₁ MIC
		(μg/mL)
-	-	4
XAM	-	4
0.25% agar	9	16
0.25% agar	14	16
0.25% agar	21	16
0.25% agar	27	16
XAM	9	32
XAM	12	32
XAM	14	32
XAM	20	32
	- XAM 0.25% agar 0.25% agar 0.25% agar 0.25% agar XAM XAM	

Next, we compared the fitness of the early and endpoint Oct-TriA₁ mutants to that of the WT parent strain (Figure 3.2C). The WT E. coli used for generating mutants from the 0.25% agar lane was pre-adapted to this SAGE medium as previously described [241]. To account for any changes in fitness due to adaptation to XAM, we also passaged the WT strain through antibiotic-free XAM 3 times to produce a XAM-adapted WT strain (Materials and Methods). All evolved mutants showed longer lag times (though differences with A51 did not reach statistical significance) and lower growth rates, yields and AUCs (area under the growth curves), indicating that Oct-TriA₁ resistance imposed a large fitness cost (Figure 3.2C). In general, the XAM-generated mutants showed larger fitness deficits, even though the fitness of the XAM-adapted WT was comparable to the WT in every metric measured. Interestingly, the XAM CM strain showed a clear diauxic growth pattern (Supplementary Figure 3.4). While a delayed release of glucose from degradation of xanthan gum could affect growth during our long evolution experiment, the stability of xanthan gum makes it unlikely for significant amounts of monomers to be released in the medium at 37 °C since it remains stable over multiple years at temperatures above 70 °C and was insufficient to maintain bacterial growth [253,254] (Supplementary Figure 3.1). This strain harbored a deletion in the nuo operon, which codes for a NADH/ubiquinone oxidoreductase that shuttles electrons from NADH into the electron transport chain [255,256]. When cells grow in the presence of glucose, they excrete acetate [257]. As cells deplete glucose from media, they switch to uptaking acetate [258], shifting from glycolysis to TCA cycle and gluconeogenesis [257]. In nuo mutants, high NADH/NAD⁺ ratios inhibit enzymes involved in the TCA cycle, drastically slowing growth and potentially giving rise to the diauxic growth pattern we observed [255,258]. However, what causes subsequent resumption of growth during diauxie is unclear [259,260].

3.2.5. Genetic analysis of Oct-TriA₁-resistant mutants

We whole genome sequenced four strains from our SAGE evolution experiments: A26, A51, XAM34 and XAM CM (Figure 3.3). Mutations in A26 and XAM CM were not complete subsets of A51 and XAM CM respectively, showing that different clones were selected along the SAGE lanes during these samplings. This suggests mutants that appeared early did not maintain their selective advantage, and other mutants that gained an advantage at different time points (and hence, at different states of the gradient) surpassed the earlier mutants. XAM34 had an MIC eight times that of the wildtype *E. coli* BW25113 and had eight mutations: three non-synonymous, three intergenic, and two frameshift insertions (Table 3.1, Figure 3.3). XAM CM, drawn from later in the same SAGE plate, had the same MIC and ten mutations: four non-synonymous, two intergenic, three frameshift insertions, and one frameshift deletion. Two of these were identical: a five-base deletion in *yddW* and a E26K mutation in *rpoD*. A26 had two nonsynonymous mutations and the same five-base deletion in *yddW*, while A51 had four non-synonymous mutations, one intergenic mutation, one insertion, and three frameshift mutations (including the five-base deletion in *yddW*).

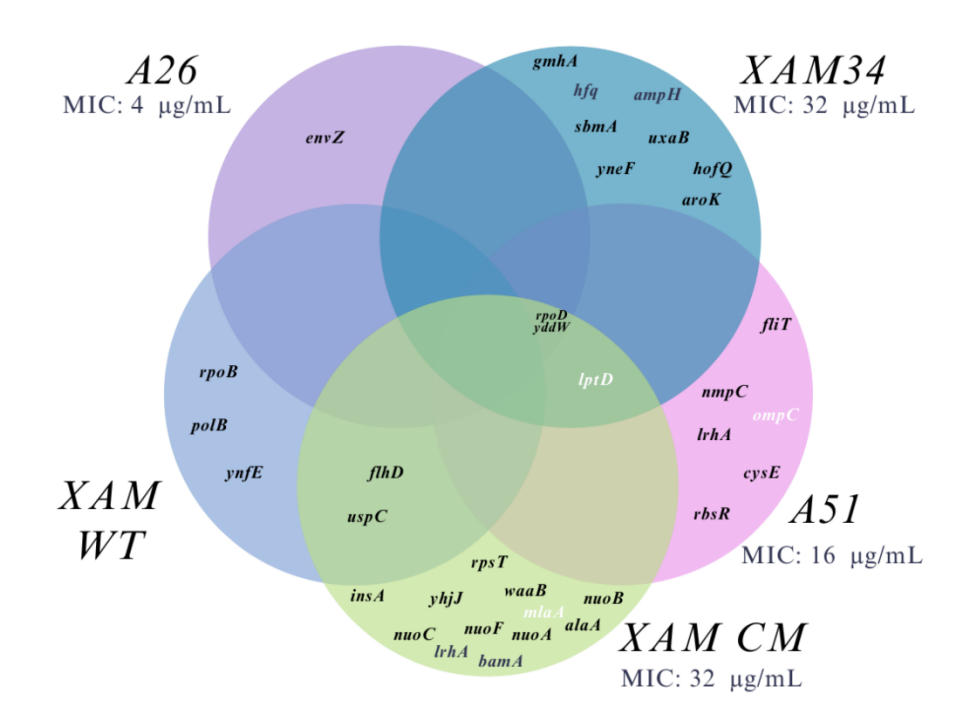


Figure 3.3 Mutations identified in the evolved strains.

A26 and A51 represent mutations observed in cells isolated at 26 mm and 51 mm in agar media; XAM 34 and XAM CM cells isolated at 34 mm and 75 mm, respectively in xanthan gum media. The highlighted mutations were selected for allelic exchange.

To separate possible resistance mutations from those that might be associated with adaptation to the ALE conditions, we sequenced the XG-adapted WT for comparison with the XAM-generated Oct-TriA₁ mutants. Only one mutation overlapped with the antibiotic-exposed samples; an intergenic mutation in $flhD \leftarrow / \rightarrow uspC$ that was also found in XAM CM. The XAM evolved strain carried a G \rightarrow T mutation in -261/-519 while the XAM CM carried a C \rightarrow A in -263/+44. flhD is involved in flagellar type II transcription activation and uspC is a universal stress protein. Changes in flhD expression may alter swimming speed, enhancing movement through the soft agar

plates [261–263]. Other mutations observed were in *rpoB*, *ynfE* and *polB* genes, genes not mutated in any of the antibiotic-exposed strains.

All strains with MICs higher than the wild type carried a single nucleotide polymorphism in lptD, creating LptD G561S (A51, XAM 34) or G561D (XAM CM). This was also the only gene to contain two mutations, with A51 having a further (GTG)3 \rightarrow 2 deletion in nucleotides 705-707. LptD is an integral component of the Lpt complex, which is essential for the assembly and transport of LPS to the outer membrane of Gram-negative bacteria [264]. Mutations were also observed in two other genes linked to LPS biosynthesis: X34 contained a SNP in gmhA, which encodes a phosphoheptose isomerase that produces the D-glycero-D-manno-heptose 7-phosphate found in the core of LPS [265], while XAM CM contained a frameshift mutation in waaB, which encodes a galactosyltransferase that appends galactose to that core [266]. Similar to polymyxin B [245], tridecaptin A₁ engages with LPS in the outer membrane to facilitate uptake into the intermembrane space and access its target [220], and these mutations strongly suggest that tridecaptin resistance is conferred by alterations in LPS structure.

Three other mutations had clear ties to the bacterial outer membrane: *mlaA* directly regulates outer membrane composition and was heavily truncated in XAM CM (MlaA W59*), while the porin gene *ompC* is implicated in both maintenance of outer membrane integrity and drug uptake [267,268]. Notably, OmpC was altered both directly through a nonsynonymous *ompC* SNP (OmpC N47S) in A51 and indirectly through a nonsynonymous SNP in the *omp* regulator *envZ* (EnvZ R253S) in A26. A SNP was also observed in *bamA* (BamA L501Q; XAM CM), part of the BAM complex [269]. BamA is responsible for inserting β-barrel proteins into the OM [269]. Mutations

in *bamA* have been related to resistance to drugs targeting this OM protein [240,270,271]. In the case of darobactin, resistance mutations in *bamA* also result in loss of virulence [272].

Gene ontology enrichment analysis mapped the remaining mutations to several key pathways, including those related to respiratory electron transport mechanisms (Supplementary Table 3.1). This suggests adaptive changes in electron transport and ATP synthesis, in addition to alterations in outer membrane assembly and biosynthesis.

3.2.6. Allelic exchange in genes involved in phospholipid transport and outer membrane assembly confirmed their involvement in resistance to Oct-TriA₁.

To investigate the effect of mutations in genes associated with phospholipid transport, we introduced the observed mutations in lptD into E. coli BW25113 via allelic exchange. This was carried out using CRISPR-Cas9/ λ -Red assisted recombineering as previously described [273,274]. Concurrently, knockouts in ompC and mlaA were obtained from the Keio collection [275]. The effect of these alterations was assessed via MIC assays, revealing that all five alterations increased the ancestral strain's MIC against Oct-TriA₁ two-fold (Supplementary Figure 3.5).

Other cationic non-ribosomal peptides (CNRP) like Polymyxin and Brevidicine [276] have a similar uptake mechanism [277] [278], Specifically, brevicidine also targets components in the inner membrane, namely phosphatidylglycerol and cardiolipin. Given the similarities in their mechanisms of action, the mutations related to LPS biosynthesis and transport conferring OctTriA1 resistance may also result in cross-resistance to brevicidine. Although we did not observe cross-resistance to Polymyxin B in our study (Supplementary Figure 3.5), it is important

to consider broader implications of cross-resistance in antimicrobial strategy development. Exploring these targets that haven't been extensively used in the clinic could provide an advantage in delaying the appearance of resistance.

The effect of the mutations on fitness was more variable. None of the mutations altered lag times during growth in MHB, but significant deviations were observed in both growth rates and max OD (Figure 3.2C). The effect of the LptD mutations on fitness varied by both site and type of mutation. Despite halving susceptibility towards OctTriA1, the extra GTG repeat had no effect on bacterial fitness, while the LptD G561D mutation was much more detrimental than the LptD G561S mutation. As no single mutation increased resistance or impaired fitness to the levels observed in XAM CM, a combination of costly mutations appears to be required for high-level resistance.

3.3. Discussion

In this study we demonstrate the first *de novo* evolution of resistance to Oct-TriA₁, with the effect of putative resistance-conferring mutations confirmed through allelic exchange. Further, we have improved the SAGE system through the incorporation of the thickening agent xanthan gum, extending the potential duration of experiments from a week to a month and enhancing selection rates. This modified system was also much more effective at selecting mutants resistant to polymyxin B, an antibiotic that is often difficult to target with other ALE systems.

In line with resistance to other D-amino acid-containing non-ribosomal peptides [279], resistance in the native producers of tridecaptins is mediated via hydrolytic D-stereospecific peptidases [280]. In contrast, the mutations we have observed are largely in genes coding for LPS biosynthesis and outer membrane homeostasis. These pathways are essential to bacterial growth, as well as

interactions with the immune system, nutrient acquisition, and toxin susceptibility [281–283]. As a result, it is unsurprising that the resistant strains we generated had significantly impaired fitness (Figure 3.2C). Similar results have been observed with other membrane-interacting antibiotics, like the polymyxins. In many pathogens mutations that confer colistin resistance significantly impairs fitness and/or virulence [284], though acquisition of the plasmids encoding colistin resistance factor *mcr-1* has a much smaller impact [285].

The factors that underpin widespread, high-level resistance are not fully understood. When evaluating evolution potential there has been a strong tendency to focus on the rate by which resistance emerges, either through mutation rate studies or ALE [219–221,286–289]. This work suggests that the nature of the mutations should also be taken into account. Each of the mutations in *lptD*, *mlaA*, and *ompC* altered the octyl-tridecaptin A₁ MIC two-fold, with little overlap between strains (Figure 3.3, 3.4). Given the overall change in susceptibility following SAGE was 8-fold, high-level resistance likely resulted from a combination of multiple mutations rather than from any single mutation. SAGE is well-suited to the serial acquisition of small-impact mutations [241], potentially explaining why it was successful when attempts to evolve resistance via serial passage through liquid culture failed [220].

Xanthan gum was able to significantly reduce synaeresis and allow SAGE experiments to extend beyond their initial limit of 7-10 days, and this media may have utility outside ALE. Syneresis causes loss of growth-promoting properties of media when cultivating slow-growing bacteria and fungus [242,290,291]. Addition of a water-binding agent like xanthan gum may preserve these properties, allowing extension of those experiments as well.

Against the rising prevalence of antibiotic resistance, "evolution-proof" or "resistance-proof" are very appealing targets [225,226]. Their discovery could greatly alleviate the growing AMR crisis, carving a path forward for the use of antibiotics for decades to come. However, since the discovery of sulfa drugs, hundreds of antibiotics have entered clinical use, with pathogens evolving resistance to each and every one of them [225]. This work underscores the genetic flexibility of bacteria, and highlights the need for stringent evolution studies during the development and discovery of new antibiotics. If resistance is to emerge, we would do well to study it *in vitro* before its appearance in pathogens.

3.4. Materials and Methods

3.4.1. Bacterial Strain and Growth Conditions

E. coli K-12 substr. BW25113 and all subsequent resistant mutants were grown in cation-adjusted Mueller Hinton Broth (MHB 2) media at 37 °C. Liquid cultures were shaken at 250 RPM, while agar cultures were grown in a static incubator.

3.4.2. Oct- $TriA_1$ synthesis

Oct-TriA₁ synthesis was performed as described by Cochrane *et al.* [229], with the following modifications. Briefly, in a manual peptide synthesizer 120.5 mg of Wang resin pre-loaded with Fmoc-Alanine at a loading of 0.6 mmol/g was swelled in dimethylformamide (DMF). The protecting group was cleaved with two twenty-minute treatments of 4:1 DMF:4-methylpiperidine. The beads were then washed three times with DMF, once with dichloromethane (DCM), then one final time with DMF. The next residue in the series was then added in 3x excess, alongside HATU

(3x excess) and diisopropylethylamine (DIPEA) (8x excess). Coupling was carried out for one hour, at which point the beads were washed as above and the Fmoc protecting group once more cleaved. This cycle was repeated for each of the peptides, with Fmoc-Glu(OtBu)-OH, Fmoc-D-Ser(OtBu)-OH, Fmoc-Dab(Boc)-OH, and Fmoc-D-Dab(Boc)-OH used for the residues with reactive side chains. The complete peptide was cleaved from the resin with a 95:2.5:2.5 solution of trifluoroacetic acid (TFA):deionized water:triisopropylsilane for 2 hours. The cleavage solvent was removed on a rotary evaporator, and the crude material was triturated three times with diethyl ether. The solid residue was then purified to homogeneity on an Agilent 1100 preparative HPLC system, using an XBridge BEH C18 OBD prep column (5 μm, 25 x 250 mm) and the following water/acetonitrile gradient system.

Time	Acetonitrile (%)
0	5
1	5
3	20
23	55
31	95
36	95

Peaks eluting around 13.2 min across multiple runs were pooled, and the identity of the peptide was confirmed via high resolution mass spectrometry on an Orbitrap LTQ Velos.

3.4.3. SAGE evolutions

SAGE plates were prepared and inoculated as described previously [241]. For SAGE plates made with XAM, MH media \pm 0.15% agar was first stirred in a flask on a hot plate and stirrer on high for 5-10 minutes. 0.2% xanthan gum was then slowly added to the stirring liquid and the mixture was allowed to stir for 2-3 minutes before autoclaving. This medium was melted on demand prior to use in SAGE plates. We checked on the plates every day to measure distance moved by the bacterial front, and we extracted bacteria only when the bacterial front moved significantly from the previous measurement. Bacteria were extracted from the point where they moved the farthest from the inoculation site. Cells were extracted from SAGE plates by pipetting up 20 μ L of the gel and transferring it into 5 mL MH media for culturing. Overnight growth was streaked on MH plates and single colonies were used to prepare glycerol stocks.

3.4.4. MIC Assays

MICs were determined via broth microdilution, following CLSI guidelines [292]. Briefly, antibiotics were serially diluted in 96-well plates and mixed with bacteria at a final concentration of 5 x 10⁵ CFU/mL. Plates were incubated at 37 °C without shaking for 16-20 h, and the MIC was recorded as the lowest concentration that visibly inhibited growth.

3.4.5. Synaeresis tests

Water loss from different gel mixtures was measured as described by Banerjee et al. [251] with the following modifications. Agar concentrations ranging from 0.2-2% were first stirred in a flask on a hot plate for 5-10 minutes. 0.25% xanthan gum, guar gum or pectin was then slowly added to the stirring liquid, which was allowed to stir for 2-3 minutes. Flasks were transferred to a 37 °C

shaker and shaken overnight at 250 rpm to produce a smooth, homogenous mixture. The flasks were then autoclaved, and 20 ml of each liquid was transferred to 50 mL centrifuge tubes. Tubes were allowed to cool at room temperature, then stored at 4 °C overnight. Initial masses of the tubes were recorded (~30 g on average) before centrifugation at 1000 rpm for 30 mins at 25 °C. Centrifugation broke the gel structure, making it difficult to decant water out of the tubes without losing gel mass. To extract the free liquid, tubes were instead left upright with their caps open, and a folded filter paper was used to wick away the water over 30 minutes. The filter papers were then carefully removed to minimize the loss of gel mass, and the final tube masses were recorded. Water loss was calculated as the difference between the initial and the final masses of the tubes.

3.4.6. Bacterial Motility tests

Bacterial migration speeds on different gel compositions were measured as described by Croze et al. [243]. The media were prepared as described above. 30 mL of each mixture was then poured in separate petri dishes, and the plates were left to set overnight at room temperature. 2 μL of overnight bacterial culture was placed on the center of each petri dish, and the inoculum was allowed to dry/absorb for an hour. 9 mL of mineral oil was overlaid on each plate, and all plates were then incubated at 37 °C without shaking, lid side up. The diameter of growth was measured 6 h post incubation.

3.4.7. Generation of the XAM-adapted WT strain

12 mL of antibiotic-free XAM was poured in a SAGE lane and allowed to cool and solidify. 50 μL of overnight WT bacterial culture was then inoculated on one side and the inoculum was allowed to dry/absorb for 30 minutes. 2.5 mL of mineral oil was overlaid on the gel, and the plate was incubated at 37 °C. The next day, cells were extracted from the end of the lane as described

above, then grown overnight. These cells were used to inoculate a second antibiotic-free XAM lane and the whole process was repeated. Following three consecutive passes, cells were streaked on agar, and a single colony was designated as the XAM-adapted WT strain.

3.4.8. Fitness measurements

1 μL of overnight bacterial culture was added to 99 μL of MH broth in 96 well plates. Lids were treated with 0.05% Triton X-100 in 20% ethanol to reduce fogging [293]. Absorbance readings (595 nm) were recorded using a plate reader at 5 min intervals for 24 h (Tecan Sunrise). Area under the growth curves were calculated in GraphPad Prism. All other metrics were generated using Dashing Growth Curves [294].

3.4.9. WGS and variant calling

Whole genomes were extracted using a bacterial genomic DNA extraction kit following the manufacturer's instructions (Bio Basic Inc, Cat: BS624). Whole genome sequencing was performed at SeqCenter using the Illumina NovaSeq X Plus sequencer, which generated 2x151 bp paired-end reads. The Breseq v0.37.1 pipeline was used for variant calling with bowtie2 v2.4.5 and R v4.2.2 [295].

3.4.10. Gene ontology enrichment analysis

Mutations observed in all of the evolved strains were analyzed for enrichment of gene ontology groups using the ShinyGO package v0.741 [296]. The p-value cut-off for the False Discovery Rate (FDR) was set to 0.05 against *E. coli* MG1655, a K12 strain. Several previously reported differences between MG1655 and BW25113 were identified and excluded from the analysis [297]; most notably deletion of the *araBAD* and *rhaDAB* operons, replacement of a section of the *lacZ*

gene with four *rrnB* terminators, and a frameshift mutation in *hsdR* that causes a premature stop codon.

3.4.11. Allelic exchange mutant generation

Allelic exchange of the selected mutated genes was carried out using the no-SCAR (Scarless Cas9 assisted recombineering) method, as previously described [273,274]. In short, retargeting of the pKDsgRNA plasmid was constructed for the lptD gene region of interest through CPEC cloning in a way that the mutation would disrupt the PAM site or the 12 bp seed region. Cas9 counterselection was achieved by sequentially transforming pCas9cr4 and the retargeted pKDsgRNA and electroporating dsDNA containing the desired mutation. Following induction of λ -Red and Cas9, the successful mutants were verified and the plasmids were cured of the plasmids to render them susceptible to Chloramphenicol and Spectinomycin.

3.4.12. Keio collection strains Kan cassette curing

Keio collection strains were cured of the kanamycin resistance cassette through FLP-recombinase-mediated recombination, using the pCP20 plasmid as previously described [275,298]. Subsequent curing of temperature sensitive pCP20 plasmid yielded Kan^S, Amp^S for MIC determination.

3.4.13. Strains

Strain	Genotype	Reference
E. coli BW25113	Δ(araD-araB)567 Δ(rhaD- rhaB)568 ΔlacZ4787 (::rrnB- 3) hsdR514 rph-1	[275]
E. coli BW25113 lptD G561S	$\Delta(araD-araB)$ 567 $\Delta(rhaD-$	This study

	rhaB)568 ΔlacZ4787 (::rrnB- 3) hsdR514 rph-1 lptDG561S	
E. coli BW25113 lptD G61D	Δ(araD-araB)567 Δ(rhaD- rhaB)568 ΔlacZ4787 (::rrnB- 3) hsdR514 rph-1 lptDG561D	This study
E. coli BW25113 lptD(GTG)3→2	Δ (araD-araB)567 Δ (rhaD-rhaB)568 Δ lacZ4787 (::rrnB-3) hsdR514 rph- 1Δ lptD(GTG)3 \rightarrow 2	This study
E. coli BW25113mlaA (vacJ) JW2343-1	F-, $\Delta(araD-araB)$ 567, $\Delta lacZ4787(::rrnB-3), \lambda$ -, $\Delta mlaA754::kan, rph-1,$ $\Delta(rhaD-rhaB)$ 568, $hsdR$ 514	[275]
E. coli BW25113 ΔompC JW2203-1	F-, Δ(<i>araD-araB</i>)567, Δ <i>lacZ</i> 4787(::rrnB-3), λ-, Δ <i>ompC</i> 768::kan, <i>rph</i> -1, Δ(<i>rhaD-rhaB</i>)568, <i>hsdR</i> 514	[275]

Chapter 4. Large scale laboratory evolution uncovers clinically relevant collateral antibiotic sensitivity

Chowdhury FR, Banari V, Lesnic V, Zhanel GG, and Findlay BL; International Journal of

Antimicrobial Agents 2025, 107564.

Available at: doi.org/10.1016/j.ijantimicag.2025.107564

4.1. Introduction

Antibiotic resistance is spreading at an alarming rate, claiming the lives of over 1.2 million people

every year [12]. Developing strategies to slow down resistance evolution has become essential to

combat antibiotic resistance [299]. Sequential antibiotic therapy, where antibiotics are

administered in a chronological sequence in an individual patient, has emerged as a potential

strategy to slow down the evolution of resistance [300]. In principle, this strategy interrupts the

selection of resistant populations by changing the selective pressure via switching treatment to a

different drug [116]. Evolutionary trade-offs like collateral sensitivity (CS) have been proposed to

improve the success of such sequential therapies by limiting the rate of bacterial evolution

[123,128,301]. We now have numerous studies that have described large networks of collateral

sensitivities in different bacteria [52,128,134,152,302]. However, investigations on their

evolutionary repeatability via large scale experimental evolution are scarce, but are essential for

successful clinical application [139]. In addition, different laboratories use different adaptive

laboratory evolution (ALE) platforms that are difficult to standardize [52,128,152,303,304]. Since

evolutionary outcomes can vary depending on the bacterial microenvironment [139,305], it is

important to determine the effect of the choice of the ALE platform on CS evolution.

In this study, we evolve 20-24 lineages of *Escherichia coli* to screen for CS between four drug

pairs reported to exhibit CS, using three different ALE platforms widely used to study evolution

82

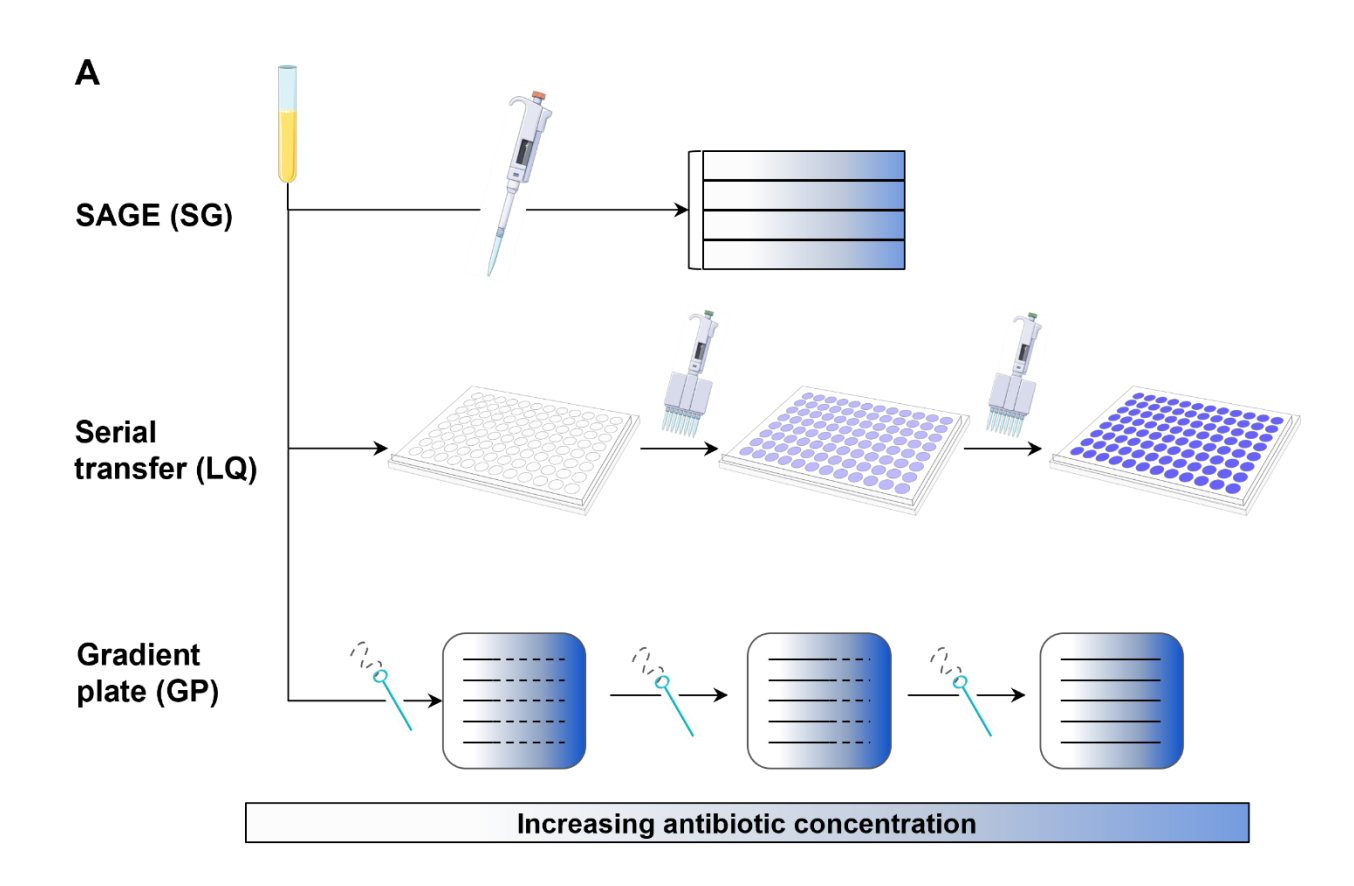
and CS [55]. We find that serial transfer and gradient plating-based ALE platforms agree well on the frequencies of CS, cross-resistance (CR) and resistance levels. However, the soft agar gradient evolution (SAGE) platform produces substantially lower frequencies of CS and higher incidence of CR compared to the other two platforms. To test the relevance of these CS/CR predictions from the different ALE platforms, we analyze antimicrobial susceptibility data from over 750 clinical uropathogenic multidrug resistant (MDR) E. coli strains to test for the presence of CS/CR relationships. We find that CS is almost entirely absent, but neutrality or CR is prevalent. However, we observe a significant association between increasing omadacycline (a third generation tetracycline) resistance and reduced colistin (polymyxin E) resistance. Interestingly, out of the four drug pairs screened in our ALE experiments, SAGE showed significant CS in only one of them: a tigecycline (TIG) (a third generation tetracycline) and polymyxin B (POL) pair. Using genomics and phenotypic analysis, we describe, for the first time, the mechanism of polymyxin B CS in tigecycline-resistant bacteria. Our results highlight the power of large-scale ALE experiments in predicting repeatable CS relationships that hold potential to reduce resistance in MDR bacteria in the clinic.

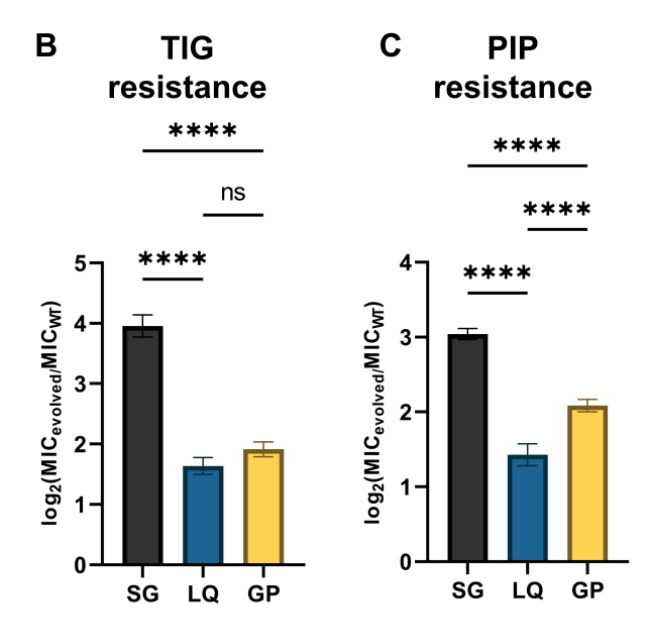
4.2. Results

4.2.1. SAGE produces lower collateral sensitivities and higher cross resistances compared to other ALE platforms

We evolved 20-24 mutants against tigecycline (TIG) and piperacillin (PIP) separately using three different ALE platforms [55]: SAGE [69], serial transfer liquid culture-based method (LQ) [48], and gradient plates (GP) [51] (Figure 4.1A). We also investigated CS profiles for nitrofurantoin (NIT) and ciprofloxacin (CIP), but were unable to achieve resistance at high enough frequencies

in LQ (NIT, CIP) or GP (CIP) to generate the necessary sample sizes (Supplementary Table 4.1). SAGE also produced 8-16-fold increases in relative MIC (MIC of evolved lineage/MIC of WT) of TIG and PIP, while levels from LQ and GP were limited to 2-4-fold increases (Figure 4.1B, C) before incurring frequent extinctions. SAGE presents a smooth continuous gradient of antibiotic





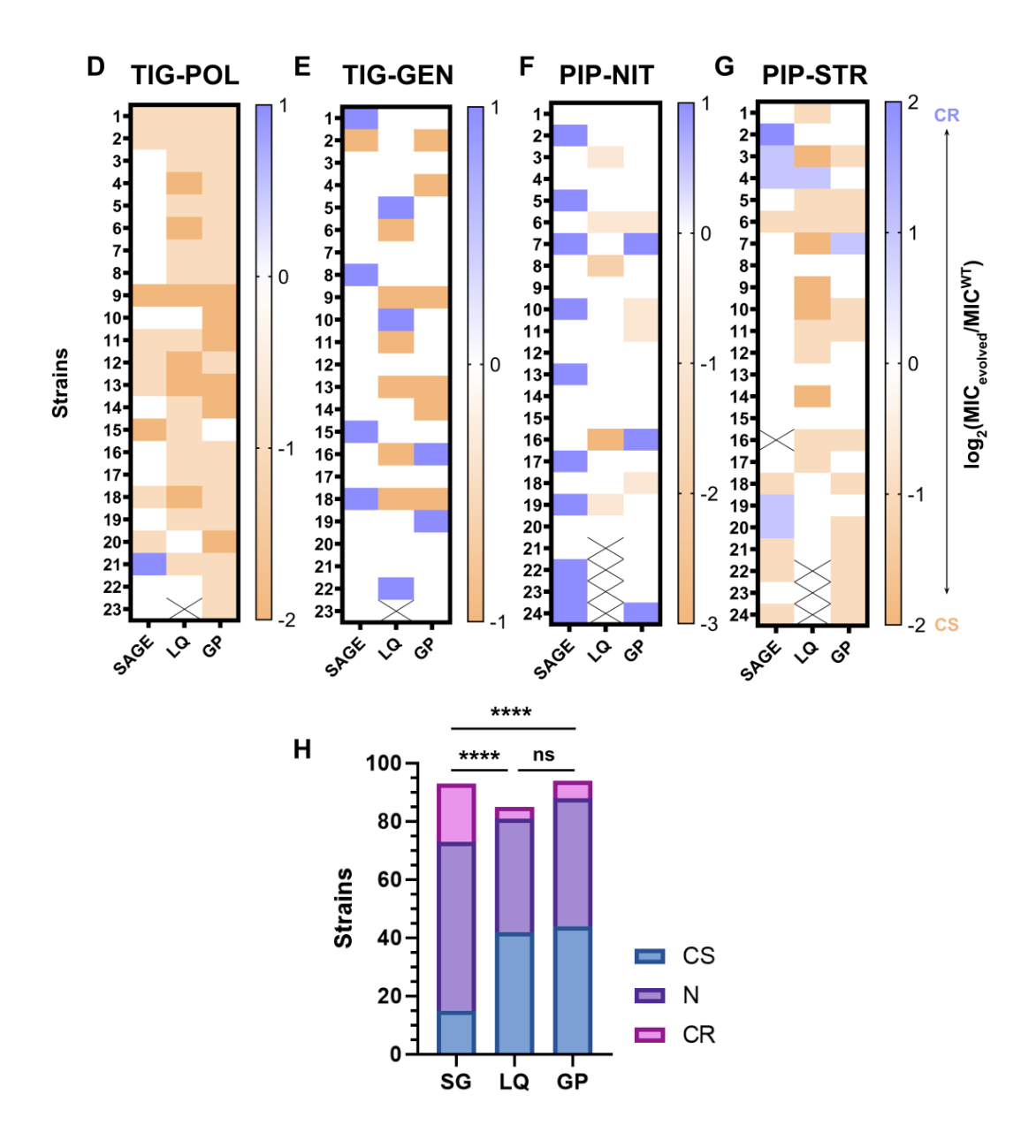


Figure 4.1 Evolution of antibiotic resistance using three different ALEs.

(A) Schematic of the ALE platforms used to evolve resistance in this study. (B) Relative TIG and (C) PIP MICs of evolved mutants. ****p<0.0001, one-way ANOVA with Bonferroni correction. (D) - (G) CS profiles of mutants evolved to TIG and PIP. The labels on top show the antibiotics against which resistance was evolved and CS were measured. For example, "TIG-POL" denotes the POL CS measurements of TIG resistant mutants. (H) Combined CS, N and CR distributions from the three ALE platforms. SG = SAGE. ****p<0.0001, one-way ANOVA with Bonferroni correction. Statistical analyses were performed by comparing relative MICs of mutants from each platform.

in soft agar instead of the 2-fold stepwise increasing gradients present in the serial transfer-based method (LQ) [17]. Because of this, SAGE allows selection of small-effect mutations which may not confer resistances high enough to survive in 2-fold increasing gradients [20]. These mutations may help explain the higher MICs reached through SAGE. Even in GP, daily passaging of a random mutant in the plate introduces a sampling bottleneck which may not select cells with small-effect mutations.

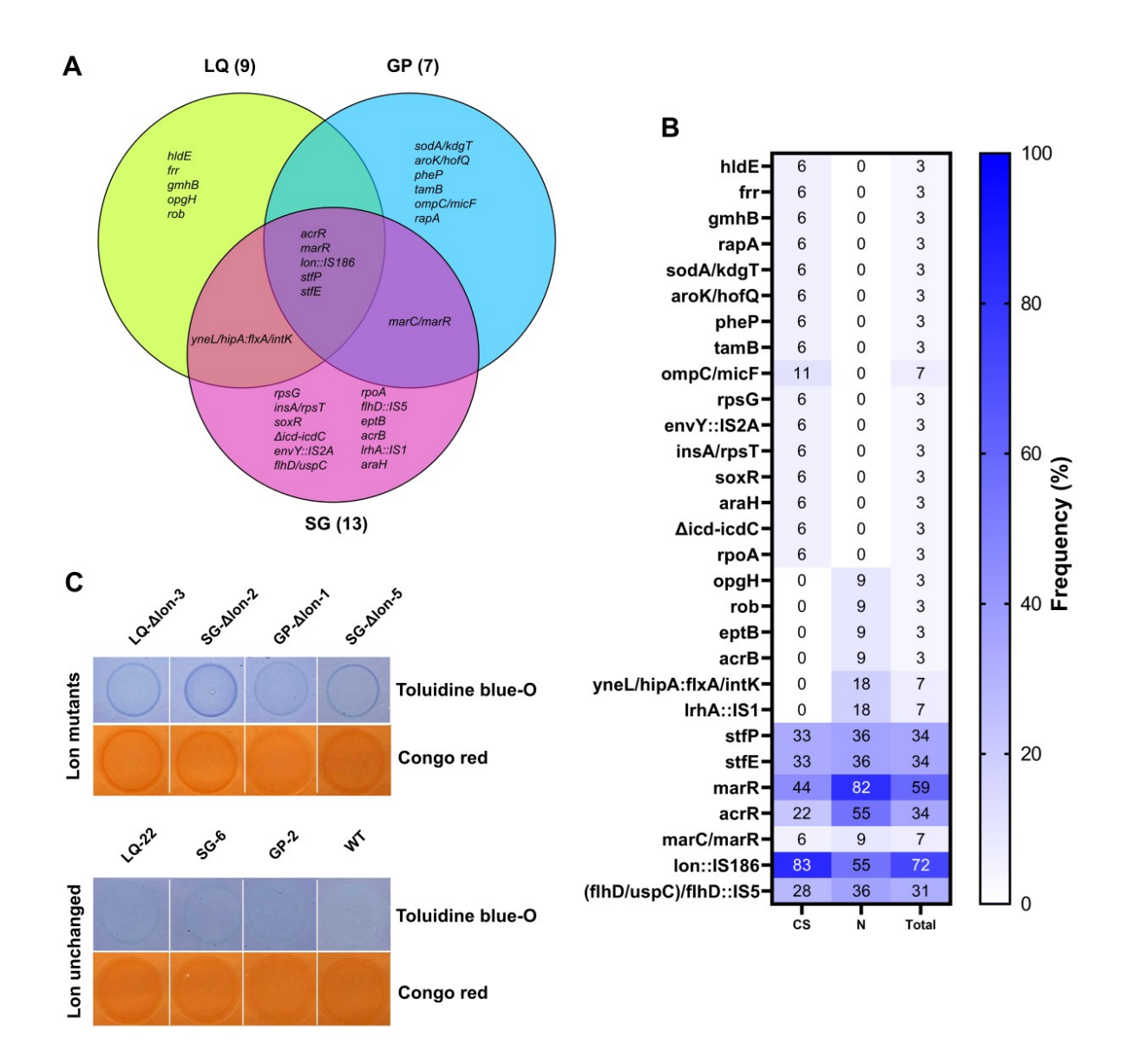
Next, we screened for CS towards POL and gentamicin GEN in the TIG-resistant lineages [52] and NIT and streptomycin (STR) in the PIP-resistant lineages [52,128]. A large proportion of TIG-resistant lineages exhibited CS to POL: ~86% from LQ, ~96% from GP, and ~39% from SAGE (Figure 4.1D) (Supplementary Figure 4.1). We previously reported the presence of reciprocal CS between the POL -TIG pair [306]. CS towards GEN was low in all platforms, with LQ and GP showing CS in ~26% of lineages and SAGE in only ~4% (Figure 4.1E) (Supplementary Figure 4.1). Cross resistance (CR) towards POL was almost entirely absent, and CR to GEN was present at very low frequencies (Figure 4.1D, E) (Supplementary Figure 4.1).

CS towards NIT was rare in the PIP-resistant lineages, present in only ~17-25% of the LQ and GP strains and absent in the SAGE strains (Figure 4.1F) (Supplementary Figure 4.1). By contrast CR was common in the SAGE lineages, with ~42% less susceptible to NIT (Figure 4.1F) (Supplementary Figure 4.1). About 50% of the PIP-resistant lineages from LQ and GP, and 21% from SAGE showed CS towards STR (Figure 4.1G) (Supplementary Figure 4.1). ~20% of the SAGE mutants showed CR towards STR, but again this CR was rare in the other two platforms. Overall, ~16% of SAGE mutants showed CS compared to 49% and 47% from LQ and GP

respectively (Figure 4.1H). Incidence of CR in SAGE mutants was much higher at about 21% than the 4-6% in LQ and GP mutants (Figure 4.1H).

4.2.2. Tigecycline resistance evolves via similar pathways across ALE platforms

To compare the genomic adaptations of lineages evolved through the three different platforms and to identify differences in mutational profiles between strains that evolved CS and strains that did not, we whole genome sequenced 29 lineages adapted to TIG: nine from LQ (six with POL CS and three neutral), seven from GP (six with POL CS and one neutral) and 13 from SAGE (six with POL CS, six neutral, and one with POL CR) (Figure 4.2A). The genome profile of the lineage that showed POL CR from SAGE was a complete subset of the mutations appearing in the CS lineages, and was excluded from further analysis suspecting a two-fold random variation in MIC [307]. Lineages acquired ~1.2 mutations per strain from LQ, ~1.7 strain from GP, and ~1.5 mutations per strain from SAGE (Figure 4.2A). SAGE generated several mutations unique from the other platforms, presumably because it selects for mutants that have improved growth rates and motility [145,241] which are often seen as compensatory mutations in antibiotic resistant bacteria [110– 113,119,172]. Strains from all platforms showed mutations in one or more of the following genes involved in TIG resistance: lon, acrR, and marR (Figure 4.2A) (Supplementary Figure 4.2A). Deactivation of the Lon protease, often achieved via mutations in its promoter region, spares the MarA, RamA and SoxS activators from degradation, increasing expression of genes that mediate resistance like acrAB [126,308]. Mutations in AcrR and MarR more directly relieve repression of the acrAB and marRAB operons, increasing efflux activity to drive TIG resistance [308]. The primary method by which TIG resistance evolved is therefore through increased expression of efflux pumps, regardless of the evolutionary system.



D

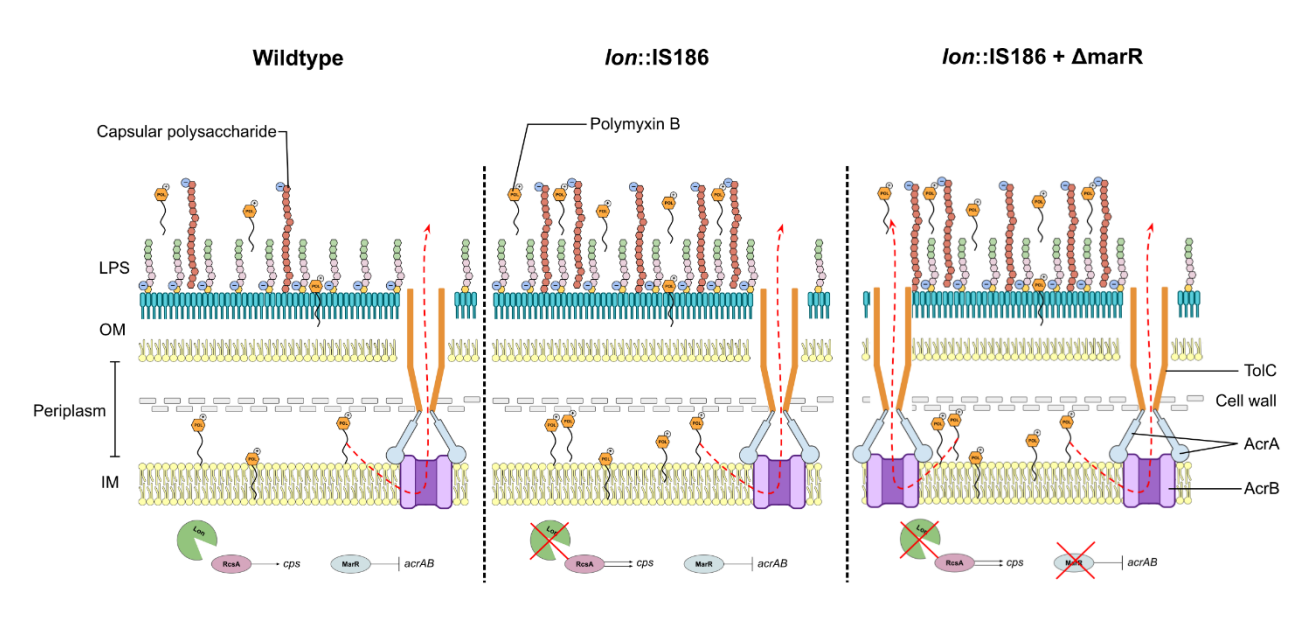


Figure 4.2 Genomic and phenotypic analysis reveals mechanism of POL CS in TIG resistant mutants.

(A) Venn diagram showing common mutations between TIG mutants evolved from the three different platforms. The numbers in brackets denote the total number of mutants sequenced from that platform. (B) Frequency at which a mutation in the genes listed on the vertical axis appeared in all 29 mutants sequenced in this study, stratified by POL CS and N. "Total" denotes frequencies at which a mutation appeared among all strains. "sodA/kdgT" refers to an intergenic mutation between the genes sodA and kdgT. "envY::1S2A" denotes that gene envY was interrupted by the insertion element IS2A. "Δicd-icdC" refers to a deletion that affects all genes between and including icd and icdC. "yneL/hipA:flxA/intK" refers to a new junction between the intergenic regions of yneL/hipA and flxA/intK. Two different flhD mutations: (flhD/uspC) and flhD:IS5 were grouped together and reported as "(flhD/uspC)/flhD:IS5". (C) Toluidine blue-O and Congo red binding assays for four randomly picked Lon mutants and four with Lon intact. The strain IDs of the mutants are noted at the top of the panels. Strain IDs contain information about the platform used, and the lineage that was picked. For example, "LQ-Δlon-3" = Lon mutant from the LQ platform, with "3" denoting that it is the third lineage out of the 22 generated through this platform. "LQ-22" = the 22nd lineage from the platform, with no mutation in Lon. WT = wildtype. (D) The role of Lon and MarR mutations in POL CS. Left panel: WT cells. Lon degrades RcsA, limiting the expression of capsular polysaccharide genes (cps). MarR expression negatively regulates AcrAB expression. Middle panel: Lon deactivation to evolve TIG resistance spares RcsA from

degradation, allowing expression of cps genes and causing the production of capsular polysaccharides. Increased negative charge on the membrane due to these polysaccharides causes increased accumulation of the polycationic POL, making cells more susceptible to POL. Right panel: MarR deactivating mutations associated with TIG resistance allow increased AcrAB expression, increasing the number of efflux pumps that are able to pump out POL molecules, neutralizing POL CS.

4.2.3. Polymyxin collateral sensitivity is linked to Lon protease deactivation

While POL CS in TIG-resistant *E. coli* has been previously reported [52,306], the mechanism of POL CS remains unknown. Since CS was abundant in strains evolved through all three platforms, we hypothesized that mutation(s) that 1) occurred in all three platforms, 2) appeared frequently and 3) appeared more frequently in strains exhibiting CS may be responsible for POL CS. We tallied the frequencies of each mutation stratified by CS and neutrality (Figure 4.2B) (Supplementary Figure 4.2) and found that the *lon*::IS186 mutation, previously reported to be a mutation hotspot [309], was the only mutation that met these criteria (Figure 4.2B) (Supplementary Figure 4.2).

Cells that lack Lon activity accumulate the transcriptional regular RcsA, which is a positive regulator of capsular polysaccharide (exopolysaccharide) synthesis [310,311]. Increased exopolysaccharides has been shown to increase sensitivity to POL by increasing concentration of POL around the outer membrane in *Klebsiella* [312]. We hypothesized that our TIG-resistant Lon mutants were overproducing exopolysaccharides, which in turn were making them more susceptible to POL. To test this, we randomly picked and grew three strains with the Lon mutation, three without the Lon mutation, and one with both the Lon and marR mutations on plates

containing toluidine blue-O, congo red and ruthenium red. Toluidine blue-O binds to negatively charged polysaccharides, congo red binds to amyloid fibers like curli, and ruthenium red binds to acidic exopolysaccharides [313]. The Lon mutants were preferentially stained by toluidine blue-O and congo red (Figure 4.2C), confirming that our Lon mutants overproduced exopolysaccharides. We did not see any difference between colonies grown on ruthenium red (data not shown). Based on these results, we propose that *lon*::IS186 mutants overproduce negatively charged exopolysaccharides which increase POL accumulation around the cells, rendering them hypersensitive towards the antibiotic (Figure 4.2D).

4.2.4. MarR deactivation neutralizes Lon deactivation-driven polymyxin collateral sensitivity

If Lon mutations produced the POL CS phenotype in the TIG resistant cells, resistance to TIG that did not confer POL CS must have either occurred via a different pathway, or the CS effect of the Lon mutation may have been masked via secondary mutations. Candidate mutations that occurred frequently and preferentially in cells that remained neutral to POL were in the efflux regulators acrR and marR (Figure 4.2B) (Supplementary Figure 4.2), known to confer resistance to TIG [314,315]. This suggests that cells that bypass Lon mutations to achieve resistance via efflux upregulation avoid POL CS.

Fifty-five percent of the neutral strains also exhibited the Lon mutation (Figure 4.2B). How do strains that carry this mutation mask the CS phenotype? To answer this question, we narrowed our analysis to the SAGE mutants where we had an equal distribution of cells with CS and neutral phenotype sequenced (Supplementary Figure 4.2). While 100% of the neutral strains had a MarR mutation, 67% of them also carried the *lon*::IS186 mutation. Since deactivation of MarR allows

upregulation of TIG and POL efflux [126,308,316], we hypothesized that deactivation of MarR on a *lon*::IS186 background neutralizes the CS phenotype associated with Lon mutants (Figure 4.2D). To test this, we constructed the pUC57-marR plasmid and introduced it into four POL-neutral strains that showed both the marR and *lon*::IS186 mutations. Strain 3 showed a 2 bp deletion mutation and strain 5 introduced a premature stop codon in marR (Table 4.1) which should both significantly reduce or completely abolish marR activity [317]. Mutation in the 104th amino acid that changes the glycine carried by strain 4 (Table 4.1) has been associated with reduced *marR* activity [318]. The AAGGCTGG duplication causes a frameshift mutation which should also affect marR activity (Table 4.1) [319]. Introduction of pUC67-marR converted three of the four strains from neutral to CS to POL, and increased susceptibility in the wildtype strain (Table 4.1). This suggested that cells that mutated MarR gained the ability to resist POL at a magnitude large enough to neutralize CS due to the *lon*::IS186 mutation. Reintroduction of MarR on a plasmid then reduced efflux levels, reverting the effects of the MarR mutation.

Table 4.1 Changes in POL MIC after introduction of the pUC57-marR plasmid in strains with different MarR mutations.

Strain	MarR allele	POL MIC (μg/mL)
WT	-	0.25
TIG-SG-N-3	Δ2 bp coding (428-429/435 nt)	0.25
TIG-SG-N-4	G104S	0.25

TIG-SG-N-5	Q117*	0.25
TIG-SG-N-7	$(AAGGCTGG)_{1\rightarrow 2}$	0.25
WT + pUC57	-	0.25
TIG-SG-N-3 + pUC57	Δ2 bp coding (428-429/435 nt)	0.25
TIG-SG-N-4 + pUC57	G104S	0.25
TIG-SG-N-5 + pUC57	Q117*	0.25
TIG-SG-N-7 + pUC57	$(AAGGCTGG)_{1\rightarrow 2}$	0.125
WT + pUC57-marR	-	0.125
TIG-SG-N-3 + pUC57-marR	Δ2 bp coding (428-429/435 nt)	0.125
TIG-SG-N-4 + pUC57-marR	G104S	0.125
TIG-SG-N-5 + pUC57-marR	Q117*	0.125
TIG-SG-N-7 + pUC57-marR	$(AAGGCTGG)_{1\rightarrow 2}$	0.125

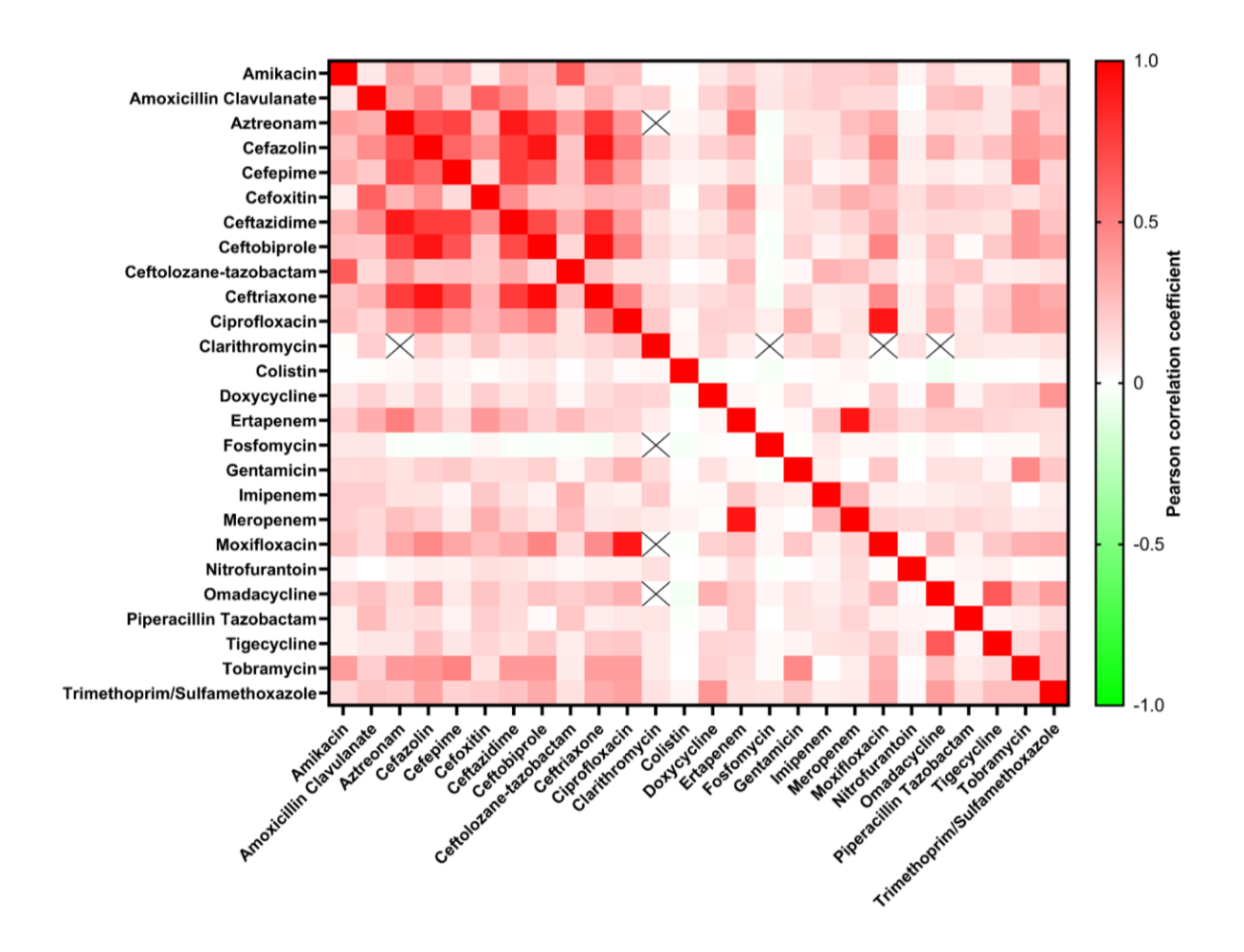
MarR mutations cannot completely explain neutrality: a significant number of strains that carried *marR* mutations showed CS towards POL (Figure 4.2B) (Supplementary Figure 4.2). Additional mutations in these strains such as HldE (D-beta-D-heptose 7-phosphate kinase), GmhB (D-

glycero-beta-D-manno-heptose-1,7-bisphosphate 7-phosphatase) and TamB (translocation and assembly module subunit) (Figure 4.2B) (Supplementary Figure 4.2) involved in LPS biosynthesis and maintenance [126,320,321] and may have played a role in POL sensitivity.

4.2.5. Strong intra-class cross-resistance, but not collateral sensitivity, is prevalent in clinical E. coli

The goal of identifying any CS relationship is to ultimately apply it in antibiotic sequences or combinations that are resilient against resistance evolution in the clinic. To test for the presence of collateral effects of resistance in pathogenic *E. coli*, we calculated the Pearson correlation coefficients between MIC data to serve as a proxy for cross resistances and collateral sensitivities from 779 uropathogenic *E. coli* strains from the CANWARD surveillance study (Supplementary Table 4.2) [322]. We identified strong cross-resistance between drugs of the same class, particularly between β-lactams (Figure 4.3A). Very little negative correlation (collateral sensitivity) was present in the dataset, which appears to be common in clinical datasets [323]. The largest negative correlation of -0.05 was seen between omadacycline (OMC) and colistin (COL).





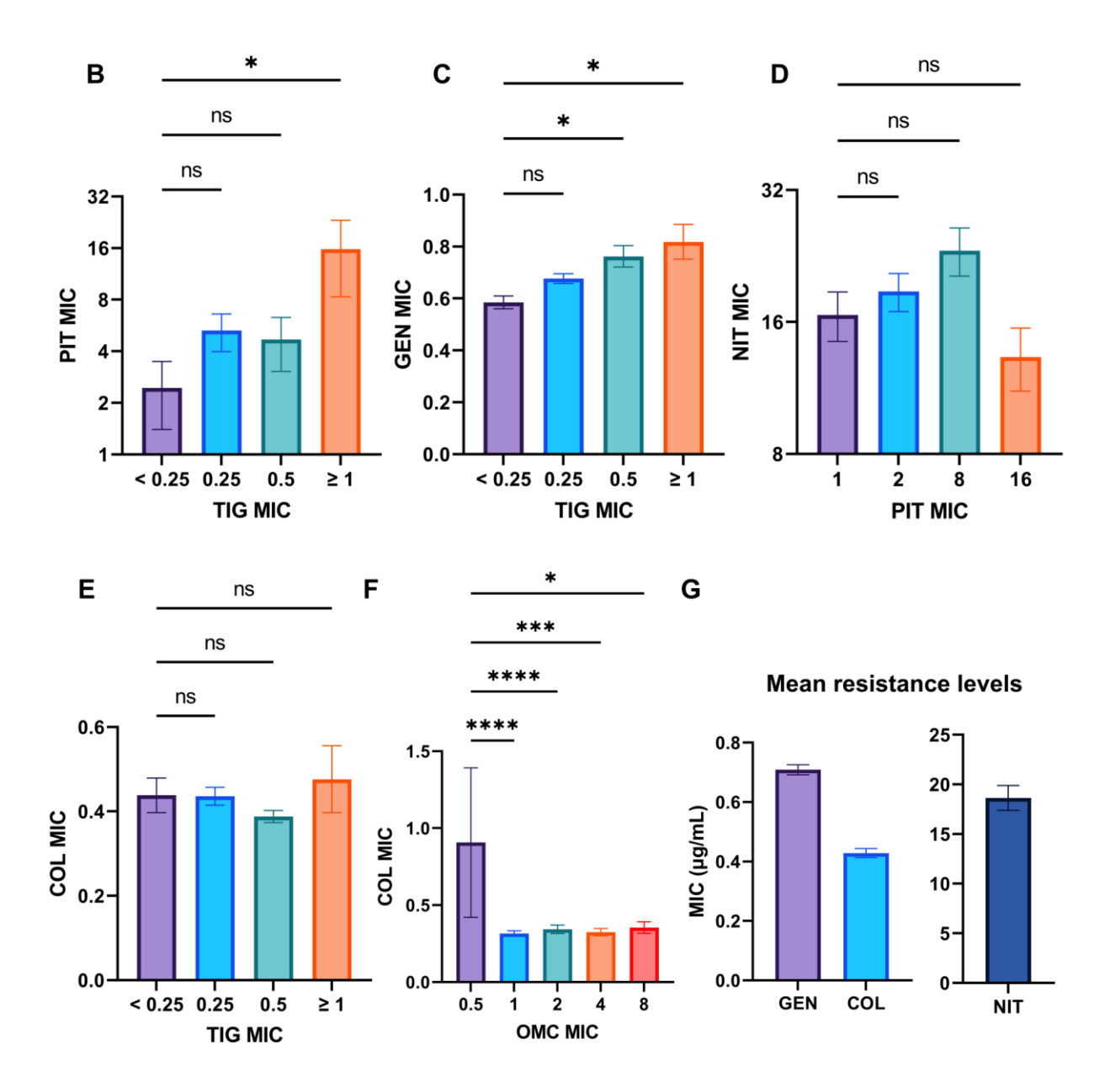


Figure 4.3 Uropathogenic *E. coli* antimicrobial susceptibilities reveal a rare CS relationship predicted by laboratory evolution.

(A) Pearson correlation coefficients between MICs of each antibiotic with every other antibiotic in the dataset. A value of 1 denotes a perfect positive correlation (strong CR), 0 denotes no correlation, while a -1 denotes a perfect negative correlation (strong CS). (B) - (F) Relationship between resistances to drugs labelled on the x- and y-axes. *p<0.05, ****p<0.001, ****p<0.0001, one-way ANOVA with Bonferroni correction. (G) Mean resistance levels of antibiotics on the x-axis from the whole dataset.

4.2.6. CS relationships rarely appear in clinical strains and their prevalence is best predicted by SAGE

We looked more closely at the clinical antibiotic susceptibility data to identify smaller changes in resistance. Specifically, we looked at the TIG-GEN, PIP-NIT and TIG-POL relationships to compare with our ALE results. PIP-STR was not included since STR was not among the drugs in the clinical dataset. Since our ALE adaptations only included chromosomal changes, it was important to limit our analysis to resistance conferred by chromosomal mutations instead of mobile elements. TIG is unaffected by Tet(M), tet(A), tet(B),tet(C), tet(D), and tet(K) mobile resistance determinants [324]. Plasmid-encoded tet(X) genes that code for TIG inactivating enzymes and confer high TIG resistance with MICs ranging from 8-16 μg/mL are rare [325,326], and our dataset did not contain TIG MICs >2 μg/mL. Chromosomal TIG resistance generally arises from increased efflux mediated by AcrAB-TolC in *E. coli* [308], and to further confirm that TIG resistance was largely chromosome mediated in our clinical dataset, we hypothesized that PIT (piperacillin/tazobactam) resistance should go up with increasing TIG resistance since PIP is susceptible to efflux. As expected, PIT resistance did increase with increasing TIG MIC in the clinical strains (Figure 4.3B).

Next, we looked at how GEN MICs varied with increasing TIG MIC. We removed GEN MICs > 4 μg/mL from the analysis because these MICs were more likely to be conferred by plasmid-borne aminoglycoside modifying enzymes [327]. We observed a steady increase in GEN MICs with increasing TIG MIC among the remaining isolates (Figure 4.3C). From our ALE experiments, LQ and GP showed CS in over 25% of the strains, but SAGE in ~4%, while CR was present in 17% of strains (Figure 4.1E) (Supplementary Figure 4.1).

NIT MIC changes with PIT resistance did not reach statistical significance, but showed an increasing trend up to 8 μ g/mL of PIT resistance. From the ALE results, LQ and GP lineages showed CS in 17-25% of the strains with none from SAGE (Figure 4.1F) (Supplementary Figure 4.1). Over 40% of the SAGE lineages were cross-resistant to NIT (Figure 4.1F) (Supplementary Figure 4.1).

POL was not included in the clinical antimicrobial susceptibility data, so we examined the TIG-colistin (COL) relationship instead. Colistin and POL have very similar structures and near-identical activity *in vitro* [328]. For the first time in the analysis, we see small but statistically insignificant reductions in COL resistance with up to 0.5 μg/mL of TIG MIC (Figure 4.3E). During this analysis, we observed that mean COL resistance dropped significantly with resistance to another third generation tetracycline, omadacycline (OMC) (Figure 4.3F, G) [329]. As OMC MIC increased from 0.5 to 1 μg/mL, COL MIC dropped ~three-fold (Figure 4.3F). ~86-96% of LQ and GP lineages and ~39% of SAGE lineages showed CS to POL (Figure 4.1D) (Supplementary Figure 4.1).

4.3. Discussion

In this study we investigated the repeatability of CS evolution in four reported drug pairs. With large sample sizes of 20-24 lineages we examined three different ALE platforms, testing the robustness of CS interactions to changes in evolutionary conditions and identifying possible ALE-specific biases. We found that SAGE allowed rapid evolution of high level resistance to antibiotics while still producing core resistance-conferring mutations comparable to other ALE platforms

(Figure 4.1B, C) (Figure 4.2A) (Supplementary Figure 4.2). SAGE consistently produced lower frequencies of CS and higher cases of CR compared to the serial transfer and gradient platingbased methods (Figure 4.1D-G) in the TIG - GEN, PIP - NIT and PIP - STR drug pairs. This best matched antimicrobial susceptibility data from over 750 clinical MDR E. coli strains, in which CR and neutrality were abundant but indications of CS relationships were almost entirely absent (Figure 4.3A). Importantly, we found no negative correlations between TIG - GEN, PIP - NIT and PIP - STR, and instead found evidence of cross-resistance (Figure 4.3C-E). This suggests that while CS relationships may regularly appear through laboratory evolutions, their application in the clinic needs to be carefully assessed. If the effect of CS is minimal in clinical strains, the usefulness of CS relationships elucidated from ALE experiments may be inflated. Out of the four drug pairs tested, SAGE produced substantial CS in only one of them, the TIG - POL pair (~39%; Figure 4.1D, H). From the clinical data, we observed that resistance to COL decreased with another thirdgeneration tetracycline, omadacyline (Figure 4.3F) [329]. The fact that this CS relationship appeared frequently in all three ALE platforms (Figure 4.1D) and held among MDR clinical strains suggests that this could be potentially exploitable to select against resistance, and that SAGE may be able to predict these important relationships.

We previously showed the presence of reciprocal CS between the TIG-POL drug pair [306], but the mechanism of CS was unknown. In this study we showed that tigecycline resistant Lon mutants produced increased extracellular polysaccharides, rendering them more susceptible to POL. From the ubiquity of the Lon mutations in our data and prior reports, it is likely that this mutation is the first step towards clinical TIG resistance [308,330], and hence the COL sensitivity in clinical strains may be driven by the same mechanism. Cells may bypass the CS to POL by either

increasing efflux through mutations in regulators like MarR, or by acquiring second step efflux regulator mutations after Lon deactivation (Figure 4.2B-D), suggesting the observed COL sensitivity may be transitory or that increased efflux may have undetected fitness costs.

Second step mutations in efflux regulators AcrR and MarR appeared more frequently in SAGE compared to LQ and GP (Supplementary Figure 4.2) and could partly be responsible for the low CS in SAGE lineages. In contrast to our findings, one study showed that accumulation of second step resistance mutations conferred collateral sensitivity over resistance to antibiotics [133]. However, in that study, efflux mutations were the first step mutations, with second step mutations conferring the CS they observed [133]. This is in line with our and others' findings that efflux mutations often confer broad-spectrum CR [107,331]. Another study showed how CS varies at a population level, with lineages that showed CS early during evolution getting replaced by mutants that acquired changes in genes with milder CS effects [134]. Results from this study suggest that this can also occur at the strain level. Together, we suggest that the evolutionary timeline of CS cannot be generalized and must be studied on a case-by-case basis, possibly at the antibiotic and the bacterial species level.

The usefulness of CS has been debated, due in part to its dependence on the repeatability of evolution [54]. Our results show that CS can indeed often appear at only low frequencies (Figure 4.1E-G), and is strongly linked to the specific mechanism by which cells become resistant. Our highly repeatable TIG-POL CS relationship was dependent on selection of the same *lon*::IS186 mutation across almost all sequenced lineages that exhibited CS. While this limits the number of CS interactions that may be worth pursuing, this also offers hope that robust CS that appear in

complicated evolutionary landscapes in healthcare may be achieved via targeting collateral effects tied to readily accessible mutational hotspots.

From our attempts at evolving large sample sizes against multiple antibiotics via the different ALEs, we found that generating large numbers of resistant mutants was easier with SAGE (Supplementary Table 4.1), though the number of mutations per strain and the core resistance determinants selected for were similar to the other platforms tested (Figure 4.2A). This should facilitate ALE experimentation at scale in laboratories that do not have ready access to robotics.

Overall, we discovered a mechanism by which TIG resistance reliably conferred CS to POL by leveraging large scale laboratory evolution and showed that these biological effects were observed and reproducible in more than 750 clinical MDR *E. coli* strains. We highlighted the importance of large scale ALE experiments to generate robust profiles of collateral effects and showed that SAGE better predicts CS relationships that can help reduce antibiotic resistance in the clinic.

4.4. Materials and Methods

4.4.1. Bacterial strain and growth conditions

E. coli K-12 substr. BW25113 (WT) was grown aerobically at 37 °C with 250 rpm shaking in Muller Hinton (MH) broth. All evolved mutants were grown in MH broth supplemented with appropriate concentration of antibiotics.

4.4.2. Susceptibility assays

MICs were performed using the EUCAST standard broth microdilution method [332].

4.4.3. ALE experiments

SAGE, serial transfer and gradient plating-based evolutions were performed as described before [48,50,51,107,145,306]. To prepare a SAGE plate, MH media with 0.15% agar was stirred and heated, followed by slow addition of 0.2% xanthan gum before autoclaving [20]. This liquid was supplemented with antibiotics and poured into 4-well plates that were propped up on one side using p1000 pipette tips. After this layer was set, a second layer of antibiotic free medium was added to create an even surface, and plates were incubated overnight at room temperature to allow diffusion. For SAGE, the maximum concentration of antibiotics are listed in the table below. Maximum concentrations were determined from experiments to determine suitable concentrations that consistently generated mutants above clinical breakpoints. All SAGE plates were incubated for a fixed duration of seven days, which we found to be sufficient for cells to reach the end of the plates [306,333]. For serial transfers, evolutions were started at 1/8th the WT MIC of the antibiotic by transferring 1 µL of overnight culture of WT bacteria into 99 µL of MH broth containing appropriate concentration of the antibiotic. Plates were incubated for 18-20 h, then 1 µL from all wells showing growth were transferred onto the 1/4th MIC plate and so on, until the concentration listed in the table below was reached (i.e., a total of six transfers). Passaging beyond the listed concentration incurred significant loss of strains due to extinctions. For gradient plates, maximum antibiotic concentrations are listed below. Plates were made in square dishes (Falcon, Cat. No.:

351112) and were streaked towards the higher end of the antibiotic gradient after 18-20 h of incubation until growth was observed within the last grid of the plates.

Antibiotic	Maximum concentration in SAGE
TIG	5 μg/mL
PIP	40 μg/mL

Antibiotic	Maximum concentration evolved to during
	serial transfers
TIG	4x MIC, 1 μg/mL
PIP	4x MIC, 4 μg/mL

Antibiotic Maximum concentration in l		Days taken to reach end of	
	gradient plates	plates	
TIG	5 μg/mL	5 days	
PIP	80 μg/mL	5-7 days	

4.4.4. Whole genome sequencing and analysis

Genomes were extracted using the Bio Basic genomic DNA kit (Cat. no.: BS624). Sequencing and variant calling was performed by Sequence (USA), on an Illumina NextSeq 2000. Variant calling was carried out using Breseq (80). Reference sequence CP009273.1 was used for variant calling.

All mutations reported had a frequency of a 100% over a sequencing depth of ~100-120x. Coverage of 99-100% was achieved for all mutants sequenced. WGS data is available under the NCBI Sequence Read Archive BioProject: PRJNA1220725NCBI. Figure 4.2 and Supplementary Figure 4.2 were built using R and GraphPad Prism.

4.4.5. Exopolysaccharide assay

MH + 1.5% agar was separately supplemented with 150 μ g/ml Congo red, 40 μ g/ml toluidine blue O or 40 μ g/ml ruthenium red (AK Scientific) [313]. All plates also contained 0.5 μ g/mL of TIG. 10 μ L of overnight cultures grown in MH broth + 0.5 μ g/mL of TIG were spotted onto these plates.

4.4.6. MarR complementation

The MarR fragment was synthesized based on its sequence available in the NCBI reference sequence CP009273.1, and inserted into the pUC57 MCS by Bio Basic Inc. The ligated plasmid was sequence verified before use in experiments. Cells were chemically transformed separately with the empty vector or pUC57-marR [334]. We determined from separate experiments with this plasmid that IPTG induction was not required for sufficient marR production: cells transformed with this plasmid showed reduced efflux activity as measured by chloramphenical resistance [164] but increasing concentrations of IPTG did not significantly change this resistance level (data not shown).

4.4.7. Clinical strains and data analysis

Antibiotic susceptibility data of 779 uropathogenic *E. coli* strains was obtained from the CANWARD surveillance study [322]. The Pearson correlation coefficients and MIC data extraction were performed using custom Python scripts.

4.4.8. Data and materials availability:

WGS data is available under the NCBI Sequence Read Archive BioProject: PRJNA1220725.

Chapter 5. Sequential antibiotic exposure restores antibiotic susceptibility

Chowdhury FR and Findlay BL; *Journal of Antimicrobial Chemotherapy* (revisions submitted as of writing this thesis).

Preprint available (under an older version of the title of this paper) at: doi.org/10.1101/2024.11.06.622341

5.1. Introduction

Antibiotic resistance is associated with 4.7 million deaths every year and is projected to claim 40 million lives by the year 2050 [12,335]. As pathogens are adapting to antibiotics faster than new drugs can be developed, alternative strategies to curb resistance are necessary [336]. One proposed strategy is to use existing drugs to design sequential or cyclic antibiotic treatment regimens with drugs applied one after the other at either defined time intervals or as resistance successively emerges [83,107,117]. Rapid switching delays but does not halt the evolution of resistance, and so as resistance emerges to drug A the cycle degrades. Proper selection of drug B is proposed to increase the time required for multidrug resistance to emerge, or even allow resensitization to A [83,123].

A few studies have proposed specific drug pairs for cyclic antibiotic therapy [128,337], but large scale evolutionary studies that probe the frequencies at which these pairs successfully hinder evolution or reverse resistance (resensitize) are missing. These effects must be evolutionarily repeatable to be useful in therapy [139]. In this work, we leverage the soft agar gradient evolution (SAGE) platform [69,107] to sequentially evolve resistance against four drug pairs proposed for cyclic therapy in 16 replicate populations of *Escherichia coli* K-12 substr. BW25113. We show that the drug pairs gentamicin (GEN) – piperacillin (PIP) and PIP – GEN drive 50% of the populations extinct, while the other two: ciprofloxacin (CIP) – GEN and polymyxin B (POL) –

tigecycline (TIG) do not hinder resistance evolution. Upon the evolution of resistance to the second drug in the cycle the GEN – PIP pair showed no significant GEN resensitization, the PIP – GEN and CIP – GEN pairs produced a 2-fold reduction in mean resistance to the first drug, while the POL – TIG pair showed a 64-fold reduction in POL resistance in every replicate population tested. To date, extinctions and resensitizations in cyclic therapy have been theoretically linked to forward collateral sensitivity (CS), where resistance to the first drug A in the cycle causes CS to the second drug B. In our data, we find no correlation between forward CS within drugs and extinctions or resensitizations. However, we find that if resistance to drug B in naive cells frequently produces CS to drug A, cells initially resistant to drug A are often rendered more susceptible to A when resistance to B emerges (Figure 1). We term this CS interaction backward CS (Figure 1), since CS to A evolves with resistance to B (CS direction: B to A) but antibiotics are applied in a sequence of A to B. To elaborate, consider a situation where the sequential treatment regimen is the application of antibiotic A, followed by the application of antibiotic B (treatment direction: A to B). If, via susceptibility measurements, it is determined that resistance to antibiotic A in naive bacteria induces CS to antibiotic B, we would say that this antibiotic sequence exhibits forward collateral sensitivity. If, instead, resistance to antibiotic B is known to induce CS to antibiotic A in naive bacteria, we would say that this antibiotic sequence exhibits backward collateral sensitivity. We find that backward collateral sensitivity helps bring down resistance levels even when bacteria sequentially acquire resistance to A and then B. We illustrate the role of forward and backward CS this by showing that in the aminoglycoside-β-lactam pair gentamicin and piperacillin, gentamicin resistant populations exhibit widespread forward CS towards piperacillin, but subsequent exposure of cells with piperacillin CS to piperacillin does not lead to increased extinctions or significant gentamicin resistance reduction. However, when we expose PIP resistant bacteria to GEN (PIP – GEN pair; frequent CS in the opposite direction: backward CS), we see a 2-fold reduction in median PIP resistance. We use whole genome sequencing and efflux measurements to show that this reduction is driven by the weakening of PIP efflux in the GEN adapted strains. The effects of backward CS extend beyond the GEN – PIP pair, and we find polymyxin B (POL) – tigecycline (TIG) to be a pair that highly favors resensitization to POL. Our results show the importance of considering the direction of CS and drug switching in designing effective cyclic therapies.

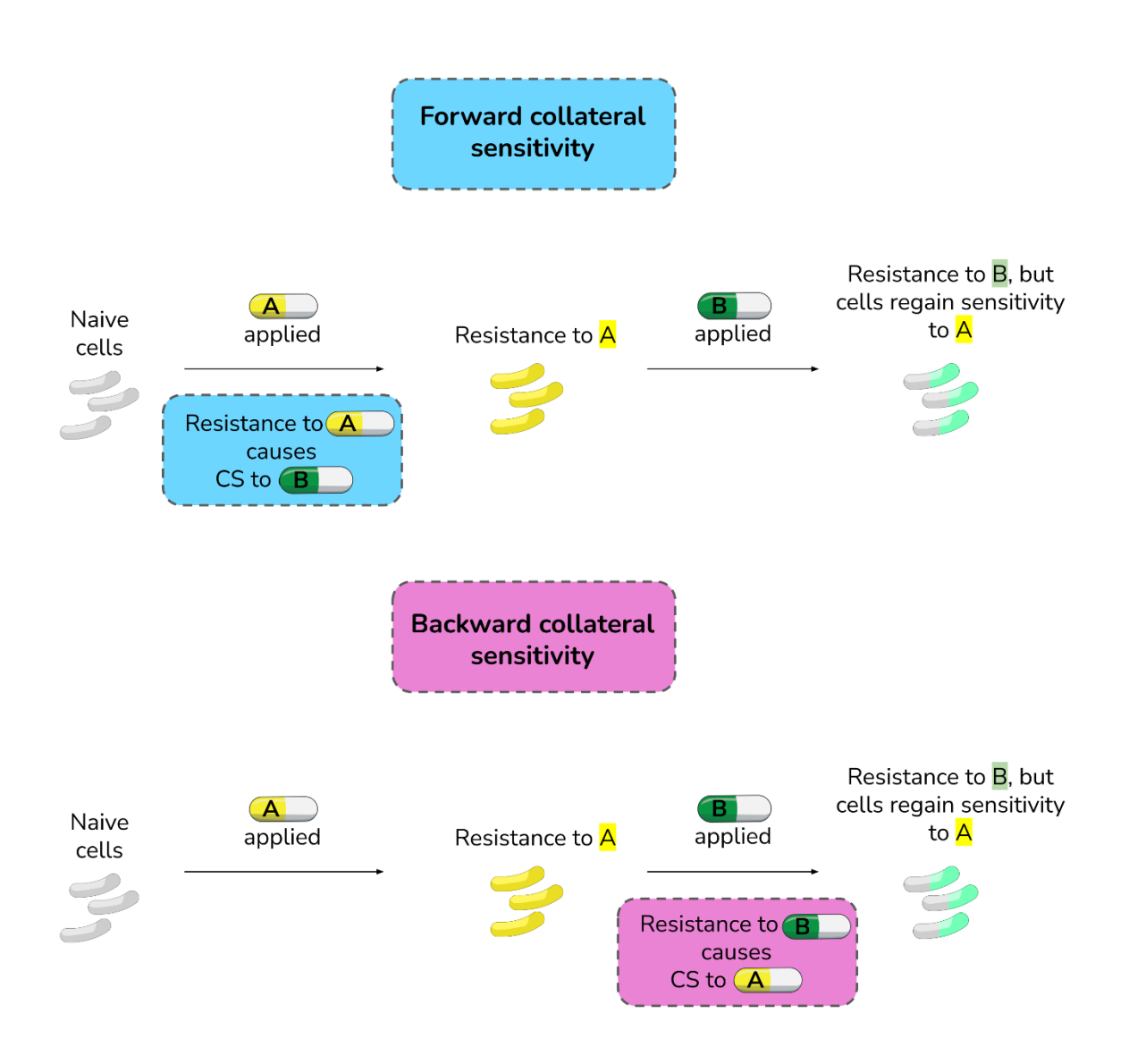


Figure 5.1 The concept of forward and backward collateral sensitivity.

5.2. Results

5.2.1. A SAGE-based evolution platform to test pairwise drug sequences

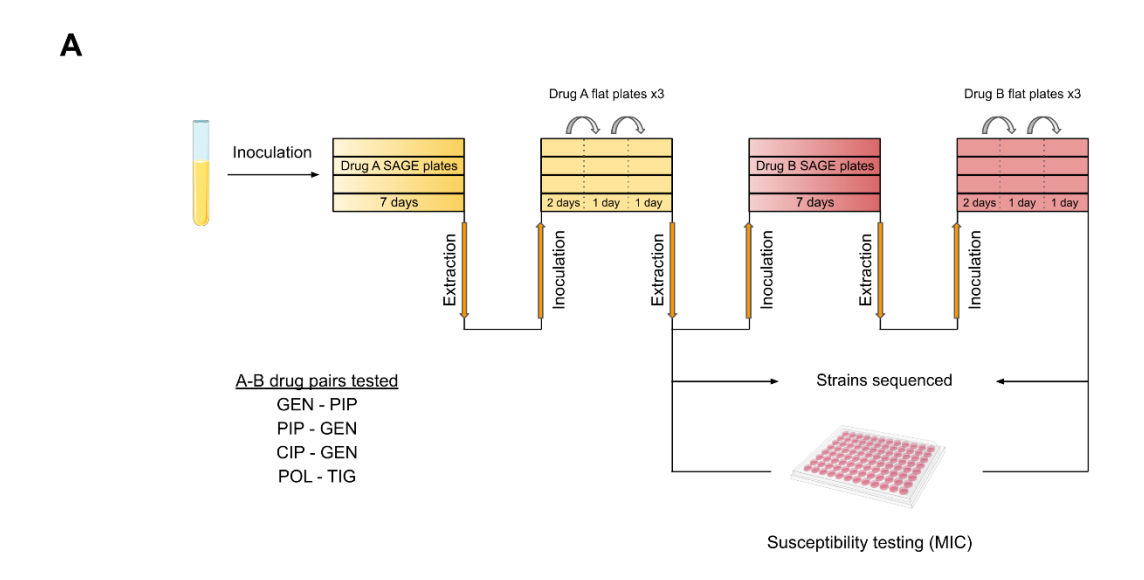
We began with four drug pairs proposed for cyclic therapies with reported forward CS between either the drugs or the drug classes: gentamicin (GEN) – piperacillin (PIP) [128], PIP – GEN [128,337], ciprofloxacin (CIP) – GEN [53], and polymyxin B (POL) – tigecycline (TIG) [337].

First, we used SAGE to generate 16 independent replicates of Escherichia coli K-12 substr. BW25113 (WT) that were resistant to the first component of each drug pair at levels above clinical breakpoints [69] (Figure 5.2A). The sole exception was POL, where we generated 15 strains. Highlevel POL resistance was infrequent, and to generate 15 lineages required 88 starting replicates. Next, we passed these mutants through soft agar "flat plates" three times in series (Figure 5.2A). These plates contained the antibiotic from the prior challenge, at a concentration equal to half the minimum inhibitory concentration (MIC) of the antibiotic following SAGE. We included flat plates for three reasons: 1) general growth defects like slow growth rates, common after genomic adaptation to antibiotics [75] can appear as false CS during MIC plate readouts [337], 2) there were conflicting reports about the stability of CS [128,338], and 3) we wanted to study CS interactions that are not easily reverted via compensatory mutations. We previously showed that flat plates accelerate movement of chloramphenicol-resistant strains through soft agar, significantly improving growth rates in liquid media and allowing for resistance evolution to a subsequent antibiotic at near-wildtype frequencies [107]. We find here that the effect is general, with similar effects on GEN resistant strains (Figure 5.2B). Replicates were then screened for resistance to the challenge antibiotic and for CS towards the second drug in the pair (Figure 5.2C, D). After SAGE evolution, the majority of the strains exhibited resistance levels above clinical breakpoints [339] for all the antibiotics tested (Figure 5.1C). WT MICs are listed in Table 5.1.

Table 5.1 WT MICs.

Antibiotic	MIC (μg/mL)
GEN	0.5

PIP	1
CIP	0.0625
POL	0.25
TIG	0.25



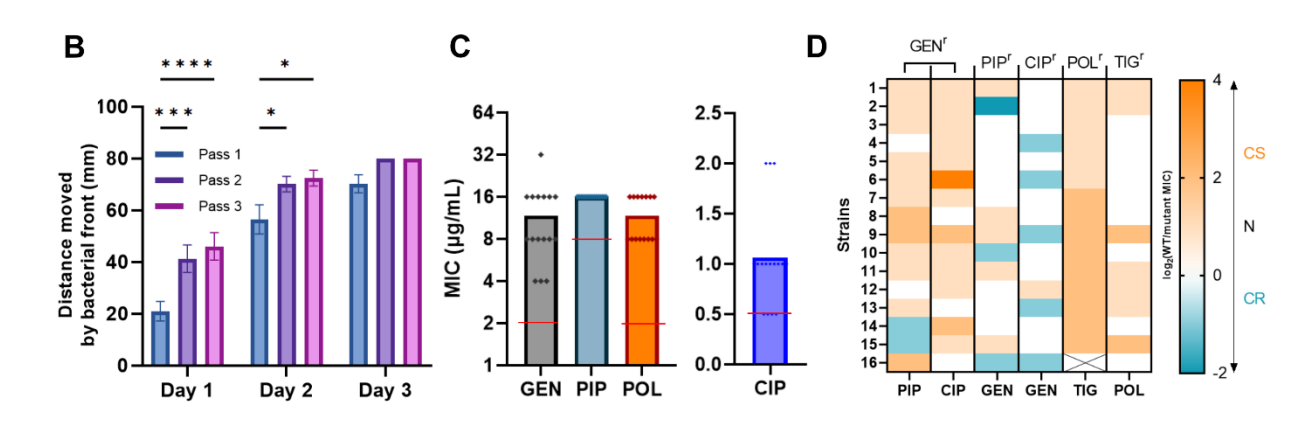


Figure 5.2 A SAGE-based evolution platform to study sequential antibiotic application.

(A) Bacteria were inoculated in parallel into SAGE lanes containing antibiotic gradients, then incubated to generate resistant mutants. After 7 days, mutants were harvested and passed through three successive flat plates containing sub-inhibitory concentrations of the initial antibiotic. (B) Flat plates improve bacterial fitness in GEN resistant cells, as

measured by distance swam (n= 16). (C) Following SAGE bacteria are resistant at or above clinical breakpoints. Red lines indicate the resistance breakpoints (n= 15 for POL, n= 16 for all other antibiotics). (D) Heatmap showing CS interactions between drugs. Bacteria are resistant to the drug labelled on the top of a column, and the label on the bottom shows CS readouts towards that drug. CS and CR are shown on a log2 scale. *p<0.05, ***p<0.001, ***p<0.0001, two-way ANOVA with Tukey's multiple comparisons test.

PIP CS in GEN resistant replicates and TIG CS in POL resistant replicates occurred frequently, with little to no cross-resistance (CR) (Figure 5.2D). PIP resistant strains showed moderate GEN CS, while CIP resistant strains showed GEN CS in only 1/16 replicates. Our GEN – PIP CS results reinforce previous reports that aminoglycoside – β-lactam pairs exhibit reciprocal CS [128,337], but some reported CS interactions, such as between CIP – GEN [53], may either be infrequent or be mitigated via compensatory evolution.

Table 5.2 Mutations in the PIP and PIP-GEN adapted strains that affect efflux and the electron transport chain respectively.

A

	PIP resistant	
Gene	Function	Ref.
mprA	Negative regulator of the multidrug transporter operon <i>emrAB</i> .	[166]
acrR	Regulator of RND efflux pump components AcrAB.	[340]
marR	Repressor of the multiple antibiotic resistance operon <i>marRAB</i> .	[165]

B

	PIP-GEN resistant	
Gene	Function	Ref.
clsC	Cardiolipin synthase C, supports respiratory supercomplex organization.	[341]
ubiD	Involved in ubiquinone biosynthesis.	[342]
arcB	Aerobic respiration control sensor protein, member of the two-component regulatory system ArcB/ArcA.	[343]
fre	NAD(P)H-flavin reductase, involved in transmembrane electron transfer.	[344]

5.2.2. Forward CS does not promote extinctions, resistance drops or resensitizations in clonal populations

With a collection of strains with complete CS (POL – TIG), almost no CS (CIP – GEN), and a mix of both CS and CR (PIP – GEN and GEN – PIP) we then evaluated whether forward CS improves extinction rates and/or promotes resistance drops and resensitizations, by subjecting each resistant replicate to the second drug in its series (Figure 5.2A). We considered strains as resensitized to antibiotic A when both the following conditions were met: 1) resistance drops at least 4x from prior evolved MICs and 2) the MIC reduced to the clinical breakpoint or below. We set a strict definition for resensitization to accommodate for possible discrepancies due to random 2-fold MIC changes [307]. Strains were considered extinct when cells could not be recovered after extraction from within 1.5 cm of the end of the SAGE plates.

We found that both the GEN – PIP and PIP – GEN pairs caused 8/16 of the replicates to go extinct (Figure 5.3A), even with significant differences in the prevalence of forward CS (Figure 5.2D).

The extinctions occurred despite compensatory evolution in the flat plates, indicating a stable hurdle in adaptation to the second drug. The failures were not due to the antibiotic challenge alone, as generation of resistance to GEN or PIP in WT populations resulted in no extinctions (Figure 5.3A). The other two drug pairs did not show any extinctions, including the POL – TIG pair, which had ubiquitous forward CS (Figure 5.2D).

To maintain the sample size for subsequent tests with the GEN – PIP and PIP – GEN pairs, extinct replicates were re-run using the same SAGE setup. This allowed recovery of 6/8 of the extinct replicates in the GEN – PIP pair, but only 1/8 in the PIP – GEN pair, the pair with lower incidence of forward CS (Figure 5.3A, 2D). We found no association between the replicates that went extinct and their CS status towards drug B in the GEN – PIP and PIP – GEN pairs (Figure 5.3B). This suggests that factors outside CS may drive extinctions in a sequential regimen.

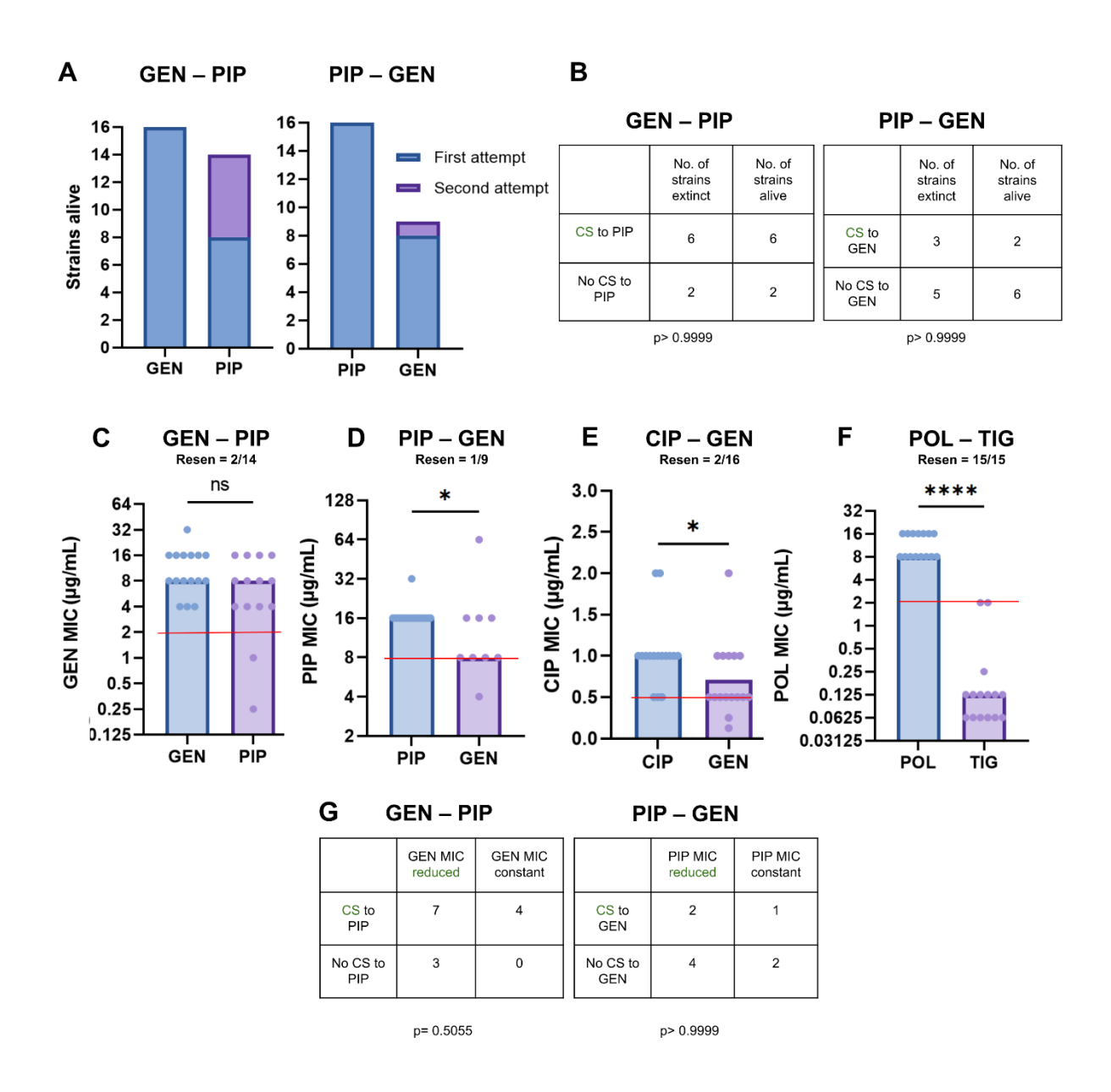


Figure 5.3 Extinctions, MIC reductions and resensitizations in drug pairs.

(A) The GEN – PIP and PIP – GEN pairs cause frequent extinctions (n= 16 for both pairs). (B) Extinctions cannot be correlated with the incidence of CS (Fisher's exact test). (C) The GEN – PIP pair does not cause a significant reduction in GEN MIC (n= 16 after evolution to GEN, n= 14 after evolution to PIP). (D) and (E) PIP – GEN and CIP – GEN cause a 2x reduction in median PIP and CIP resistance, respectively (n= 16 after evolution to PIP and CIP, n= 9 after evolution to GEN following PIP and n= 16 after evolution to GEN following CIP resistance). (F) The POL – TIG pair causes reliable resensitization and a large POL resistance drop (n= 15). Red lines indicate the resistance breakpoints.

(F) and (G) Extinctions cannot be correlated with the incidence of CS (Fisher's exact test). Resen = resensitizations. *p<0.05, ****p<0.0001, Mann-Whitney test.

To test the link between CS and reduced levels of resistance we first measured drug A resistance levels after exposure to drug B in the extant replicates. The GEN – PIP pair produced no significant drop in median resistance levels following PIP evolution, with 2/14 replicates resensitized to GEN (Figure 5.3C). The PIP – GEN and CIP – GEN pairs produced a 2-fold reduction in median drug A resistance, and 1/9 and 2/16 resensitizations respectively (Figure 5.3D, E). POL – TIG showed a remarkable 64x reduction in median POL resistance, achieving resensitizations in all 16 replicates (Figure 5.3F).

Next, we looked for associations between forward CS and drug A resistance drops. However, only 1/16 CIP resistant replicates showed GEN CS in the CIP – GEN pair, while all POL resistant replicates were resensitized to POL. Insufficient CS in the CIP – GEN pair, and the presence of only resensitized replicated in the POL – TIG pair made them unsuitable for this analysis. From the GEN – PIP and PIP – GEN pairs, we found no associations between the number of strains with reduced drug A resistance and forward CS (Figure 5.3G). This suggests forward CS may not play a significant role in resistance mitigation in a sequential regimen when clonal populations are involved. Overall, we found that the GEN – PIP and PIP – GEN pairs can cause reliable bacterial extinctions, with 3/4 drug pairs tested producing significant drug A resistance drops. However, extinctions and resistance drops were not associated with drug B CS, and resensitizations remained low.

5.2.3. Backward CS can drive resistance drops

First, we showed that removal of antibiotic pressure does not resensitize bacteria to PIP or CIP (Supplementary Figure 5.1, supplementary figure 5.2). To explain the mechanism that drove the resistance drops we first looked into the PIP – GEN pair, in which 5/9 replicates showed reduced PIP MIC after exposure to GEN (Figure 5.3C). GEN resistance is known to partially arise via mutations that weaken the proton motive force (PMF) [124] which may disrupt the efflux-driven PIP resistance [345]. To test if PIP resistance is driven by efflux in our strains, we first sequenced three replicates after PIP exposure from the PIP – GEN pair (Figure 5.2A). Two of the three PIP-adapted strains showed mutations in genes known to affect efflux: *mprA* [346], *marR* [347], or *acrR* [340] (Figure 5.4A, Table 5.2A). All three strains also displayed CR to the antibiotics chloramphenicol (CHL) and tetracycline (TET) and the organic solvent hexanes. (Figure 5.4C, D, E). CHL, TET and hexanes are all known substrates of efflux pumps in *E. coli*, indicating increased efflux capacity in the PIP-adapted strains [348–350].

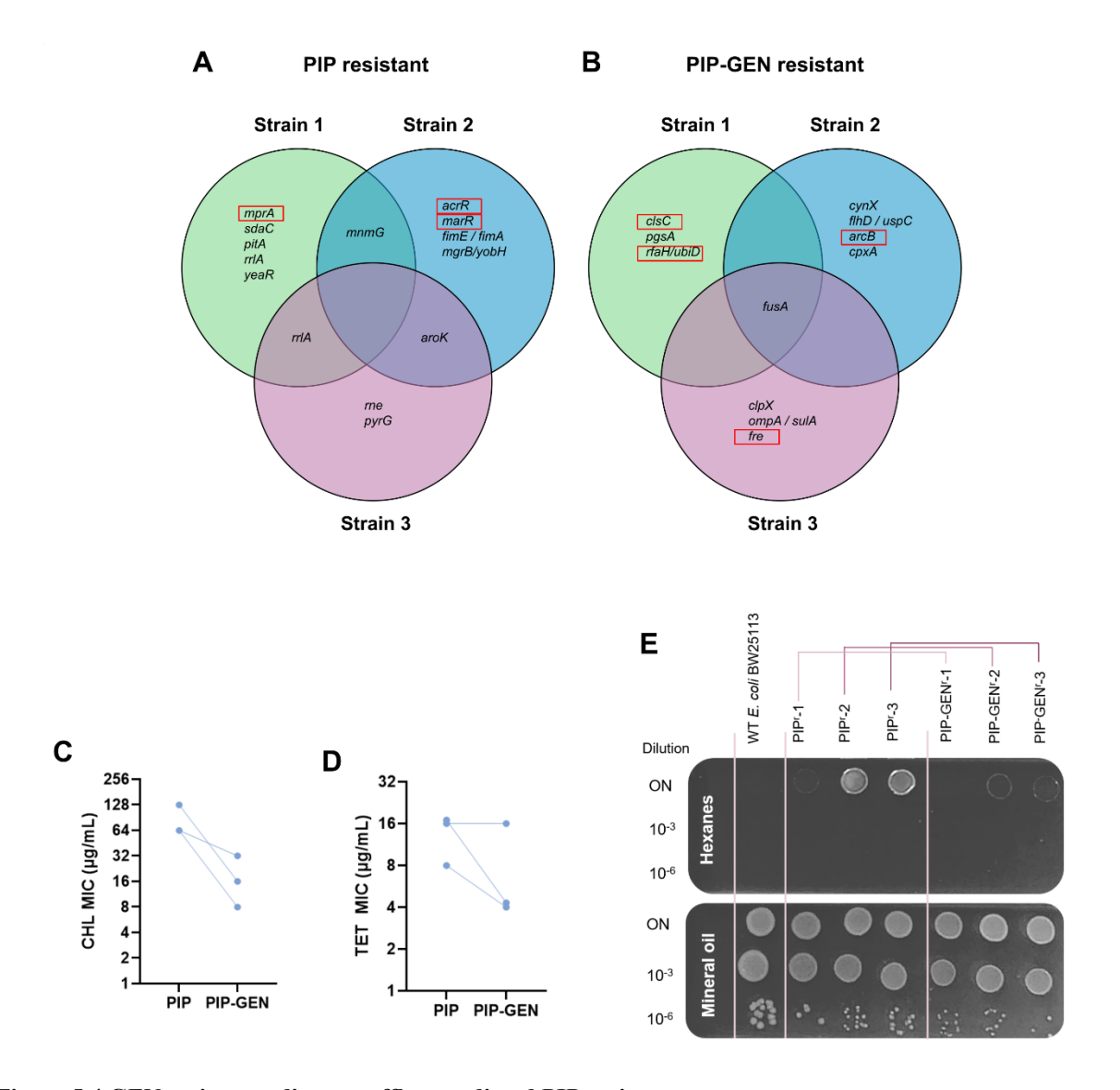


Figure 5.4 GEN resistance disrupts efflux-mediated PIP resistance.

(A) and (B) Mutations identified in 3 strains. Genes boxed in red are involved in efflux activity or the electron transport chain (Table 5.2). (C) and (D) PIP-resistant strains are cross-resistant to CHL and TET, suggesting efflux upregulation in these strains. "PIP-GEN" strains that were sequentially adapted to PIP and GEN have on average increased CHL and TET susceptibility. (E) Hexanes tolerance test. All strains show good growth under mineral oil. The WT failed to grow under hexanes, while PIP resistant strains 2 and 3, and to a lesser extent, strain 1, showed growth on the undiluted spots. This ability is almost entirely lost upon GEN adaptation, suggesting efflux disruption. Representative picture from 3 independent experiments.

To elucidate the effects of GEN resistance, we then sequenced three strains after GEN adaptation (Figure 5.2A). All three acquired mutations in *fusA* (Figure 5.4B), which codes for the elongation factor G and is known to confer gentamicin resistance [351]. Additionally, every strain acquired mutations in genes involved in the electron transport chain: *clsC* [341], *ubiD* [342], *arcB* [343], or *fre* [344] (Table 5.2B). CHL resistance, TET resistance, and solvent tolerance all dropped following GEN adaptation (Figure 5.4C, D, E), showing that these mutations negatively affect efflux. The backward CS towards PIP that frequently arises with GEN resistance (Figure 5.2D, first column) may hence stem from a reduction in efflux. The median drop in PIP resistance levels after exposure to GEN also corresponds to the magnitude of backward PIP CS exhibited by WT cells resistant to GEN (Figure 5.2D first column, 5.3D).

To test if backward CS can also explain the resistance drops in CIP – GEN and POL – TIG pairs, we separately evolved 16 replicates against GEN and TIG to check the presence of backward CS towards CIP and POL respectively. GEN resistance imposed CIP CS in 13/16 strains (2x CS in 10, 4x CS one and 8x in two) (Figure 5.2D). Efflux is important in CIP resistance [352], and the efflux weakening effects of GEN resistance (Figure 5.4 C-E) could also be imparting the CIP CS. Again, the increase in CIP sensitivity in the CIP – GEN pair was equal to the magnitude of backward CIP CS (Figure 5.3E, Figure 5.2D, second column). Based on these results, we suggest that backward CS may disrupt resistance in A – B drug pairs, increasing drug A sensitivity. The effect of TIG resistance was more complex.

5.2.4. POL resensitization is multifactorial

TIG resistance caused 2x POL CS in 5/16 strains and $\geq 4x$ CS in 2/16 strains (our limit of detection was 0.0625 μg/mL; MIC assays with wells clear at 0.0625 μg/mL were recorded as ≥4x CS) (Figure 5.2D, sixth column). Reciprocal CS between POL and TIG has been reported in E. coli before [337], but the mechanism of CS remains unknown. The resensitizations in the POL – TIG pair were generally stronger than the backward CS we observed, and with half of the POL – TIG replicates lacking CS (Figure 5.2D), backwards CS alone could not explain the median 64x increase in POL susceptibility. As POL MICs were measured after TIG SAGE evolutions and the flat plates (step 9 in Figure 5.5), it is possible that the change in susceptibility was due to heteroresistance or compensatory mutations [353]. To identify the experimental stage at which the POL resensitizations occurred, we first revived four randomly selected POL resistant strains and passaged them five times through antibiotic free soft agar plates (Figure 5.5A, Supplementary figure 5.1). We measured POL MICs after each passage (Figure 5, 2 to 6), and found a maximum 2x reduction in POL MICs (Figure 5.5B). Next, we revived the same four lineages from frozen stocks, but this time from stages 7 - 10 (Figure 5.5A) and measured their POL MICs. 1 out of the 4 strains was resensitized to POL during or immediately after evolution against TIG, while the rest showed a 0-4x reduction at this stage (Figure 5.5B). POL susceptibility in the other three strains was restored over the first TIG flat plate, which caused a 2-128x reduction in POL resistance. Subsequent TIG flat plates had no effect (Figure 5.5B). This suggests that cells with both POL and TIG resistance take evolutionary paths that promote phenotypic resistance reversion above what is achievable through the simple removal of POL selection pressure [123,141].

Α

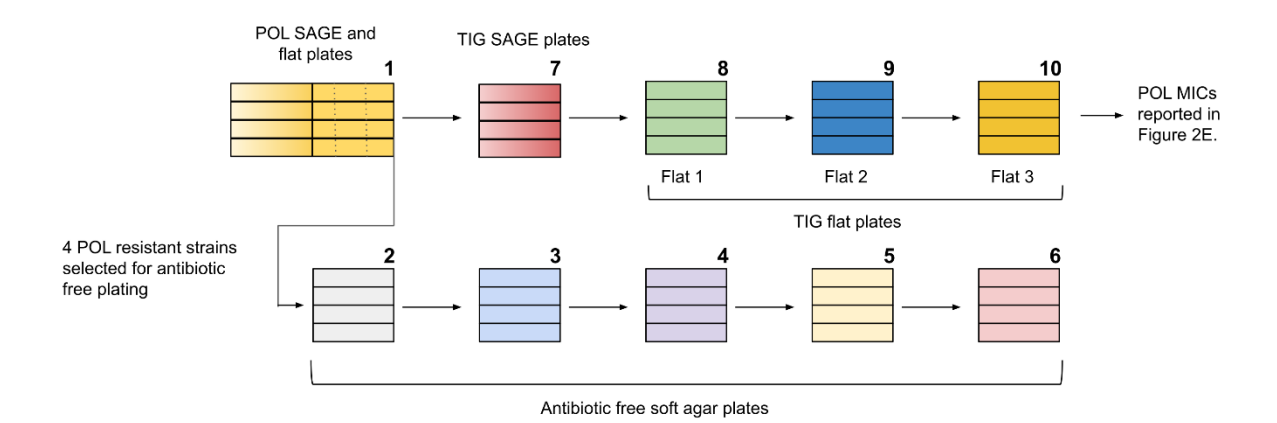


Figure 5.5 Resensitization of POL resistant strains.

(A) Scheme showing the steps of POL and TIG sequential resistance evolution. Numbers represent the stages at which POL MICs were performed. (B) POL MICs at different stages of evolution.

5.3. Discussion

In this study we investigated four drug pairs proposed for cyclic therapy, generating 16 independent replicates of E. coli that were sequentially adapted to each drug in the pair. Owing to our large sample sizes, we were able to produce data on the reliability of these cyclic therapies i.e., the frequencies at which they drive extinctions and resensitizations and the frequencies they fall to escape mutants that generate multidrug resistance.

We found varying degrees of extinctions in these pairs. GEN – PIP and PIP – GEN appeared to be potent drug pairs since both the pairs drove 50% of the bacterial populations extinct (Figure 5.3A). However, other proposed drug pairs like CIP - GEN [53] and POL - TIG [337] exhibited no extinctions, highlighting the importance of large scale laboratory evolutions to determine drug pairs that hinder resistance.

The GEN - PIP drug pair produced no significant reduction in resistance (Figure 5.3C). Looking at the spread of the data, the importance of a large data set becomes clear. While a number of strains ended up losing resistance, an almost equal number of strains either retained or gained resistance, making small sample sizes vulnerable to biases.

Optimal drug pairs for cyclic therapies are thought to have been ones with forward CS [53,128,354]. Contrary to this, we found no significant associations between forward CS and bacterial extinction or antibiotic resensitization. Evolution of resistance to GEN led to frequent PIP CS (Figure 5.2D) but cells with and without PIP CS were equally likely to have reduced GEN resistance following evolution to PIP (Figure 5.3G). While PIP exposure did render half of the lineages extinct (Figure 5.3A), extinction was not correlated with the presence or absence of CS (Figure 5.3B). In contrast, backward CS appeared to promote reduction resistance levels. Both the PIP – GEN and CIP – GEN pairs had high rates of backward CS and reductions in drug A resistance following the evolution of resistance to drug B (Figure 5.2D, Figure 5.3D, E). Our genomic analyses and efflux activity measurements showed that increased PIP sensitivity in the PIP – GEN pair was driven by the disruption of efflux capacity (Figure 5.4, Table 5.2), and may have also

played a role in CIP CS. Backward CS was present, but not identified, in a prior study of CS pairs with reciprocal CS interactions [128], and our work suggests that backward CS may be partly responsible for the resensitizations seen in that study.

All SAGE evolutions were conducted over a fixed period, with mutants extracted after seven days of incubation from within 1.5 cm of the end of the plates. This design allowed us to set a fixed benchmark to report adaptation rates and extinctions, but does not allow us to comment on if the speed at which resistance evolved was affected by the presence of CS. Future studies that track movement in SAGE plates could potentially answer this question.

The POL – TIG pair showed a 100% rate of POL resensitization, producing an impressive 64x drop in median POL resistance levels. While backward CS was also observed in this pair (Figure 5.2D, first reported by Imamovic *et al.* as reciprocal CS [337]), the magnitude of POL resistance reductions exceeded what would be expected from CS alone. Our results indicated that multiple mechanisms contributed to POL resensitization: removal of POL selection, adaptation to TIG, and probably most importantly, compensatory evolution in the POL and TIG resistant populations. These resensitizations may be especially relevant for chronic diseases in which TIG and either POL or the polymyxin B analogue colistin see current use [355], such as cystic fibrosis [356].

Taken together, we suggest that backward, but not forward, CS may play an important role in reducing resistance levels in drug pairs. The weakening of efflux mechanisms upon exposure to a second antibiotic, as seen in the PIP – GEN, and possibly the CIP – GEN pair, may provide an approach for developing more effective sequential drug therapies aimed at reducing resistance. We also provide support for the idea that an aminoglycoside – β -lactam pair can frequently promote bacterial extinction. Our results highlight the importance of thorough laboratory investigation of

drug pairs and of considering the directionality of CS interactions when designing sequential drug therapies to build pairs more resilient against bacterial evolution.

5.4. Materials and Methods

5.4.1. Bacterial strain and growth conditions

E. coli K-12 substr. BW25113 and all subsequent resistant mutants were grown in Mueller Hinton (MH) media at 37 °C. Growth media was supplemented with appropriate antibiotics when growing mutants or extracting mutants from SAGE plates.

5.4.2. SAGE Evolutions

SAGE plates were set up to generate resistant mutants as described before [69]. All SAGE plates were made with Muller Hinton (MH) media + 0.15% agar + 0.2% xanthan gum (XAM) [71]. Antibiotic concentrations are listed in the table below, and were determined from trial SAGE experiments to evolve strains with MICs above clinical breakpoints within seven days. All SAGE plates were incubated for a fixed duration of seven days. Mutants were extracted from within 1.5 cm of the end of the lanes by pipetting 20 μL of the gel into Muller Hinton (MH) broth supplemented with the challenge antibiotic at a concentration = 2x the WT MIC (Table 5.1). Extracts were taken from regions with clear signs of growth. If no growth was apparent, extracts were pipetted from a random site within 1.5 cm of the end of the lane. A replicate was considered extinct if no growth was visible after overnight incubation in the antibiotic-supplemented MH broth.

Antibiotic	Concentration (μg/mL)
GEN	5
PIP	40
CIP	1
POL	10
TIG	5

5.4.3. MIC assays

MICs were measured using the microdilution method outlined by the CLSI [214]. Dilutions of antibiotics were prepared in MH broth and inoculated with bacteria at a final concentration = 1/200 of 0.5 McFarland standardized inoculum in non-treated 96-well plates. Plates were then incubated overnight and the MIC was recorded as the lowest concentration of antibiotic that prevented visible bacterial growth.

5.4.4. Flat plates

Flat plates were prepared as previously described [107]. First, the MIC of the antibiotic that was in prior SAGE plates was determined for all strains that completed their SAGE plates. Next, we created flat lanes specific for each strain by pouring ~12 mL of XAM supplemented with the antibiotic at a concentration = ½ the MIC of that strain in a lane of a four-well dish. This allowed maintenance of the SAGE-evolved resistance phenotype during compensatory evolution. XAM media was used for all flat plates. Plates were inoculated as described before [69]. Each replicate passed three consecutive flat lanes (Figure 5.2A, Figure 5.5). The first flat plate was incubated for

two days, and the second and the third for one day (Figure 5.2A). The 16 GEN resistant strains were used to determine the appropriate flat plate incubation times, and all three passes for these strains were incubated for three days instead (Figure 5.3B). Extractions were carried out as described in the "SAGE evolutions" section, but were not limited to the 1.5 cm region of the end of the lanes. Instead, cells were extracted from where the cells had moved the farthest.

5.4.5. Whole genome sequencing and analysis

Genomes were extracted from strains revived from frozen stock using the Bio Basic genomic DNA kit (Cat. no.: BS624). Sequencing and variant calling was performed by Sequencer (USA). Sequencing was performed on an Illumina NextSeq 2000, and demultiplexing, quality control, and adapter trimming was performed with bcl-convert (v3.9.3). Variant calling was carried out using Breseq under default settings (80). NCBI reference sequence CP009273.1 for E. coli K-12 substr. BW25113 was used for variant calling. Figures showing common mutations in the three strains in Figure 5.4A and B were made using the R package *ggvenn*. For the PIP-GEN resistant strains, mutations acquired during PIP adaptation were removed before analysis.

5.4.6. Hexanes tolerance assay

The solvent tolerance test was performed using a protocol adapted from Ikehata *et al* [357]. Overnight cultures for each strain were diluted 10^3 and 10^6 times in MH broth and 5 μ L spotted on MH agar surface. Spots were allowed to air dry, then the surface was either covered with \sim 3 mm of hexanes (ACS Grade, Caledon Laboratory Chemicals, SKU: 5500-1-40) or mineral oil. Plates

were sealed with parafilm and left in the fume hood to incubate for five days at room temperature.

Plates needed refilling with hexanes every day due to evaporation.

5.4.7. Antibiotic free soft agar plates

Plates were prepared similarly to the flat plates described before but without antibiotics. Strains were inoculated on one end of these plates and were incubated for one day. Strains were then extracted, cultured in antibiotic free MH broth and inoculated in a second plate. This process was repeated to achieve a total of five passes (Supplementary Figure 5.1). Broth cultured extracts were also streaked on antibiotic free MH petri plates. Cells from petri plates were used to perform MIC tests.

Chapter 6. Tripartite loops reverse antibiotic resistance

Published record: Chowdhury FR and Findlay BL; Molecular Biology and Evolution 2025, 42

(6)

Available at: https://doi.org/10.1093/molbev/msaf115

6.1. Introduction

Bacterial infections claim 7.7 million lives each year, of which 4.95 million are associated with

antibiotic resistance [335]. The slow pace of antibiotic development is failing to keep up with

bacterial evolution, pushing us towards a post-antibiotic era [358–360]. Tipping the scales in our

favor in the fight against antibiotic resistance will require alternative strategies beyond the

discovery or invention of new drugs to combat antibiotic resistance. One potential approach to

slow down resistance evolution is to employ existing drugs in a sequence, with drugs administered

one after the other at either predetermined times or as resistance arises [83,117]. Experimental and

computational evolution studies indicate that sequential antibiotic regimens can constrain

resistance evolution [86,128,303,361–363], and incorporation of collateral sensitivity (CS) is

thought to allow maintenance of sensitivity to the alternating drugs indefinitely [52,84,128,364].

Unfortunately, studies on the effectiveness, importance and repeatability of CS have produced

mixed results [134]. Some experimental evolution studies report repeatable CS interactions

[128,152,303], while others show weak reproducibility [54,132,137,140,152]. Reports also

suggest that sequential antibiotic therapy can constrain resistance evolution independently of CS

[140,141]. While the effect of CS on resistance evolution is anchored in several excellent studies

which have identified a number of possible drug pairings, most pairings have been experimentally

verified using a relatively limited number of evolutionary replicates (2-8 replicates in general)

[52,128,361]. Reproducibility is critical for the use of CS in the clinic, and the evolutionary trade-

129

offs that are at the core of sequential or cyclic regimens must be repeatable. Absent large scale experimental evolution studies, it is unclear which drug cycles will fail, how often they will fail, and whether those failure rates can be limited.

In a previous study [306], we showed that in a gentamicin (GEN) - piperacillin (PIP) pairwise cycle previously suggested for cyclic therapies [52,128], GEN resistant *Escherichia coli* lineages frequently evolved hypersensitivity towards piperacillin (PIP) but subsequent PIP evolution failed to reverse resistance or reduce adaptation rates, predominantly producing multidrug resistant mutants instead. The repeatability of CS evolution was low even in some previously reported CS-pairs, and there was a lack of complete antibiotic resensitization in most of the pairs tested [306]. This showed that CS interactions often fall apart due to lack of repeatability of evolution, and that pairwise cycles often do not achieve the level of resensitization required for cyclic regimens.

In this study, we ask if mutants that fail to be resensitized in a pairwise cycle can be salvaged, with susceptibility to one or both of the initial antibiotics restored. Although resistant mutants possess strong selective advantages in environments containing the antibiotic of interest, those mutations render them less fit in antibiotic free environments [75,107]. Reversion to susceptibility is then favoured, either through competition by naive cells or by compensatory mutations that enhance fitness but lower resistance levels (phenotypic reversion) [141,194,365]. As it is infeasible to prescribe an antibiotic-free period during an ongoing infection, we instead incorporate a third antibiotic into the series, creating a tripartite loop (Figure 6.1A). We choose this third drug with a mechanism of action distinct from the other two, limiting the potential for cross resistance [366,367]. We evolve replicates of *Escherichia coli* K-12 substr. BW25113 (wildtype, WT; n =

16) through experimental tripartite loops using a soft agar gradient evolution (SAGE) based platform [69]. The large sample size allows us to capture repeatable evolutionary outcomes. Because compensatory evolution can frequently mitigate the effects of evolutionary trade-offs [108–111], we include "flat plates" after every evolution step (Figure 1A). Flat plates have been previously shown to reveal robust fitness trade-offs [252,306]. Using this setup, we find that evolution of nitrofurantoin (NIT) resistance reliably restores GEN susceptibility in bacteria resistant to GEN and PIP when bacteria are evolved against drugs in the order GEN-PIP-NIT. This loop is effectively bidirectional, with NIT resistant bacteria reliably resensitized through a NIT-PIP-GEN loop. This effect is not limited to NIT, as a suboptimal drug like doxycycline (DOX), against which the majority of the GEN and PIP-resistant strains were cross-resistant, was able to reinstate GEN sensitivity. We find that to bypass the fitness loss associated with multidrug resistance, cells rewire their metabolic pathways, concurrently restoring susceptibility to the first drug in the series. All resensitizations we observe occur independently of CS interactions between component drugs in the loop. Extending our strategy to clinical strains, we then restore NIT sensitivity in clinical E. coli isolates that were initially resistant to NIT via sequential evolution against PIT (piperacill1in/tazobactam) and GEN. Resensitization occurs even when bacteria bypass chromosomal PIP adaptations by mutating β-lactamases. Overall, we demonstrate that in some cases the multidrug resistance that arises in pairwise loops can be reversed by extending to tripartite loops, experimentally validating a path to more effective and more resilient cyclic antibiotic therapies.

6.2. Results

6.2.1. Tripartite drug loops that resensitize bacteria to antibiotics

We previously reported using soft agar gradient evolution (SAGE) to generate 16 independent replicates of Escherichia coli K-12 substr. BW25113 (WT) resistant to both GEN and PIP [306], a drug pair previously proposed to promote resensitization [52,128]. Out of the 16 strains, two strains went extinct during PIP evolution, while the majority of the remaining 14 maintained resistance to GEN (Figure 6.1B) (Supplementary Figure 6.1A, F) [306]. In this study, we screened for drugs that could resensitize these strains to GEN, extending our experimental design to incorporate evolution against a third drug "C" (Figure 6.1A). We used SAGE to evolve resistance to antibiotics [241], and after each stage of evolution, resistant lineages entered flat plates containing sub-inhibitory concentration of the challenge antibiotic (Figure 1A). We incorporated flat plates into our experimental design to prioritize evolutionary trade-offs that are less susceptible to compensatory evolution [252,306]. Fitness costs linked to resistance mutations are welldocumented, but "cost-free" mutants frequently emerge in the clinic by offsetting these costs through compensatory mutations [108–111]. If laboratory-generated resistance-associated tradeoffs can be readily alleviated, their therapeutic potential may be limited. We previously showed that flat plates can generate fitter mutants through compensatory evolution rapidly, ameliorating fitness deficits [252,306]. Any trade-offs associated with the evolution of resistance in this study are therefore expected to be resilient against compensatory mutations.

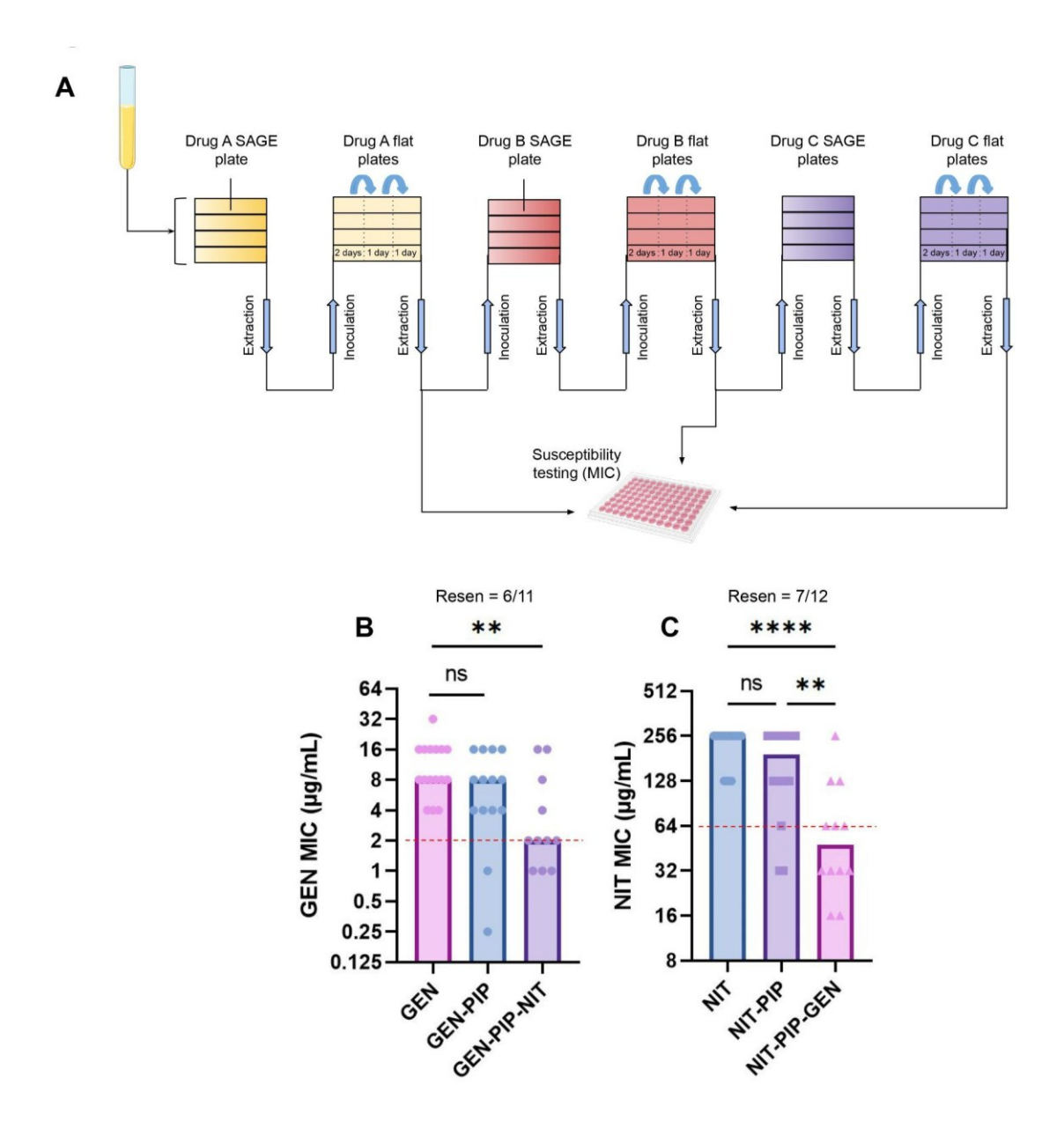


Figure 6.1 Tripartite loops improve antibiotic resensitization.

(A) SAGE is used to study three-drug cyclic regimens or tripartite loops. Bacteria were inoculated into soft agar containing antibiotic gradients to generate resistant mutants (n = 16). SAGE plates were incubated for a fixed duration of 7 days, after which mutants were harvested and passed through three "flat plates" containing the same antibiotic from the prior SAGE plate at a concentration = ½ the evolved MIC of the mutants. The incubation period for each flat passage is noted in the figure. MIC and CS profiles of mutants were determined after the end of the flat plates. (B) GEN MICs of strains that passed through the GEN-PIP-NIT tripartite loop. The y-axis denotes the GEN MICs and the x-axis denotes the sequence of antibiotics against which the strains were evolved. For example, the GEN-PIP bar

shows the GEN MICs of strains that were sequentially evolved to GEN and PIP (as shown in (A)). (C) NIT MICs of strains that passed through the NIT-PIP-GEN loop. Resen = resensitization counts. Dotted red lines indicate the clinical breakpoint (EUCAST). Bars represent the median MICs. **p<0.01, ****p<0.0001, Kruskal-Wallis with uncorrected Dunn's test.

Evolution of NIT resistance reduced the GEN resistance of seven out of eleven strains to or below the clinical breakpoint, while driving three lineages extinct (Supplementary Figure 6.1A), with a median 8-fold drop in GEN MIC (Figure 6.1B, Supplementary Figure 6.1F). To account for possible random fluctuations in MIC measurements [307] affecting resensitization counts, we defined antibiotic resensitization as a four-fold or greater reduction in MIC compared to levels evolved when they first encountered the antibiotic, in addition to reduction at or below the clinical breakpoint. Using this definition, NIT resistance resensitized six out of eleven strains to GEN (Figure 6.1B).

To determine the effect of subsequent evolution against GEN, we subjected the six strains to GEN SAGE plates again, keeping the concentration of GEN equal to their first exposure. Although resensitized, the GEN MIC of these strains were 2-4-folds higher than the WT, making this a 2-4-fold smaller GEN challenge than the one faced by the WT (Supplementary Figure 6.1F). While we achieved a 100% evolution rate following the first GEN SAGE plate with WT bacteria (Supplementary Figure 6.1A) [306], 3/6 lineages went extinct in this second exposure (Supplementary Figure 6.1B). This shows that not only were these strains resensitized to GEN, but their ability to develop GEN resistance was also impaired.

When we measured NIT resistance in the three surviving mutants, we observed a 4-fold to 16-fold reduction in NIT resistance levels, rendering all three strains resensitized to NIT (Supplementary Figure 6.1D). This hinted at a possibility of bidirectionality in this loop, where GEN and NIT resistance were mutually exclusive. To test this at scale, we restarted our evolution experiments with 16 replicates, this time evolving resistance sequentially to NIT, PIP and then GEN. Following evolution against GEN we saw a ~5-fold reduction in median NIT resistance (Figure 6.1C). Nine out of 12 strains that completed this challenge fell at or below the NIT resistance breakpoint, with 7/12 reaching resensitization (Figure 6.1C) (Supplementary Figure 6.1G). There were no extinctions on exposure to NIT or PIP, but four strains went extinct during GEN evolution (Supplementary Figure 6.1C).

When strains were evolved sequentially to PIP, GEN and NIT, NIT had no significant impact on PIP susceptibility (Supplementary Figure 6.1E). This showed that ordering of GEN, PIP and NIT was critical for achieving resensitization, but when applied correctly produced significant resensitizations.

6.2.2. PIP resistance is important for resensitization

Stratifying results from each step of the GEN-PIP-NIT loop by final GEN MIC revealed that strains which were ultimately resensitized to GEN exhibited decreased GEN resistance following PIP adaptation, while those that maintained GEN resistance after NIT were unchanged by evolution against PIP (Figure 6.2A, B). Similarly, stratifying NIT resensitized and resistant strains from the NIT-PIP-GEN loop revealed that PIP evolution reduced NIT resistance by 2-fold in the resensitized strains, but not in the resistant ones (Figure 6.2C, D). Overall, strains evolved through

an intervening PIP evolution step exhibited a 4-fold reduction in GEN resistance on NIT exposure, as opposed to a 2-fold difference when the PIP step was omitted (Figure 6.1B, 6.2E). This suggests that the incorporation of a third drug allows for resensitizations which would not be possible in pairwise loops.

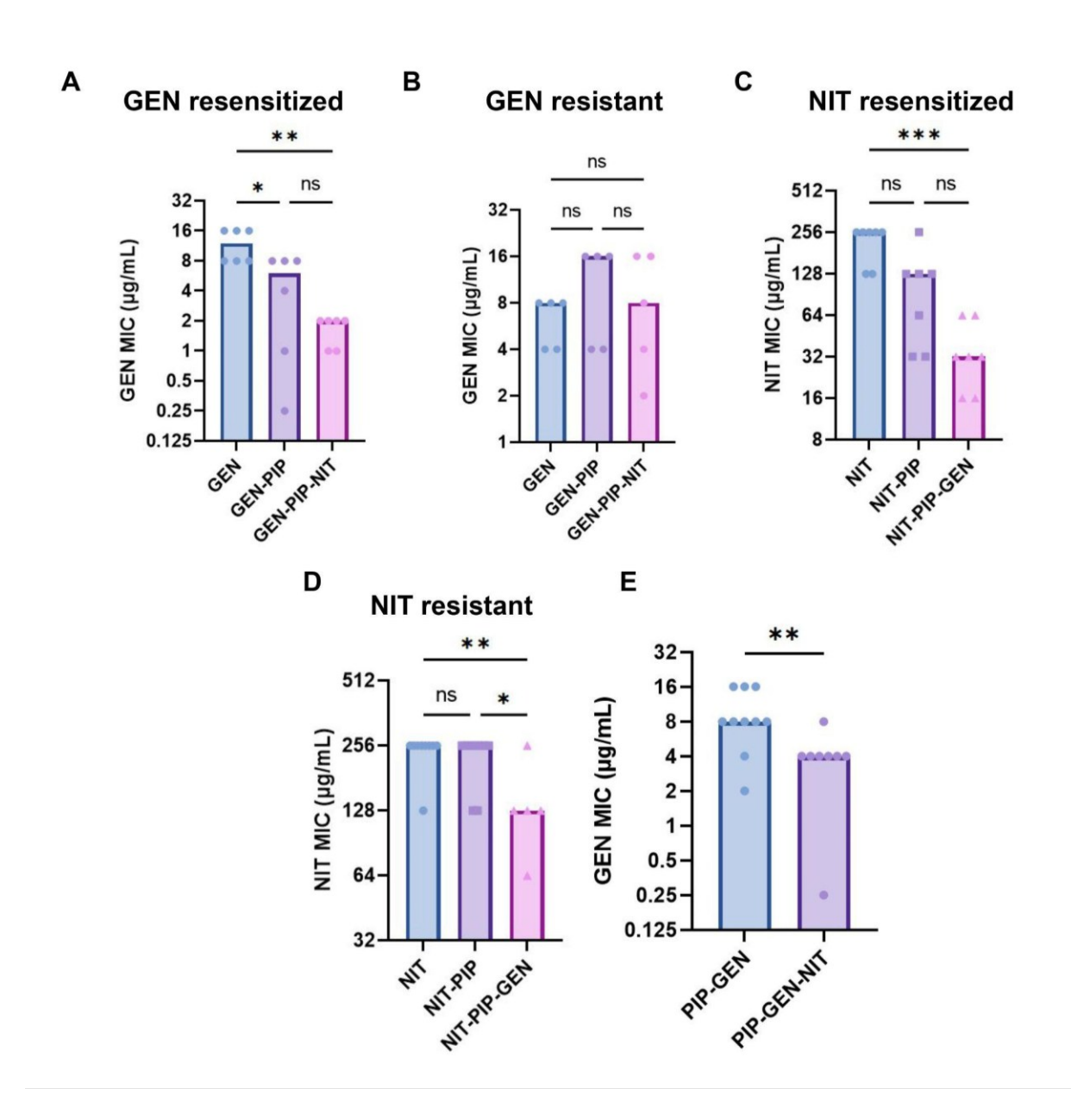


Figure 6.2 PIP aids resensitization in tripartite loops.

(A) GEN MICs of GEN-resensitized and (B) GEN-resistant strains that passed through the GEN-PIP-NIT loop. (C) NIT MICs of NIT resensitized and (D) resistant strains that passed through the NIT-PIP-GEN loop. *p<0.05, **p<0.01, ****p<0.001, ****p<0.001, ****p<0.0001, Kruskal-Wallis with uncorrected Dunn's test. (E) GEN MIC of strains that passed through a PIP-GEN-NIT tripartite loop. MICs after the PIP step are not shown. For all graphs, the y-axis denotes the MICs and the x-axis denotes the sequence of antibiotics against which the strains were evolved before measuring the MICs. For example, the PIP-GEN-NIT bar shows the GEN MICs of strains that were sequentially evolved to PIP, GEN and NIT.**p<0.01, Mann Whitney test. Bars represent the median MICs.

6.2.3. Resensitizations are independent of CS and principally mitigate fitness loss

To identify the driver of GEN resensitizations in the GEN-PIP-NIT loop, we first examined the effect of forward CS [306] to NIT. To avoid missing even a weak connection between CS and resensitizations we included all strains that showed any reduction in GEN resistance upon NIT evolution in the analysis.

We found no correlation between NIT CS in the GEN and PIP multidrug-resistant strains and reductions in GEN resistance (Figure 6.3A, B: left column; Supplementary Figure 6.1F: GEN MICs panel). To test if backward CS [306] helped resensitize bacteria to GEN, we evolved 16 WT strains to NIT (flat plates included) and measured their GEN CS. The concept of forward and backward CS in sequential regimens was recently defined [306]. Briefly, in a sequential therapy transitioning from GEN to PIP, for example, if resistance to GEN leads to CS to PIP (i.e., CS from GEN to PIP), this is referred to as forward CS since the CS aligns with the direction of drug switching. If resistance to PIP results in CS to GEN (CS from PIP to GEN) and the sequence of drug application remains GEN to PIP, we describe this as backward CS as the CS runs opposite to

the direction of evolution. When CS occurs in both directions, the drug pair is said to exhibit reciprocal CS [130]. It is important to note that the designation of CS as forward or backward is always relative to the direction of drug switching.

Only 6/16 of these strains showed 2-fold CS to GEN (and just one with 2-fold PIP CS) (Figure 6.3B; Supplementary Figure 6.1G: GEN MICs panel). In contrast, >50% of the strains were resensitized to GEN in the GEN-PIP-NIT loop, with a median 4-fold drop in resistance (Figure 6.1A). This remained true for the NIT-PIP-GEN loop, with few CS interactions between the drugs (Supplementary Figure 6.1G). The resensitizations we observed appeared to be largely independent of forward CS, and while backward CS may have played a role, it was not strong enough to resensitize strains to the extent that we observed.

To test if the specific mechanism that conferred NIT resistance drove GEN resensitization, we evolved GEN-PIP multidrug-resistant lineages against doxycycline (DOX), a tetracycline antibiotic with a different mechanism of action from NIT, GEN, or PIP [368] (n = 8). Despite most of the eight mutants showing cross-resistance to doxycycline (Figure 6.3C), 5/8 strains dropped their GEN resistance to or below the resistance breakpoint, with 3/8 reaching resensitization (Figure 6.3D). This provided further support that switching treatment to drugs towards which bacteria exhibit CS is not required for resensitization, and indicated factors other than specific resistance pathways contributed to the resensitizations we observed.

Next, we hypothesized that the cumulative fitness costs of maintaining multiple drug resistance may promote the adoption of evolutionary paths that ameliorate these costs, resulting in phenotypic reversion. To test this, we measured strain fitness after each evolution step in the GEN-PIP-NIT, NIT-PIP-GEN and PIP-GEN-NIT tripartite loops, using area under growth curves (AUC) as a proxy for fitness (Supplementary Figure 6.2) [107,140]. In the GEN-PIP-NIT loop we found only a small drop in average fitness after each evolution step, which did not reach statistical significance (Supplementary Figure 6.2A). However, stratifying strains on the basis of resensitization to GEN revealed a clear difference in fitness (Figure 6.3E-G). Strains that were resensitized to GEN upon NIT evolution either saw small gains or marginal losses in fitness (Figure 6.3E, G), while those that retained GEN resistance lost significantly more fitness on average, with none gaining fitness (Figure 6.3F, G).

The results of the NIT-PIP-GEN loop were less clear. We observed large fitness losses after every step of evolution, with the evolution of GEN resistance in particular producing extremely unfit mutants (Supplementary Figure 6.2B). Two of the seven NIT resensitized strains exhibited moderate to large fitness gains upon GEN evolution but none of the five NIT resistant strains did (Supplementary Figure 6.2D-F). However, the differences in Δ AUC between the resensitized and resistant groups did not reach statistical significance (Supplementary Figure 6.2F).

Strains from the PIP-GEN-NIT loop showed a large fitness drop as they moved from PIP to GEN, but did not show a significant change in fitness following NIT evolution (Supplementary Figure 6.2C). Given the increased burden of resistance to three separate antibiotics, we expected that a constant AUC would correspond to significant resensitization. However, only one lineage exhibited increased PIP susceptibility, and that was following GEN evolution, not NIT (Supplementary Figure 6.1E). Looking more closely into the MIC profiles of these strains revealed

that while there were no significant changes in PIP susceptibility, 7/8 strains had increased GEN susceptibility following NIT exposure (Figure 6.3C). As GEN resistance was consistently associated with the largest fitness penalties (Supplementary Figure 6.2), this may have off-set a fitness penalty from acquiring NIT resistance, while leaving the less costly PIP resistance unchanged. Overall, the tripartite loops led to higher fitness costs and increased resensitization compared to pairwise loops.

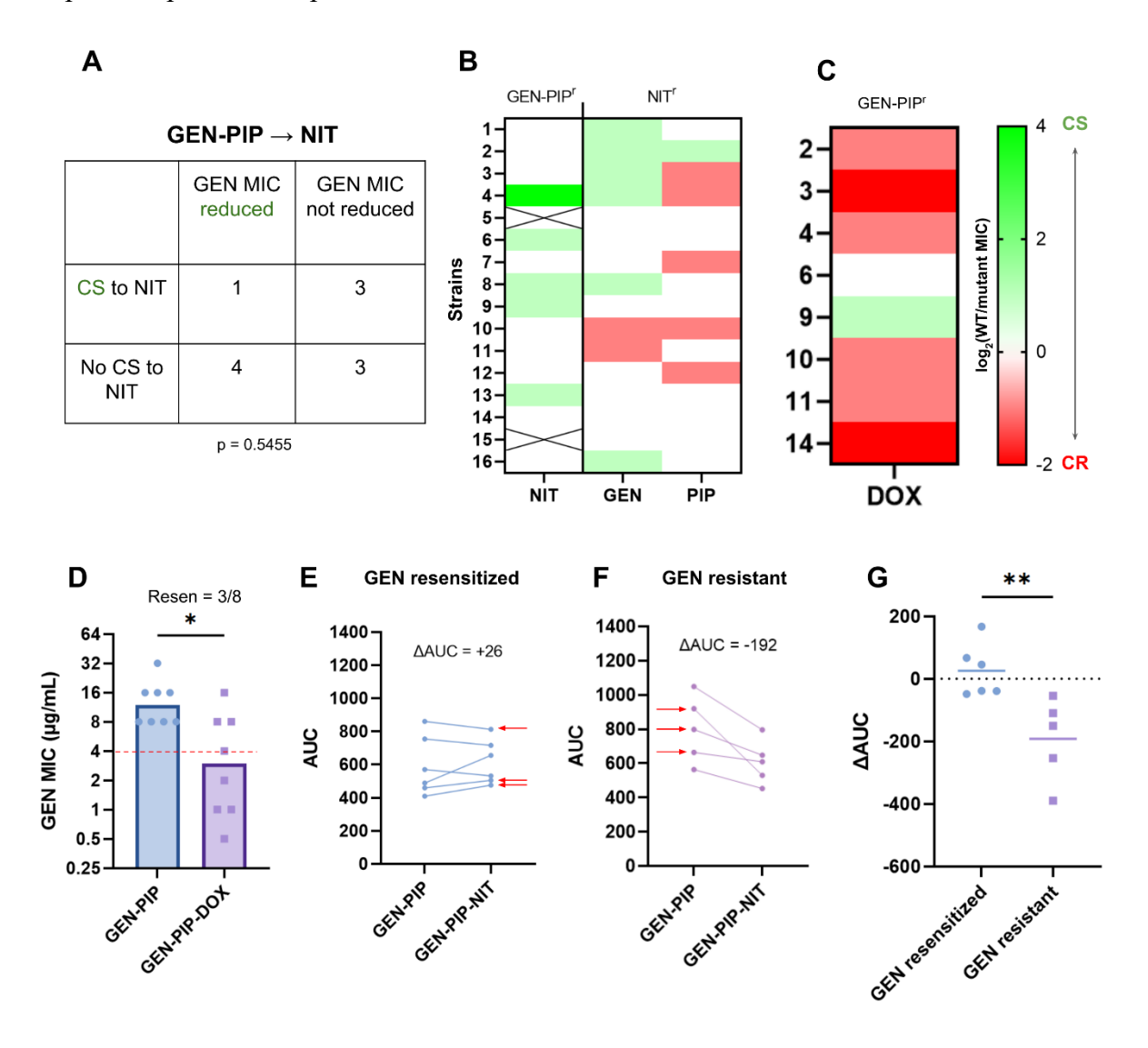


Figure 6.3 Resensitization does not correlate with CS but mitigates fitness loss.

(A) Contingency table for the 11 strains which evolved NIT resistance through the GEN-PIP-NIT loop, showing no associations between CS and GEN resensitizations. Fisher's exact test. (B) First column: NIT CS of the GEN and PIP

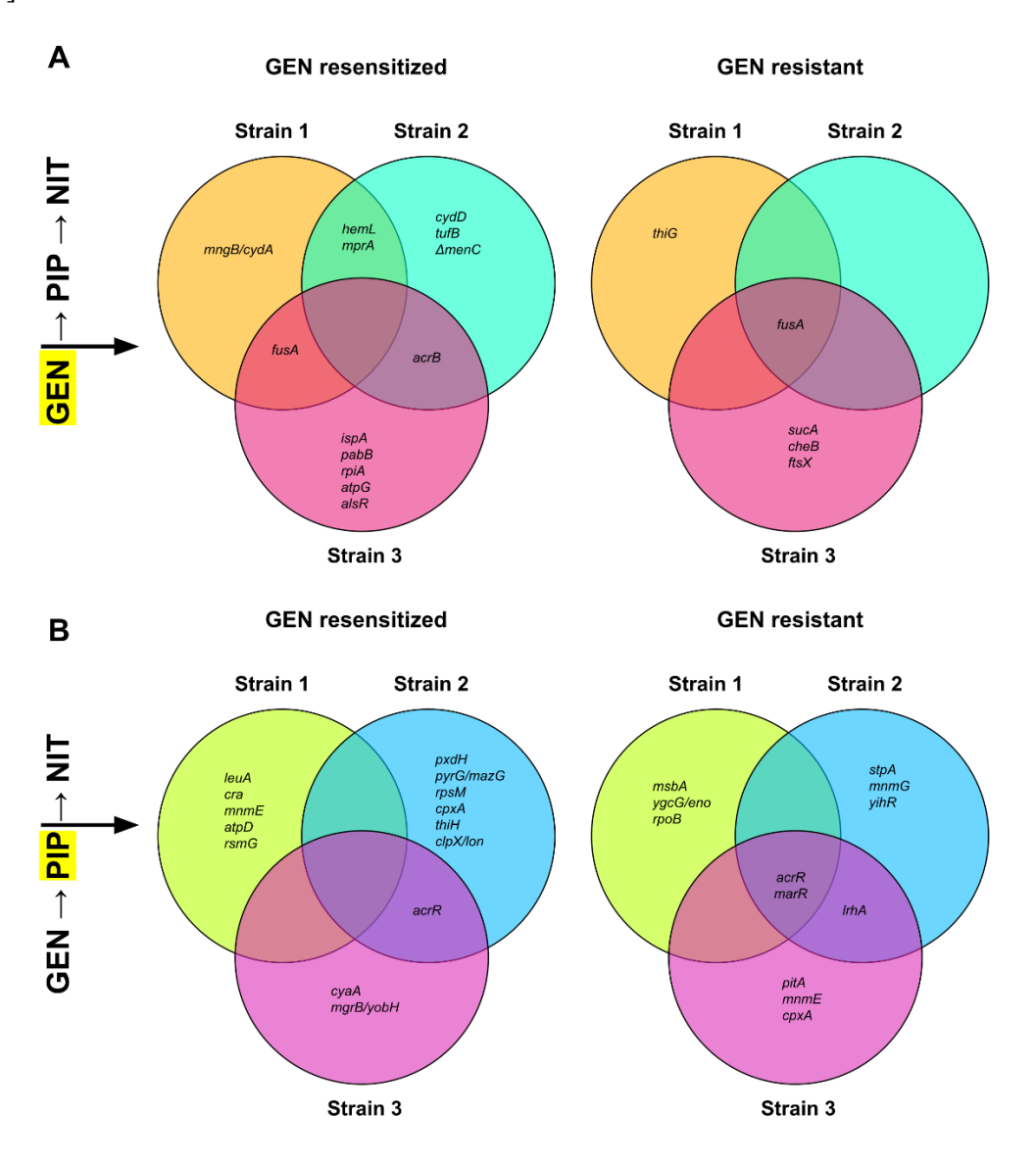
evolved mutants from the GEN-PIP-NIT loop. Second column: GEN and PIP CS of WT bacteria evolved to NIT. CS interactions are reported on a log2 scale. (C) DOX MICs of an eight strain subset of the GEN and PIP evolved mutants from the GEN-PIP-NIT loop. CS interactions are reported on a log2 scale. The y-axis denotes the ID of the strains that were picked for DOX MIC testing. (D) GEN MICs of the subset that passed through the GEN-PIP-DOX loop. The x-axis denotes the sequence of antibiotics against which the strains were evolved before measuring GEN MICs. For example, the GEN-PIP-DOX bar shows the GEN MICs of strains that were sequentially evolved to GEN, PIP and DOX. Dotted red line indicate the clinical breakpoint. Bars represent the median MICs. *p<0.05, Mann Whitney test. (E) and (F) AUCs of strains before and after NIT evolution for GEN-resensitized and GEN-resistant strains respectively. The x-axis denotes the sequence of antibiotics against which the strains were evolved before measuring AUCs. GEN-PIP = before NIT evolution, GEN-PIP-NIT = after NIT evolution. ΔAUC is the average of the difference between post and pre NIT AUCs. For the GEN resistant group, we considered every strain that did not meet our resensitization criteria as resistant. This resulted in the inclusion of one strain that was below the GEN resistant breakpoint but did not reach our resensitization standard. Red arrows indicate the strains that were sequenced. (G) ΔAUC of individual strains plotted, grouped by resensitized and resistant. Horizontal lines represent the mean. **p<0.01, unpaired t test.

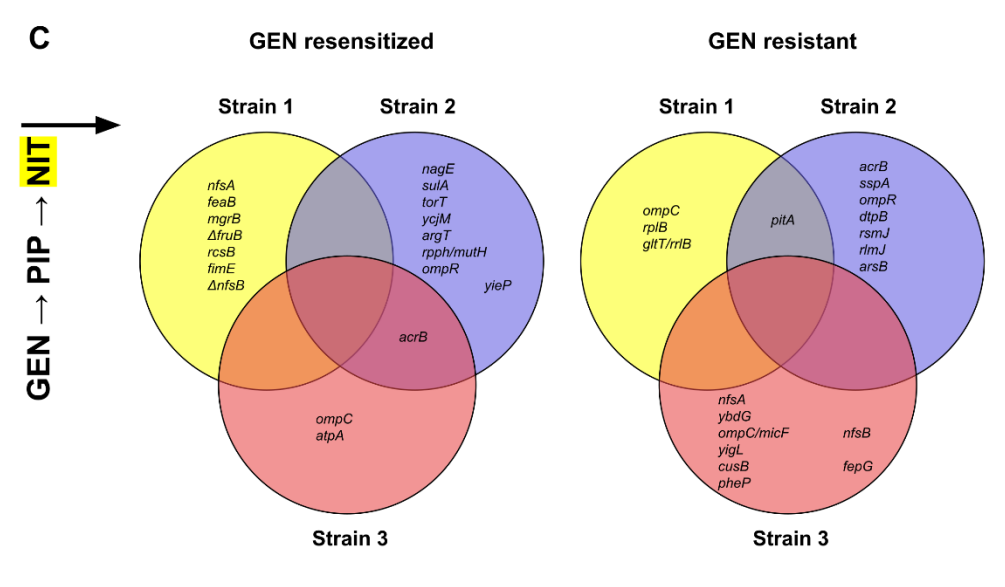
6.2.4. Whole genome sequencing sheds light on resistance and resensitization mechanisms

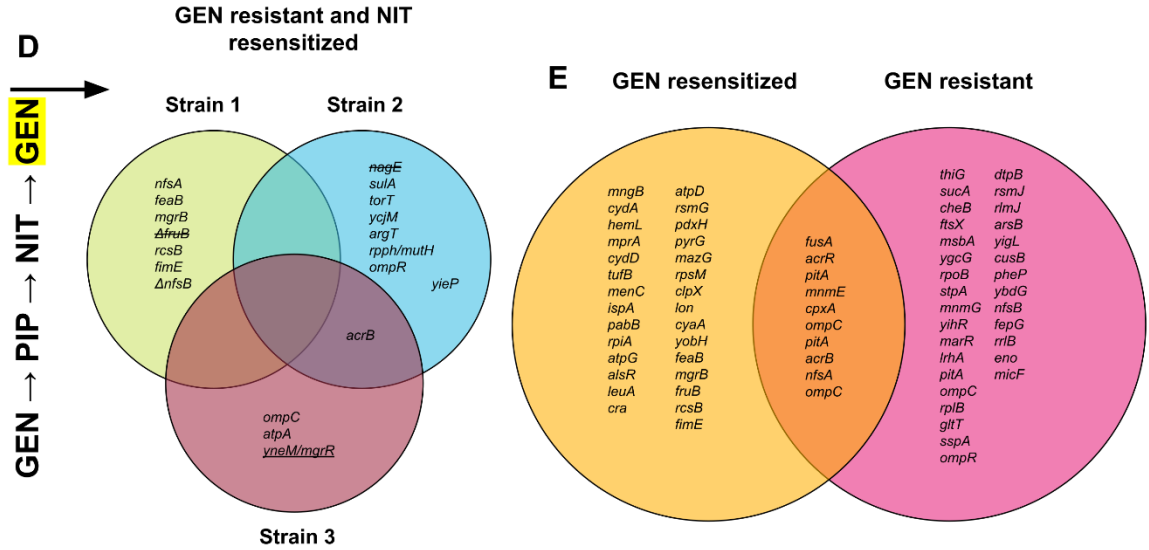
To understand the genetic basis of the resistance and resensitization observed, we sequenced the genome of six lineages from the GEN-PIP-NIT loop: three that were resensitized to GEN and three that remained resistant to GEN after NIT evolution (Supplementary Figure 6.1D). Each lineage was sequenced following every evolution experiment (Figure 6.1A), allowing us to reconstruct all six evolutionary trajectories (Figure 6.4A-D).

Five of the six lineages acquired their initial GEN resistance through mutations in the translation elongation factor G, *fusA*, mutations that are known to reduce gentamicin's ability to bind to the

ribosome (Figure 6.4A) [369]. Even though both the GEN resensitized and resistant groups evolved similar GEN MICs (Supplementary Figure 6.1F), the resensitized strains contained multiple additional mutations in genes involved in the electron transport: *hemL* [370], *cydA* [371], *cydD* [372], *menC* [373], and *atpG* [374] (Figure 6.4A). Mutations in the electron transport chain can provide GEN resistance either by disrupting drug uptake or reducing ribosomal protein levels [375,376].







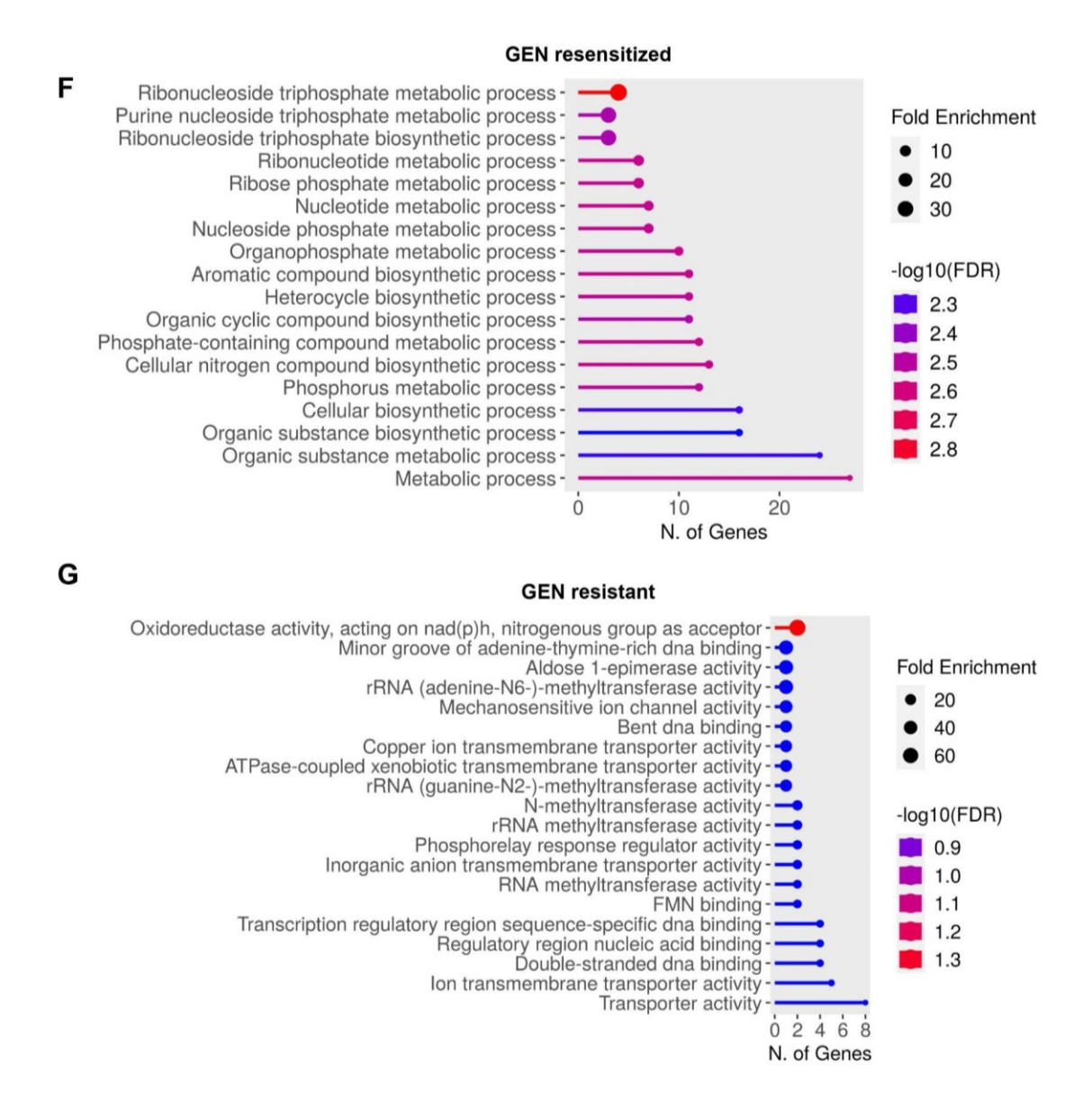


Figure 6.4 Tracking genomic changes through the GEN-PIP-NIT loop.

(A) - (D) Venn diagrams show overlapping and unique mutations in the GEN-resensitized and GEN-resistant strains from the three strains sequenced. The label on the left denotes when the strains were sequenced, with the most recent evolution step highlighted. Mutations that appeared in one step were carried forward to the next step, but are only displayed the first time they appeared in this figure. Strikethroughs denote mutations that appeared in a prior step but were not present in the current step. Underlined mutation in D, strain 3 represents a newly acquired mutation absent from strain 3 in C. (E) Venn diagram showing all overlapping and unique mutations between the GEN resensitized and GEN resistant group, pooled from every step (GEN-PIP-NIT only). (F) and (G). GO term enrichment analysis of unique mutations in the GEN resensitized and GEN resistant groups.

Five out of the six lineages acquired mutations in the efflux regulators acrR and marR following exposure to PIP, changes known to confer β -lactam resistance (Figure 6.4B) [377]. Mutations in the resensitized group also included other genes involved in β -lactam resistance such as cpxA and cyaA [378,379]; genes involved in carbon, amino acid, and vitamin metabolism: cra [380], leuA [381], pdxH and thiH [382,383]; and the ribosomal genes rsmG and rpsM [384,385] (Figure 6.4B). The resistant group did not show any clear mutations in genes involved in metabolism or the ribosome.

All NIT-resistant mutants acquired mutations in one or more of the genes involved in NIT resistance: *nfsA*, *nfsB* [386], *sulA* (essential for NIT resistance in *lon* mutants) [123], *ompR* [387] and *ompC* [388,389] (Figure 6.4A). Both GEN-resensitized and GEN-resistant lineages showed multiple mutations involved in transmembrane transporters. The resensitized group acquired mutations in genes involved in the sugar phosphotransferase transport system: *fruB* [390] and *nagE* [391], which also have putative roles in aminoglycoside uptake [81], while the resistant strains gained mutations in metal ion, amino acid and peptide transporters instead: *cusB* [392], *fepG* [393], *pitA* [394], *dptB* [395], and *pheP* [396] (Figure 6.4A). A gentamicin uptake assay suggested that these transport related mutations in the GEN resensitized strains may have slightly increased GEN penetration, but the results did not reach statistical significance (Supplementary Figure 6.3)

To elucidate how differences between the GEN-resensitized and GEN-resistant groups could affect their propensity towards resensitization, we first identified overlapping and unique mutations between the two groups following NIT evolution (Figure 6.4E). Common mutations were mostly

those known to confer resistance to GEN, PIP, or NIT, as discussed above. To categorize the remainder, we ran GO term enrichment analyses on the non-overlapping gene sets. Every hit from the resensitized group that was above the enrichment FDR cutoff was involved in metabolic processes (Figure 6.4F), whereas no significant enrichment was found in the resistant group. Manually removing the FDR cutoff (by setting it to 0.99) identified processes involved in transport and DNA-binding (Figure 6.4G). Mutations in metabolic processes are often involved in compensatory evolution to mitigate fitness costs and phenotypic reversion of resistance [397–400], which supports our observation of the little to no loss (but rather a slight increase) in fitness in the GEN resensitized strains (Figure 6.3C), in contrast to the significant fitness loss in the resistant group (Figure 6.3D). These genomic and fitness outcomes suggest that cells become resistant to antibiotics using similar mechanisms, but bifurcate at the level of fitness cost compensation. Cells that adopt pathways that help mitigate their fitness losses also reverse their resistance to the earlier drugs, strongly suggesting a correlation between the two phenotypes.

Since we also saw a surprising drop in NIT resistance after reacquisition of GEN resistance from the GEN-PIP-NIT-GEN series in all three non-extinct lineages, (Supplementary Figure 6.1D), we looked at the genome sequence of these NIT resensitized strains (Figure 6.4D). After reacquisition of GEN resistance, the genomic profile of the three strains looked almost identical (Figure 6.4C and D) except that strain 1 was replaced by a mutant with an intact *fruB* gene possibly via elevation of a low frequency mutant in the population, while strain 2 reverted its *nagE* mutation (Figure 6.4D). Both genes are involved in sugar transport. It is unclear how reversion of these mutations allowed GEN resistance reacquisition. There are no direct reports of nitrofurantoin being transported inside the cell via these transporters, but both *nagE* and *fruB* have been reported to

carry other drugs like streptozotocin and fosfomycin [401,402]. Since the *nagE* and *fruB* mutations are the only differences between the GEN-sensitive-NIT-resistant and GEN-resistant-NIT-sensitive strains (Figure 6.4C and D), it is likely that these mutations play a role in GEN and/or NIT resistance levels.

6.2.5. NIT-PIP-GEN loop reduces clinically acquired NIT resistance

To test if a tripartite loop can reduce clinically acquired drug resistance, we obtained four previously reported NIT-resistant uropathogenic *E. coli* clinical isolates [403]: strains A, B, C and D (renamed for this study) (Figure 6.5A). The strains were all resistant to NIT at varying levels (Figure 5B-E), and were isolated using sampling criteria designed to avoid repeated collection of the same isolates [403]. Next, we started sequential SAGE evolutions with eight replicates for each strain (Figure 6.5A). Three of the four strains (A, C, and D) were confirmed to have β -lactamase(s) via MIC testing (PIP MIC > 64 μ g/mL, PIP/tazobactam MIC \leq 4/4 μ g/mL), so we opted to replace the PIP SAGE plates with PIT (PIP/tazobactam) plates which contained the same PIP concentrations used in the rest of study in combination with a flat tazobactam concentration of 4 μ g/mL throughout the plate [404]. Subsequent GEN SAGE plates remained the same. These strains showed an extinction pattern similar to our NIT-PIP-GEN evolutions using the laboratory strain, with PIT evolution not incurring any extinctions and GEN evolution causing a ~31% extinction (10/32 strains extinct) comparable to the 25% with the laboratory strain (Supplementary Figure 6.1C) (Supplementary Figure 6.4A).

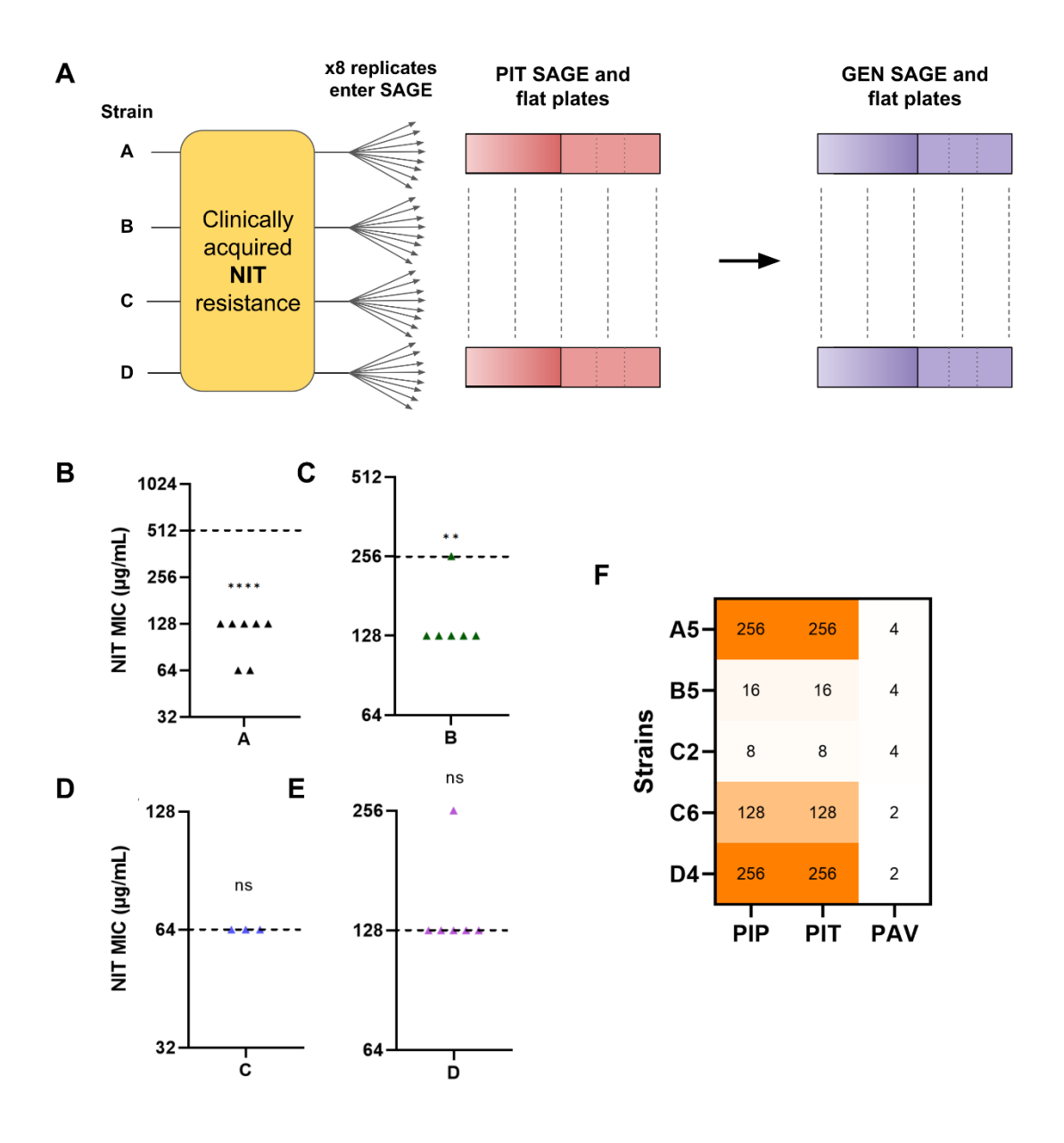


Figure 6.5 The NIT-PIP-GEN loop reduces clinically acquired NIT resistance.

(A) Four uropathogenic clinical E. coli strains resistant to NIT were used to start sequential PIT and GEN evolution. Each strain started 8 replicates in SAGE. The rest of the experimental evolution design remained identical to the one used for the laboratory strain. (B), (C), (D) and (E) NIT MICs of the clinical replicates post GEN adaptation. The dotted line represents NIT MICs of the parental strain pre SAGE adaptation. Labels on the x-axis denote the parental strain of the replicates for which the MICs are displayed. **p< 0.01, ****p<0.0001, one sample t-test. (F) PIP, PIP and PAV MICs of five clinical replicates after PIT exposure. PIT = piperacillin + tazobactam (4 μ g/mL), PAV = piperacillin + avibactam (4 μ g/mL). The y-axis denotes the strain ID where A5 = the 5th replicate from strain A.

Post GEN evolution, strain A showed a 4-fold median reduction in NIT resistance with 5/8 replicates showing MICs of 128 μg/ML, two dropping to 64 μg/mL (below the NIT clinical breakpoint), and one going extinct (Figure 6.5B) (Supplementary Figure 6.4A). Strain B showed a 2-fold median reduction in NIT resistance, with 5/8 strains dropping to 128 μg/mL down from 256 μg/mL of the parent strain and two going extinct (Figure 6.5C) (Supplementary Figure 6.4A). 5/8 replicates of strain C went extinct (Supplementary Figure 6.4A), and the rest of the replicates did not show a significant drop in NIT resistance, and neither did the six surviving replicates of strain D (Figure 6.5D, E).

6.2.6. Bypassing chromosomal adaptations against PIP does not abolish resensitizations

When we measured PIT MICs of the clinical replicates after PIT SAGE plates, we noticed resistance levels that were 8-16-folds higher (Supplementary Figure 6.4B) than the PIP resistance levels we observed after PIP SAGE plates using our laboratory strain (Supplementary Figure 6.1F, G). These high resistance levels were limited to strains A and D, and to a smaller extent C, which were also the strains that contained at least one β -lactamase that inactivated PIP. All 8 replicates of Strain B, which was originally sensitive to PIP (and hence did not require tazobactam for PIP activity) evolved an MIC of 16 μ g/mL, similar to the laboratory strain. This led us to hypothesize that instead of chromosomal adaptations against PIP during the PIT exposure, the β -lactamase bearing strains may have mutated their β -lactamase to resist tazobactam instead.

We picked five of these PIT resistant strains and measured their PIP MICs, but this time in combination with the non- β -lactam β -lactamase inhibitor avibactam (at a flat concentration of 4 μ g/mL) (PAV) [405]. Addition of avibactam increased PIP sensitivity by 64-128 folds, returning

MICs to within 2-fold of the PIP MICs of the parental strain (Figure 6.5F) (Supplementary Figure 6.4B), indicating that the PIP resistance was mediated by a change in the β-lactamase that allowed cells to bypass inhibition by tazobactam. Replicate B5 also saw a small 4-fold drop in PIP resistance which may be due to the modest antibacterial activity of avibactam against *E. coli* [406]. Despite avoiding chromosomal adaptations to PIP, we still observed almost identical extinction frequencies in all four clinical strains (Supplementary Figure 6.1C) (Supplementary Figure 6.4A) and frequent and significant resistance drops in strains A and B (Figure 6.5B, C).

6.3. Discussion

Cyclic antibiotic therapies have been proposed as a way to combat the rise of antibiotic resistance [128,303,361–363]. The success of such regimens is thought to hinge on CS interactions between the component drugs [52,84,128,364]. However, to date, CS has seen no application in the clinic since its first description in 1952 [51] and since its proposed benefits in cyclic therapies, partly because of the unreliability and rarity of CS [54,132,137,152]. In a previous study we showed that CS, when applied in the correct direction during cyclic therapies, can help resensitize bacteria to antibiotics [306]. However, we observed that the repeatability of CS evolution was low even in drug pairs with reported CS interactions, typified by small resistance drops and low resensitization frequencies, which may readily lead to the emergence of multidrug-resistant mutants [306].

In this study, we explored the potential of extending pairwise regimens to longer "tripartite loops". We found that the tripartite loop GEN-PIP-NIT significantly improved resensitization frequencies as compared to the previously proposed GEN-PIP pairwise loop [52,128,306], going from ~14% [306] to ~54% of lineages (Figure 6.1B). The loop was also invertible, with NIT-PIP-GEN reliably

resensitizing bacteria to NIT (Figure 6.1C). Resensitizations were independent of CS (Figure 6.3A, B) (Supplementary Figure 6.1F, G), and did not appear to be driven by NIT-specific resistance mutations. The resensitization was at least partially independent of drug identity, as extending the GEN-PIP loop with DOX, against which the bacteria showed cross-resistance, produced GEN-resensitized strains (Figure 6.3C, D).

When GEN-resensitized strains from the GEN-PIP-NIT loop were subjected to GEN again, we found that the antibiotic posed a significant evolutionary challenge, with three out of the six strains going extinct during SAGE (Supplementary Figure 6.1B). We did not observe extinctions when WT bacteria were exposed to GEN (Supplementary Figure 6.1A), implying that multidrug-resistant bacteria have constrained evolutionary paths that limit further resistance development. In fact, the three mutants that were able to reacquire GEN resistance dropped their NIT resistance in the process, showcasing the difficulty in maintaining multiple resistance mechanisms.

Unlike in the laboratory, rapid drug cycling in patients may not be possible due to pharmacokinetic factors [86], and the resulting longer evolutionary periods can allow for compensatory evolution which can mitigate evolutionary trade-offs like CS [134,137,407]. While this complicates CS-based cyclic therapies, our study shows that compensatory evolution can be leveraged to drive phenotypic reversion of resistance. We tracked fitness of resensitized and resistant bacteria throughout our tripartite loops, demonstrating that the sequential adaptation to three antibiotics increased fitness penalties compared to pairwise loops (Supplementary Figure 6.2), possibly due to the need to carry multiple independent resistance phenotypes. Strains could overcome this fitness loss through resensitization, e.g. to GEN (Figure 6.3E, Figure 6.4), or could persist with

poor growth (Figure 6.3F) [407]. This interplay was also apparent in the PIP-GEN-NIT loop, again through resensitization of GEN (Figure 6.3D). Since GEN evolution imposed the largest penalties in our experiments, it appears to be ideal for incorporation into drug cycling protocols. Our GO term enrichment analyses also clearly show evidence of metabolic rewiring associated with compensatory evolution [397–400] in resensitized strains that are missing from the resistant ones (Figure 6.4F, G), and the fitness and genomic analyses taken together suggests a strong association between compensatory evolution and resistance reversion.

In further support of longer cyclic regimens, we showed that despite the fact that PIP evolution failed to produce significant resensitizations (Figure 6.1B, C) (Supplementary Figure 6.1 F, G) [306], it aided in bringing down resistance to the initial drug in both the GEN-PIP-NIT loop and NIT-PIP-GEN loops (Figure 6.2A-D), which turned to full resensitizations after evolution against the last drug in the series. Additionally, tripartite loops continued to drive bacterial extinction (Supplementary Figure 6.1A - C), reinforcing prior work on sequential regimens [128,306].

When we compared the NIT resistant vs NIT resensitized strains from the GEN-PIP-NIT-GEN sequence (Figure 6.4D), we discovered that the genomes of the two groups were almost identical, except that the NIT resensitized strains reinstated two sugar transporter mutations. Elucidation of the exact mechanism of NIT resensitization will require further studies, but our data suggests a possible, previously unreported role for sugar transporters in NIT resistance (Figure 6.4C, D).

Our results from the evolutions using uropathogenic clinical strains show that our suggested tripartite loops may be effective even against diverse genetic backgrounds and when resistance evolution is complicated via plasmid-bound evolution, showing potential for translation into the clinic. Overall, we suggest that tripartite loops can improve antibiotic resensitization and allow continuation of antibiotic cycling even if pairwise cycles fail, without being limited by CS requirements. With our antibiotic development pipeline failing to keep up with resistance emergence, such cyclic therapies may prolong the lifespan of our existing antibiotics.

6.4. Materials and Methods

6.4.1. Bacterial strain and growth conditions

Escherichia coli K-12 substr. BW25113 and the evolved lineages were cultured in Muller Hinton (MH) media at 37 °C. Antibiotics were added to the growth media as needed to grow or isolate resistant mutants from SAGE plates. The clinical samples were streaked on tryptic soy agar (TSA) plates containing $64 \,\mu\text{g/mL}$ of NIT, and pure cultures were obtained by transferring a single colony from each strain onto MH agar plates. These were then used for all subsequent experiments.

6.4.2. SAGE evolutions

Evolutions were performed as previously described [145,306]. SAGE evolved mutants were extracted from within 1.5 cm of the end of the plates after seven days of incubation into MH broth containing the challenge antibiotic at a concentration = 2x the WT MIC. Strains were considered extinct when they could not be recovered after extraction from within 1.5 cm of the end of the SAGE plates [306]. Mutants that went extinct were given a second chance at evolution using the same parameters as before. This allowed us to maintain a larger sample size through the extinction events that occurred at different steps of evolution, and we report both the initial and final

extinction counts (Supplementary Figure 6.1A - C). Antibiotic concentrations in SAGE are listed below, and were determined from trial SAGE experiments to reliably evolve strains with MICs above the clinical breakpoints for each antibiotic [339].

Antibiotic	Concentration (µg/mL)
GEN	5
PIP	40
NIT	80

6.4.3. Susceptibility testing

Minimum inhibitory concentrations (MIC) of antibiotics were determined using the broth microdilution method as described by the CLSI [214]. Antibiotics were diluted in MH broth, then serially diluted across 96 well plates. Bacteria were inoculated at a concentration of 1/200 of a 0.5 McFarland standard. Plates were incubated overnight at 37 °C without shaking, and the MIC was recorded as the lowest antibiotic concentration that prevented visible bacterial growth. For PIT and PAV MICs, tazobactam or avibactam respectively was added at a fixed concentration of 4 μg/mL to all the wells in the test plates [404,405].

6.4.4. Flat plates

Flat plates were prepared as previously described [306]. First, the evolved MIC of the antibiotic used in the preceding SAGE plates was determined for all strains that completed SAGE evolution.

Next, specific lanes were created for each strain by pouring approximately 12 mL medium supplemented with the antibiotic at half the MIC of that strain into four-well dishes. This allowed for the maintenance of the resistance gained from SAGE during compensatory evolution. Each replicate underwent three consecutive passages on these flat plates (Figure 6.1A). The first plate was incubated for two days, and the second and third plates for one day (Figure 6.1A). Unlike during SAGE evolutions, where extractions were limited to within the final 1.5 cm of the plates, cells from flat plates were extracted from the farthest point of growth. PIT flat plates contained tazobactam at a fixed concentration of 4 µg/mL in combination with appropriate [PIP] [404].

6.4.5. Fitness measurements

Growth curves for each strain were made by tracking absorbance readings at 595 nm of 1/100 dilutions of overnight cultures using a plate reader (Tecan Sunrise) for 24 h. Plate lids were treated with 0.05% Triton X-100 in 20% ethanol to reduce fogging [212]. AUCs were calculated using GraphPad Prism.

6.4.6. Whole genome sequencing

Genomic DNA was extracted using the Bio Basic genomic DNA kit (Cat. no.: BS624). Sequencing and variant calling were performed by Sequenter (USA) on an Illumina NextSeq 2000, and demultiplexing, quality control, and adapter trimming were performed with bcl-convert (v3.9.3). Variant calling was performed using Breseq under default settings [295]. NCBI reference sequence CP009273.1 was used for variant calling. Common mutations were identified using custom R scripts and Venn diagrams were based on the output of the R package *ggvenn*.

6.4.7. Term enrichment analysis

To identify pathways affected the mutations ShinyGO by observed, v0.81(https://bioinformatics.sdstate.edu/go/) was used. For GEN resensitized strains, the following parameters were used: Species: Escherichia coli str. K-12 substr. MG1655 STRINGdb; DB: Go Biological processes; FDR: Default of 0.05. Resistant strains produced no result using these parameters. These parameters were modified by removing the FDR cutoff to produce the results shown in Figure 6.4G. The modified parameters were: DB: GO Molecular Function; FDR: set to 0.99.

6.4.8. Gentamicin uptake assay

Gentamicin uptake was measured using a modified version of a previously reported protocol [408]. 300 μL of overnight bacterial cultures were transferred into 30 mL of MH broth in conical flasks and incubated at 37 °C with 250 rpm shaking until log phase was reached. The log phase of each strain was estimated from their growth curves. OD at 600 nm was then measured for each strain, and cells were either concentrated or diluted to reach an OD of 0.4. 100 μL of cells were transferred into microcentrifuge tubes, and GEN was added at a concentration of 100 μg/mL. Tubes were allowed to incubate at 37 °C with 1000 rpm shaking on a heat block for 15 minutes. Tubes were then chilled on ice for five minutes, then centrifuged at 12,000 g for two minutes. 5 μL of the supernatants were used to spot WT *E. coli* seeded MH agar plates, and left to air dry. Plates were incubated overnight, then photographed from a fixed distance of 29 cm. Images were analyzed by fitting circles around the inhibition zones and measuring the area in px² using ImageJ [409].

Measurements were taken from 6 independent replicates for each strain. The three resensitized strains that were sequenced (Supplementary Figure 6.1F) were also used to perform this test.

Chapter 7. General Discussion

Antibiotic resistance is fundamentally an evolutionary challenge, requiring solutions grounded in evolutionary principles. In this work, I demonstrated how large-scale laboratory evolution can help us understand this problem better, and how we can use the knowledge gained to build antibiotic therapies that are resilient against evolution. By exploring the dynamics of resistance evolution and its associated trade-offs from over a thousand laboratory-generated mutants across various drug sequences, I shed light on how fitness costs of resistance shape the outcomes of sequential antibiotic regimens.

7.1. Key Findings

A platform for discovering fitness costs of resistance that are resilient against compensatory evolution was developed.

In chapter 2, I showed that growth impairments associated with resistance evolution can impede the evolution of subsequent resistance, and that this effect may be applicable in a variety of antibiotics and bacteria. Since compensatory evolution is a powerful means by which bacteria escape the effects of the fitness costs of resistance, I reported a simple, soft agar gradient evolution (SAGE)-based method to discover trade-offs that are stable against compensatory evolution.

Xanthan gum massively reduces synaeresis from agar-based hydrogels.

Synaeresis, the spontaneous expulsion of water from agar hydrogels, causes significant loss of growth-promoting properties of solid growth medium during long incubations, and limits the evolution of resistance in SAGE. In chapter 3, I reported that the addition of xanthan gum can reduce synaeresis by ~70% in low-strength agar-based media, and can significantly enhance resistance evolution in SAGE.

"Evolution proof" antibiotics may just be "laboratory-evolution proof".

In chapter 3, I described the evolution of *de novo* resistance to the antibiotic tridecaptin A_1 via an improved SAGE method, an antibiotic against which resistance evolution was not reported despite previous laboratory evolution attempts. Antibiotics such as tridecaptin A_1 have been labelled "evolution proof", but my results suggested that failures to generate resistance in the laboratory may be more related to the experimental evolution methods used. If history is any guide, evolution will continue to find ways to overcome our antibiotics. The real question is whether we can stay ahead by predicting the evolutionary paths it might take.

SAGE evolutions better predict clinical collateral phenotypes.

In chapter 4, I reported results from large scale evolution of antibiotic resistance and collateral phenotypes (collateral sensitivity and cross-resistance) using three different evolution platforms: serial transfer based, gradient plating-based, and SAGE. Upon comparison, I found that SAGE produced very few instances of collateral sensitivity but exhibited cross-resistance and neutrality at high frequencies when compared to the other platforms. This resembled collateral interactions identified from a clinical dataset of over 750 clinical uropathogenic multidrug resistant *E. coli* strains.

SAGE predicted a collateral sensitivity relationship found in the clinic.

In chapter 4, I found that SAGE showed significant CS in only one out of the four drug pairs investigated: a tigecycline (a third generation tetracycline) and polymyxin B pair. We observed a significant association between increasing omadacycline (a third generation tetracycline)

resistance and reduced colistin (polymyxin E) resistance in a clinical dataset of multidrug resistant *E. coli* strains.

A novel mechanism of collateral sensitivity was discovered.

In chapter 4, I explained how resistance to tigecycline can make cells hypersensitive to polymyxin B. I showed that tigecycline-resistant cells inactivate the Lon protease, leading to overproduction of negatively charged exopolysaccharides and enhancing binding of the polycationic antibiotic polymyxin B, rendering cells hypersensitive to it.

Large scale evolutions are essential for accurate prediction of repeatable collateral sensitivity.

In chapter 5, I found that reported collateral sensitivity interactions can have very low repeatability.

A ciprofloxacin - gentamicin pair with reported collateral sensitivity produced only ~6% collateral sensitivity when 16 independent evolutionary replicates were probed. Repeatability is essential for application of evolutionary strategies in the clinic to combat resistance. My experimental design provides a platform for large scale screening for the evolution of repeatable collateral phenotypes.

Forward and backward collateral sensitivities were defined for the first time, revealing that only backward collateral sensitivity plays a critical role in resensitization.

I broke down reciprocal collateral sensitivity into forward and backward collateral sensitivities in reference with the direction of sequential therapy in chapter 5. Forward collateral sensitivity was found to not be significantly associated with antibiotic resensitizations, while backward collateral sensitivity appeared to play a major role.

Tigecycline resistance causes a dramatic 64-fold polymyxin B-resensitization.

In chapter 5, I discovered that polymyxin B resistant *E. coli* were completely resensitized to polymyxin B when tigecycline resistance developed. Every one of the 16 evolutionary replicates were resensitized, with an average 64-fold drop in polymyxin B resistance. In addition with the tigecycline - polymyxin B relationship I reported in chapter 4, this drug pair appears to be a potent drug pair with strong reciprocal CS interactions with potential for clinical application.

A novel, collateral sensitivity-independent sequential regimen termed "tripartite loop" was described that exploits cumulative fitness costs to repeatably guide bacteria towards resensitization.

In chapter 5, I showed that complete antibiotic resensitizations below clinical breakpoints are rare in pairwise sequential regimens. In chapter 6, I developed extended sequential antibiotic regimens, termed "tripartite loops", designed to resensitize bacteria by exploiting cumulative fitness costs. I described tripartite loops composed of the clinically relevant drugs gentamicin, piperacillin and nitrofurantoin and showed that sequential evolution of resistance through these sequences repeatably resensitized bacteria to antibiotics below clinical breakpoints. This strategy proved more effective than pairwise regimens and was successful in multidrug-resistant clinical isolates, even when evolution was complicated via plasmid-bound mutations.

7.2. Limitations

Before investigating the role of collateral sensitivity in sequential antibiotic therapies, I dedicated significant effort, detailed in chapters three and four, to developing the SAGE platform and validating its clinical relevance. While SAGE offers important insights into resistance and collateral phenotypes, it remains an *in vitro* model and cannot fully replicate the complexities of

real infections. Advancing towards more physiologically relevant experimental evolution platforms will be important to test the broader applicability and translational potential of these findings.

One of the primary goals of this study was to bring to light evolutionary trade-offs that appear frequently and are generalizable across different genetic backgrounds of *E. coli*. This was done through inclusion of a large number of independent evolutionary replicates and different clinical isolates. Since evolution is highly dependent on the genetic background [410,411], extending these results to other bacterial pathogens will require further validation.

Results from this work showed that the accumulating fitness burden of acquiring multiple drug resistances was associated with antibiotic resensitizations. Further experimental work will be necessary to establish a causal relationship between fitness penalties and antibiotic resensitization.

Chromosomal mutations are a major driver of antibiotic resistance [412–414] and formed the primary focus of this thesis. However, horizontal gene transfer of mobile genetic elements (MGEs), such as plasmids, also plays a significant role in the spread of resistance. Understanding how MGEs influence the outcomes of sequential antibiotic treatments will be an important direction for future research.

7.3. Future Work

Specialized culture media that mimic infection environments like the cystic fibrosis lung [415] and intracellular vacuoles of macrophages [416] have been developed to better reflect *in vivo*

conditions. In fact, some excellent work has been done recently on developing mice as *in vivo* models of evolution [417]. However, conducting large-scale evolution experiments directly in *in vivo* models will be challenging and impractical for early-stage discovery of robust evolutionary trade-offs. A more feasible and powerful approach will be to integrate physiologically relevant media into platforms like SAGE, enabling high-throughput screening under infection-mimicking conditions. Promising candidates identified through this strategy can then be advanced to *in vivo* validation, an essential next step to confirm their relevance in real-world infections and move them closer to clinical application.

WHO's critical and high-risk bacterial pathogens list includes *Acinetobacter baumannii*, multidrug resistant Enterobacterales, *Salmonella* Typhi, *Shigella* spp, *Enterococcus faecium*, *Pseudomonas*, *aeruginosa*, *Neisseria gonnorrhoeae* and *Staphylococcus aureus*. This study focused on *E. coli*, a representative of multidrug-resistant Enterobacterales. The evolutionary and sequential antibiotic strategies developed here can serve as a blueprint for tackling other clinically significant pathogens on this list.

In chapter 2, I described an experimental framework to discover evolutionary trade-offs that are stable against compensatory evolution. Identifying such trade-offs is essential since trade-offs in the clinic are often neutralized via compensatory evolution. Expanding the search for discovering more robust trade-offs can improve the availability of optimal antibiotic sequences for wider application.

In chapters 4 and 5, I identified the polymyxin–tigecycline pair as a powerful reciprocal drug combination capable of driving dramatic antibiotic resensitization, with promising potential for clinical application in resistance management. While chapter 5 explores key contributors to this effect, the exact mechanism remains unclear. A multiomics approach applied on the large number of mutants produced in this work can help shed light into the mechanism of this exciting drug pair.

SAGE evolution experiments in this study were carried out over a fixed seven-day period. This standardized experimental design enabled consistent benchmarking of adaptation rates and extinction events. However, it limited our ability to assess whether the presence of collateral sensitivity influenced the speed of resistance evolution. Future studies that track bacterial movement across the SAGE plates could provide valuable insights into how CS shapes evolutionary kinetics.

Chapter 6 described the identification of a novel, invertible tripartite antibiotic loop composed of the clinically relevant antibiotics gentamicin, piperacillin and nitrofurantoin that produced antibiotic resensitizations and drove bacterial extinction even when tested against clinical bacterial isolates. The experimental design reported in this chapter can be used, possibly with additional SAGE media modifications to mimic infection specific conditions, to discover additional tripartite loops which can limit resistance during long antibiotic exposures.

The genomic tracking of evolutionary trajectories in chapter 6 uncovered interesting leads, most notably, a potential role for the sugar phosphotransferase transport system in modulating resistance and hypersensitivity to gentamicin and nitrofurantoin. The system's ubiquitous presence in

bacteria and complete absence in eukaryotes makes it an attractive target for the development of new antimicrobials. Uncovering the roles of the mutations in this pathway may open new avenues for antibiotic development or antibiotic resensitization strategies.

The described tripartite loop showed exciting potential to resensitize nitrofurantoin resistant clinical *E. coli* isolates. Whole genome sequencing of these mutants to uncover the genetic changes and their evolutionary trajectories can provide important information on how resistance reversion in clinical strains compares to that observed in laboratory-evolved strains. Such comparisons can help us understand the underlying genetic factors that cause bacteria to "phenotypically converge" towards antibiotic resensitization and ultimately design evolutionary strategies that repeatably hinder resistance evolution.

Acquisition of resistance-conferring plasmids can bypass the need for chromosomal mutations [418], potentially avoiding the fitness costs associated with those mutations. However, carrying resistance plasmids often imposes its own fitness burden on bacteria [419]. I showed that the presence of resistance-coding plasmids in clinical *E. coli* isolates did not significantly compromise the efficacy of tripartite loops. A more detailed investigation into how the fitness costs associated with plasmids can be leveraged to manage the spread of resistance, and the influence of plasmids on sequential therapies will be important to build robust treatment strategies.

7.4. Conclusion

My work advances our understanding of antibiotic resistance evolution and presents the importance of the integration of evolutionary principles into the design of antibiotic therapies.

Through refinement of the SAGE platform [69], I reported a high-throughput experimental evolution platform capable of capturing robust fitness trade-offs that shape bacterial adaptation. Leveraging this platform, I showed how resistance-associated fitness costs can slow subsequent adaptation, disrupt pathways to resistance evolution and drive resensitization to antibiotics.

A xanthan gum-supplemented SAGE medium massively improved the water-retention capacity of the system, improving its resistance generation potential. Using this platform, I challenged the notion of "evolution-proof" antibiotics proposed to resist the emergence of resistance. I was able to generate mutants resistant to Oct-TriA₁, a lipopeptide previously believed to be refractory to resistance evolution [146], within nine days. In collaboration with Laura Domínguez Mercado, we identified for the first time the genetic mechanism underlying *de novo* resistance to this compound. This finding suggests that no antibiotic is immune to evolution and highlights the need for platforms like SAGE to proactively predict resistance mechanisms before clinical deployment. Identifying such escape routes early is crucial for guiding preclinical development, surveillance planning, and therapy design [218].

I discovered a clinically relevant collateral sensitivity interaction through the largest experimental comparison of laboratory evolution platforms to date. SAGE predicted a rare but robust collateral sensitivity between third-generation tetracyclines (tigecycline and omadacycline) and the last-resort polymyxin-class antibiotics (polymyxin B and colistin). I also explained a previously unknown mechanism of collateral sensitivity between these drugs. I showed that resistance to tigecycline induced hypersensitivity to polymyxins via Lon protease deactivation and consequent overproduction of negatively charged exopolysaccharides, enhancing binding of the cationic

drugs. This finding provides one of the few mechanistically supported examples of collateral sensitivity with translational potential and highlights the importance of scale and platform choice in predicting clinically actionable collateral interactions.

Contrary to prior assumptions, I showed that collateral sensitivity is not a universally reliable phenomenon; its repeatability and impact on resistance evolution are highly context-dependent. Through a thorough analysis of sequential regimens and dissection of reciprocal collateral sensitivity into forward and backward CS, I demonstrated that only backward CS, where resistance to the second drug increases susceptibility to the first, consistently contributes to meaningful resensitization. However, even these effects were modest in magnitude, prompting a pivot toward strategies beyond CS alone.

This led to the development of tripartite antibiotic loops: sequential regimens composed of three clinically relevant drugs. I showed that these loops exploit the cumulative fitness burden of evolving multiple resistances, forcing bacteria into evolutionary paths that either reverse previous resistance or lead to extinction. The loops proved not only repeatable but also robust across diverse clinical isolates, including those carrying plasmid-borne resistance determinants. This represents a significant advancement in designing evolutionarily resilient therapies capable of resensitizing or eliminating multidrug-resistant pathogens.

Collectively, this work highlights the potential of using evolutionary constraints to limit resistance evolution. Large-scale experimental evolution can help discover predictable resistance pathways, identify stable evolutionary bottlenecks, and guide the rational design of antibiotic regimens that

are both durable and translatable. As we face an era of dwindling antibiotic innovation [420], this evolution-based framework offers a path ahead for extending the lifespan of our existing drugs and restoring their utility against multidrug resistant bacterial pathogens.

References

- [1] Cook MA, Wright GD. The past, present, and future of antibiotics. Sci Transl Med 2022;14:eabo7793. https://doi.org/10.1126/scitranslmed.abo7793.
- [2] Adedeji WA. THE TREASURE CALLED ANTIBIOTICS. Ann Ib Postgrad Med 2016;14:56–7.
- [3] Antibiotics are the basis of modern medicine. Wellcome 2020. https://wellcome.org/news/antibiotics-are-basis-modern-medicine-these-projects-aim-keep-it-way (accessed March 26, 2025).
- [4] Turkulov V, Brkić S, Doder R, Vukadinov J, Sević S, Canak G. [Application of antibiotics in vulnerable groups]. Med Pregl 2010;63 Suppl 1:33–6.
- [5] Antibiotics Uses. NhsUk 2017. https://www.nhs.uk/conditions/antibiotics/uses/ (accessed March 26, 2025).
- [6] Hutchings MI, Truman AW, Wilkinson B. Antibiotics: past, present and future. Curr Opin Microbiol 2019;51:72–80. https://doi.org/10.1016/j.mib.2019.10.008.
- [7] CDC. About Antimicrobial Resistance. Antimicrob Resist 2024. https://www.cdc.gov/antimicrobial-resistance/about/index.html (accessed March 7, 2025).
- [8] Antimicrobial resistance. WHO n.d. https://www.who.int/news-room/fact-sheets/detail/antimicrobial-resistance (accessed March 7, 2025).
- [9] Van Boeckel TP, Pires J, Silvester R, Zhao C, Song J, Criscuolo NG, et al. Global trends in antimicrobial resistance in animals in low- And middle-income countries. Science 2019;365. https://doi.org/10.1126/science.aaw1944.
- [10] Rolfe R, Kwobah C, Muro F, Ruwanpathirana A, Lyamuya F, Bodinayake C, et al. Barriers to implementing antimicrobial stewardship programs in three low- and middle-income country tertiary care settings: findings from a multi-site qualitative study. Antimicrob Resist Infect Control 2021;10:60. https://doi.org/10.1186/s13756-021-00929-4.
- [11] Murray CJ, Ikuta KS, Sharara F, Swetschinski L, Aguilar GR, Gray A, et al. Global burden of bacterial antimicrobial resistance in 2019: a systematic analysis. The Lancet 2022;399:629–55. https://doi.org/10.1016/S0140-6736(21)02724-0.
- [12] Naghavi M, Vollset SE, Ikuta KS, Swetschinski LR, Gray AP, Wool EE, et al. Global burden of bacterial antimicrobial resistance 1990–2021: a systematic analysis with forecasts to 2050. The Lancet 2024;404:1199–226. https://doi.org/10.1016/S0140-6736(24)01867-1.
- [13] Bush K, Bradford PA. β-Lactams and β-Lactamase Inhibitors: An Overview. Cold Spring Harb Perspect Med 2016;6:a025247. https://doi.org/10.1101/cshperspect.a025247.
- [14] Abraham EP. A glimpse of the early history of the cephalosporins. Rev Infect Dis 1979;1:99–105. https://doi.org/10.1093/clinids/1.1.99.

- [15] Marshall WF, Blair JE. The Cephalosporins. Mayo Clin Proc 1999;74:187–95. https://doi.org/10.4065/74.2.187.
- [16] Armstrong T, Fenn SJ, Hardie KR. JMM Profile: Carbapenems: a broad-spectrum antibiotic. J Med Microbiol 2021;70:001462. https://doi.org/10.1099/jmm.0.001462.
- [17] Brewer NS, Hellinger WC. The Monobactams. Mayo Clin Proc 1991;66:1152–7. https://doi.org/10.1016/S0025-6196(12)65797-8.
- [18] Sykes RB, Bonner DP. Discovery and development of the monobactams. Rev Infect Dis 1985;7 Suppl 4:S579-593. https://doi.org/10.1093/clinids/7.supplement 4.s579.
- [19] Krause KM, Serio AW, Kane TR, Connolly LE. Aminoglycosides: An Overview. Cold Spring Harb Perspect Med 2016;6:a027029. https://doi.org/10.1101/cshperspect.a027029.
- [20] Nelson ML, Levy SB. The history of the tetracyclines. Ann N Y Acad Sci 2011;1241:17–32. https://doi.org/10.1111/j.1749-6632.2011.06354.x.
- [21] Appelbaum PC, Hunter PA. The fluoroquinolone antibacterials: past, present and future perspectives. Int J Antimicrob Agents 2000;16:5–15. https://doi.org/10.1016/S0924-8579(00)00192-8.
- [22] Dinos GP. The macrolide antibiotic renaissance. Br J Pharmacol 2017;174:2967–83. https://doi.org/10.1111/bph.13936.
- [23] Ledger EVK, Sabnis A, Edwards AM. Polymyxin and lipopeptide antibiotics: membrane-targeting drugs of last resort. Microbiology 2022;168:001136. https://doi.org/10.1099/mic.0.001136.
- [24] Blaskovich MAT, Hansford KA, Butler MS, Jia Z, Mark AE, Cooper MA. Developments in Glycopeptide Antibiotics. ACS Infect Dis 2018;4:715–35. https://doi.org/10.1021/acsinfecdis.7b00258.
- [25] Davies J, Davies D. Origins and evolution of antibiotic resistance. Microbiol Mol Biol Rev MMBR 2010;74:417–33. https://doi.org/10.1128/MMBR.00016-10.
- [26] Nothias L-F, Knight R, Dorrestein PC. Antibiotic discovery is a walk in the park. Proc Natl Acad Sci 2016;113:14477–9. https://doi.org/10.1073/pnas.1618221114.
- [27] Clardy J, Fischbach MA, Currie CR. The natural history of antibiotics. Curr Biol 2009;19:R437–41. https://doi.org/10.1016/j.cub.2009.04.001.
- [28] Sengupta S, Chattopadhyay MK, Grossart H-P. The multifaceted roles of antibiotics and antibiotic resistance in nature. Front Microbiol 2013;4. https://doi.org/10.3389/fmicb.2013.00047.
- [29] D'Costa VM, King CE, Kalan L, Morar M, Sung WWL, Schwarz C, et al. Antibiotic resistance is ancient. Nature 2011;477:457–61. https://doi.org/10.1038/nature10388.
- [30] Dobrindt U, Zdziarski J, Salvador E, Hacker J. Bacterial genome plasticity and its impact on adaptation during persistent infection. Int J Med Microbiol 2010;300:363–6. https://doi.org/10.1016/j.ijmm.2010.04.010.
- [31] Tooke CL, Hinchliffe P, Bragginton EC, Colenso CK, Hirvonen VHA, Takebayashi Y, et al. β-Lactamases and β-Lactamase Inhibitors in the 21st Century. J Mol Biol 2019;431:3472–500. https://doi.org/10.1016/j.jmb.2019.04.002.
- [32] Ramirez MS, Tolmasky ME. Aminoglycoside Modifying Enzymes. Drug Resist Updat Rev Comment Antimicrob Anticancer Chemother 2010;13:151–71. https://doi.org/10.1016/j.drup.2010.08.003.
- [33] Zhou G, Wang Q, Wang Y, Wen X, Peng H, Peng R, et al. Outer Membrane Porins Contribute to Antimicrobial Resistance in Gram-Negative Bacteria. Microorganisms 2023;11:1690. https://doi.org/10.3390/microorganisms11071690.

- [34] Papkou A, Hedge J, Kapel N, Young B, MacLean RC. Efflux pump activity potentiates the evolution of antibiotic resistance across S. aureus isolates. Nat Commun 2020;11:3970. https://doi.org/10.1038/s41467-020-17735-y.
- [35] Lambert PA. Bacterial resistance to antibiotics: Modified target sites. Adv Drug Deliv Rev 2005;57:1471–85. https://doi.org/10.1016/j.addr.2005.04.003.
- [36] Sun D, Jeannot K, Xiao Y, Knapp CW. Editorial: Horizontal Gene Transfer Mediated Bacterial Antibiotic Resistance. Front Microbiol 2019;10. https://doi.org/10.3389/fmicb.2019.01933.
- [37] Silver LL. Challenges of Antibacterial Discovery. Clin Microbiol Rev 2011;24:71–109. https://doi.org/10.1128/cmr.00030-10.
- [38] WHO report highlights shortage of new antibiotics | CIDRAP n.d. https://www.cidrap.umn.edu/who-report-highlights-shortage-new-antibiotics (accessed January 15, 2023).
- [39] Gupta SK, Nayak RP. Dry antibiotic pipeline: Regulatory bottlenecks and regulatory reforms. J Pharmacol Pharmacother 2014;5:4–7. https://doi.org/10.4103/0976-500X.124405.
- [40] Blujepa (gepotidacin) approved by US FDA for treatment of uncomplicated urinary tract infections (uUTIs) in female adults and paediatric patients 12 years of age and older | GSK 2025. https://www.gsk.com/en-gb/media/press-releases/blujepa-gepotidacin-approved-by-us-fda-for-treatment-of-uncomplicated-urinary-tract-infections/ (accessed March 31, 2025).
- [41] Terreni M, Taccani M, Pregnolato M. New Antibiotics for Multidrug-Resistant Bacterial Strains: Latest Research Developments and Future Perspectives. Molecules 2021;26:2671. https://doi.org/10.3390/molecules26092671.
- [42] Jacobs A. W.H.O. Warns That Pipeline for New Antibiotics Is Running Dry. N Y Times 2020.
- [43] WHO publishes list of bacteria for which new antibiotics are urgently needed n.d. https://www.who.int/news/item/27-02-2017-who-publishes-list-of-bacteria-for-which-new-antibiotics-are-urgently-needed (accessed January 15, 2023).
- [44] Nurjadi D, Schulenburg H, Niemann S, Zinkernagel AS, Rupp J. Are we overlooking the obvious? Bacterial evolution is at the heart of antimicrobial resistance. Lancet Microbe 2025;0. https://doi.org/10.1016/j.lanmic.2024.101069.
- [45] McDonald MJ. Microbial Experimental Evolution a proving ground for evolutionary theory and a tool for discovery. EMBO Rep 2019;20:e46992. https://doi.org/10.15252/embr.201846992.
- [46] Lenski RE. Experimental evolution and the dynamics of adaptation and genome evolution in microbial populations. ISME J 2017;11:2181–94. https://doi.org/10.1038/ismej.2017.69.
- [47] Hirasawa T, Maeda T. Adaptive Laboratory Evolution of Microorganisms: Methodology and Application for Bioproduction. Microorganisms 2023;11:92. https://doi.org/10.3390/microorganisms11010092.
- [48] Vinchhi R, Jena C, Matange N. Adaptive laboratory evolution of antimicrobial resistance in bacteria for genetic and phenotypic analyses. STAR Protoc 2023;4:102005. https://doi.org/10.1016/j.xpro.2022.102005.

- [49] Maeda T, Iwasawa J, Kotani H, Sakata N, Kawada M, Horinouchi T, et al. High-throughput laboratory evolution reveals evolutionary constraints in Escherichia coli. Nat Commun 2020;11:5970. https://doi.org/10.1038/s41467-020-19713-w.
- [50] Krist AC, Showsh SA. Experimental Evolution of Antibiotic Resistance in Bacteria. Am Biol Teach 2007;69:94–7. https://doi.org/10.1662/0002-7685(2007)69[94:EEOARI]2.0.CO;2.
- [51] Szybalski W, Bryson V. Genetic studies on microbial cross resistance to toxic agents i. J Bacteriol 1952;64:489–99. https://doi.org/10.1128/jb.64.4.489-499.1952.
- [52] Imamovic L, Sommer MOA. Use of Collateral Sensitivity Networks to Design Drug Cycling Protocols That Avoid Resistance Development. Sci Transl Med 2013;5:204ra132-204ra132. https://doi.org/10.1126/SCITRANSLMED.3006609.
- [53] Podnecky NL, Fredheim EGA, Kloos J, Sørum V, Primicerio R, Roberts AP, et al. Conserved collateral antibiotic susceptibility networks in diverse clinical strains of Escherichia coli. Nat Commun 2018;9:3673. https://doi.org/10.1038/s41467-018-06143-y.
- [54] Nichol D, Rutter J, Bryant C, Hujer AM, Lek S, Adams MD, et al. Antibiotic collateral sensitivity is contingent on the repeatability of evolution. Nat Commun 2019 101 2019;10:1–10. https://doi.org/10.1038/s41467-018-08098-6.
- [55] Krajewska J, Tyski S, Laudy AE. In Vitro Resistance-Predicting Studies and In Vitro Resistance-Related Parameters—A Hit-to-Lead Perspective. Pharmaceuticals 2024;17:1068. https://doi.org/10.3390/ph17081068.
- [56] Maeda T, Furusawa C. Laboratory Evolution of Antimicrobial Resistance in Bacteria to Develop Rational Treatment Strategies. Antibiotics 2024;13:94. https://doi.org/10.3390/antibiotics13010094.
- [57] Toprak E, Veres A, Yildiz S, Pedraza JM, Chait R, Paulsson J, et al. Building a morbidostat: an automated continuous-culture device for studying bacterial drug resistance under dynamically sustained drug inhibition. Nat Protoc 2013;8:555–67. https://doi.org/10.1038/nprot.2013.021.
- [58] Drake DR, Brogden KA. Continuous-Culture Chemostat Systems and Flowcells as Methods to Investigate Microbial Interactions. Polymicrob. Dis., ASM Press; 2002.
- [59] Dragosits M, Mattanovich D. Adaptive laboratory evolution principles and applications for biotechnology. Microb Cell Factories 2013;12:64. https://doi.org/10.1186/1475-2859-12-64.
- [60] Ekkers DM, Branco dos Santos F, Mallon CA, Bruggeman F, van Doorn GS. The omnistat: A flexible continuous-culture system for prolonged experimental evolution. Methods Ecol Evol 2020;11:932–42. https://doi.org/10.1111/2041-210X.13403.
- [61] Stefano Ugolini G, Wang M, Secchi E, Pioli R, Ackermann M, Stocker R. Microfluidic approaches in microbial ecology. Lab Chip 2024;24:1394–418. https://doi.org/10.1039/D3LC00784G.
- [62] Yuan L, Straub H, Shishaeva L, Ren Q. Microfluidics for Biofilm Studies. Annu Rev Anal Chem 2023;16:139–59. https://doi.org/10.1146/annurev-anchem-091522-103827.
- [63] Duncombe TA, Tentori AM, Herr AE. Microfluidics: reframing biological enquiry. Nat Rev Mol Cell Biol 2015;16:554–67. https://doi.org/10.1038/nrm4041.
- [64] Baym M, Lieberman TD, Kelsic ED, Chait R, Gross R, Yelin I, et al. Spatiotemporal microbial evolution on antibiotic landscapes. Science 2016;353:1147–51. https://doi.org/10.1126/science.aag0822.

- [65] This might be the coolest visualization of evolution ever | Vox n.d. https://www.vox.com/2016/9/8/12852924/evolution-bacteria-timelapse-video-megaharvard (accessed April 16, 2025).
- [66] Scutti S. Giant petri dish helps you 'see' antibiotic resistance. CNN 2016. https://www.cnn.com/2016/09/08/health/giant-petri-dish-antibiotic-resistance/index.html (accessed April 16, 2025).
- [67] Scientists Build Giant Petri Dish to Film Bacteria Resistance | American Association for the Advancement of Science (AAAS) n.d. https://www.aaas.org/news/scientists-build-giant-petri-dish-film-bacteria-resistance (accessed April 16, 2025).
- [68] Pesheva E. A cinematic approach to drug resistance. Harv Gaz 2016. https://news.harvard.edu/gazette/story/2016/09/a-cinematic-approach-to-drug-resistance/(accessed April 16, 2025).
- [69] Ghaddar N, Hashemidahaj M, Findlay BL. Access to high-impact mutations constrains the evolution of antibiotic resistance in soft agar. Sci Rep 2018 81 2018;8:1–10. https://doi.org/10.1038/s41598-018-34911-9.
- [70] Hermsen R, Deris JB, Hwa T. On the rapidity of antibiotic resistance evolution facilitated by a concentration gradient. Proc Natl Acad Sci U S A 2012;109:10775–80. https://doi.org/10.1073/pnas.1117716109.
- [71] Chowdhury FR, Mercado LD, Kharitonov K, Findlay BL. *De novo* evolution of antibiotic resistance to Oct-TriA1. Microbiol Res 2025;293:128056. https://doi.org/10.1016/j.micres.2025.128056.
- [72] Dheda K, Lenders L, Magombedze G, Srivastava S, Raj P, Arning E, et al. Drug-Penetration Gradients Associated with Acquired Drug Resistance in Patients with Tuberculosis. Am J Respir Crit Care Med 2018;198:1208–19. https://doi.org/10.1164/rccm.201711-2333OC.
- [73] Wu A, Loutherback K, Lambert G, Estévez-Salmerón L, Tlsty TD, Austin RH, et al. Cell motility and drug gradients in the emergence of resistance to chemotherapy. Proc Natl Acad Sci 2013;110:16103–8. https://doi.org/10.1073/pnas.1314385110.
- [74] Maharjan R, Ferenci T. The fitness costs and benefits of antibiotic resistance in drug-free microenvironments encountered in the human body. Environ Microbiol Rep 2017;9:635–41. https://doi.org/10.1111/1758-2229.12564.
- [75] Melnyk AH, Wong A, Kassen R. The fitness costs of antibiotic resistance mutations. Evol Appl 2015;8:273–83. https://doi.org/10.1111/eva.12196.
- [76] Enne VI, Delsol AA, Davis GR, Hayward SL, Roe JM, Bennett PM. Assessment of the fitness impacts on Escherichia coli of acquisition of antibiotic resistance genes encoded by different types of genetic element. J Antimicrob Chemother 2005;56:544–51. https://doi.org/10.1093/jac/dki255.
- [77] Lenski RE. Bacterial evolution and the cost of antibiotic resistance. Int Microbiol Off J Span Soc Microbiol 1998;1:265–70.
- [78] Lenormand T, Harmand N, Gallet R. Cost of resistance: an unreasonably expensive concept. Rethink Ecol 2018;3:51–70. https://doi.org/10.3897/rethinkingecology.3.31992.
- [79] Wistrand-Yuen E, Knopp M, Hjort K, Koskiniemi S, Berg OG, Andersson DI. Evolution of high-level resistance during low-level antibiotic exposure. Nat Commun 2018;9:1599. https://doi.org/10.1038/s41467-018-04059-1.

- [80] Taber HW, Mueller JP, Miller PF, Arrow AS. Bacterial uptake of aminoglycoside antibiotics. Microbiol Rev 1987;51:439–57. https://doi.org/10.1128/mr.51.4.439-457.1987.
- [81] Lang M, Carvalho A, Baharoglu Z, Mazel D. Aminoglycoside uptake, stress, and potentiation in Gram-negative bacteria: new therapies with old molecules. Microbiol Mol Biol Rev 2023;87:e00036-22. https://doi.org/10.1128/mmbr.00036-22.
- [82] Vogwill T, MacLean RC. The genetic basis of the fitness costs of antimicrobial resistance: a meta-analysis approach. Evol Appl 2015;8:284–95. https://doi.org/10.1111/eva.12202.
- [83] Andersson DI, Hughes D. Antibiotic resistance and its cost: is it possible to reverse resistance? Nat Rev Microbiol 2010;8:260–71. https://doi.org/10.1038/nrmicro2319.
- [84] Baym M, Stone LK, Kishony R. Multidrug evolutionary strategies to reverse antibiotic resistance. Science 2016;351:aad3292. https://doi.org/10.1126/science.aad3292.
- [85] Rajer F, Sandegren L. The Role of Antibiotic Resistance Genes in the Fitness Cost of Multiresistance Plasmids. mBio 2022;13:e03552-21. https://doi.org/10.1128/mbio.03552-21.
- [86] Nyhoegen C, Uecker H. Sequential antibiotic therapy in the laboratory and in the patient. J R Soc Interface 2023;20:20220793. https://doi.org/10.1098/rsif.2022.0793.
- [87] Fuentes-Hernandez A, Plucain J, Gori F, Pena-Miller R, Reding C, Jansen G, et al. Using a Sequential Regimen to Eliminate Bacteria at Sublethal Antibiotic Dosages. PLOS Biol 2015;13:e1002104. https://doi.org/10.1371/JOURNAL.PBIO.1002104.
- [88] Lau JSY, Korman TM, Woolley I. Life-long antimicrobial therapy: where is the evidence? J Antimicrob Chemother 2018;73:2601–12. https://doi.org/10.1093/jac/dky174.
- [89] Horne M, Woolley I, Lau JSY. The Use of Long-term Antibiotics for Suppression of Bacterial Infections. Clin Infect Dis Off Publ Infect Dis Soc Am 2024;79:848–54. https://doi.org/10.1093/cid/ciae302.
- [90] CDCTB. Tuberculosis (TB) Treatment for TB Disease. Cent Dis Control Prev 2025. https://www.cdc.gov/tb/topic/treatment/tbdisease.htm (accessed March 26, 2025).
- [91] Antibiotics | Cystic Fibrosis Foundation n.d. https://www.cff.org/managing-cf/antibiotics (accessed March 26, 2025).
- [92] Spellberg B, Rice LB. Duration of Antibiotic Therapy: Shorter Is Better. Ann Intern Med 2019;171:210–1. https://doi.org/10.7326/M19-1509.
- [93] de la Fuente-Nunez C, Cesaro A, Hancock REW. Antibiotic failure: Beyond antimicrobial resistance. Drug Resist Updat 2023;71:101012. https://doi.org/10.1016/j.drup.2023.101012.
- [94] Roemhild R, Schulenburg H. Evolutionary ecology meets the antibiotic crisis. Evol Med Public Health 2019;2019:37–45. https://doi.org/10.1093/emph/eoz008.
- [95] Hope W, Nambiar S, O'Brien S, Sharland M, Paterson DL, Yin M, et al. Combining antibiotics to tackle antimicrobial resistance. Nat Microbiol 2025;10:813–6. https://doi.org/10.1038/s41564-025-01969-x.
- [96] Pena-Miller R, Laehnemann D, Jansen G, Fuentes-Hernandez A, Rosenstiel P, Schulenburg H, et al. When the Most Potent Combination of Antibiotics Selects for the Greatest Bacterial Load: The Smile-Frown Transition. PLOS Biol 2013;11:e1001540. https://doi.org/10.1371/journal.pbio.1001540.
- [97] Hegreness M, Shoresh N, Damian D, Hartl D, Kishony R. Accelerated evolution of resistance in multidrug environments. Proc Natl Acad Sci 2008;105:13977–81. https://doi.org/10.1073/pnas.0805965105.

- [98] Lázár V, Snitser O, Barkan D, Kishony R. Antibiotic combinations reduce Staphylococcus aureus clearance. Nature 2022;610:540–6. https://doi.org/10.1038/s41586-022-05260-5.
- [99] Chang JY, Shim K-N, Tae CH, Lee KE, Lee J, Lee KH, et al. Triple therapy versus sequential therapy for the first-line Helicobacter pylori eradication. BMC Gastroenterol 2017;17:16. https://doi.org/10.1186/s12876-017-0579-8.
- [100] Su D-J, Chang M-H, Yang J-C, Ni Y-H, Hsu H-Y, Wu J-F. Fourteen-day sequential therapy is superior to 7-day triple therapy as first-line regimen for *Helicobacter pylori* infected children. J Formos Med Assoc 2022;121:202–9. https://doi.org/10.1016/j.jfma.2021.03.001.
- [101] Zullo A, De Francesco V, Hassan C, Morini S, Vaira D. The sequential therapy regimen for Helicobacter pylori eradication: a pooled-data analysis. Gut 2007;56:1353–7. https://doi.org/10.1136/gut.2007.125658.
- [102] Wu D-C, Hsu P-I, Wu J-Y, Opekun AR, Kuo C-H, Wu I-C, et al. Sequential and Concomitant Therapy With Four Drugs Is Equally Effective for Eradication of H pylori Infection. Clin Gastroenterol Hepatol 2010;8:36-41.e1. https://doi.org/10.1016/j.cgh.2009.09.030.
- [103] Hepatology TLG&. The problem of antimicrobial resistance in chronic liver disease. Lancet Gastroenterol Hepatol 2022;7:495. https://doi.org/10.1016/S2468-1253(22)00130-3.
- [104] Pailhoriès H, Herrmann J-L, Velo-Suarez L, Lamoureux C, Beauruelle C, Burgel P-R, et al. Antibiotic resistance in chronic respiratory diseases: from susceptibility testing to the resistome. Eur Respir Rev 2022;31. https://doi.org/10.1183/16000617.0259-2021.
- [105] Nelson CP, Hoberman A, Shaikh N, Keren R, Mathews R, Greenfield SP, et al. Antimicrobial Resistance and Urinary Tract Infection Recurrence. Pediatrics 2016;137:e20152490. https://doi.org/10.1542/peds.2015-2490.
- [106] López-Causapé C, Rojo-Molinero E, Macià MD, Oliver A. The problems of antibiotic resistance in cystic fibrosis and solutions. Expert Rev Respir Med 2015;9:73–88. https://doi.org/10.1586/17476348.2015.995640.
- [107] Chowdhury FR, Findlay BL. Fitness Costs of Antibiotic Resistance Impede the Evolution of Resistance to Other Antibiotics. ACS Infect Dis 2023;9:1834–45. https://doi.org/10.1021/acsinfecdis.3c00156.
- [108] Sander P, Springer B, Prammananan T, Sturmfels A, Kappler M, Pletschette M, et al. Fitness Cost of Chromosomal Drug Resistance-Conferring Mutations. Antimicrob Agents Chemother 2002;46:1204–11. https://doi.org/10.1128/aac.46.5.1204-1211.2002.
- [109] Ramadhan AA, Hegedus E. Survivability of vancomycin resistant enterococci and fitness cost of vancomycin resistance acquisition. J Clin Pathol 2005;58:744–6. https://doi.org/10.1136/jcp.2004.024091.
- [110] Eckartt KA, Delbeau M, Munsamy-Govender V, DeJesus MA, Azadian ZA, Reddy AK, et al. Compensatory evolution in NusG improves fitness of drug-resistant M. tuberculosis. Nature 2024;628:186–94. https://doi.org/10.1038/s41586-024-07206-5.
- [111] Goig GA, Menardo F, Salaam-Dreyer Z, Dippenaar A, Streicher EM, Daniels J, et al. Effect of compensatory evolution in the emergence and transmission of rifampicin-resistant Mycobacterium tuberculosis in Cape Town, South Africa: a genomic epidemiology study. Lancet Microbe 2023;4:e506–15. https://doi.org/10.1016/S2666-5247(23)00110-6.

- [112] Szamecz B, Boross G, Kalapis D, Kovács K, Fekete G, Farkas Z, et al. The Genomic Landscape of Compensatory Evolution. PLOS Biol 2014;12:e1001935. https://doi.org/10.1371/journal.pbio.1001935.
- [113] Loftie-Eaton W, Bashford K, Quinn H, Dong K, Millstein J, Hunter S, et al. Compensatory mutations improve general permissiveness to antibiotic resistance plasmids. Nat Ecol Evol 2017;1:1354–63. https://doi.org/10.1038/s41559-017-0243-2.
- [114] Knopp M, Andersson DI. Amelioration of the Fitness Costs of Antibiotic Resistance Due To Reduced Outer Membrane Permeability by Upregulation of Alternative Porins. Mol Biol Evol 2015;32:3252–63. https://doi.org/10.1093/molbev/msv195.
- [115] Hibbing ME, Fuqua C, Parsek MR, Peterson SB. Bacterial competition: surviving and thriving in the microbial jungle. Nat Rev Microbiol 2010;8:15–25. https://doi.org/10.1038/nrmicro2259.
- [116] Merker M, Tueffers L, Vallier M, Groth EE, Sonnenkalb L, Unterweger D, et al. Evolutionary Approaches to Combat Antibiotic Resistance: Opportunities and Challenges for Precision Medicine. Front Immunol 2020;11.
- [117] Melnikov SV, Stevens DL, Fu X, Kwok HS, Zhang J-T, Shen Y, et al. Exploiting evolutionary trade-offs for posttreatment management of drug-resistant populations. Proc Natl Acad Sci U S A 2020;117:17924–31. https://doi.org/10.1073/pnas.2003132117.
- [118] Turnidge J, Paterson DL. Setting and Revising Antibacterial Susceptibility Breakpoints. Clin Microbiol Rev 2007;20:391–408. https://doi.org/10.1128/CMR.00047-06.
- [119] Li F, Wang J, Jiang Y, Guo Y, Liu N, Xiao S, et al. Adaptive Evolution Compensated for the Plasmid Fitness Costs Brought by Specific Genetic Conflicts. Pathogens 2023;12:137. https://doi.org/10.3390/pathogens12010137.
- [120] Ventola CL. The Antibiotic Resistance Crisis. Pharm Ther 2015;40:277–83.
- [121] Yoshida M, Reyes SG, Tsuda S, Horinouchi T, Furusawa C, Cronin L. Time-programmable drug dosing allows the manipulation, suppression and reversal of antibiotic drug resistance in vitro. Nat Commun 2017;8:15589. https://doi.org/10.1038/ncomms15589.
- [122] Yekani M, Azargun R, Sharifi S, Nabizadeh E, Nahand JS, Ansari NK, et al. Collateral sensitivity: An evolutionary trade-off between antibiotic resistance mechanisms, attractive for dealing with drug-resistance crisis. Health Sci Rep 2023;6:e1418. https://doi.org/10.1002/hsr2.1418.
- [123] Roemhild R, Andersson DI. Mechanisms and therapeutic potential of collateral sensitivity to antibiotics. PLOS Pathog 2021;17:e1009172. https://doi.org/10.1371/JOURNAL.PPAT.1009172.
- [124] Lázár V, Singh GP, Spohn R, Nagy I, Horváth B, Hrtyan M, et al. Bacterial evolution of antibiotic hypersensitivity. Mol Syst Biol 2013;9:700. https://doi.org/10.1038/MSB.2013.57.
- [125] Roemhild R, Linkevicius M, Andersson DI. Molecular mechanisms of collateral sensitivity to the antibiotic nitrofurantoin. PLOS Biol 2020;18:e3000612. https://doi.org/10.1371/journal.pbio.3000612.
- [126] Linkevicius M, Sandegren L, Andersson DI. Mechanisms and fitness costs of tigecycline resistance in Escherichia coli. J Antimicrob Chemother 2013;68:2809–19. https://doi.org/10.1093/jac/dkt263.

- [127] Rosenkilde CEH, Munck C, Porse A, Linkevicius M, Andersson DI, Sommer MOA. Collateral sensitivity constrains resistance evolution of the CTX-M-15 β-lactamase. Nat Commun 2019;10:618. https://doi.org/10.1038/s41467-019-08529-y.
- [128] Barbosa C, Römhild R, Rosenstiel P, Schulenburg H. Evolutionary stability of collateral sensitivity to antibiotics in the model pathogen Pseudomonas aeruginosa. eLife 2019;8:e51481. https://doi.org/10.7554/eLife.51481.
- [129] Barbosa C, Trebosc V, Kemmer C, Rosenstiel P, Beardmore R, Schulenburg H, et al. Alternative Evolutionary Paths to Bacterial Antibiotic Resistance Cause Distinct Collateral Effects. Mol Biol Evol 2017;34:2229–44. https://doi.org/10.1093/molbev/msx158.
- [130] Kavanaugh LG, Flanagan JN, Steck TR. Reciprocal antibiotic collateral sensitivity in Burkholderia multivorans. Int J Antimicrob Agents 2020;56:105994. https://doi.org/10.1016/j.ijantimicag.2020.105994.
- [131] Hernando-Amado S, Sanz-García F, Martínez JL. Rapid and robust evolution of collateral sensitivity in Pseudomonas aeruginosa antibiotic-resistant mutants. Sci Adv 2020;6:eaba5493. https://doi.org/10.1126/sciadv.aba5493.
- [132] Maltas J, Wood KB. Pervasive and diverse collateral sensitivity profiles inform optimal strategies to limit antibiotic resistance. PLOS Biol 2019;17:e3000515. https://doi.org/10.1371/journal.pbio.3000515.
- [133] Maltas J, Huynh A, Wood KB. Dynamic collateral sensitivity profiles highlight opportunities and challenges for optimizing antibiotic treatments. PLOS Biol 2025;23:e3002970. https://doi.org/10.1371/journal.pbio.3002970.
- [134] Sakenova N, Cacace E, Orakov A, Huber F, Varik V, Kritikos G, et al. Systematic mapping of antibiotic cross-resistance and collateral sensitivity with chemical genetics. Nat Microbiol 2024:1–15. https://doi.org/10.1038/s41564-024-01857-w.
- [135] Wang X, Nong L, Schaar G, Jonker M, Leeuw W de, Kuile BH ter. Collateral sensitivity and cross resistance in six species of bacteria exposed to six classes of antibiotics 2024:2024.12.12.628210. https://doi.org/10.1101/2024.12.12.628210.
- [136] Mahmud HA, Wakeman CA. Navigating collateral sensitivity: insights into the mechanisms and applications of antibiotic resistance trade-offs. Front Microbiol 2024;15. https://doi.org/10.3389/fmicb.2024.1478789.
- [137] Sørum V, Øynes EL, Møller AS, Harms K, Samuelsen Ø, Podnecky NL, et al. Evolutionary Instability of Collateral Susceptibility Networks in Ciprofloxacin-Resistant Clinical Escherichia coli Strains. mBio 2022;13:e00441-22. https://doi.org/10.1128/mbio.00441-22.
- [138] Baquero F, Martínez JL, F. Lanza V, Rodríguez-Beltrán J, Galán JC, San Millán A, et al. Evolutionary Pathways and Trajectories in Antibiotic Resistance. Clin Microbiol Rev 2021;34:e00050-19. https://doi.org/10.1128/CMR.00050-19.
- [139] Allen RC, Pfrunder-Cardozo KR, Hall AR. Collateral Sensitivity Interactions between Antibiotics Depend on Local Abiotic Conditions. mSystems 2021;6:e01055-21. https://doi.org/10.1128/mSystems.01055-21.
- [140] Brepoels P, Appermans K, Pérez CA, Lories B, Marchal K, Steenackers H. Antibiotic cycling affects resistance evolution independently of collateral sensitivity. Mol Biol Evol 2022:msac257. https://doi.org/10.1093/molbev/msac257.

- [141] Dunai A, Spohn R, Farkas Z, Lázár V, Györkei Á, Apjok G, et al. Rapid decline of bacterial drug-resistance in an antibiotic-free environment through phenotypic reversion. eLife 2019;8:e47088. https://doi.org/10.7554/eLife.47088.
- [142] Trimble MJ, Mlynárčik P, Kolář M, Hancock REW. Polymyxin: Alternative Mechanisms of Action and Resistance. Cold Spring Harb Perspect Med 2016;6:a025288. https://doi.org/10.1101/cshperspect.a025288.
- [143] Divoux T, Mao B, Snabre P. Syneresis and delayed detachment in agar plates. Soft Matter 2015;11:3677–85. https://doi.org/10.1039/C5SM00433K.
- [144] Croze OA, Ferguson GP, Cates ME, Poon WCK. Migration of chemotactic bacteria in soft agar: role of gel concentration. Biophys J 2011;101:525–34. https://doi.org/10.1016/j.bpj.2011.06.023.
- [145] Chowdhury FR, Mercado LD, Kharitonov K, Findlay BL. *De novo* evolution of antibiotic resistance to Oct-TriA1. Microbiol Res 2025;293:128056. https://doi.org/10.1016/j.micres.2025.128056.
- [146] Cochrane SA, Findlay B, Bakhtiary A, Acedo JZ, Rodriguez-Lopez EM, Mercier P, et al. Antimicrobial lipopeptide tridecaptin A1 selectively binds to Gram-negative lipid II. Proc Natl Acad Sci 2016;113:11561–6. https://doi.org/10.1073/pnas.1608623113.
- [147] Bell G, MacLean C. The Search for 'Evolution-Proof' Antibiotics. Trends Microbiol 2018;26:471–83. https://doi.org/10.1016/j.tim.2017.11.005.
- [148] Pinheiro F. Predicting the evolution of antibiotic resistance. Curr Opin Microbiol 2024;82:102542. https://doi.org/10.1016/j.mib.2024.102542.
- [149] LaCroix RA, Palsson BO, Feist AM. A Model for Designing Adaptive Laboratory Evolution Experiments. Appl Environ Microbiol 2017;83:e03115-16. https://doi.org/10.1128/AEM.03115-16.
- [150] Van den Bergh B, Swings T, Fauvart M, Michiels J. Experimental Design, Population Dynamics, and Diversity in Microbial Experimental Evolution. Microbiol Mol Biol Rev 2018;82:10.1128/mmbr.00008-18. https://doi.org/10.1128/mmbr.00008-18.
- [151] Chowdhury FR, Banari V, Lesnic V, Zhanel GG, Findlay BL. Large scale laboratory evolution uncovers clinically relevant collateral antibiotic sensitivity 2025:2025.02.07.637158. https://doi.org/10.1101/2025.02.07.637158.
- [152] Podnecky NL, Fredheim EGA, Kloos J, Sørum V, Primicerio R, Roberts AP, et al. Conserved collateral antibiotic susceptibility networks in diverse clinical strains of Escherichia coli. Nat Commun 2018;9:3673. https://doi.org/10.1038/s41467-018-06143-y.
- [153] Lázár V, Martins A, Spohn R, Daruka L, Grézal G, Fekete G, et al. Antibiotic-resistant bacteria show widespread collateral sensitivity to antimicrobial peptides. Nat Microbiol 2018;3:718–31. https://doi.org/10.1038/s41564-018-0164-0.
- [154] Jacobs A. U.N. Issues Urgent Warning on the Growing Peril of Drug-Resistant Infections. N Y Times 2019.
- [155] Dadgostar P. Antimicrobial Resistance: Implications and Costs. Infect Drug Resist 2019;12:3903–10. https://doi.org/10.2147/IDR.S234610.
- [156] Van Boeckel TP, Pires J, Silvester R, Zhao C, Song J, Criscuolo NG, et al. Global trends in antimicrobial resistance in animals in low- and middle-income countries. Science 2019;365:eaaw1944. https://doi.org/10.1126/science.aaw1944.
- [157] Dawes EA. Growth and Survival of Bacteria. In: Poindexter JS, Leadbetter ER, editors. Bact. Nat. Vol. 3 Struct. Physiol. Genet. Adapt., Boston, MA: Springer US; 1989, p. 67–187. https://doi.org/10.1007/978-1-4613-0803-4_2.

- [158] Palma V, Gutiérrez MS, Vargas O, Parthasarathy R, Navarrete P. Methods to Evaluate Bacterial Motility and Its Role in Bacterial–Host Interactions. Microorganisms 2022;10:563. https://doi.org/10.3390/microorganisms10030563.
- [159] Geisel N, Vilar JMG, Rubi JM. Optimal Resting-Growth Strategies of Microbial Populations in Fluctuating Environments. PLOS ONE 2011;6:e18622. https://doi.org/10.1371/journal.pone.0018622.
- [160] Nichol D, Jeavons P, Fletcher AG, Bonomo RA, Maini PK, Paul JL, et al. Steering Evolution with Sequential Therapy to Prevent the Emergence of Bacterial Antibiotic Resistance. PLOS Comput Biol 2015;11:e1004493. https://doi.org/10.1371/journal.pcbi.1004493.
- [161] Nichol D, Rutter J, Bryant C, Hujer A, Lek S, Adams M, et al. Antibiotic collateral sensitivity is contingent on the repeatability of evolution 2019. https://doi.org/10.1038/s41467-018-08098-6.
- [162] Beckley AM, Wright ES. Identification of antibiotic pairs that evade concurrent resistance via a retrospective analysis of antimicrobial susceptibility test results. Lancet Microbe 2021;2:e545–54. https://doi.org/10.1016/S2666-5247(21)00118-X.
- [163] Barbosa C, Römhild R, Rosenstiel P, Schulenburg H. Evolutionary stability of collateral sensitivity to antibiotics in the model pathogen Pseudomonas aeruginosa. eLife 2019;8:e51481. https://doi.org/10.7554/eLife.51481.
- [164] Langevin AM, El Meouche I, Dunlop MJ. Mapping the Role of AcrAB-TolC Efflux Pumps in the Evolution of Antibiotic Resistance Reveals Near-MIC Treatments Facilitate Resistance Acquisition. mSphere 2020;5:e01056-20. https://doi.org/10.1128/mSphere.01056-20.
- [165] Sulavik MC, Gambino LF, Miller PF. The MarR repressor of the multiple antibiotic resistance (mar) operon in Escherichia coli: prototypic member of a family of bacterial regulatory proteins involved in sensing phenolic compounds. Mol Med 1995;1:436–46.
- [166] Zhang H, Ma Y, Liu P, Li X. Multidrug resistance operon emrAB contributes for chromate and ampicillin co-resistance in a Staphylococcus strain isolated from refinery polluted river bank. SpringerPlus 2016;5:1648. https://doi.org/10.1186/s40064-016-3253-7.
- [167] Ariza RR, Li Z, Ringstad N, Demple B. Activation of multiple antibiotic resistance and binding of stress-inducible promoters by Escherichia coli Rob protein. J Bacteriol 1995;177:1655–61. https://doi.org/10.1128/jb.177.7.1655-1661.1995.
- [168] Soto SM. Role of efflux pumps in the antibiotic resistance of bacteria embedded in a biofilm. Virulence 2013;4:223–9. https://doi.org/10.4161/viru.23724.
- [169] Nishino K, Yamasaki S, Nakashima R, Zwama M, Hayashi-Nishino M. Function and Inhibitory Mechanisms of Multidrug Efflux Pumps. Front Microbiol 2021;12.
- [170] Nikaido H. Antibiotic Resistance Caused by Gram-Negative Multidrug Efflux Pumps. Clin Infect Dis 1998;27:S32–41.
- [171] Anes J, McCusker MP, Fanning S, Martins M. The ins and outs of RND efflux pumps in Escherichia coli. Front Microbiol 2015;6.
- [172] Olivares Pacheco J, Alvarez-Ortega C, Alcalde Rico M, Martínez JL. Metabolic Compensation of Fitness Costs Is a General Outcome for Antibiotic-Resistant Pseudomonas aeruginosa Mutants Overexpressing Efflux Pumps. mBio 2017;8:e00500-17. https://doi.org/10.1128/mBio.00500-17.

- [173] Juhas M, Ajioka JW. Identification and validation of novel chromosomal integration and expression loci in Escherichia coli flagellar region 1. PloS One 2015;10:e0123007. https://doi.org/10.1371/journal.pone.0123007.
- [174] Khamari B, Adak S, Chanakya PP, Lama M, Peketi ASK, Gurung SA, et al. Prediction of nitrofurantoin resistance among Enterobacteriaceae and mutational landscape of in vitro selected resistant Escherichia coli. Res Microbiol 2022;173:103889. https://doi.org/10.1016/j.resmic.2021.103889.
- [175] Gerrish PJ, Lenski RE. The fate of competing beneficial mutations in an asexual population. Genetica 1998;102:127–44. https://doi.org/10.1023/A:1017067816551.
- [176] Łapińska U, Voliotis M, Lee KK, Campey A, Stone MRL, Tuck B, et al. Fast bacterial growth reduces antibiotic accumulation and efficacy. eLife 2022;11:e74062. https://doi.org/10.7554/eLife.74062.
- [177] Tao K, Watanabe S, Narita S, Tokuda H. A Periplasmic LolA Derivative with a Lethal Disulfide Bond Activates the Cpx Stress Response System. J Bacteriol 2010;192:5657–62. https://doi.org/10.1128/JB.00821-10.
- [178] Choi U, Lee C-R. Distinct Roles of Outer Membrane Porins in Antibiotic Resistance and Membrane Integrity in Escherichia coli. Front Microbiol 2019;10.
- [179] Tajima T, Yokota N, Matsuyama S, Tokuda H. Genetic analyses of the in vivo function of LolA, a periplasmic chaperone involved in the outer membrane localization of Escherichia coli lipoproteins. FEBS Lett 1998;439:51–4. https://doi.org/10.1016/s0014-5793(98)01334-9.
- [180] Pelchovich G, Schreiber R, Zhuravlev A, Gophna U. The contribution of common rpsL mutations in Escherichia coli to sensitivity to ribosome targeting antibiotics. Int J Med Microbiol IJMM 2013;303:558–62. https://doi.org/10.1016/j.ijmm.2013.07.006.
- [181] Sandegren L, Andersson DI. Bacterial gene amplification: implications for the evolution of antibiotic resistance. Nat Rev Microbiol 2009;7:578–88. https://doi.org/10.1038/nrmicro2174.
- [182] Hjort K, Nicoloff H, Andersson DI. Unstable tandem gene amplification generates heteroresistance (variation in resistance within a population) to colistin in Salmonella enterica. Mol Microbiol 2016;102:274–89. https://doi.org/10.1111/mmi.13459.
- [183] Greulich P, Scott M, Evans MR, Allen RJ. Growth-dependent bacterial susceptibility to ribosome-targeting antibiotics. Mol Syst Biol 2015;11:0796. https://doi.org/10.15252/msb.20145949.
- [184] Jagielski T, Ignatowska H, Bakuła Z, Dziewit Ł, Napiórkowska A, Augustynowicz-Kopeć E, et al. Screening for Streptomycin Resistance-Conferring Mutations in Mycobacterium tuberculosis Clinical Isolates from Poland. PLoS ONE 2014;9:e100078. https://doi.org/10.1371/journal.pone.0100078.
- [185] Melchionna MV, Gullett JM, Bouveret E, Shrestha HK, Abraham PE, Hettich RL, et al. Bacterial Homologs of Progestin and AdipoQ Receptors (PAQRs) Affect Membrane Energetics Homeostasis but Not Fluidity. J Bacteriol 2022;204:e0058321. https://doi.org/10.1128/jb.00583-21.
- [186] Bruni GN, Kralj JM. Membrane voltage dysregulation driven by metabolic dysfunction underlies bactericidal activity of aminoglycosides. eLife n.d.;9:e58706. https://doi.org/10.7554/eLife.58706.
- [187] Xing Y, Kang X, Zhang S, Men Y. Specific phenotypic, genomic, and fitness evolutionary trajectories toward streptomycin resistance induced by pesticide co-stressors in

- Escherichia coli. ISME Commun 2021;1:1–11. https://doi.org/10.1038/s43705-021-00041-z.
- [188] Zogaj X, Nimtz M, Rohde M, Bokranz W, Römling U. The multicellular morphotypes of Salmonella typhimurium and Escherichia coli produce cellulose as the second component of the extracellular matrix. Mol Microbiol 2001;39:1452–63. https://doi.org/10.1046/j.1365-2958.2001.02337.x.
- [189] Serra DO, Richter AM, Hengge R. Cellulose as an architectural element in spatially structured Escherichia coli biofilms. J Bacteriol 2013;195:5540–54. https://doi.org/10.1128/JB.00946-13.
- [190] Reizer J, Reizer A, Saier MH. Novel phosphotransferase system genes revealed by bacterial genome analysis--a gene cluster encoding a unique Enzyme I and the proteins of a fructose-like permease system. Microbiol Read Engl 1995;141 (Pt 4):961–71. https://doi.org/10.1099/13500872-141-4-961.
- [191] Zelcbuch L, Lindner SN, Zegman Y, Vainberg Slutskin I, Antonovsky N, Gleizer S, et al. Pyruvate Formate-Lyase Enables Efficient Growth of Escherichia coli on Acetate and Formate. Biochemistry 2016;55:2423–6. https://doi.org/10.1021/acs.biochem.6b00184.
- [192] Criswell D, Tobiason VL, Lodmell JS, Samuels DS. Mutations Conferring Aminoglycoside and Spectinomycin Resistance in *Borrelia burgdorferi*. Antimicrob Agents Chemother 2006;50:445–52. https://doi.org/10.1128/AAC.50.2.445-452.2006.
- [193] Kenney TJ, Churchward G. Cloning and sequence analysis of the rpsL and rpsG genes of Mycobacterium smegmatis and characterization of mutations causing resistance to streptomycin. J Bacteriol 1994;176:6153–6.
- [194] Hernando-Amado S, Laborda P, Valverde JR, Martínez JL. Rapid Decline of Ceftazidime Resistance in Antibiotic-Free and Sublethal Environments Is Contingent on Genetic Background. Mol Biol Evol 2022;39:msac049. https://doi.org/10.1093/molbev/msac049.
- [195] Pao SS, Paulsen IT, Saier MH. Major facilitator superfamily. Microbiol Mol Biol Rev MMBR 1998;62:1–34. https://doi.org/10.1128/MMBR.62.1.1-34.1998.
- [196] Daley DO, Rapp M, Granseth E, Melén K, Drew D, von Heijne G. Global topology analysis of the Escherichia coli inner membrane proteome. Science 2005;308:1321–3. https://doi.org/10.1126/science.1109730.
- [197] Dassler T, Maier T, Winterhalter C, Böck A. Identification of a major facilitator protein from Escherichia coli involved in efflux of metabolites of the cysteine pathway. Mol Microbiol 2000;36:1101–12. https://doi.org/10.1046/j.1365-2958.2000.01924.x.
- [198] Saier MH, Reddy VS, Tsu BV, Ahmed MS, Li C, Moreno-Hagelsieb G. The Transporter Classification Database (TCDB): recent advances. Nucleic Acids Res 2016;44:D372-379. https://doi.org/10.1093/nar/gkv1103.
- [199] Wang H, Yin X, Wu Orr M, Dambach M, Curtis R, Storz G. Increasing intracellular magnesium levels with the 31-amino acid MgtS protein. Proc Natl Acad Sci U S A 2017;114:5689–94. https://doi.org/10.1073/pnas.1703415114.
- [200] Weaver J, Mohammad F, Buskirk AR, Storz G. Identifying Small Proteins by Ribosome Profiling with Stalled Initiation Complexes. mBio 2019;10:e02819-18. https://doi.org/10.1128/mBio.02819-18.
- [201] Lee H-J, Gottesman S. sRNA roles in regulating transcriptional regulators: Lrp and SoxS regulation by sRNAs. Nucleic Acids Res 2016;44:6907–23. https://doi.org/10.1093/nar/gkw358.

- [202] Jonas K, Edwards AN, Simm R, Romeo T, Römling U, Melefors O. The RNA binding protein CsrA controls cyclic di-GMP metabolism by directly regulating the expression of GGDEF proteins. Mol Microbiol 2008;70:236–57. https://doi.org/10.1111/j.1365-2958.2008.06411.x.
- [203] Sandegren L, Lindqvist A, Kahlmeter G, Andersson DI. Nitrofurantoin resistance mechanism and fitness cost in Escherichia coli. J Antimicrob Chemother 2008;62:495–503. https://doi.org/10.1093/jac/dkn222.
- [204] Sargentini NJ, Gularte NP, Hudman DA. Screen for genes involved in radiation survival of Escherichia coli and construction of a reference database. Mutat Res 2016;793–794:1–14. https://doi.org/10.1016/j.mrfmmm.2016.10.001.
- [205] Amundsen SK, Taylor AF, Chaudhury AM, Smith GR. recD: the gene for an essential third subunit of exonuclease V. Proc Natl Acad Sci U S A 1986;83:5558–62. https://doi.org/10.1073/pnas.83.15.5558.
- [206] Frenoy A, Bonhoeffer S. Death and population dynamics affect mutation rate estimates and evolvability under stress in bacteria. PLoS Biol 2018;16:e2005056. https://doi.org/10.1371/journal.pbio.2005056.
- [207] Sanz-García F, Gil-Gil T, Laborda P, Blanco P, Ochoa-Sánchez L-E, Baquero F, et al. Translating eco-evolutionary biology into therapy to tackle antibiotic resistance. Nat Rev Microbiol 2023:1–15. https://doi.org/10.1038/s41579-023-00902-5.
- [208] Ocampo PS, Lázár V, Papp B, Arnoldini M, Abel zur Wiesch P, Busa-Fekete R, et al. Antagonism between bacteriostatic and bactericidal antibiotics is prevalent. Antimicrob Agents Chemother 2014;58:4573–82. https://doi.org/10.1128/AAC.02463-14.
- [209] Batra A, Roemhild R, Rousseau E, Franzenburg S, Niemann S, Schulenburg H. High potency of sequential therapy with only β-lactam antibiotics. eLife 2021;10:e68876. https://doi.org/10.7554/eLife.68876.
- [210] Amor DR, Gore J. Fast growth can counteract antibiotic susceptibility in shaping microbial community resilience to antibiotics. Proc Natl Acad Sci 2022;119:e2116954119. https://doi.org/10.1073/pnas.2116954119.
- [211] Melnyk AH, McCloskey N, Hinz AJ, Dettman J, Kassen R. Evolution of Cost-Free Resistance under Fluctuating Drug Selection in Pseudomonas aeruginosa. mSphere 2017;2:e00158-17. https://doi.org/10.1128/mSphere.00158-17.
- [212] Brewster JD. A simple micro-growth assay for enumerating bacteria. J Microbiol Methods 2003;53:77–86. https://doi.org/10.1016/S0167-7012(02)00226-9.
- [213] Sprouffske K, Wagner A. Growthcurver: an R package for obtaining interpretable metrics from microbial growth curves. BMC Bioinformatics 2016;17:172. https://doi.org/10.1186/s12859-016-1016-7.
- [214] CLSI. M07: Dilution AST for Aerobically Grown Bacteria CLSI 2018. https://clsi.org/standards/products/microbiology/documents/m07/ (accessed January 12, 2020).
- [215] Deatherage DE, Barrick JE. Identification of mutations in laboratory-evolved microbes from next-generation sequencing data using breseq. Methods Mol Biol Clifton NJ 2014;1151:165–88. https://doi.org/10.1007/978-1-4939-0554-6 12.
- [216] Murray CJ, Ikuta KS, Sharara F, Swetschinski L, Robles Aguilar G, Gray A, et al. Global burden of bacterial antimicrobial resistance in 2019: a systematic analysis. The Lancet 2022;399:629–55. https://doi.org/10.1016/S0140-6736(21)02724-0/ATTACHMENT/B227DEB3-FF04-497F-82AC-637D8AB7F679/MMC1.PDF.

- [217] Jacobs A. U.N. Issues Urgent Warning on the Growing Peril of Drug-Resistant Infections. N Y Times 2019.
- [218] Bonomo RA, Perez F, Hujer AM, Hujer KM, Vila AJ. The Real Crisis in Antimicrobial Resistance: Failure to Anticipate and Respond. Clin Infect Dis 2024:ciad758. https://doi.org/10.1093/cid/ciad758.
- [219] Ling LL, Schneider T, Peoples AJ, Spoering AL, Engels I, Conlon BP, et al. A new antibiotic kills pathogens without detectable resistance. Nature 2015;517:455–9. https://doi.org/10.1038/nature14098.
- [220] Cochrane SA, Findlay B, Bakhtiary A, Acedo JZ, Rodriguez-Lopez EM, Mercier P, et al. Antimicrobial lipopeptide tridecaptin A1 selectively binds to Gram-negative lipid II. Proc Natl Acad Sci 2016;113:11561–6. https://doi.org/10.1073/pnas.1608623113.
- [221] Stokes JM, Yang K, Swanson K, Jin W, Cubillos-Ruiz A, Donghia NM, et al. A deep learning approach to antibiotic discovery. Cell 2020;180:688-702.e13. https://doi.org/10.1016/j.cell.2020.01.021.
- [222] Ge Y, MacDonald DL, Holroyd KJ, Thornsberry C, Wexler H, Zasloff M. In vitro antibacterial properties of pexiganan, an analog of magainin. Antimicrob Agents Chemother 1999;43:782–8. https://doi.org/10.1128/AAC.43.4.782.
- [223] Mcguire JM, Wolfe RN, Ziegler DW. Vancomycin, a new antibiotic. II. In vitro antibacterial studies. Antibiot Annu 1955;3:612–8.
- [224] Shukla R, Lavore F, Maity S, Derks MGN, Jones CR, Vermeulen BJA, et al. Teixobactin kills bacteria by a two-pronged attack on the cell envelope. Nature 2022;608:390–6. https://doi.org/10.1038/s41586-022-05019-y.
- [225] Bell G, MacLean C. The Search for 'Evolution-Proof' Antibiotics. Trends Microbiol 2018;26:471–83. https://doi.org/10.1016/j.tim.2017.11.005.
- [226] Upadhayay A, Ling J, Pal D, Xie Y, Ping F-F, Kumar A. Resistance-proof antimicrobial drug discovery to combat global antimicrobial resistance threat. Drug Resist Updat 2023;66:100890. https://doi.org/10.1016/j.drup.2022.100890.
- [227] Lohans CT, Huang Z, van Belkum MJ, Giroud M, Sit CS, Steels EM, et al. Structural Characterization of the Highly Cyclized Lantibiotic Paenicidin A via a Partial Desulfurization/Reduction Strategy. J Am Chem Soc 2012;134:19540–3. https://doi.org/10.1021/ja3089229.
- [228] Shoji J, Hinoo H, Sakazaki R, Kato T, Wakisaka Y, Mayama M, et al. Isolation of tridecaptins A, B and C (studies on antibiotics from the genus Bacillus. XXIII). J Antibiot (Tokyo) 1978;31:646–51. https://doi.org/10.7164/antibiotics.31.646.
- [229] Cochrane SA, Lohans CT, Brandelli JR, Mulvey G, Armstrong GD, Vederas JC. Synthesis and Structure—Activity Relationship Studies of N-Terminal Analogues of the Antimicrobial Peptide Tridecaptin A1. J Med Chem 2014;57:1127–31. https://doi.org/10.1021/jm401779d.
- [230] Ballantine RD, McCallion CE, Nassour E, Tokajian S, Cochrane SA. Tridecaptin-inspired antimicrobial peptides with activity against multidrug-resistant Gram-negative bacteria. MedChemComm 2019;10:484–7. https://doi.org/10.1039/c9md00031c.
- [231] Cochrane SA, Findlay B, Vederas JC, Ratemi ES. Key residues in octyl-tridecaptin A1 analogues linked to stable secondary structures in the membrane. Chembiochem Eur J Chem Biol 2014;15:1295–9. https://doi.org/10.1002/cbic.201402024.

- [232] WHO publishes list of bacteria for which new antibiotics are urgently needed n.d. https://www.who.int/news/item/27-02-2017-who-publishes-list-of-bacteria-for-which-new-antibiotics-are-urgently-needed (accessed January 15, 2023).
- [233] Wang H, Ishchenko A, Skudlarek J, Shen P, Dzhekieva L, Painter RE, et al. Cerastecins inhibit membrane lipooligosaccharide transport in drug-resistant Acinetobacter baumannii. Nat Microbiol 2024;9:1244–55. https://doi.org/10.1038/s41564-024-01667-0.
- [234] Zampaloni C, Mattei P, Bleicher K, Winther L, Thäte C, Bucher C, et al. A novel antibiotic class targeting the lipopolysaccharide transporter. Nature 2024;625:566–71. https://doi.org/10.1038/s41586-023-06873-0.
- [235] Pahil KS, Gilman MSA, Baidin V, Clairfeuille T, Mattei P, Bieniossek C, et al. A new antibiotic traps lipopolysaccharide in its intermembrane transporter. Nature 2024;625:572–7. https://doi.org/10.1038/s41586-023-06799-7.
- [236] Werneburg M, Zerbe K, Juhas M, Bigler L, Stalder U, Kaech A, et al. Inhibition of Lipopolysaccharide Transport to the Outer Membrane in Pseudomonas aeruginosa by Peptidomimetic Antibiotics. ChemBioChem 2012;13:1767–75. https://doi.org/10.1002/cbic.201200276.
- [237] Srinivas N, Jetter P, Ueberbacher BJ, Werneburg M, Zerbe K, Steinmann J, et al. Peptidomimetic Antibiotics Target Outer-Membrane Biogenesis in Pseudomonas aeruginosa. Science 2010;327:1010–3. https://doi.org/10.1126/science.1182749.
- [238] Zhang X, Li Y, Wang W, Zhang J, Lin Y, Hong B, et al. Identification of an anti-Gramnegative bacteria agent disrupting the interaction between lipopolysaccharide transporters LptA and LptC. Int J Antimicrob Agents 2019;53:442–8. https://doi.org/10.1016/j.ijantimicag.2018.11.016.
- [239] Imai Y, Meyer KJ, Iinishi A, Favre-Godal Q, Green R, Manuse S, et al. A new antibiotic selectively kills Gram-negative pathogens. Nature 2019;576:459–64. https://doi.org/10.1038/s41586-019-1791-1.
- [240] Kaur H, Jakob RP, Marzinek JK, Green R, Imai Y, Bolla JR, et al. The antibiotic darobactin mimics a β -strand to inhibit outer membrane insertase. Nature 2021;593:125–9. https://doi.org/10.1038/s41586-021-03455-w.
- [241] Ghaddar N, Hashemidahaj M, Findlay BL. Access to high-impact mutations constrains the evolution of antibiotic resistance in soft agar. Sci Rep 2018 81 2018;8:1–10. https://doi.org/10.1038/s41598-018-34911-9.
- [242] Divoux T, Mao B, Snabre P. Syneresis and delayed detachment in agar plates. Soft Matter 2015;11:3677–85. https://doi.org/10.1039/C5SM00433K.
- [243] Croze OA, Ferguson GP, Cates ME, Poon WCK. Migration of chemotactic bacteria in soft agar: role of gel concentration. Biophys J 2011;101:525–34. https://doi.org/10.1016/j.bpj.2011.06.023.
- [244] Sánchez VE, Bartholomai GB, Pilosof AMR. Rheological properties of food gums as related to their water binding capacity and to soy protein interaction. LWT Food Sci Technol 1995;28:380–5. https://doi.org/10.1016/0023-6438(95)90021-7.
- [245] Trimble MJ, Mlynárčik P, Kolář M, Hancock REW. Polymyxin: Alternative Mechanisms of Action and Resistance. Cold Spring Harb Perspect Med 2016;6:a025288. https://doi.org/10.1101/cshperspect.a025288.
- [246] Liao W, Lin J, Jia H, Zhou C, Zhang Y, Lin Y, et al. Resistance and Heteroresistance to Colistin in *Escherichia coli* Isolates from Wenzhou, China. Infect Drug Resist 2020;13:3551–61. https://doi.org/10.2147/IDR.S273784.

- [247] Andersson DI, Nicoloff H, Hjort K. Mechanisms and clinical relevance of bacterial heteroresistance. Nat Rev Microbiol 2019;17:479–96. https://doi.org/10.1038/s41579-019-0218-1.
- [248] Hjort K, Nicoloff H, Andersson DI. Unstable tandem gene amplification generates heteroresistance (variation in resistance within a population) to colistin in *Salmonella enterica*. Mol Microbiol 2016;102:274–89. https://doi.org/10.1111/mmi.13459.
- [249] Yoshida M, Reyes SG, Tsuda S, Horinouchi T, Furusawa C, Cronin L. Time-programmable drug dosing allows the manipulation, suppression and reversal of antibiotic drug resistance *in vitro*. Nat Commun 2017;8:15589. https://doi.org/10.1038/ncomms15589.
- [250] Einhorn-Stoll U. Pectin-water interactions in foods From powder to gel. Food Hydrocoll 2018;78:109–19. https://doi.org/10.1016/j.foodhyd.2017.05.029.
- [251] Banerjee S, Bhattacharya S. Compressive textural attributes, opacity and syneresis of gels prepared from gellan, agar and their mixtures. J Food Eng 2011;102:287–92. https://doi.org/10.1016/j.jfoodeng.2010.08.025.
- [252] Chowdhury FR, Findlay BL. Fitness Costs of Antibiotic Resistance Impede the Evolution of Resistance to Other Antibiotics. ACS Infect Dis 2023;9:1834–45. https://doi.org/10.1021/acsinfecdis.3c00156.
- [253] Seright RS, Henrici BJ. Xanthan Stability at Elevated Temperatures. SPE Reserv Eng 1990;5:52–60. https://doi.org/10.2118/14946-PA.
- [254] Jouenne S. Polymer flooding in high temperature, high salinity conditions: Selection of polymer type and polymer chemistry, thermal stability. J Pet Sci Eng 2020;195:107545. https://doi.org/10.1016/j.petrol.2020.107545.
- [255] Prüss BM, Nelms JM, Park C, Wolfe AJ. Mutations in NADH:ubiquinone oxidoreductase of *Escherichia coli* affect growth on mixed amino acids. J Bacteriol 1994;176:2143–50.
- [256] Van den Bergh B, Schramke H, Michiels JE, Kimkes TEP, Radzikowski JL, Schimpf J, et al. Mutations in respiratory complex I promote antibiotic persistence through alterations in intracellular acidity and protein synthesis. Nat Commun 2022;13:546. https://doi.org/10.1038/s41467-022-28141-x.
- [257] Shimada T, Tanaka K. Use of a Bacterial Luciferase Monitoring System To Estimate Real-Time Dynamics of Intracellular Metabolism in *Escherichia coli*. Appl Environ Microbiol 2016;82:5960–8. https://doi.org/10.1128/AEM.01400-16.
- [258] Shimada T, Nakazawa K, Tachikawa T, Saito N, Niwa T, Taguchi H, et al. Acetate overflow metabolism regulates a major metabolic shift after glucose depletion in *Escherichia coli*. FEBS Lett 2021;595:2047–56. https://doi.org/10.1002/1873-3468.14151.
- [259] Chu D, Barnes DJ. The lag-phase during diauxic growth is a trade-off between fast adaptation and high growth rate. Sci Rep 2016;6:25191. https://doi.org/10.1038/srep25191.
- [260] Salvy P, Hatzimanikatis V. Emergence of diauxie as an optimal growth strategy under resource allocation constraints in cellular metabolism. Proc Natl Acad Sci 2021;118:e2013836118. https://doi.org/10.1073/pnas.2013836118.
- [261] Barker CS, Prüß BM, Matsumura P. Increased Motility of *Escherichia coli* by Insertion Sequence Element Integration into the Regulatory Region of the flhD Operon. J Bacteriol 2004;186:7529–37. https://doi.org/10.1128/jb.186.22.7529-7537.2004.
- [262] Lee C, Park C. Mutations upregulating the flhDC operon of *Escherichia coli* K-12. J Microbiol Seoul Korea 2013;51:140–4. https://doi.org/10.1007/s12275-013-2212-z.

- [263] Wang X, Wood TK. IS5 inserts upstream of the master motility operon flhDC in a quasi-Lamarckian way. ISME J 2011;5:1517–25. https://doi.org/10.1038/ismej.2011.27.
- [264] Chng S-S, Ruiz N, Chimalakonda G, Silhavy TJ, Kahne D. Characterization of the two-protein complex in *Escherichia coli* responsible for lipopolysaccharide assembly at the outer membrane. Proc Natl Acad Sci U S A 2010;107:5363–8. https://doi.org/10.1073/pnas.0912872107.
- [265] Taylor PL, Blakely KM, Leon GP de, Walker JR, McArthur F, Evdokimova E, et al. Structure and Function of Sedoheptulose-7-phosphate Isomerase, a Critical Enzyme for Lipopolysaccharide Biosynthesis and a Target for Antibiotic Adjuvants. J Biol Chem 2008;283:2835–45. https://doi.org/10.1074/jbc.M706163200.
- [266] Qian J, Garrett TA, Raetz CRH. In vitro assembly of the outer core of the lipopolysaccharide from *Escherichia coli* K-12 and *Salmonella* Typhimurium. Biochemistry 2014;53:1250–62. https://doi.org/10.1021/bi4015665.
- [267] Choi U, Lee C-R. Distinct Roles of Outer Membrane Porins in Antibiotic Resistance and Membrane Integrity in *Escherichia coli*. Front Microbiol 2019;10:953. https://doi.org/10.3389/fmicb.2019.00953.
- [268] Chong Z-S, Woo W-F, Chng S-S. Osmoporin OmpC forms a complex with MlaA to maintain outer membrane lipid asymmetry in *Escherichia coli*. Mol Microbiol 2015;98:1133–46. https://doi.org/10.1111/mmi.13202.
- [269] Lehman KM, Grabowicz M. Countering Gram-Negative Antibiotic Resistance: Recent Progress in Disrupting the Outer Membrane with Novel Therapeutics. Antibiot Basel Switz 2019;8:163. https://doi.org/10.3390/antibiotics8040163.
- [270] Luther A, Urfer M, Zahn M, Müller M, Wang S-Y, Mondal M, et al. Chimeric peptidomimetic antibiotics against Gram-negative bacteria. Nature 2019;576:452–8. https://doi.org/10.1038/s41586-019-1665-6.
- [271] Hart EM, Mitchell AM, Konovalova A, Grabowicz M, Sheng J, Han X, et al. A small-molecule inhibitor of BamA impervious to efflux and the outer membrane permeability barrier. Proc Natl Acad Sci U S A 2019;116:21748–57. https://doi.org/10.1073/pnas.1912345116.
- [272] Huang L, Wang M, Mo T, Liu M, Biville F, Zhu D, et al. Role of LptD in Resistance to Glutaraldehyde and Pathogenicity in *Riemerella anatipestifer*. Front Microbiol 2019;10:1443. https://doi.org/10.3389/fmicb.2019.01443.
- [273] Reisch CR, Prather KLJ. The no-SCAR (Scarless Cas9 Assisted Recombineering) system for genome editing in *Escherichia coli*. Sci Rep 2015;5:15096. https://doi.org/10.1038/srep15096.
- [274] Reisch CR, Prather KLJ. Scarless Cas9 Assisted Recombineering (no-SCAR) in *Escherichia coli*, an Easy-to-Use System for Genome Editing. Curr Protoc Mol Biol 2017;117:31.8.1-31.8.20. https://doi.org/10.1002/cpmb.29.
- [275] Baba T, Ara T, Hasegawa M, Takai Y, Okumura Y, Baba M, et al. Construction of *Escherichia coli* K-12 in-frame, single-gene knockout mutants: the Keio collection. Mol Syst Biol 2006;2:2006.0008. https://doi.org/10.1038/msb4100050.
- [276] Li Y-X, Zhong Z, Zhang W-P, Qian P-Y. Discovery of cationic nonribosomal peptides as Gram-negative antibiotics through global genome mining. Nat Commun 2018;9:3273. https://doi.org/10.1038/s41467-018-05781-6.
- [277] Zhao X, Zhong X, Yang S, Deng K, Liu L, Song X, et al. Elucidating the Mechanism of Action of the Gram-Negative-Pathogen-Selective Cyclic Antimicrobial Lipopeptide

- Brevicidine. Antimicrob Agents Chemother 2023;67:e00010-23. https://doi.org/10.1128/aac.00010-23.
- [278] Manioglu S, Modaresi SM, Ritzmann N, Thoma J, Overall SA, Harms A, et al. Antibiotic polymyxin arranges lipopolysaccharide into crystalline structures to solidify the bacterial membrane. Nat Commun 2022;13:6195. https://doi.org/10.1038/s41467-022-33838-0.
- [279] Li Y-X, Zhong Z, Hou P, Zhang W-P, Qian P-Y. Resistance to nonribosomal peptide antibiotics mediated by D-stereospecific peptidases. Nat Chem Biol 2018;14:381–7. https://doi.org/10.1038/s41589-018-0009-4.
- [280] Bann SJ, Ballantine RD, Cochrane SA. The tridecaptins: non-ribosomal peptides that selectively target Gram-negative bacteria. RSC Med Chem 2021;12:538–51. https://doi.org/10.1039/D0MD00413H.
- [281] Liu Y-F, Yan J-J, Lei H-Y, Teng C-H, Wang M-C, Tseng C-C, et al. Loss of Outer Membrane Protein C in *Escherichia coli* Contributes to Both Antibiotic Resistance and Escaping Antibody-Dependent Bactericidal Activity. Infect Immun 2012;80:1815–22. https://doi.org/10.1128/IAI.06395-11.
- [282] Simpson BW, Trent MS. Pushing the envelope: LPS modifications and their consequences. Nat Rev Microbiol 2019;17:403–16. https://doi.org/10.1038/s41579-019-0201-x.
- [283] Phan K, Ferenci T. The fitness costs and trade-off shapes associated with the exclusion of nine antibiotics by OmpF porin channels. ISME J 2017;11:1472–82. https://doi.org/10.1038/ismej.2016.202.
- [284] Wang Y, Luo Q, Xiao T, Zhu Y, Xiao Y. Impact of Polymyxin Resistance on Virulence and Fitness among Clinically Important Gram-Negative Bacteria. Engineering 2022;13:178–85. https://doi.org/10.1016/j.eng.2020.11.005.
- [285] Tietgen M, Semmler T, Riedel-Christ S, Kempf VAJ, Molinaro A, Ewers C, et al. Impact of the colistin resistance gene mcr-1 on bacterial fitness. Int J Antimicrob Agents 2018;51:554–61. https://doi.org/10.1016/j.ijantimicag.2017.11.011.
- [286] Sommer MOA, Munck C, Toft-Kehler RV, Andersson DI. Prediction of antibiotic resistance: time for a new preclinical paradigm? Nat Rev Microbiol 2017;15:689–96. https://doi.org/10.1038/nrmicro.2017.75.
- [287] Cirz RT, Chin JK, Andes DR, de Crécy-Lagard V, Craig WA, Romesberg FE. Inhibition of Mutation and Combating the Evolution of Antibiotic Resistance. PLoS Biol 2005;3:e176. https://doi.org/10.1371/journal.pbio.0030176.
- [288] Martin JK, Sheehan JP, Bratton BP, Moore GM, Mateus A, Li SH-J, et al. A Dual-Mechanism Antibiotic Kills Gram-Negative Bacteria and Avoids Drug Resistance. Cell 2020;181:1518-1532.e14. https://doi.org/10.1016/j.cell.2020.05.005.
- [289] Martinez JL, Baquero F. Mutation Frequencies and Antibiotic Resistance. Antimicrob Agents Chemother 2000;44:1771–7.
- [290] Savinova TA, Bocharova YA, Mayansky NA, Chebotar IV. Application of Dimethicone to Prevent Culture Media from Drying in Microbiological Diagnostics. Mod Technol Med 2023;15:14–9. https://doi.org/10.17691/stm2023.15.1.02.
- [291] Laserna EC, Uyenco F, Epifanio E, Veroy RL, Cajipe GJB. Carrageenan from Eucheuma striatum (Schmitz) in Media for Fungal and Yeast Cultures. Appl Environ Microbiol 1981;42:174–5.

- [292] CLSI. M07: Dilution AST for Aerobically Grown Bacteria CLSI 2018. https://clsi.org/standards/products/microbiology/documents/m07/ (accessed January 12, 2020).
- [293] Brewster JD. A simple micro-growth assay for enumerating bacteria. J Microbiol Methods 2003;53:77–86. https://doi.org/10.1016/S0167-7012(02)00226-9.
- [294] Reiter MA, Vorholt JA. Dashing Growth Curves: a web application for rapid and interactive analysis of microbial growth curves. BMC Bioinformatics 2024;25:67. https://doi.org/10.1186/s12859-024-05692-y.
- [295] Barrick JE, Colburn G, Deatherage DE, Traverse CC, Strand MD, Borges JJ, et al. Identifying structural variation in haploid microbial genomes from short-read resequencing data using breseq. BMC Genomics 2014;15:1039. https://doi.org/10.1186/1471-2164-15-1039.
- [296] Ge SX, Jung D, Yao R. ShinyGO: a graphical gene-set enrichment tool for animals and plants. Bioinformatics 2020;36:2628–9. https://doi.org/10.1093/bioinformatics/btz931.
- [297] Grenier F, Matteau D, Baby V, Rodrigue S. Complete Genome Sequence of *Escherichia coli* BW25113. Genome Announc 2014;2:e01038-14. https://doi.org/10.1128/genomeA.01038-14.
- [298] Datsenko KA, Wanner BL. One-step inactivation of chromosomal genes in *Escherichia coli* K-12 using PCR products. Proc Natl Acad Sci U S A 2000;97:6640–5.
- [299] Bo L, Sun H, Li Y-D, Zhu J, Wurpel JND, Lin H, et al. Combating antimicrobial resistance: the silent war. Front Pharmacol 2024;15. https://doi.org/10.3389/fphar.2024.1347750.
- [300] Roemhild R, Barbosa C, Beardmore RE, Jansen G, Schulenburg H. Temporal variation in antibiotic environments slows down resistance evolution in pathogenic Pseudomonas aeruginosa. Evol Appl 2015;8:945–55. https://doi.org/10.1111/eva.12330.
- [301] Imamovic L, Ellabaan MMH, Machado AMD, Citterio L, Wulff T, Molin S, et al. Drug-Driven Phenotypic Convergence Supports Rational Treatment Strategies of Chronic Infections. Cell 2018;172:121-134.e14. https://doi.org/10.1016/j.cell.2017.12.012.
- [302] Hernando-Amado S, Sanz-García F, Martínez J. Rapid and robust evolution of collateral sensitivity in Pseudomonas aeruginosa antibiotic-resistant mutants 2020. https://doi.org/10.1126/sciadv.aba5493.
- [303] Hernando-Amado S, Laborda P, Martínez JL. Tackling antibiotic resistance by inducing transient and robust collateral sensitivity. Nat Commun 2023;14:1723. https://doi.org/10.1038/s41467-023-37357-4.
- [304] Jahn LJ, Munck C, Ellabaan MMH, Sommer MOA. Adaptive Laboratory Evolution of Antibiotic Resistance Using Different Selection Regimes Lead to Similar Phenotypes and Genotypes. Front Microbiol 2017;8. https://doi.org/10.3389/fmicb.2017.00816.
- [305] Laborda P, Martínez JL, Hernando-Amado S. Evolution of Habitat-Dependent Antibiotic Resistance in Pseudomonas aeruginosa. Microbiol Spectr 2022;10:e00247-22. https://doi.org/10.1128/spectrum.00247-22.
- [306] Chowdhury FR, Findlay BL. Backward collateral sensitivity can restore antibiotic susceptibility 2024:2024.11.06.622341. https://doi.org/10.1101/2024.11.06.622341.
- [307] Culp EJ, Waglechner N, Wang W, Fiebig-Comyn AA, Hsu Y-P, Koteva K, et al. Evolution-guided discovery of antibiotics that inhibit peptidoglycan remodelling. Nature 2020;578:582–7. https://doi.org/10.1038/s41586-020-1990-9.

- [308] Grossman TH. Tetracycline Antibiotics and Resistance. Cold Spring Harb Perspect Med 2016;6:a025387. https://doi.org/10.1101/cshperspect.a025387.
- [309] SaiSree L, Reddy M, Gowrishankar J. IS186 Insertion at a Hot Spot in thelon Promoter as a Basis for Lon Protease Deficiency of Escherichia coli B: Identification of a Consensus Target Sequence for IS186 Transposition. J Bacteriol 2001;183:6943–6. https://doi.org/10.1128/jb.183.23.6943-6946.2001.
- [310] Stout V, Torres-Cabassa A, Maurizi MR, Gutnick D, Gottesman S. RcsA, an unstable positive regulator of capsular polysaccharide synthesis. J Bacteriol 1991;173:1738–47. https://doi.org/10.1128/jb.173.5.1738-1747.1991.
- [311] Torres-Cabassa AS, Gottesman S. Capsule synthesis in Escherichia coli K-12 is regulated by proteolysis. J Bacteriol 1987;169:981–9. https://doi.org/10.1128/jb.169.3.981-989.1987.
- [312] D'Angelo F, Rocha EPC, Rendueles O. The Capsule Increases Susceptibility to Last-Resort Polymyxins, but Not to Other Antibiotics, in Klebsiella pneumoniae. Antimicrob Agents Chemother n.d.;67:e00127-23. https://doi.org/10.1128/aac.00127-23.
- [313] Ferrières Lionel, Aslam SN, Cooper RM, Clarke DJ. The yjbEFGH locus in Escherichia coli K-12 is an operon encoding proteins involved in exopolysaccharide production. Microbiology 2007;153:1070–80. https://doi.org/10.1099/mic.0.2006/002907-0.
- [314] Ma X, Xi W, Yang D, Zhao L, Yu W, He Y, et al. Collateral sensitivity between tetracyclines and aminoglycosides constrains resistance evolution in carbapenem-resistant Klebsiella pneumoniae. Drug Resist Updat 2023;68:100961. https://doi.org/10.1016/j.drup.2023.100961.
- [315] Sharma P, Haycocks JRJ, Middlemiss AD, Kettles RA, Sellars LE, Ricci V, et al. The multiple antibiotic resistance operon of enteric bacteria controls DNA repair and outer membrane integrity. Nat Commun 2017;8:1444. https://doi.org/10.1038/s41467-017-01405-7.
- [316] Warner DM, Levy SB. Different effects of transcriptional regulators MarA, SoxS and Rob on susceptibility of Escherichia coli to cationic antimicrobial peptides (CAMPs): Rob-dependent CAMP induction of the marRAB operon. Microbiology 2010;156:570–8. https://doi.org/10.1099/mic.0.033415-0.
- [317] Williams LE, Wernegreen JJ. Sequence Context of Indel Mutations and Their Effect on Protein Evolution in a Bacterial Endosymbiont. Genome Biol Evol 2013;5:599–605. https://doi.org/10.1093/gbe/evt033.
- [318] Kumaraswami M, Schuman JT, Seo SM, Kaatz GW, Brennan RG. Structural and biochemical characterization of MepR, a multidrug binding transcription regulator of the Staphylococcus aureus multidrug efflux pump MepA. Nucleic Acids Res 2009;37:1211–24. https://doi.org/10.1093/nar/gkn1046.
- [319] Praski Alzrigat L, Huseby DL, Brandis G, Hughes D. Fitness cost constrains the spectrum of marR mutations in ciprofloxacin-resistant Escherichia coli. J Antimicrob Chemother 2017;72:3016–24. https://doi.org/10.1093/jac/dkx270.
- [320] Kneidinger B, Marolda C, Graninger M, Zamyatina A, McArthur F, Kosma P, et al. Biosynthesis Pathway of ADP-l-glycero-β-d-manno-Heptose in Escherichia coli. J Bacteriol 2002;184:363–9. https://doi.org/10.1128/jb.184.2.363-369.2002.
- [321] Josts I, Stubenrauch CJ, Vadlamani G, Mosbahi K, Walker D, Lithgow T, et al. The Structure of a Conserved Domain of TamB Reveals a Hydrophobic β Taco Fold. Structure 2017;25:1898-1906.e5. https://doi.org/10.1016/j.str.2017.10.002.

- [322] Denisuik AJ, Garbutt LA, Golden AR, Adam HJ, Baxter M, Nichol KA, et al. Antimicrobial-resistant pathogens in Canadian ICUs: results of the CANWARD 2007 to 2016 study. J Antimicrob Chemother 2019;74:645–53. https://doi.org/10.1093/jac/dky477.
- [323] Herencias C, Álvaro-Llorente L, Ramiro-Martínez P, Fernández-Calvet A, Muñoz-Cazalla A, DelaFuente J, et al. β-lactamase expression induces collateral sensitivity in Escherichia coli. Nat Commun 2024;15:4731. https://doi.org/10.1038/s41467-024-49122-2.
- [324] Petersen PJ, Jacobus NV, Weiss WJ, Sum PE, Testa RT. In Vitro and In Vivo Antibacterial Activities of a Novel Glycylcycline, the 9-t-Butylglycylamido Derivative of Minocycline (GAR-936). Antimicrob Agents Chemother 1999;43:738–44. https://doi.org/10.1128/aac.43.4.738.
- [325] Zeng Y, Lu J, Liu C, Ling Z, Sun Q, Wang H, et al. A method for screening tigecycline-resistant gene *tet*(X) from human gut. J Glob Antimicrob Resist 2021;24:29–31. https://doi.org/10.1016/j.jgar.2020.11.010.
- [326] Sun J, Chen C, Cui C-Y, Zhang Y, Liu X, Cui Z-H, et al. Plasmid-encoded tet(X) genes that confer high-level tigecycline resistance in Escherichia coli. Nat Microbiol 2019;4:1457–64. https://doi.org/10.1038/s41564-019-0496-4.
- [327] Jakobsen L, Sandvang D, Jensen VF, Seyfarth AM, Frimodt-Møller N, Hammerum AM. Gentamicin susceptibility in *Escherichia coli* related to the genetic background: problems with breakpoints. Clin Microbiol Infect 2007;13:830–2. https://doi.org/10.1111/j.1469-0691.2007.01751.x.
- [328] Nation RL, Velkov T, Li J. Colistin and Polymyxin B: Peas in a Pod, or Chalk and Cheese? Clin Infect Dis Off Publ Infect Dis Soc Am 2014;59:88–94. https://doi.org/10.1093/cid/ciu213.
- [329] Heidrich CG, Mitova S, Schedlbauer A, Connell SR, Fucini P, Steenbergen JN, et al. The Novel Aminomethylcycline Omadacycline Has High Specificity for the Primary Tetracycline-Binding Site on the Bacterial Ribosome. Antibiotics 2016;5:32. https://doi.org/10.3390/antibiotics5040032.
- [330] Nicoloff H, Andersson DI. Lon protease inactivation, or translocation of the gene, potentiate bacterial evolution to antibiotic resistance. Mol Microbiol 2013;90:1233–48. https://doi.org/10.1111/mmi.12429.
- [331] Webber MA, Piddock LJV. The importance of efflux pumps in bacterial antibiotic resistance. J Antimicrob Chemother 2003;51:9–11. https://doi.org/10.1093/jac/dkg050.
- [332] EUCAST: MIC determination n.d. https://www.eucast.org/ast_of_bacteria/mic_determination/?no_cache=1 (accessed December 25, 2021).
- [333] Chowdhury FR, Findlay BL. Tripartite loops reverse antibiotic resistance 2025:2025.01.04.631305. https://doi.org/10.1101/2025.01.04.631305.
- [334] Chung CT, Niemela SL, Miller RH. One-step preparation of competent Escherichia coli: transformation and storage of bacterial cells in the same solution. Proc Natl Acad Sci U S A 1989;86:2172–5. https://doi.org/10.1073/pnas.86.7.2172.
- [335] Murray CJL, Ikuta KS, Sharara F, Swetschinski L, Aguilar GR, Gray A, et al. Global burden of bacterial antimicrobial resistance in 2019: a systematic analysis. The Lancet 2022;399:629–55. https://doi.org/10.1016/S0140-6736(21)02724-0.
- [336] Ventola CL. The antibiotic resistance crisis: part 1: causes and threats. P T Peer-Rev J Formul Manag 2015;40:277–83.

- [337] Imamovic L, Sommer MOA. Use of Collateral Sensitivity Networks to Design Drug Cycling Protocols That Avoid Resistance Development. Sci Transl Med 2013;5:204ra132-204ra132. https://doi.org/10.1126/SCITRANSLMED.3006609.
- [338] Sørum V, Øynes EL, Møller AS, Harms K, Samuelsen Ø, Podnecky NL, et al. Evolutionary Instability of Collateral Susceptibility Networks in Ciprofloxacin-Resistant Clinical Escherichia coli Strains. mBio 2022;13:e00441-22. https://doi.org/10.1128/mbio.00441-22.
- [339] eucast: Clinical breakpoints and dosing of antibiotics n.d. https://www.eucast.org/clinical breakpoints (accessed October 10, 2022).
- [340] Adler M, Anjum M, Andersson DI, Sandegren L. Combinations of mutations in envZ, ftsI, mrdA, acrB and acrR can cause high-level carbapenem resistance in Escherichia coli. J Antimicrob Chemother 2016;71:1188–98. https://doi.org/10.1093/jac/dkv475.
- [341] Hryc CF, Mallampalli VKPS, Bovshik EI, Azinas S, Fan G, Serysheva II, et al. Structural insights into cardiolipin replacement by phosphatidylglycerol in a cardiolipin-lacking yeast respiratory supercomplex. Nat Commun 2023;14:2783. https://doi.org/10.1038/s41467-023-38441-5.
- [342] Gulmezian M, Hyman KR, Marbois BN, Clarke CF, Javor GT. The role of UbiX in *Escherichia coli* coenzyme Q biosynthesis. Arch Biochem Biophys 2007;467:144–53. https://doi.org/10.1016/j.abb.2007.08.009.
- [343] Georgellis D, Kwon O, Lin EC. Quinones as the redox signal for the arc two-component system of bacteria. Science 2001;292:2314–6. https://doi.org/10.1126/science.1059361.
- [344] Schröder I, Johnson E, de Vries S. Microbial ferric iron reductases. FEMS Microbiol Rev 2003;27:427–47. https://doi.org/10.1016/S0168-6445(03)00043-3.
- [345] Seoane AS, Levy SB. Characterization of MarR, the repressor of the multiple antibiotic resistance (mar) operon in Escherichia coli. J Bacteriol 1995;177:3414–9.
- [346] Lomovskaya O, Lewis K, Matin A. EmrR is a negative regulator of the Escherichia coli multidrug resistance pump EmrAB. J Bacteriol 1995;177:2328–34. https://doi.org/10.1128/jb.177.9.2328-2334.1995.
- [347] Beggs GA, Brennan RG, Arshad M. MarR family proteins are important regulators of clinically relevant antibiotic resistance. Protein Sci Publ Protein Soc 2020;29:647–53. https://doi.org/10.1002/pro.3769.
- [348] Brunelle BW, Bearson BL, Bearson SMD. Chloramphenicol and tetracycline decrease motility and increase invasion and attachment gene expression in specific isolates of multidrug-resistant Salmonella enterica serovar Typhimurium. Front Microbiol 2015;5:801. https://doi.org/10.3389/fmicb.2014.00801.
- [349] Aono R, Tsukagoshi N, Yamamoto M. Involvement of Outer Membrane Protein TolC, a Possible Member of the mar-sox Regulon, in Maintenance and Improvement of Organic Solvent Tolerance of Escherichia coli K-12. J Bacteriol 1998;180:938–44. https://doi.org/10.1128/jb.180.4.938-944.1998.
- [350] Pourahmad Jaktaji R, Zargampoor F. Expression of TolC and Organic Solvent Tolerance of Escherichia Coli Ciprofloxacin Resistant Mutants. Iran J Pharm Res IJPR 2017;16:1185–9.
- [351] Evgrafov MR de, Faza M, Asimakopoulos K, Sommer M. Systematic Investigation of Resistance Evolution to Common Antibiotics Reveals Conserved Collateral Responses across Common Human Pathogens 2020. https://doi.org/10.1128/AAC.01273-20.

- [352] Shariati A, Arshadi M, Khosrojerdi MA, Abedinzadeh M, Ganjalishahi M, Maleki A, et al. The resistance mechanisms of bacteria against ciprofloxacin and new approaches for enhancing the efficacy of this antibiotic. Front Public Health 2022;10:1025633. https://doi.org/10.3389/fpubh.2022.1025633.
- [353] Andersson DI, Nicoloff H, Hjort K. Mechanisms and clinical relevance of bacterial heteroresistance. Nat Rev Microbiol 2019;17:479–96. https://doi.org/10.1038/s41579-019-0218-1
- [354] Hernando-Amado S, Sanz-García F, Martínez JL. Rapid and robust evolution of collateral sensitivity in Pseudomonas aeruginosa antibiotic-resistant mutants. Sci Adv 2020;6:eaba5493. https://doi.org/10.1126/sciadv.aba5493.
- [355] Entenza JM, Moreillon P. Tigecycline in combination with other antimicrobials: a review of in vitro, animal and case report studies. Int J Antimicrob Agents 2009;34:8.e1-9. https://doi.org/10.1016/j.ijantimicag.2008.11.006.
- [356] Parkins MD, Elborn JS. Newer antibacterial agents and their potential role in cystic fibrosis pulmonary exacerbation management. J Antimicrob Chemother 2010;65:1853–61. https://doi.org/10.1093/jac/dkq245.
- [357] Ikehata Y, Doukyu N. Improving the organic solvent tolerance of *Escherichia coli* with vanillin, and the involvement of an AcrAB-TolC efflux pump in vanillin tolerance. J Biosci Bioeng 2022;133:347–52. https://doi.org/10.1016/j.jbiosc.2021.12.015.
- [358] Reardon S. WHO warns against "post-antibiotic" era. Nature 2014. https://doi.org/10.1038/nature.2014.15135.
- [359] Lack of innovation set to undermine antibiotic performance and health gains n.d. https://www.who.int/news/item/22-06-2022-22-06-2022-lack-of-innovation-set-to-undermine-antibiotic-performance-and-health-gains (accessed December 2, 2024).
- [360] Dutescu IA, Hillier SA. Encouraging the Development of New Antibiotics: Are Financial Incentives the Right Way Forward? A Systematic Review and Case Study. Infect Drug Resist 2021;14:415–34. https://doi.org/10.2147/IDR.S287792.
- [361] Hernando-Amado S, Sanz-García F, Martínez JL. Rapid and robust evolution of collateral sensitivity in Pseudomonas aeruginosa antibiotic-resistant mutants. Sci Adv 2020;6:eaba5493. https://doi.org/10.1126/sciadv.aba5493.
- [362] Kim S, Lieberman TD, Kishony R. Alternating antibiotic treatments constrain evolutionary paths to multidrug resistance. Proc Natl Acad Sci U S A 2014;111:14494–9. https://doi.org/10.1073/pnas.1409800111.
- [363] Aulin LBS, Liakopoulos A, van der Graaf PH, Rozen DE, van Hasselt JGC. Design principles of collateral sensitivity-based dosing strategies. Nat Commun 2021;12:5691. https://doi.org/10.1038/s41467-021-25927-3.
- [364] Hall MD, Handley MD, Gottesman MM. Is resistance useless? Multidrug resistance and collateral sensitivity. Trends Pharmacol Sci 2009;30:546–56. https://doi.org/10.1016/j.tips.2009.07.003.
- [365] Allen RC, Engelstädter J, Bonhoeffer S, McDonald BA, Hall AR. Reversing resistance: different routes and common themes across pathogens. Proc R Soc B Biol Sci 2017;284:20171619. https://doi.org/10.1098/rspb.2017.1619.
- [366] Lozano-Huntelman NA, Singh N, Valencia A, Mira P, Sakayan M, Boucher I, et al. Evolution of antibiotic cross-resistance and collateral sensitivity in Staphylococcus epidermidis using the mutant prevention concentration and the mutant selection window. Evol Appl 2020;13:808–23. https://doi.org/10.1111/eva.12903.

- [367] Lázár V, Nagy I, Spohn R, Csörgő B, Györkei Á, Nyerges Á, et al. Genome-wide analysis captures the determinants of the antibiotic cross-resistance interaction network. Nat Commun 2014;5:4352. https://doi.org/10.1038/ncomms5352.
- [368] Holmes NE, Charles PGP. Safety and Efficacy Review of Doxycycline. Clin Med Ther 2009;1:CMT.S2035. https://doi.org/10.4137/CMT.S2035.
- [369] Rodriguez de Evgrafov MC, Faza M, Asimakopoulos K, Sommer MOA. Systematic Investigation of Resistance Evolution to Common Antibiotics Reveals Conserved Collateral Responses across Common Human Pathogens. Antimicrob Agents Chemother 2020;65:10.1128/aac.01273-20. https://doi.org/10.1128/aac.01273-20.
- [370] Choby JE, Skaar EP. Heme Synthesis and Acquisition in Bacterial Pathogens. J Mol Biol 2016;428:3408–28. https://doi.org/10.1016/j.jmb.2016.03.018.
- [371] Cotter PA, Melville SB, Albrecht JA, Gunsalus RP. Aerobic regulation of cytochrome d oxidase (cydAB) operon expression in Escherichia coli: roles of Fnr and ArcA in repression and activation. Mol Microbiol 1997;25:605–15. https://doi.org/10.1046/j.1365-2958.1997.5031860.x.
- [372] Poole RK, Gibson F, Wu G. The cydD gene product, component of a heterodimeric ABC transporter, is required for assembly of periplasmic cytochrome c and of cytochrome bd in Escherichia coli. FEMS Microbiol Lett 1994;117:217–23. https://doi.org/10.1111/j.1574-6968.1994.tb06768.x.
- [373] Kurosu M, Begari E. Vitamin K2 in Electron Transport System: Are Enzymes Involved in Vitamin K2 Biosynthesis Promising Drug Targets? Molecules 2010;15:1531–53. https://doi.org/10.3390/molecules15031531.
- [374] Ofori-Anyinam B, Riley AJ, Jobarteh T, Gitteh E, Sarr B, Faal-Jawara TI, et al. Comparative genomics shows differences in the electron transport and carbon metabolic pathways of *Mycobacterium africanum* relative to *Mycobacterium tuberculosis* and suggests an adaptation to low oxygen tension. Tuberculosis 2020;120:101899. https://doi.org/10.1016/j.tube.2020.101899.
- [375] Shan Y, Lazinski D, Rowe S, Camilli A, Lewis K. Genetic Basis of Persister Tolerance to Aminoglycosides in Escherichia coli. mBio 2015;6:10.1128/mbio.00078-15. https://doi.org/10.1128/mbio.00078-15.
- [376] Shiraliyev R, Orman MA. Metabolic disruption impairs ribosomal protein levels, resulting in enhanced aminoglycoside tolerance. eLife 2024;13. https://doi.org/10.7554/eLife.94903.2.
- [377] Dulanto Chiang A, Dekker JP. Efflux pump-mediated resistance to new beta lactam antibiotics in multidrug-resistant gram-negative bacteria. Commun Med 2024;4:1–9. https://doi.org/10.1038/s43856-024-00591-y.
- [378] Jing W, Liu J, Wu S, Li X, Liu Y. Role of cpxA Mutations in the Resistance to Aminoglycosides and β-Lactams in Salmonella enterica serovar Typhimurium. Front Microbiol 2021;12.
- [379] Gross R, Yelin I, Lázár V, Datta MS, Kishony R. Beta-lactamase dependent and independent evolutionary paths to high-level ampicillin resistance. Nat Commun 2024;15:5383. https://doi.org/10.1038/s41467-024-49621-2.
- [380] Shimada T, Fujita N, Maeda M, Ishihama A. Systematic search for the Cra-binding promoters using genomic SELEX system. Genes Cells 2005;10:907–18. https://doi.org/10.1111/j.1365-2443.2005.00888.x.

- [381] Somers JM, Amzallag A, Middleton RB. Genetic Fine Structure of the Leucine Operon of Escherichia coli K-12. J Bacteriol 1973;113:1268–72. https://doi.org/10.1128/jb.113.3.1268-1272.1973.
- [382] di Salvo ML, Ko T-P, Musayev FN, Raboni S, Schirch V, Safo MK. Active site structure and stereospecificity of *Escherichia coli* pyridoxine-5'-phosphate oxidase1. J Mol Biol 2002;315:385–97. https://doi.org/10.1006/jmbi.2001.5254.
- [383] Kriek M, Martins F, Challand MR, Croft A, Roach PL. Thiamine Biosynthesis in Escherichia coli: Identification of the Intermediate and By-Product Derived from Tyrosine. Angew Chem Int Ed 2007;46:9223–6. https://doi.org/10.1002/anie.200702554.
- [384] Okamoto S, Tamaru A, Nakajima C, Nishimura K, Tanaka Y, Tokuyama S, et al. Loss of a conserved 7-methylguanosine modification in 16S rRNA confers low-level streptomycin resistance in bacteria. Mol Microbiol 2007;63:1096–106. https://doi.org/10.1111/j.1365-2958.2006.05585.x.
- [385] Hoang L, Fredrick K, Noller HF. Creating ribosomes with an all-RNA 30S subunit P site. Proc Natl Acad Sci 2004;101:12439–43. https://doi.org/10.1073/pnas.0405227101.
- [386] Dulyayangkul P, Sealey JE, Lee WWY, Satapoomin N, Reding C, Heesom KJ, et al. Improving nitrofurantoin resistance prediction in Escherichia coli from whole-genome sequence by integrating NfsA/B enzyme assays. Antimicrob Agents Chemother 2024;68:e00242-24. https://doi.org/10.1128/aac.00242-24.
- [387] Le VVH, Davies IG, Moon CD, Wheeler D, Biggs PJ, Rakonjac J. Novel 5-Nitrofuran-Activating Reductase in Escherichia coli. Antimicrob Agents Chemother 2019;63:e00868-19. https://doi.org/10.1128/AAC.00868-19.
- [388] Hussein M, Sun Z, Hawkey J, Allobawi R, Judd LM, Carbone V, et al. High-level nitrofurantoin resistance in a clinical isolate of Klebsiella pneumoniae: a comparative genomics and metabolomics analysis. mSystems 2023;9:e00972-23. https://doi.org/10.1128/msystems.00972-23.
- [389] Mohakud NK, Panda RK, Singh D, Patra SD, Simnani FZ, Sinha A, et al. Intrinsic insights to antimicrobial effects of Nitrofurantoin to multi drug resistant *Salmonella enterica* serovar Typhimurium ms202. Biomed Pharmacother 2023;165:115180. https://doi.org/10.1016/j.biopha.2023.115180.
- [390] Reizer J, Reizer A, Saier MH. Novel phosphotransferase system genes revealed by bacterial genome analysis--a gene cluster encoding a unique Enzyme I and the proteins of a fructose-like permease system. Microbiol Read Engl 1995;141 (Pt 4):961–71. https://doi.org/10.1099/13500872-141-4-961.
- [391] Peri KG, Waygood EB. Sequence of cloned enzyme IIN-acetylglucosamine of the phosphoenolpyruvate:N-acetylglucosamine phosphotransferase system of Escherichia coli. Biochemistry 1988;27:6054–61. https://doi.org/10.1021/bi00416a034.
- [392] Outten FW, Huffman DL, Hale JA, O'Halloran TV. The Independent *cue* and *cus*Systems Confer Copper Tolerance during Aerobic and Anaerobic Growth in *Escherichia coli* *. J Biol Chem 2001;276:30670–7. https://doi.org/10.1074/jbc.M104122200.
- [393] Chenault SS, Earhart CF. Identification of hydrophobic proteins FepD and FepG of the Escherichia coli ferrienterobactin permease. Microbiology 1992;138:2167–71. https://doi.org/10.1099/00221287-138-10-2167.
- [394] Beard SJ, Hashim R, Wu G, Binet MRB, Hughes MN, Poole RK. Evidence for the transport of zinc(II) ions via the Pit inorganic phosphate transport system in Escherichia

- coli. FEMS Microbiol Lett 2000;184:231–5. https://doi.org/10.1111/j.1574-6968.2000.tb09019.x.
- [395] Harder D, Stolz J, Casagrande F, Obrdlik P, Weitz D, Fotiadis D, et al. DtpB (YhiP) and DtpA (TppB, YdgR) are prototypical proton-dependent peptide transporters of Escherichia coli. FEBS J 2008;275:3290–8. https://doi.org/10.1111/j.1742-4658.2008.06477.x.
- [396] Cosgriff AJ, Brasier G, Pi J, Dogovski C, Sarsero JP, Pittard AJ. A Study of AroP-PheP Chimeric Proteins and Identification of a Residue Involved in Tryptophan Transport. J Bacteriol 2000;182:2207–17. https://doi.org/10.1128/jb.182.8.2207-2217.2000.
- [397] Zampieri M, Enke T, Chubukov V, Ricci V, Piddock L, Sauer U. Metabolic constraints on the evolution of antibiotic resistance. Mol Syst Biol 2017;13:917. https://doi.org/10.15252/msb.20167028.
- [398] Fondi M, Bosi E, Presta L, Natoli D, Fani R. Modelling microbial metabolic rewiring during growth in a complex medium. BMC Genomics 2016;17:970. https://doi.org/10.1186/s12864-016-3311-0.
- [399] RICHARDSON AR, SOMERVILLE GA, SONENSHEIN AL. Regulating the Intersection of Metabolism and Pathogenesis in Gram-positive Bacteria. Microbiol Spectr 2015;3:10.1128/microbiolspec.MBP-0004–2014. https://doi.org/10.1128/microbiolspec.MBP-0004-2014.
- [400] Durão P, Trindade S, Sousa A, Gordo I. Multiple Resistance at No Cost: Rifampicin and Streptomycin a Dangerous Liaison in the Spread of Antibiotic Resistance. Mol Biol Evol 2015;32:2675–80. https://doi.org/10.1093/molbev/msv143.
- [401] Lengeler J. Characterisation of mutants of Escherichia coli K12, selected by resistance to streptozotocin. Mol Gen Genet MGG 1980;179:49–54. https://doi.org/10.1007/BF00268445.
- [402] Gil-Gil T, Ochoa-Sánchez LE, Martínez JL. The Antibiotic Fosfomycin Mimics the Effects of the Intermediate Metabolites Phosphoenolpyruvate and Glyceraldehyde-3-Phosphate on the Stenotrophomonas maltophilia Transcriptome. Int J Mol Sci 2021;23:159. https://doi.org/10.3390/ijms23010159.
- [403] Bielec F, Brauncajs M, Pastuszak-Lewandoska D. Nitrofuran Derivatives Cross-Resistance Evidence—Uropathogenic Escherichia coli Nitrofurantoin and Furazidin In Vitro Susceptibility Testing. J Clin Med 2023;12:5166. https://doi.org/10.3390/jcm12165166.
- [404] Ambrose PG, Bhavnani SM, Jones RN. Pharmacokinetics-Pharmacodynamics of Cefepime and Piperacillin- Tazobactam against Escherichia coli and Klebsiella pneumoniae Strains Producing Extended-Spectrum β-Lactamases: Report from the ARREST Program. Antimicrob Agents Chemother 2003;47:1643–6. https://doi.org/10.1128/AAC.47.5.1643-1646.2003.
- [405] Nichols WW, Stone GG, Newell P, Broadhurst H, Wardman A, MacPherson M, et al. Ceftazidime-Avibactam Susceptibility Breakpoints against Enterobacteriaceae and Pseudomonas aeruginosa. Antimicrob Agents Chemother 2018;62:10.1128/aac.02590-17. https://doi.org/10.1128/aac.02590-17.
- [406] Berkhout J, Melchers MJ, van Mil AC, Nichols WW, Mouton JW. In Vitro Activity of Ceftazidime-Avibactam Combination in In Vitro Checkerboard Assays. Antimicrob Agents Chemother 2015;59:1138–44. https://doi.org/10.1128/AAC.04146-14.

- [407] Durão P, Balbontín R, Gordo I. Evolutionary Mechanisms Shaping the Maintenance of Antibiotic Resistance. Trends Microbiol 2018;26:677–91. https://doi.org/10.1016/j.tim.2018.01.005.
- [408] Chen Z, Gao Y, Lv B, Sun F, Yao W, Wang Y, et al. Hypoionic Shock Facilitates Aminoglycoside Killing of Both Nutrient Shift- and Starvation-Induced Bacterial Persister Cells by Rapidly Enhancing Aminoglycoside Uptake. Front Microbiol 2019;10. https://doi.org/10.3389/fmicb.2019.02028.
- [409] Schneider CA, Rasband WS, Eliceiri KW. NIH Image to ImageJ: 25 years of image analysis. Nat Methods 2012;9:671–5. https://doi.org/10.1038/nmeth.2089.
- [410] Wong A. Epistasis and the Evolution of Antimicrobial Resistance. Front Microbiol 2017;8:246. https://doi.org/10.3389/fmicb.2017.00246.
- [411] Horton JS, Taylor TB. Mutation bias and adaptation in bacteria. Microbiology 2023;169:001404. https://doi.org/10.1099/mic.0.001404.
- [412] Gomez JE, Kaufmann-Malaga BB, Wivagg CN, Kim PB, Silvis MR, Renedo N, et al. Ribosomal mutations promote the evolution of antibiotic resistance in a multidrug environment. eLife n.d.;6:e20420. https://doi.org/10.7554/eLife.20420.
- [413] Espedido BA, Gosbell IB. Chromosomal mutations involved in antibiotic resistance in Staphylococcus aureus. Front Biosci-Sch 2012;4:900–15. https://doi.org/10.2741/S307.
- [414] The Effects on Human Health of Subtherapeutic Use of Antimicrobials in Animal Feeds. Washington, D.C.: National Academies Press; 1980. https://doi.org/10.17226/21.
- [415] Ruhluel D, O'Brien S, Fothergill JL, Neill DR. Development of liquid culture media mimicking the conditions of sinuses and lungs in cystic fibrosis and health 2022. https://doi.org/10.12688/f1000research.125074.2.
- [416] N. Tsai C, Massicotte M-A, R. MacNair C, N. Perry J, D. Brown E, K. Coombes B. Screening under infection-relevant conditions reveals chemical sensitivity in multidrug resistant invasive non-typhoidal Salmonella (iNTS). RSC Chem Biol 2023;4:600–12. https://doi.org/10.1039/D3CB00014A.
- [417] Higazy D, Pham AD, van Hasselt C, Høiby N, Jelsbak L, Moser C, et al. In vivo evolution of antimicrobial resistance in a biofilm model of Pseudomonas aeruginosa lung infection. ISME J 2024;18:wrae036. https://doi.org/10.1093/ismejo/wrae036.
- [418] Castañeda-Barba S, Top EM, Stalder T. Plasmids, a molecular cornerstone of antimicrobial resistance in the One Health era. Nat Rev Microbiol 2024;22:18–32. https://doi.org/10.1038/s41579-023-00926-x.
- [419] San Millan A, MacLean RC. Fitness Costs of Plasmids: a Limit to Plasmid Transmission. Microbiol Spectr 2017;5:10.1128/microbiolspec.mtbp-0016–2017. https://doi.org/10.1128/microbiolspec.mtbp-0016-2017.
- [420] WHO Warns That Pipeline for New Antibiotics Is Running Dry. Carb-X n.d. https://carb-x.org/carb-x-news/who-warns-that-pipeline-for-new-antibiotics-is-running-dry/ (accessed August 28, 2022).

Appendices

Supplementary Materials for Chapter 2

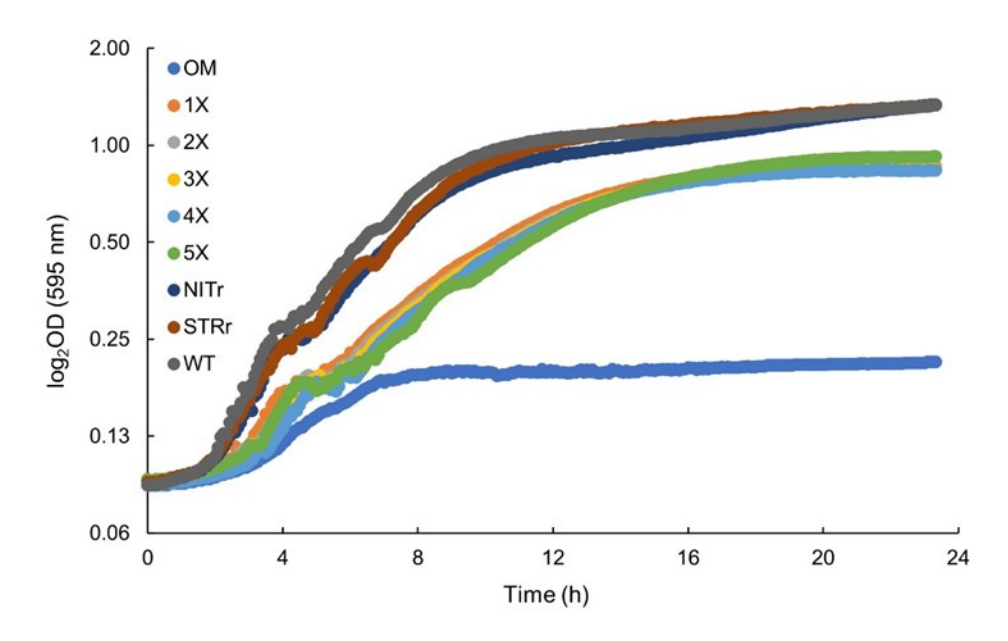


Figure S2.1: Additional growth curves. A STR and a NIT-resistant (NITr and STRr, evolved on the wildtype background) strain showed little difference in their growth curves when compared to the WT, indicating cost-free resistance mechanisms. 1X - 5X represent the OM cells after 1-5 passes through flat [CHL] SAGE lanes. Multiple passages through flat [CHL] SAGE lanes did not result in significant improvement in fitness, showing that the majority of fitness gains are realized after the primary pass.

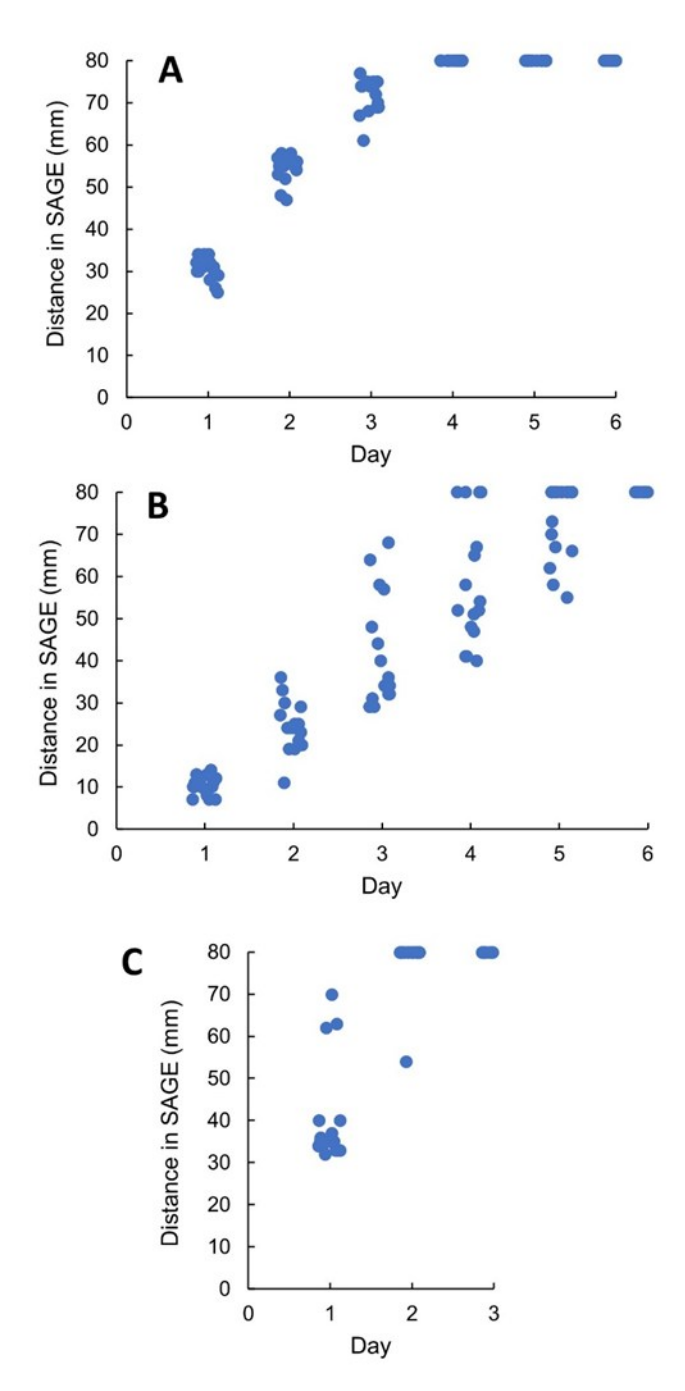


Figure S2.2: (A) WT populations showed little variation in evolution of NIT-resistance in SAGE. (B) OM replicates showed large variation in evolution of NIT-resistance in SAGE. (C) Resistance to STR evolved in WT populations via a highly repeatable pattern in SAGE. Variation along the horizontal axis is random jitter added to separate overlapping points. N = 16 for all SAGE evolutions.

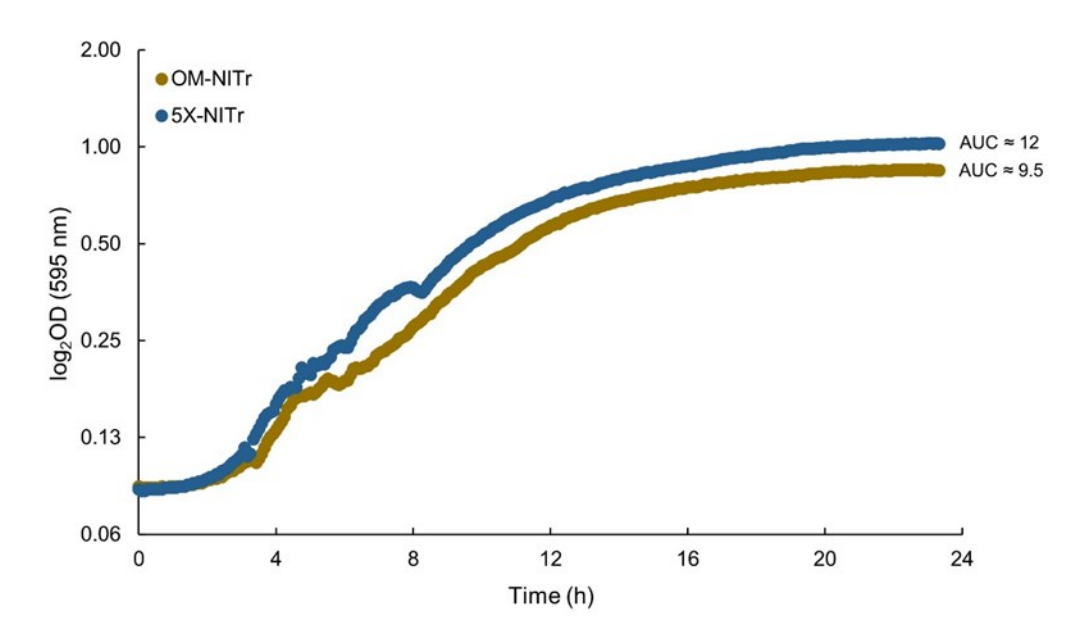


Figure S2.3: A NIT-evolved 5X (5X-NITr) replicate showed a moderate increase in fitness compared to a NIT-evolved OM replicate (OM-NITr).

Table S2.1: We observed no significant difference between the distance moved by the OM in NIT SAGE plates inoculated with either stationary phase OM or OM with inoculum size expanded to match that of the WT, except for a small statistical significance on day 3. p values are from two-sample t-tests assuming unequal variances.

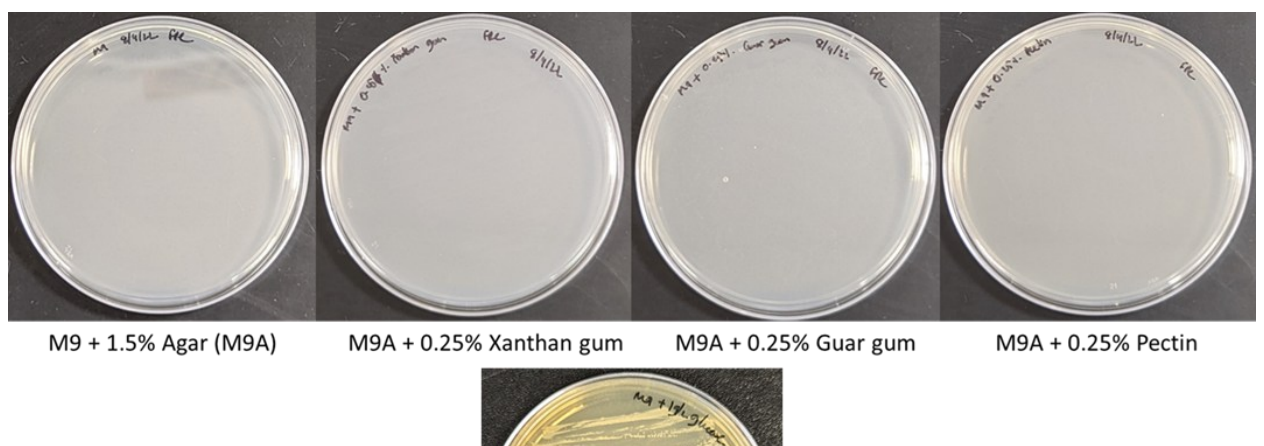
	OM (mm) (overnight	Distance moved by OM (mm) (inoculum standardized, n = 4)	p value
1	10.2	10.3	0.919
2	24.4	23.3	0.556
3	41.9	33.8	0.047*

4	58.5	52.5	0.363
5	73.2	66.3	0.505
6	78.6	78.7	0.939

All other supplementary materials are available here:

https://pubs.acs.org/doi/10.1021/acsinfecdis.3c00156?goto=supporting-info

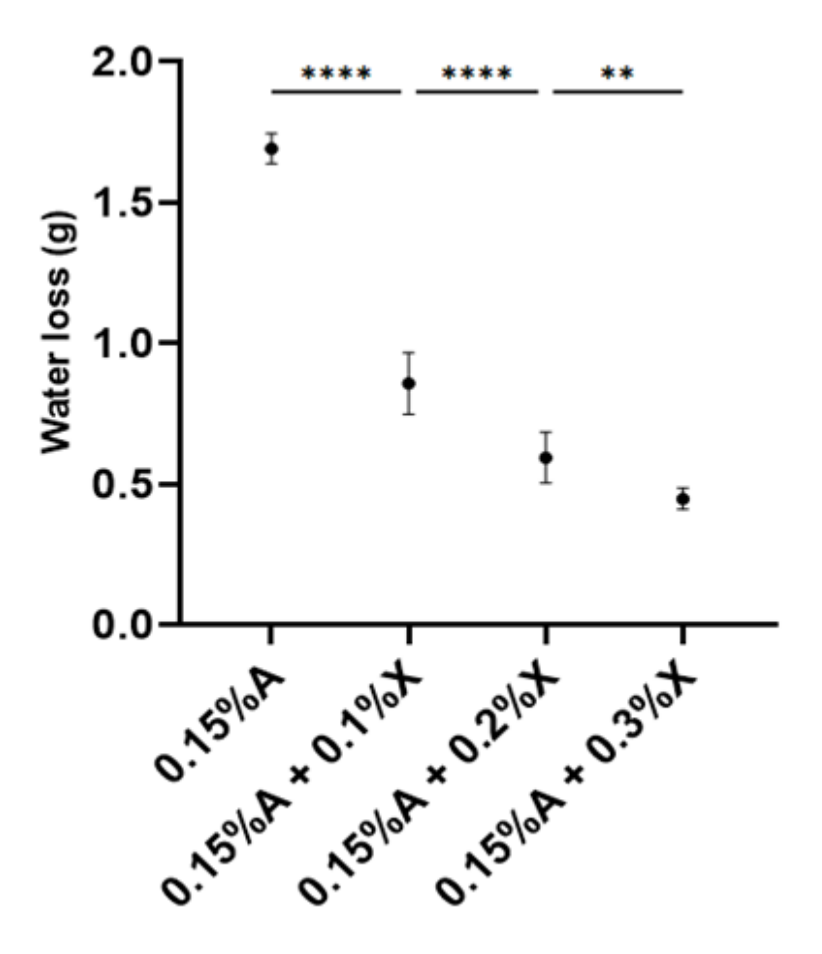
Supplementary Materials for Chapter 3



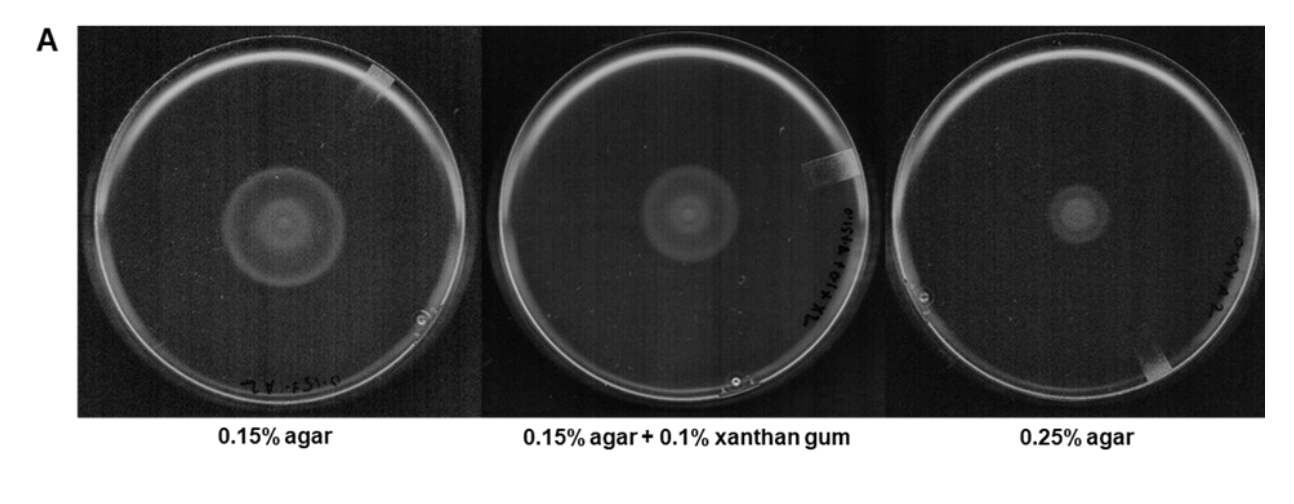


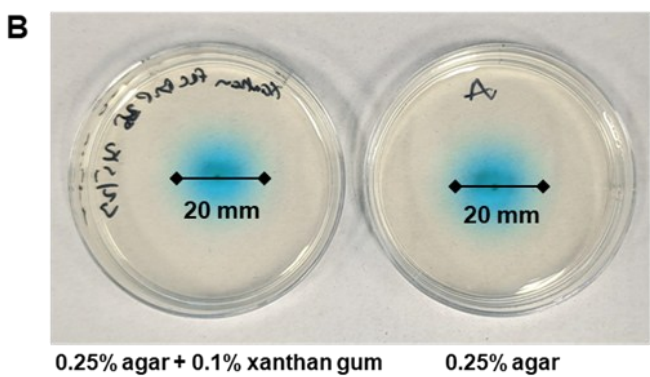
M9A + 1g/L glucose

Supplementary Figure 3.1: Growth on gelling agents. No growth was observed when *E. coli* cells were streaked on plates made with M9 + 1.5% agar (M9A) or M9A supplemented with xanthan gum, guar gum, or pectin at 0.25% w/v following 24 h of incubation. M9A supplemented with 1 g/L of glucose showed clear growth.

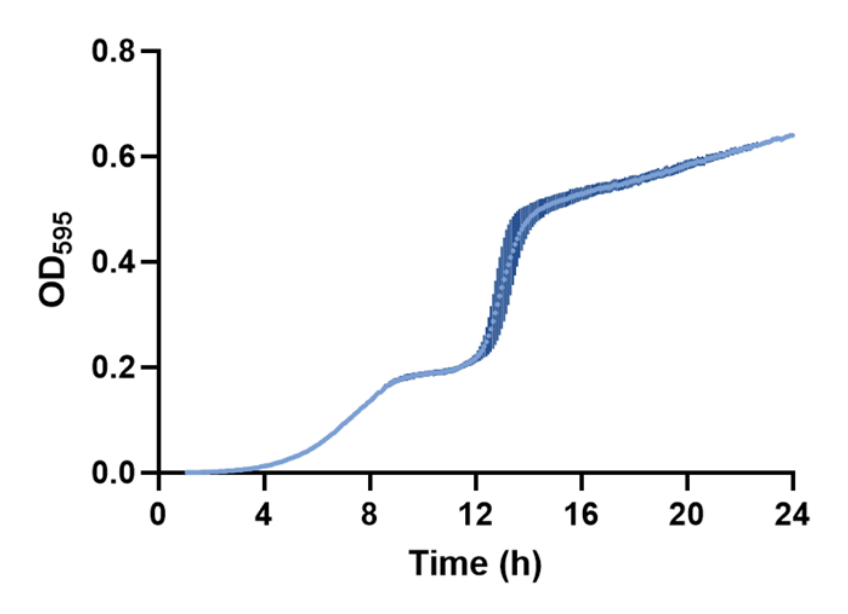


Supplementary Figure 3.2: Synaeresis at various xanthan gum concentrations. Increasing the amount of xanthan gum added to 0.15% agar medium reduces water loss, with diminishing returns at higher xanthan gum concentrations. A = agar. X = Xanthan gum. *p < 0.05, **p < 0.01, *** p < 0.001, **** p < 0.0001, one-way ANOVA with Fisher's LSD test.





Supplementary Figure 3.3: Motility and diffusion assays. (A) Cells swimming through 0.15% agar laced with 0.1% xanthan gum show increased motility relative to 0.25% agar. Representative pictures from three independent replicates are shown. (B) Diffusion rate of malachite green in 0.25% agar and 0.15% agar + 0.1% xanthan gum are similar. 2 μ L of malachite green was impregnated in the center of each plate (60 x 15 mm) made with 10 mL of media. Measurements were taken after 8 h.



Supplementary Figure 3.4: Growth of XAM CM in MHB. Cells show a diauxic growth curve.

The mean of three independent replicates is shown. Error bars indicate standard deviation.

Supplementary Table 3.1. Mutations observed in SAGE isolates.

G	75. tot				
Strain	Position	Mutation	Annotation	Gene	Description
			coding (43-47/1320		liprotein, glycosyl
A26	1563034	IS2 (-) +5 bp	nt)	yddW ←	hydrolase homolog
A26	3206481	G→A	E26K (<u>G</u> AG→ <u>A</u> AG)	rpoD →	RNA polymerase, sigma 70 (sigma D) factor
A26	3528471	G→T	R253S (<u>C</u> GC→ <u>A</u> GC)	envZ ←	sensory histidine kinase in two-component regulatory system with OmpR
A51	55429	C→T	G561S (<mark>G</mark> GT→ <u>A</u> GT)	lptD ←	LPS assembly OM complex LptDE, beta-barrel component
A51	56403	(GTG) _{3→2}	coding (705-707/2355 nt)	lptD ←	LPS assembly OM complex LptDE, beta-barrel component
A51	572569	(T) _{6→7}	intergenic (-288/-285)	$nmpC \leftarrow / \rightarrow essD$	DLP12 prophage; truncated outer membrane porin (pseudogene);IS, phage, Tn; Phage or Prophage Related; outer membrane porin protein; locus of qsr prophage/DLP12 prophage; putative phage lysis protein

Strain	Position	Mutation	Annotation	Gene	Description
A51	1563034	IS2 (-) +5 bp	coding (43-47/1320 nt)	yddW ←	liprotein, glycosyl hydrolase homolog
A51	1999224	T→A	W11R (<u>T</u> GG→ <u>A</u> GG)	fliT →	putative flagellar synthesis and assembly chaperone
A51	2306089	T→C	N47S (A <u>A</u> C→A <u>G</u> C)	$ompC \leftarrow$	outer membrane porin protein C
A51	2399791	IS2 (-) +5 bp	coding (326-330/939 nt)	lrhA ←	transcriptional repressor of flagellar, motility and chemotaxis genes
A51	3206481	G→A	E26K (<mark>G</mark> AG→ <u>A</u> AG)	$rpoD \rightarrow$	RNA polymerase, sigma 70 (sigma D) factor
A51	3775555	+A	coding (368/822 nt)	cysE ←	serine acetyltransferase
A51	3931636	C→T	T17I (A <u>C</u> A→A <u>T</u> A)	$rbsR \rightarrow$	transcriptional repressor of ribose metabolism
X34	55429	C→T	G561S (<u>G</u> GT→ <u>A</u> GT)	lptD ←	LPS assembly OM complex LptDE, beta-barrel component
X34	240136	T→C	L36P (C <u>T</u> G→C <u>C</u> G)	$gmhA \rightarrow$	D-sedoheptulose 7-phosphate isomerase
X34	391960	C→A	intergenic (-217/-135)	$ampH \leftarrow / \rightarrow sbmA$	D-alanyl-D-alanine- carboxypeptidase/end opeptidase; penicillin-binding

					protein; weak beta-lactamase/microc
					in B17 transporter
Strain	Position	Mutation	Annotation	Gene	Description
			coding		
			(43-47/1320		liprotein, glycosyl
X34	1563034	IS2 (-) +5 bp	nt)	yddW ←	hydrolase homolog
			intergenic	<i>uxaB</i> ← / ←	altronate oxidoreductase, NAD-dependent/putat ive membrane-bound
X34	1605138	C→A	(-201/+26)	yneF	diguanylate cyclase
X34	3206481	G→A	E26K (<u>G</u> AG→ <u>A</u> AG)		RNA polymerase, sigma 70 (sigma D) factor
X34	3512437	IS5 (+) +4 bp	intergenic (-14/+384)	$aroK \leftarrow / \leftarrow hofQ$	shikimate kinase I/DNA catabolic putative fimbrial transporter
X34	4390177	+T	coding (73/309 nt)	hfq o	global sRNA chaperone; HF-I, host factor for RNA phage Q beta replication
XAM CM	20771	C→A	intergenic (-263/+44)	$insA \leftarrow / \leftarrow rpsT$	IS1 repressor TnpA/30S ribosomal subunit protein S20
XAM CM	55428	C→T	G561D (G <mark>G</mark> T→G <u>A</u> T)	lptD ←	LPS assembly OM complex LptDE, beta-barrel component
XAM CM	195916	T→A	L501Q (C <u>T</u> G→C <u>A</u> G)	$bamA \rightarrow$	BamABCDE complex OM biogenesis outer membrane

					pore-forming assembly factor
Strain	Position	Mutation	Annotation	Gene	Description
XAM CM	1563034	IS2 (-) +5 bp	coding (43-47/1320 nt)	yddW ←	liprotein, glycosyl hydrolase homolog
XAM CM	1972967	IS5 (+) +4 bp	intergenic (-513/-264)	$flhD \leftarrow / \rightarrow uspC$	flagellar class II regulon transcriptional activator, with FlhC/universal stress protein
XAM CM	2394241	Δ7,687 bp		[nuoF]– [alaA]	[nuoF], nuoE, nuoC, nuoB, nuoA, lrhA, [alaA]
XAM CM	2458311	C→T	W59* (T <mark>G</mark> G→T <u>A</u> G)	mlaA ←	ABC transporter maintaining OM lipid asymmetry, OM lipoprotein component
XAM CM	3206481	G→A	E26K (<u>G</u> AG→ <u>A</u> AG)	$rpoD \rightarrow$	RNA polymerase, sigma 70 (sigma D) factor
XAM CM	3674947	+CA	coding (354/1497 nt)	yhjJ ←	putative periplasmic M16 family chaperone
XAM CM	3797305	IS5 (–) +4 bp	coding (190-193/1080 nt)	waaB ←	UDP-D-galactose:(glu cosyl)lipopolysacchar ide-1, 6-D-galactosyltransfer ase
Strain	Position	Mutation	Annotation	Gene	Description

XAM_WT	65,196	+C	coding (585/2352 nt)	polB ←	DNA polymerase II
XAM_WT	1,652,589	C→A	<i>Y88*</i> (<i>TA<mark>C→TA<u>A</u></mark></i>)	ynfE →	putative selenate reductase, periplasmic
					flagellar class II regulon transcriptional activator, with
XAM_WT	1,972,715	$G{ ightarrow} T$	intergenic (-261/-519)	$ \begin{cases} flhD \leftarrow / \rightarrow \\ uspC \end{cases} $	FlhC/universal stress protein
XAM_WT	4,171,661	A→T	$\begin{array}{c} K163N \\ (AA\underline{A} \rightarrow AA\underline{T}) \end{array}$	$rpoB \rightarrow$	RNA polymerase, beta subunit

Supplementary Table 3.2: Gene ontology groups from all of the identified mutations of the evolved strains determined with ShinyGo v0.741.

Enrichment FDR	N ¹	Pathwa y Genes	Fold Enrichme nt	Pathway	URL	Genes
1.9515679044 1107E-05	5	16	41.602822 5806452	Respiratory chain complex i	http://amigo.geneo ntology.org/amigo/ term/GO:0045271	nuoF nuoE nuoC nuoB nuoA
1.9515679044 1107E-05	5	16	41.602822 5806452	Plasma membrane respiratory chain complex i	http://amigo.geneo ntology.org/amigo/ term/GO:0045272	nuoF nuoE nuoC nuoB nuoA
1.9515679044 1107E-05	5	14	47.546082 9493088	Quinone		nuoF nuoE nuoC nuoB nuoA

Enrichment FDR	N^1	Pathwa y Genes	Fold Enrichme nt	Pathway	URL	Genes
2.0626349788 9355E-05	5	17	39.155597 7229602	NADH dehydrogenase complex	http://amigo.geneo ntology.org/amigo/ term/GO:0030964	nuoF nuoE nuoC nuoB nuoA
9.7016944712 2268E-05	5	25	26.625806 4516129	Quinone binding	http://amigo.geneo ntology.org/amigo/ term/GO:0048038	nuoF nuoE nuoC nuoB nuoA
9.7016944712 2268E-05	5	24	27.735215 0537634	Plasma membrane respirasome	http://amigo.geneo ntology.org/amigo/ term/GO:0070470	nuoF nuoE nuoC nuoB nuoA
9.7016944712 2268E-05	5	25	26.625806 4516129	Respiratory chain complex	http://amigo.geneo ntology.org/amigo/ term/GO:0098803	nuoF nuoE nuoC nuoB nuoA
0.0001143852 96756409	4	12	44.376344 0860215	Quinone		nuoF nuoE nuoB nuoA
0.0001143852 96756409	5	27	24.653524 4922342	Respirasome	http://amigo.geneo ntology.org/amigo/ term/GO:0070469	nuoF nuoE nuoC nuoB nuoA
0.0001479219 74039749	4	13	40.962779 1563275	Ubiquinone		nuoF nuoE nuoC nuoA
0.0004383166 41715869	4	17	31.324478 1783681	NADH dehydrogenase (ubiquinone) activity	http://amigo.geneo ntology.org/amigo/ term/GO:0008137	nuoF nuoC nuoB nuoA

Enrichment FDR	N^1	Pathwa y Genes	Fold Enrichme nt	Pathway	URL	Genes
0.0005138818 18946486	4	18	29.584229 390681	NADH dehydrogenase (quinone) activity	http://amigo.geneo ntology.org/amigo/ term/GO:0050136	nuoF nuoC nuoB nuoA
0.0007432115 09090046	4	20	26.625806 4516129	Ubiquinone, and fumarate reductase complex		nuoF nuoE nuoB nuoA
0.0008480425 80787152	4	21	25.357910 906298	NADH dehydrogenase activity	http://amigo.geneo ntology.org/amigo/ term/GO:0003954	nuoF nuoC nuoB nuoA
0.0016381721 3050132	4	25	21.300645 1612903	Oxidative phosphorylation		nuoF nuoE nuoB nuoA
0.0024469429 8116853	4	28	19.018433 1797235	Oxidoreductase activity, acting on nad(p)h, quinone or similar compound as acceptor	http://amigo.geneo ntology.org/amigo/ term/GO:0016655	nuoF nuoC nuoB nuoA
0.0040019759 6550932	5	62	10.736212 2788762	Oxidoreductase complex	http://amigo.geneo ntology.org/amigo/ term/GO:1990204	nuoF nuoE nuoC nuoB nuoA
0.0063920060 7085923	7	160	5.8243951 6129032	Membrane protein complex	http://amigo.geneo ntology.org/amigo/ term/GO:0098796	bamA ompC nuoF nuoE nuoC nuoB nuoA

Enrichment FDR	N^1	Pathwa y Genes	Fold Enrichme nt	Pathway	URL	Genes
0.0073435512 0593817	5	72	9.2450716 8458781	Translocase		nuoF nuoE nuoC nuoB nuoA
0.0112586016 181981	6	125	6.3901935 483871	Cell outer membrane	http://amigo.geneo ntology.org/amigo/ term/GO:0009279	lptD bamA yddW ompC mlaA hofQ
0.0113650604 47705	4	44	12.102639 2961877	Respirasome, and nitrate assimilation		nuoF nuoE nuoB nuoA
0.0148326303 699135	6	135	5.9168458 781362	Outer membrane	http://amigo.geneo ntology.org/amigo/ term/GO:0019867	lptD bamA yddW ompC mlaA hofQ
0.0148326303 699135	6	136	5.8733396 5844402	External encapsulating structure	http://amigo.geneo ntology.org/amigo/ term/GO:0030312	lptD bamA yddW ompC mlaA hofQ
0.0148326303 699135	6	135	5.9168458 781362	Macromolecule localization	http://amigo.geneo ntology.org/amigo/ term/GO:0033036	lptD bamA sbmA ompC mlaA hofQ
0.0169037765 170519	4	52	10.240694 7890819	Oxidoreductase activity, acting on nad(p)h	http://amigo.geneo ntology.org/amigo/ term/GO:0016651	nuoF nuoC nuoB nuoA

Enrichment FDR	N^1	Pathwa y Genes	Fold Enrichme nt	Pathway	URL	Genes
0.0169037765 170519	6	142	5.6251703 7710132	NAD		uxaB nuoF nuoE nuoC nuoB nuoA
0.0169037765 170519	5	92	7.2352734 9228612	Cell outer membrane		lptD bamA ompC mlaA hofQ
0.0192931642 820252	6	147	5.4338380 5134957	Catalytic complex	http://amigo.geneo ntology.org/amigo/ term/GO:1902494	nuoF nuoE nuoC nuoB nuoA cysE
0.0215782433 841346	2	6	44.376344 0860215	Phospholipid transport	http://amigo.geneo ntology.org/amigo/ term/GO:0015914	ompC mlaA
0.0215782433 841346	2	6	44.376344 0860215	Regulation of organelle assembly	http://amigo.geneo ntology.org/amigo/ term/GO:1902115	flhD fliT

Supplementary Table 3.3: Gene ontology groups, high level GO categories, from all of the identified mutations of the evolved strains determined with ShinyGo v0.74.

N ¹	High level GO category	Genes
27	Cellular process	insA1 rpsT lptD bamA gmhA ampH sbmA essD yddW uxaB yneF flhD uspC fliT ompC nuoF nuoE nuoB lrhA alaA mlaA rpoD aroK hofQ envZ cysE waaB
21	Binding	rpsT gmhA ampH sbmA yneF flhD ompC nuoF nuoE nuoC nuoB nuoA lrhA alaA rpoD aroK hofQ envZ yhjJ rbsR hfq

N ¹	High level GO category	Genes
21	Metabolic process	insA1 rpsT gmhA ampH yddW uxaB flhD nuoF nuoE nuoC nuoB nuoA lrhA alaA rpoD aroK hofQ envZ yhjJ cysE waaB
16	Catalytic activity	gmhA ampH yddW uxaB yneF nuoF nuoE nuoC nuoB nuoA alaA aroK envZ yhjJ cysE waaB
16	Cellular metabolic process	insA1 rpsT gmhA uxaB flhD nuoF nuoE nuoB lrhA alaA rpoD aroK hofQ envZ cysE waaB
15	Membrane	lptD bamA ampH sbmA yddW yneF ompC nuoF nuoE nuoC nuoB nuoA mlaA hofQ envZ
15	Primary metabolic process	insA1 rpsT gmhA ampH uxaB flhD lrhA alaA rpoD aroK hofQ envZ yhjJ cysE waaB
15	Organic substance metabolic process	insA1 rpsT gmhA ampH uxaB flhD lrhA alaA rpoD aroK hofQ envZ yhjJ cysE waaB
15	Cell periphery	lptD bamA ampH sbmA yddW yneF ompC nuoF nuoE nuoC nuoB nuoA mlaA hofQ envZ
15	Organic cyclic compound binding	rpsT ampH sbmA yneF flhD nuoF nuoC lrhA alaA rpoD aroK hofQ envZ rbsR hfq
15	Heterocyclic compound binding	rpsT ampH sbmA yneF flhD nuoF nuoC lrhA alaA rpoD aroK hofQ envZ rbsR hfq
13	Intracellular	rpsT gmhA uxaB flhD uspC fliT nuoC alaA rpoD aroK cysE waaB hfq
12	Nitrogen compound metabolic process	insA1 rpsT ampH flhD lrhA alaA rpoD aroK hofQ envZ yhjJ cysE

N ¹	High level GO category	Genes	
12	Ion binding	gmhA ampH sbmA yneF ompC nuoF nuoE nuoB alaA aroK envZ yhjJ	
10	Protein-containing complex	rpsT lptD bamA ompC nuoF nuoE nuoC nuoB nuoA cysE	
10	Biological regulation	rpsT ampH yneF flhD fliT lrhA rpoD envZ rbsR hfq	
9	Regulation of biological process	ampH yneF flhD fliT lrhA rpoD envZ rbsR hfq	
9	Response to stimulus	lptD sbmA uspC ompC alaA rpoD aroK envZ cysE	
9	Cellular component organization or biogenesis	rpsT lptD bamA gmhA ampH yddW flhD fliT mlaA	
9	Plasma membrane	ampH sbmA yneF nuoF nuoE nuoC nuoB nuoA envZ	
9	Biosynthetic process	rpsT gmhA flhD lrhA alaA rpoD aroK cysE waaB	
9	Cellular component organization	rpsT lptD bamA gmhA ampH yddW flhD fliT mlaA	
8	Localization	lptD bamA sbmA fliT ompC nuoB mlaA hofQ	
8	Small molecule binding	ampH sbmA yneF nuoF nuoC alaA aroK envZ	
8	Regulation of cellular process	yneF flhD fliT lrhA rpoD envZ rbsR hfq	
7	Establishment of localization	lptD bamA sbmA ompC nuoB mlaA hofQ	

N¹	High level GO category	Genes	
7	Membrane protein complex	bamA ompC nuoF nuoE nuoC nuoB nuoA	
6	Oxidoreductase activity	uxaB nuoF nuoE nuoC nuoB nuoA	
6	Transferase activity	yneF alaA aroK envZ cysE waaB	
6	Outer membrane	lptD bamA yddW ompC mlaA hofQ	
6	External encapsulating structure	lptD bamA yddW ompC mlaA hofQ	
6	Intrinsic component of membrane	bamA sbmA yneF ompC nuoA envZ	
6	Envelope	lptD bamA yddW ompC mlaA hofQ	
6	Macromolecule localization	lptD bamA sbmA ompC mlaA hofQ	
6	Carbohydrate derivative binding	gmhA sbmA yneF nuoF aroK envZ	
5	Regulation of metabolic process	flhD lrhA rpoD rbsR hfq	
5	Cellular component biogenesis	rpsT lptD bamA gmhA flhD	
5	Respirasome	nuoF nuoE nuoC nuoB nuoA	
5	Oxidoreductase complex	nuoF nuoE nuoC nuoB nuoA	

N ¹	High level GO category	Genes
4	Molecular function regulator	rpsT lrhA rpoD rbsR
4	Response to stress	uspC ompC alaA rpoD
4	Hydrolase activity	ampH yddW envZ yhjJ
4	Response to chemical	lptD sbmA alaA aroK
4	Positive regulation of biological process	flhD lrhA rbsR hfq
4	Negative regulation of biological process	yneF fliT lrhA hfq
4	Cellular response to stimulus	uspC ompC alaA envZ
4	Regulation of molecular function	rpsT lrhA rpoD rbsR
3	Biological adhesion	bamA yneF ompC
3	DNA-binding transcription factor activity	lrhA rpoD rbsR
3	Catabolic process	ampH uxaB hofQ
3	Response to abiotic stimulus	uspC rpoD cysE
3	Metal cluster binding	nuoF nuoE nuoB

N ¹	High level GO category	Genes
2	Transporter activity	sbmA ompC
2	Protein binding	gmhA envZ
2	Cell adhesion	bamA yneF
2	Transmembrane transporter activity	sbmA ompC
2	Regulation of cellular component biogenesis	flhDfliT
2	Interspecies interaction between organisms	essD ompC
2	Regulation of biological quality	ampH hfq
2	Cell wall organization or biogenesis	ampH yddW
2	Side of membrane	bamA envZ
1	Cell killing	essD
1	Structural molecule activity	rpsT
1	Signaling	envZ
1	Locomotion	fliT
1	Organelle	rpsT

N ¹	High level GO category	Genes
1	Cell aggregation	yneF
1	Structural constituent of ribosome	rpsT
1	Protein folding	fliT
1	Drug binding	атрН
1	Response to external stimulus	uspC
1	Carbon utilization	hofQ
1	Isomerase activity	gmhA
1	Toxin transmembrane transporter activity	sbmA
1	Cytolysis	essD
1	Enzyme regulator activity	rpsT
1	Killing of cells of other organism	essD
1	Regulation of localization	yneF
1	Amide binding	атрН
1	Regulation of locomotion	yneF

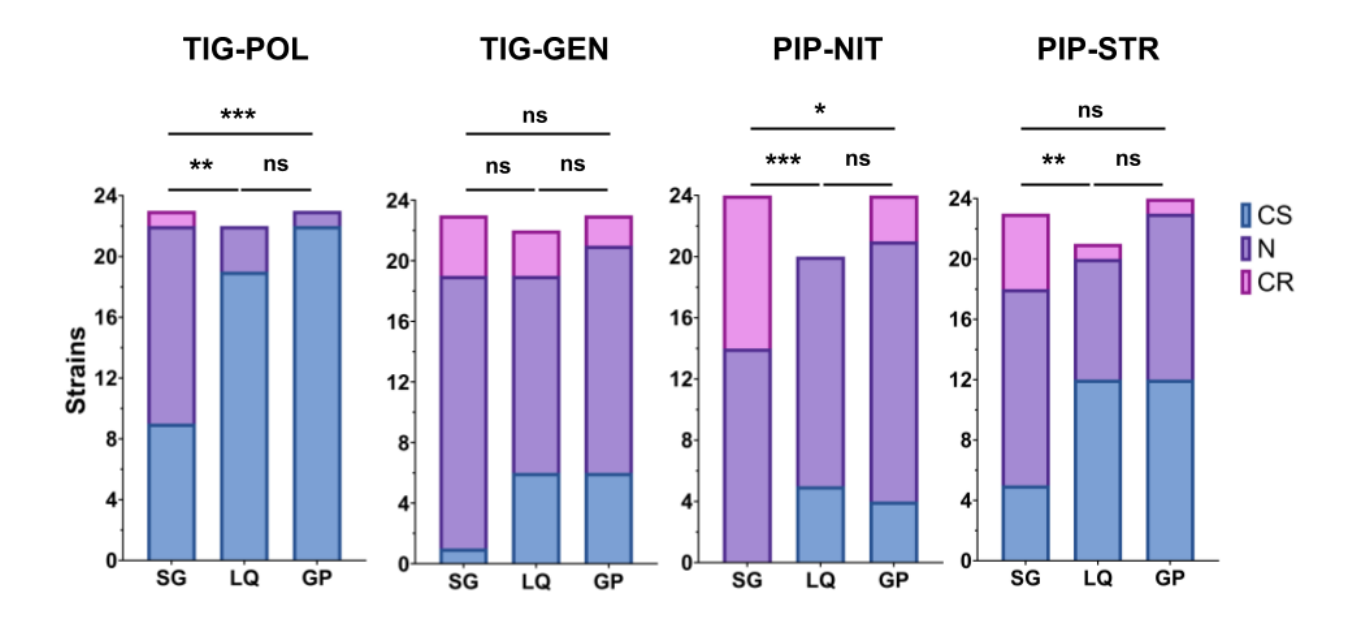
N ¹	High level GO category	Genes
1	Periplasmic space	yhjJ
1	Xenobiotic transmembrane transporter activity	sbmA
1	Non-membrane- bounded organelle	rpsT
1	Intracellular organelle	rpsT
1	Adhesion of symbiont to host	ompC
1	Regulation of response to stimulus	envZ
1	Cell motility	fliT
1	Regulation of developmental process	атрН
1	Cellular localization	bamA
1	Localization of cell	fliT
1	Intraspecies interaction between organisms	yneF
1	Molecular adaptor activity	uspC

N ¹	High level GO category	Genes
1	Aggregation of unicellular organisms	yneF
1	Sulfur compound binding	атрН
1	Ribonucleoprotein complex	rpsT

 $^{^{1}}$ N = number of genes.

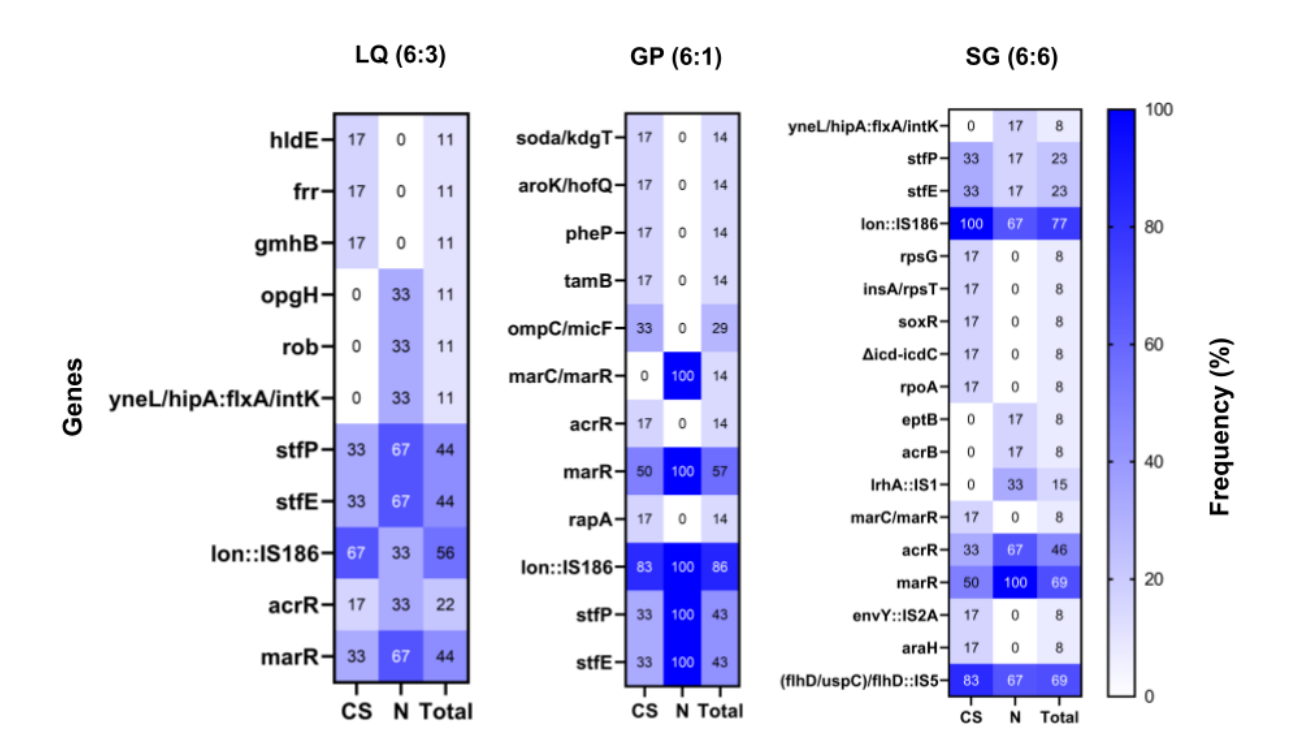
Genomic data: Available under BioProject: PRJNA1131392

Supplementary Materials for Chapter 4



Supplementary Figure 4.1: CS, N and CR distributions of the four antibiotic pairs tested, from each ALE platform. SG = SAGE. *p<0.05, ***p<0.001, ****p<0.0001, one-way ANOVA

with Bonferroni correction. Statistical analyses were performed by comparing relative MICs of mutants from each platform.

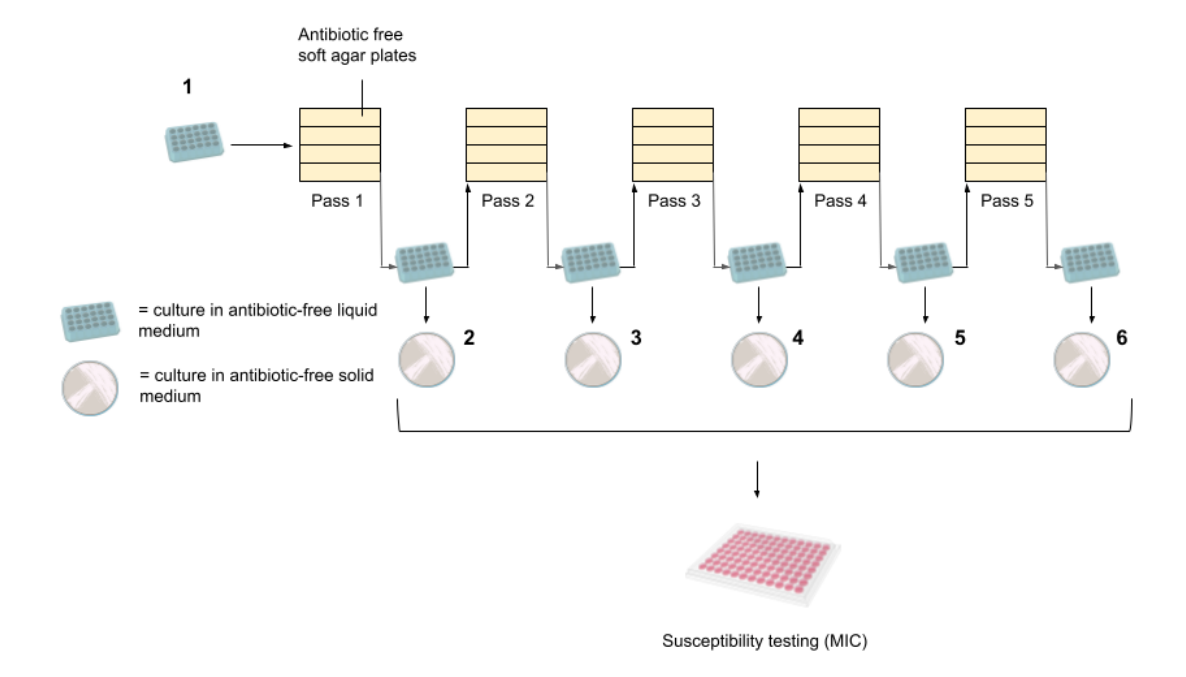


Supplementary Figure 4.2: Frequency at which a mutation in the genes listed on the vertical axis appeared in each platform. Label on top denotes the platform while (6:3) = 6 CS strains and 3 N strains. For a detailed explanation of the x-axis and gene annotations, see the legend of Figure 2 (B). SG = SAGE.

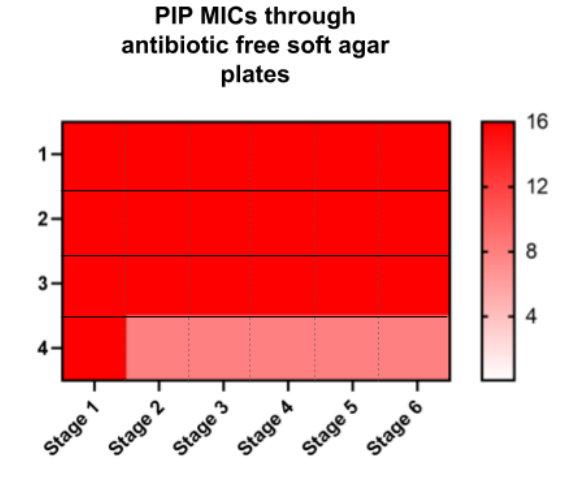
Supplementary Table 4.1: Frequencies at which each platform generated resistant mutants against the different antibiotics used in the study.

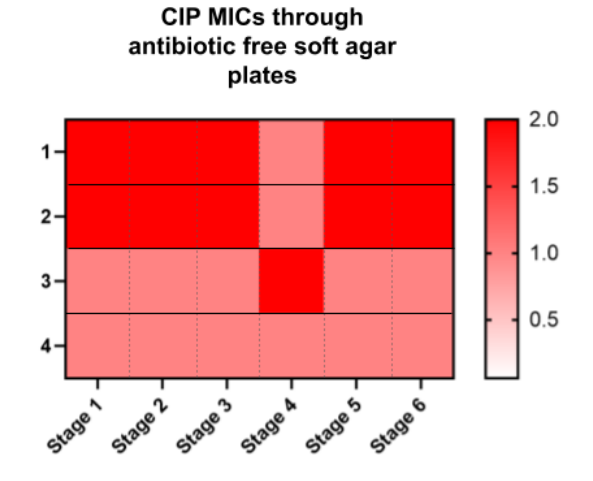
Antibiotics	ALE platform	Resistance frequency
TIG	SAGE	24 out of 24 evolutions
	LQ	22 out of 24 evolutions
	GP	23 out of 24 evolutions
PIP	SAGE	24 out of 24 evolutions
	LQ	20 out of 24 evolutions
	GP	24 out of 24 evolutions
NIT	SAGE	24 out of 24 evolutions
	LQ	3 out of 80 evolutions
	GP	24 out of 24 evolutions
CIP	SAGE	23 out of 44 evolutions
	LQ	2 out of 24 evolutions
	GP	Pilot plate showed no significant growth after 5 restreaks

Supplementary Materials for Chapter 5



Supplementary Figure 5.1: Schematic for antibiotic free soft agar passages. After the 5th pass strains have undergone 5x antibiotic free soft agar passages, 5x culturing in liquid without antibiotics, and 5x cultures on antibiotic-free solid media before being MIC tested. Numbers 1-6 represent stages at which MICs were performed. Stage 1 represents MICs of strains post resistance evolution.

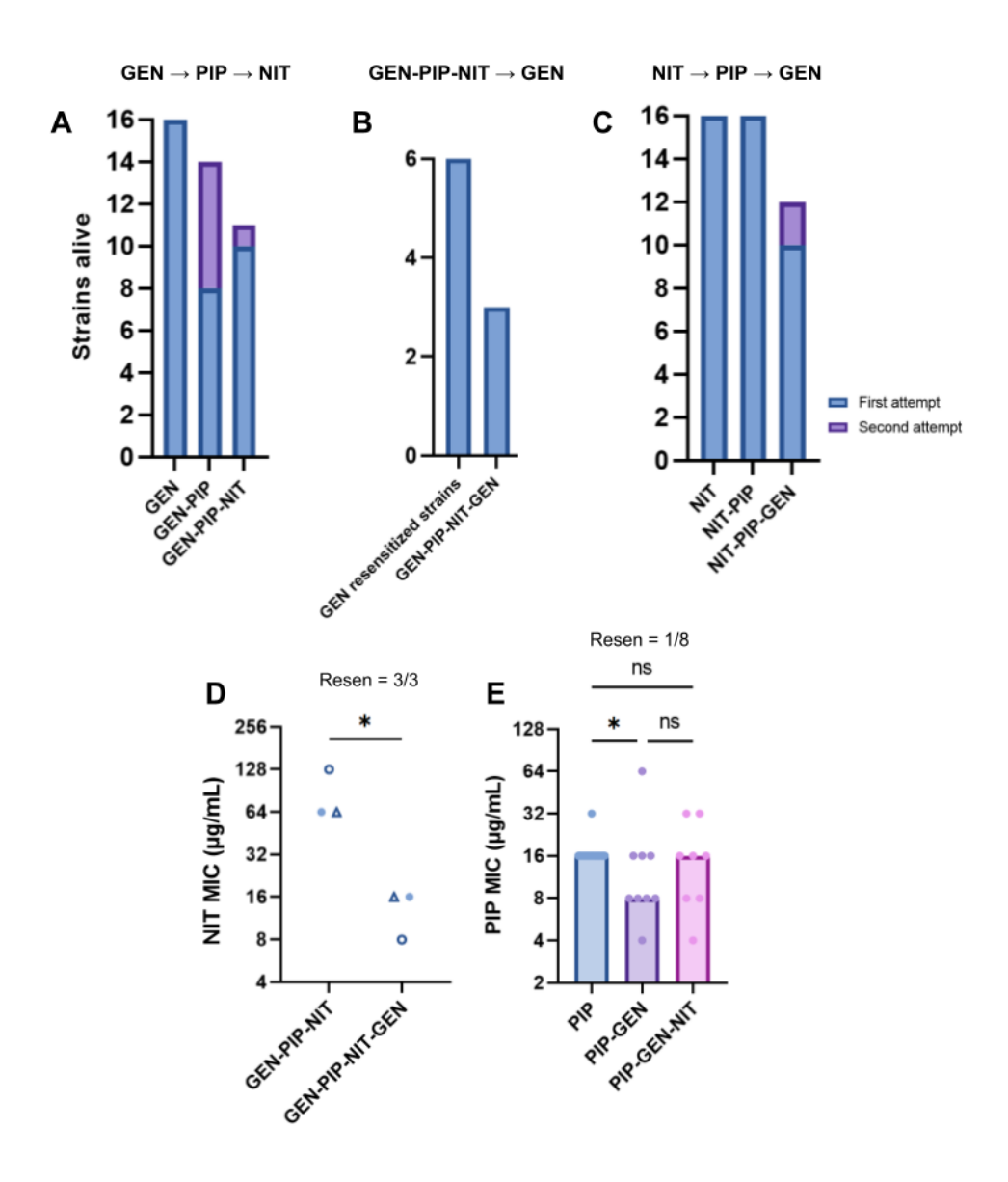


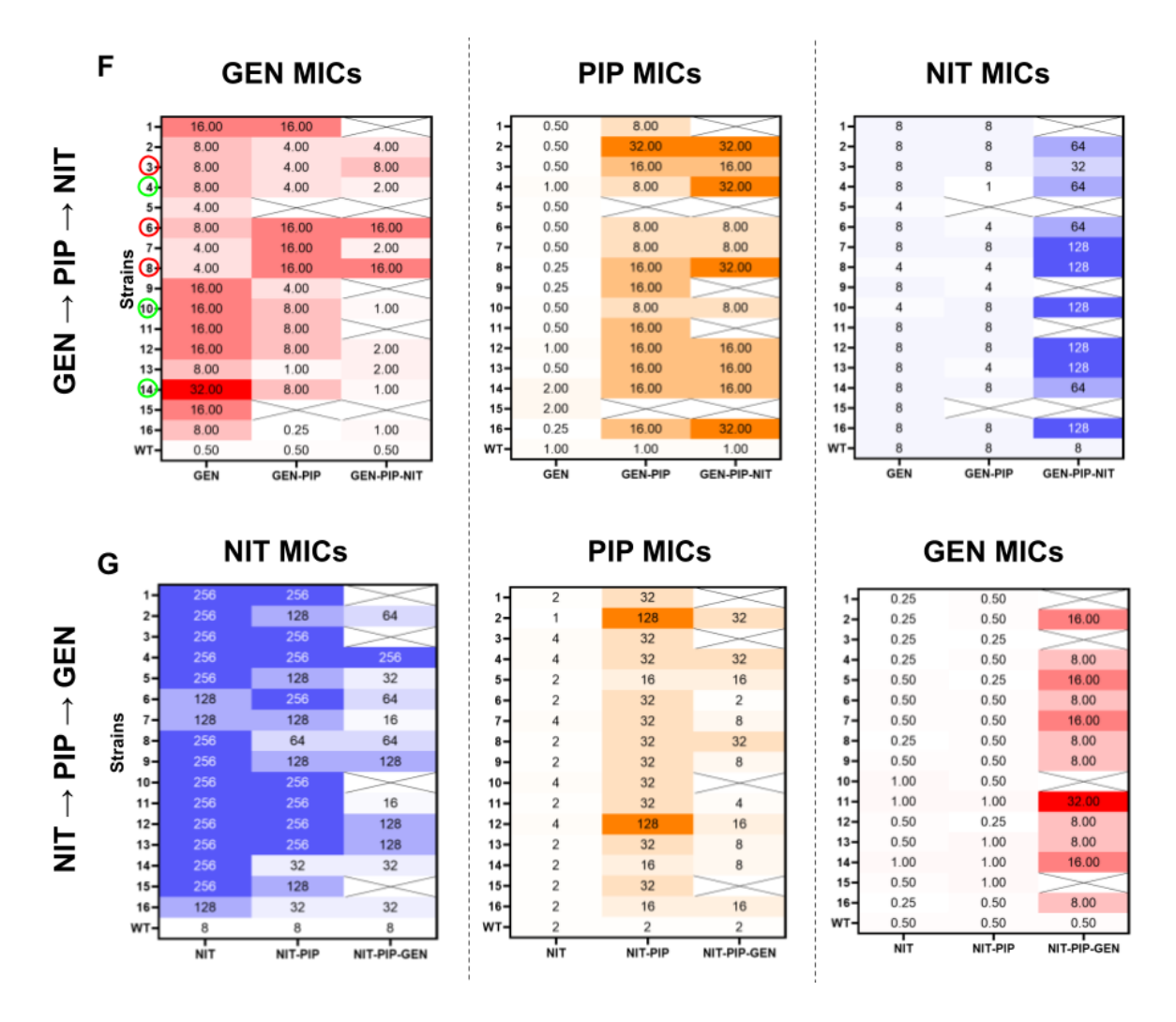


Supplementary Figure 5.2: Neither PIP or CIP MICs dropped significantly when passaged through antibiotic free medium. Passage schematic and stage numbers are on supplementary figure 5.1. Four strains that showed reduced MICs from PIP-GEN and CIP-GEN pairs were randomly selected for these tests.

Genomic data: Available under BioProject: PRJNA1207050.

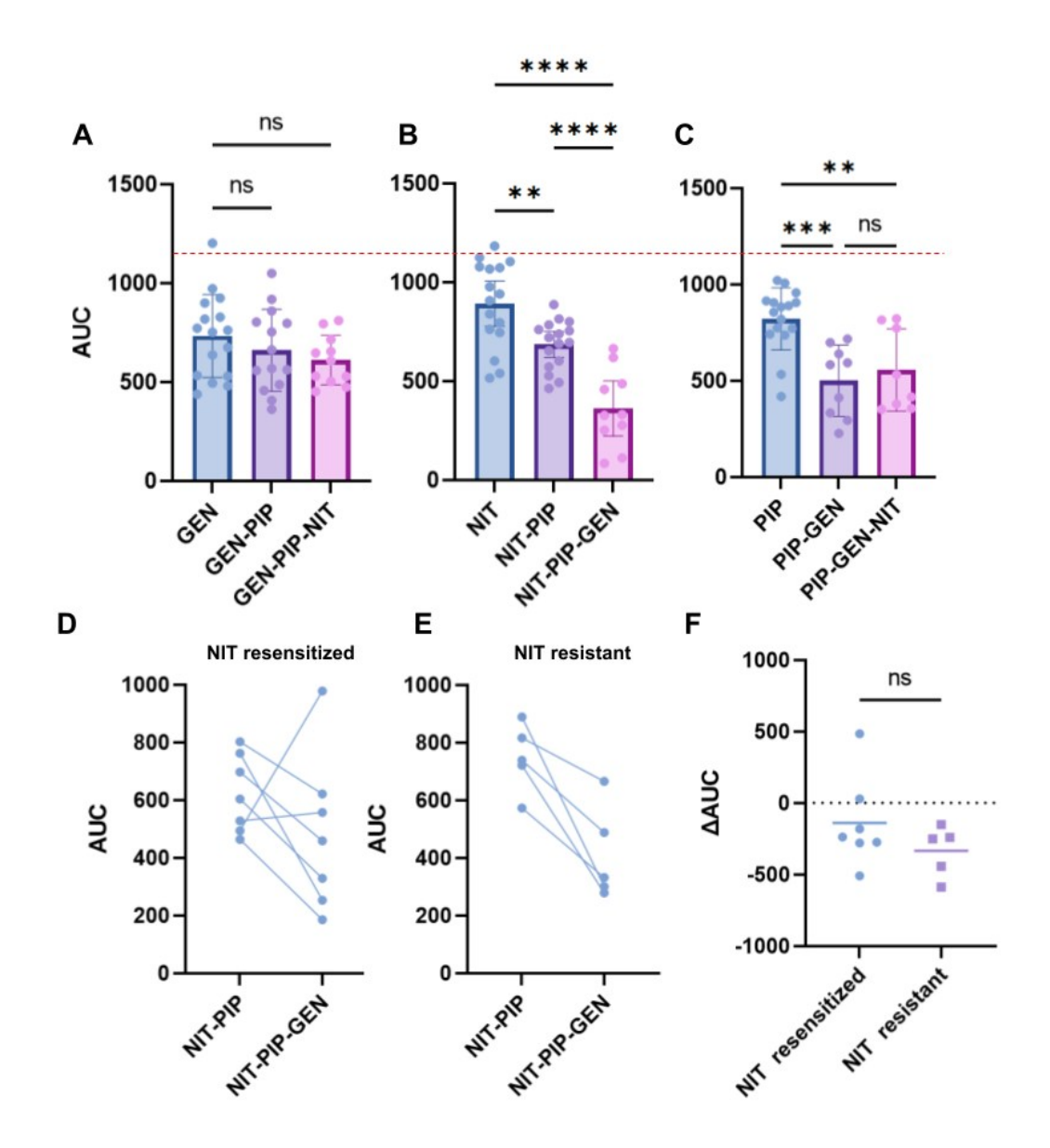
Supplementary Materials for Chapter 6





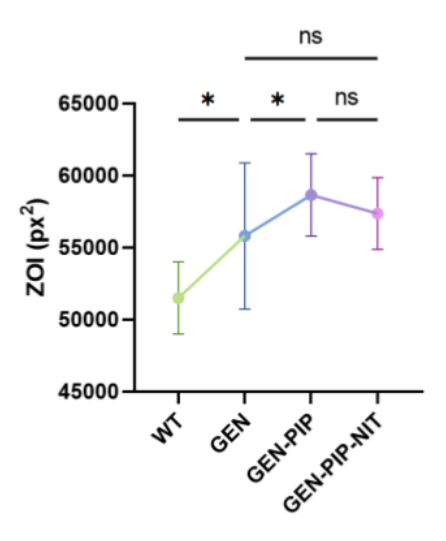
Supplementary Figure 6.1: (A) Number of non-extinct strains following each step of the GEN-PIP-NIT loop. (B) Non-extinct strains following the GEN-PIP-NIT-GEN loop. Only strains resensitized to GEN after teh GEN-PIP-NIT loop are included in the analysis. (C) Non-extinct strains following each step of the NIT-PIP-GEN loop. Purple stacked bars denote strains that went extinct on the initial pass, but survived a second attempt. (D) NIT MICs of the three non-extinct after the GEN-PIP-NIT-GEN sequence. *p<0.05, unpaired t-test (E) PIP MICs of strains that passed through the PIP-GEN-NIT loop. Bars represent the median MICs. *p<0.05, Kruskal-Wallis with uncorrected Dunn's test. (F) and (G) MICs of every strain evolved in the GEN-PIP-NIT and NIT-PIP-GEN loops. Green and red circles indicate the sequenced GEN-resensitized and GEN-

resistant strains that were sequenced, respectively. The x-axes indicate the drugs against which bacteria were evolved, with the MIC antibiotic listed at the top of each panel.

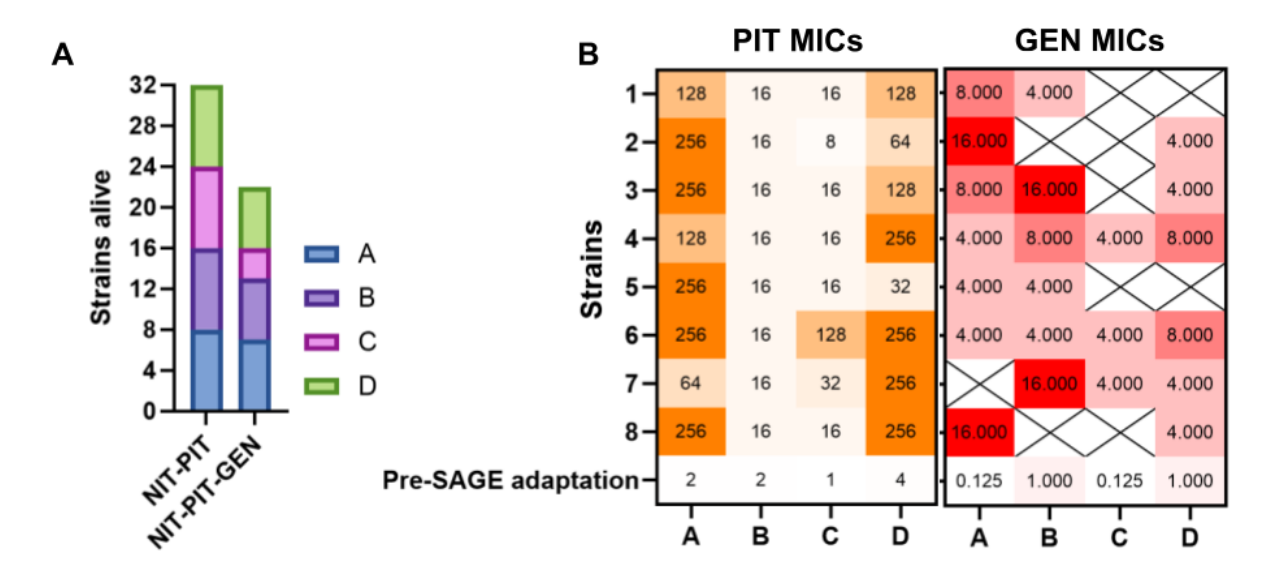


Supplementary Figure 6.2: AUC data of strains passed through (A) GEN-PIP-NIT, (B) NIT-PIP-GEN, and (C) PIP-GEN-NIT loops. The red dotted line denotes the fitness of the WT strain. Bars represent the mean with 95% CI. *p<0.05, **p<0.01, ***p<0.001, ***p<0.001, one-way ANOVA with Fisher's LSD test. (D) and (E) AUCs of strains before and after GEN evolution for

NIT-resensitized and NIT-resistant strains, respectively. The x-axes denotes the sequence of antibiotics against which the strains were evolved before measuring AUCs. (F) Δ AUC of individual strains plotted, grouped by resensitized and resistant; unpaired t test used to test significance. Means indicated by horizontal lines.



Supplementary Figure 6.3: Results from the gentamicin uptake assay. GEN was incubated with bacteria (n = 3), and then centrifuged to pellet the cells. The supernatant was used to spot E. coli seeded plates (more details in Materials and Methods). The lower the GEN uptake, the more GEN remaining in the supernatant after centrifugation and hence, the larger the ZOI. Error bars represent SD. *p<0.05 one-way ANOVA with Fisher's LSD test.



Supplementary Figure 6.4: (A) Number of non-extinct strains following each step of the (NIT)-PIT-GEN loop. NIT is omitted since the clinical strains were already NIT resistant. The different colored bars represent strain A, B, C or D. (B) PIT and GEN MICs of the clinical replicates following PIT and GEN adaptation respectively.

Genomic data: Available under BioProject: PRJNA1254677